MECHANISTIC STUDIES ON DNA GYRASE FROM *ESCHERICHIA COLI.*

by

DAVID PAUL WEINER

A thesis submitted in fulfilment of the requirements for the degree of Doctor of Philosophy at the University of Leicester.

Departments of Chemistry & Biochemistry

University of Leicester

LEICESTER LE1 7RH

UNITED KINGDOM

JULY 1992

ProQuest LLC
789 East Eisenhower Parkway
P.O. Box 1346
Ann Arbor, MI 48106-1346

To John and Marie-Louise Weiner

Acknowledgements

The work presented in this thesis was carried out in the laboratories of Professor P.M. Cullis and Dr. A. Maxwell in the Departments of Chemistry and Biochemistry, respectively.

I would like to thank Paul Cullis and Tony Maxwell for the invaluable help, advice, and encouragement that they have given me during my time in Leicester. I would also like to thank Andy Bates, Andy Jackson, Simon Dobbs, Alison Howells, Chris Wilmott, Janid Ali, and everyone else in Lab. 118 for all their help and for creating a very pleasant environment to work in. Thanks also to Mark Buttrum and John Williams for helpful discussions, to Raj Misra for guidance during the early part of my work and to John Arnold and Gerry Griffiths for help with high field NMR experiments.

Finally a special thankyou to Sarah Glassford for all of her support and inspiration.

I acknowledge the financial assistance from a studentship given to me by the S.E.R.C.

Abbreviations

A	adenine
Ad	adenosine
ATP	adenosine 5'-O-triphosphate
ADP	adenosine 5'-O-diphosphate
ADPNP	5'-adenylyl-β-γ-imidodiphosphate
$ATP_{\alpha}S$	adenosine 5'-O-(1-thiotriphosphate)
$ATP_{\beta}S$	adenosine 5'-O-(2-thiotriphosphate)
$ATP_{\gamma}S$	adenosine 5'-O-(3-thiotriphosphate)
$ADP_{\alpha}S$	adenosine 5'-O-(1-thiodiphosphate)
$ADP_{\beta}S$	adenosine 5'-O-(2-thiodiphosphate)
A_{260}	absorbance at 260 nm
DNA	deoxyribonucleic acid
BSA	bovine serum albumin
bp	base pair
ccc DNA	covalently-closed-circular DNA
o.c. DNA	open-circular (nicked) DNA
DNase	deoxyribonuclease
DTT	dithiothreitol
EDTA	ethylenediaminetetra-acetic acid
FPLC	fast protein liquid chromatography
GTP	guanosine 5'-O-triphosphate
GyrA	DNA gyrase A protein
GyrB	DNA gyrase B protein
gyrA	gene encoding GyrA
gyrB	gene encoding GyrB
HPLC	high performance liquid chromatography
IPTG	isopropyl-β-D-thiogalactopyranoside
kb	kilo-base pairs
kDa	kiloDaltons
m^7Guo	7-methyl-guanosine
m^7Gua	7-methyl-guanine
NAD^+	nicotinamide adenine dinucleotide (oxidised form)
NADH	nicotinamide adenine dinucleotide (reduced form)
NMR	nuclear magnetic resonance spectroscopy
PAGE	polyacrylamide gel electrophoresis
PEG	polyethylene glycol
P_i	inorganic phosphate
PS_i	inorganic thiophosphate
PK/LDH	Pyruvate kinase/lactate dehydrogenase
RNA	ribonucleic acid
tRNA	transfer RNA
SDS	sodium dodecyl sulphate
TEMED	N,N,N',N'-tetramethylethylenediamine
TLC	thin layer chromatography
Tris	Tris (hydroxymethyl) amino methane

ABSTRACT

DNA gyrase is an essential bacterial type II topoisomerase which couples the free energy of ATP hydrolysis to the introduction of negative supercoils into DNA. This study concentrates on the interaction of the enzyme with ATP and on the way the free energy of hydrolysis of the nucleotide is coupled to the supercoiling reaction.

Positional isotope exchange experiments, using ATP labelled with ^{18}O in the β–γ-bridge position, have shown that no detectable scrambling of the label occurs during the gyrase ATPase. This is interpreted in terms of a slow ATP off-rate in gyrase.

Gyrase-catalysed turnover of $ATP_{\gamma}S$ was found to be 300 to 1000-fold slower than ATP from supercoiling and hydrolysis measurements. This precluded the use of isotopically chiral $ATP_{\gamma}S$ to determine the stereochemistry of the gyrase ATPase, although the availability of more protein in the future may permit such a study.

Various aspects of the interaction of gyrase with diastereoisomers of $ATP_{\alpha}S$ and $ATP_{\beta}S$ have been explored which has yielded information on the type of MgATP complex handled by the enzyme and on the relationship between hydrolysis of the ATP analogues and their ability to support DNA supercoiling. Gyrase showed a strong preference for the Rp epimers of $ATP_{\alpha}S$ and $ATP_{\beta}S$ in the presence of Mg^{2+} which is consistent with the Mg^{2+} ion being coordinated to the *pro*-S oxygens of the α and β-phosphates in ATP bound to the enzyme; an α,β,γ-tridentate Mg-ATP complex with Λ-exo geometry is proposed. $ATP_{\alpha}S(Rp)$ hydrolysis appears to be well coupled to DNA supercoiling whereas $ATP_{\beta}S(Rp)$ hydrolysis is only poorly coupled to the supercoiling reaction. Two hypotheses are proposed to account for this phenomenon.

The divalent metal ion specificities of the DNA supercoiling, relaxation, and cleavage reactions of gyrase have been characterised. It was found that the cleavage reaction exhibited a greater tolerance towards different metal ions than the relaxation and supercoiling reactions; the mechanistic implications of this observation are discussed.

An N-terminal fragment of the gyrase B protein was used as a simple model for gyrase-ATP interactions. This truncated protein showed the same stereospecificity towards the diastereoisomers of $ATP_{\alpha}S$ and $ATP_{\beta}S$ as intact gyrase but the kinetics of hydrolysis of the two phosphorothioate ATP analogues showed significant differences from those with gyrase, which may be due to differences in the mechanisms of ATP hydrolysis for the two enzymes. Attempts to demonstrate reversal of stereospecifity on switching from a hard metal ion such as Mg^{2+} to a soft metal centre such as Cd^{2+} were thwarted by the inhibitory effects of Cd^{2+}.

The extent of supercoiling of pBR322 was investigated with ATP, $ATP_{\alpha}S(Rp)$, and $ATP_{\beta}S(Rp)$. With $ATP_{\beta}S(Rp)$ the rate of DNA supercoiling was very slow (since its hydrolysis is inefficiently coupled to supercoiling; see above) and the reaction did not reach a limit even after long time-courses. With ATP and $ATP_{\alpha}S(Rp)$, the supercoiling reaction was faster and did reach a limit: ATP gave a ΔLk of -46 and $ATP_{\alpha}S(Rp)$ gave a ΔLk of -47. Measurements of the displacement of the equilibrium of the reaction catalysed by arginine kinase showed that $ATP_{\alpha}S(Rp)$ has a greater free energy of hydrolysis than ATP. This energy difference corresponds closely to the extra free energy required for the additional supercoiling seen with $ATP_{\alpha}S(Rp)$. It is proposed that the extent of supercoiling in gyrase is limited by the free energy available from nucleotide hydrolysis.

TABLE OF CONTENTS

LIST OF FIGURES

Chapter 5.

Chapter 6.

Appendix I.

Chapter 1

Introduction

1.1. DNA SUPERCOILING

Discovery of DNA supercoiling.

Since the elucidation of the regular double-helical structure of DNA in the seminal paper of Watson and Crick (1953), a remarkable variety of structural deviations from this basic model has emerged. For example, in addition to B-DNA, other helical forms such as A- and Z-DNA have been characterised (Saenger, 1984), while the bending of the DNA axis has been found to be important in many interactions with proteins (Caserta *et al.*, 1989; Crothers *et al.*, 1990; Travers, 1990). Another important structural feature of DNA is the supercoiling of the helix. In fact, virtually all covalently closed-circular DNA isolated from prokaryotes and eukaryotes is in a negatively supercoiled form. Supercoiling was discovered following the finding that DNA isolated from polyoma virus formed two bands when it was centrifuged; it was deduced that this DNA was circular and that the two bands represented nicked-circular and intact supercoiled DNA (Vinograd *et al.*, 1965).

Descriptors of DNA topology.

In the standard B-DNA structure the two strands of the double helix are coiled around each other in a right-handed fashion. Thus, if the ends of the DNA are joined to give a double-stranded circle, the two strands become linked by the number of "Watson-Crick" double-helical turns in the original linear molecule. The number of times the DNA strands are interlinked is defined as the linking number (Lk or α in early literature) which is always an integer, and the number of double-helical turns in a piece of DNA is termed the twist (Tw) and is calculated from the DNA length in base-pairs (N) divided by the helical repeat (h) (see Eqn 1.1).

$$Tw = N/h \qquad \text{(eqn.1.1)}$$

For many linear and relaxed DNA's, h can be assumed to be approximately 10.5 (Rhodes and Klug, 1980). The value of N/h is not necessarily an integer; for example, in pBR322 which has 4361 bp (Watson, 1988), N/h is 415.33 (assuming h=10.5); the quantity N/h for DNA which is perfectly relaxed (under no torsional stress) is defined as Tw°. Conceptually, if linear pBR322 DNA is circularised under conditions of no torsional stress, a plasmid with a linking number which is the closest integer to Tw° (in this case +415) would be formed. The linking number of such a relaxed ccc DNA is defined as Lk° (see Eqn.1.2 below) which, by convention, is positive for right-handed DNA.

$$Lk^{\circ} (\approx Tw^{\circ}) \approx N/h \approx N/10.5 \qquad \text{(eqn. 1.2)}$$

The Lk for any two interlinked circles can be found by constraining the circles to a plane and counting the number of cross-overs (or nodes) of the two circles (Fig. 1.1). The curves are assigned a direction and each node is given a value of +1 or -1 depending on the direction of movement required to align the upper strand with the lower one. The sum of the values of all the nodes is then halved to give the linking number of the two curves. In the same way, the Lk of DNA can be assigned by constraining the duplex to a plane.

Conceptually, if the DNA was circularised under conditions where the double helix was underwound then the resulting circular plasmid would have a lower linking number than Lk°, while overwinding prior to circularisation would give a product with a greater linking number than Lk°; the change in Lk with respect to Lk° is the linking difference of the DNA (Crick *et al.*, 1979) and is given by:

$$\Delta Lk = Lk - Lk^{\circ} \qquad \text{(eqn. 1.3)}$$

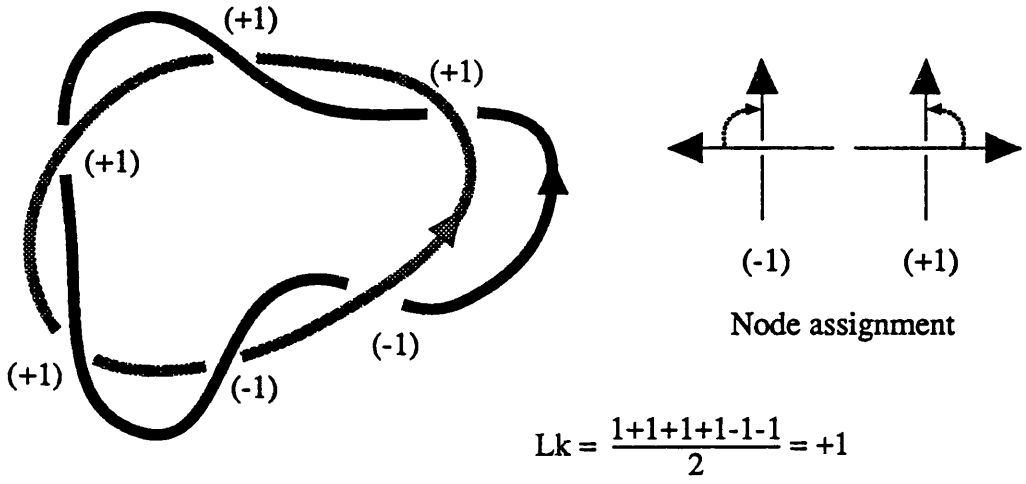

Figure 1.1. Determination of the linking number of two circles constrained to a plane. Please see text for explanation.

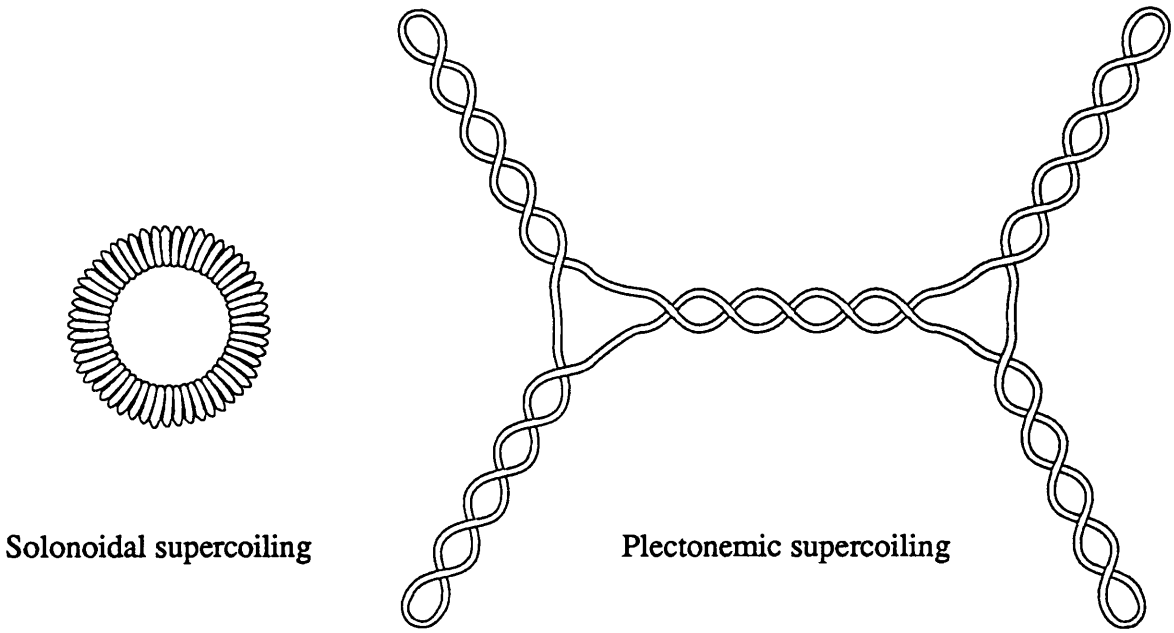

Figure 1.2. The difference between the plectonemic and solenoidal supercoiling of a plasmid of 4.6 kb with a specific linking difference of about -0.06. The plectonemically supercoiled DNA is shown as having a branched structure as seen by electron microscopy (Boles *et al.*, 1990). As can be seen from the figure, the solenoidally supercoiled DNA is considerably more compact than the plectonemically supercoiled molecule.

The linking difference can be normalised to the size of DNA circle by dividing by Lk° to give the specific linking difference (SLD or σ):

$$SLD = (Lk - Lk^\circ)/Lk^\circ \qquad \text{(eqn. 1.4)}$$

A change in linking number from the relaxed state (Lk°) results in the introduction of torsional stress into the ccc DNA which can be accommodated by either a change in the helical repeat and/or a coiling of the double helix upon itself known as supercoiling. This relationship is expressed by the following simple equations (Crick, 1976; Fuller, 1971; White, 1969);

$$Lk = Tw + Wr \qquad \text{(eqn. 1.5)}$$

$$\Delta Lk = \Delta Tw + \Delta Wr \qquad \text{(eqn. 1.6)}$$

Tw is the twist of the DNA (which has already been discussed) and Wr is the writhe of the DNA which is a measure of the contortion of the helix axis in space and can be thought of as the coiling of the helix about itself corresponding to supercoiling. It is important to note that Lk is a topological property that cannot be changed without breaking one or both of the DNA strands, while Tw and Wr are geometrical parameters that can interconvert as long as their sum is equal to Lk. (Confusion between supercoiling as a topological and a geometrical property can arise because the SLD is sometimes referred to as the extent of supercoiling or superhelical density; it is therefore more precise to avoid these terms when discussing SLD[68]).

[68]In this thesis (especially in Chapter 6), SLD is predominantly used in technical discussions. However, extent of supercoiling is also used because it is a more descriptive phrase; where it appears it is used in a topological sense and does not imply any particular geometry.

White *et al.* (1988) have developed an expression for Lk that embraces the fact that often the DNA axis lies on a surface such as when it is wrapped around a protein (eg. the histone core of a nucleosome). This treatment relates the linking number of closed DNA wrapped on a surface to the sum of two integers as follows:

$$Lk = SLk + \Phi \qquad \text{(eqn. 1.7)}$$

SLk is the surface linking number, which takes account of the effects of surface geometry on Tw and Wr, and Φ is the winding number which is a function of the helical repeat relative to the surface on which the DNA lies and can, in principle, be measured experimentally by chemical and enzymatic footprinting.

Experimental aspects of DNA supercoiling.

In introducing Lk, the concept of circularising linear DNA was used. Experimentally, nicked-circular DNA, which is under no torsional constraint since the strands are free to rotate with respect to each other, is resealed with a DNA ligase. Such an experiment with DNA of 2kb or more produces a thermal energy population consisting of a family of topoisomers differing in Lk by one (Depew and Wang, 1975; Pulleyblank *et al.*, 1975) which can be resolved by electrophoresis through an agarose gel (Keller and Wendel, 1974). In relaxed DNA the distribution of topoisomers follows a Gaussian with a standard deviation of $\sqrt{(RT/2K)}$ centred at Tw°, where R is the gas constant, T is the absolute temperature, and K is a constant roughly inversely proportional to the length of the DNA.

It follows directly from the Gaussian distribution of topoisomers that the free energy of supercoiling is proportional to the square of the linking difference of the DNA (Depew and Wang, 1975; Pulleyblank *et al.*, 1975) which agrees with data obtained from the binding of the intercalator, ethidium bromide, to nicked-circular and native supercoiled

DNA (Bauer and Vinograd, 1970; Hsieh and Wang, 1975). This indicates that for relatively large cccDNA's (approximately 2kb or more) the deformation of the helix caused by supercoiling (at least for naturally occurring ΔLk's) is an elastic process. The free energy of supercoiling for such large DNA molecules can be expressed as follows:

$$\frac{\Delta G_{sc}}{N} = NK\left(\frac{\Delta Lk}{N}\right)^2 \qquad \text{(eqn. 1.8)}$$

N is the number of bp of the DNA and NK has been shown to be largely independent of the size of the DNA circle in molecules above approximately 2kb (Horowitz and Wang, 1984; Shore and Baldwin, 1983b). The above equation is also given in Section 6.3 (Eqn. 6.6) where a further discussion of the energetics of supercoiling can be found.

For small linear DNA molecules (below about 500bp), it has been shown that the rate of ligation to closed-circular molecules, mediated by a DNA ligase, exhibits a periodic dependence on the length of the DNA with a periodicity of approximately 10bp (Shore and Baldwin, 1983a; Shore *et al.*, 1981). This is because when a DNA molecule, whose length is not an exact multiple of the helical repeat, is ligated into a circular form an amount of energy is required in order to align the two ends. For large DNA's this energy is relatively small since the distortion required to align the ends is easily accommodated by a small change in twist or writhe. However, for small DNA's (below 500bp) the deformation to align the two ends cannot be distributed over such a long stretch of DNA and a proportionately greater amount of free energy is required. Thus in small circular DNA's, the amount of energy required to change Lk by one becomes considerable and the relaxed distribution of topoisomers consists of only one or two topoisomers. The specific linking difference is related to the centre of the topoisomer distribution (as it is for larger DNA's) but in this case Lk° does not approximate to Tw° (see Eqn 1.2) and the expression for SLD becomes:

$$SLD = (Lk - Tw^{\circ})/Tw^{\circ} \qquad \text{(eqn. 1.9)}$$

The geometry of supercoiled DNA in solution has been studied by electron microscopy which has suggested that supercoiled circular DNA has a branched plectonemic conformation (Boles *et al.*, 1990; Vinograd *et al.*, 1965) as shown in Fig. 1.2. Recently, electron microscopy has also been used to determine how ΔLk is partitioned into ΔTw and ΔWr for DNA circles greater than 2kb with the finding that the ratio of ΔTw to ΔWr is approximately 1:3 (Adrian *et al.*, 1990; Boles *et al.*, 1990; Dustin *et al.*, 1991). It would be expected that for small DNA circles (below 500bp) the proportion of ΔTw would be considerably greater.

Biological significance of DNA supercoiling.

Negative supercoiling is important in many biological processes (reviewed in Bates and Maxwell (In press)). The free energy of negative supercoiling assists processes that require the unwinding or denaturation of DNA such as DNA replication, transcription, and recombination. In addition negative supercoiling facilitates a variety of DNA structural transitions such as the formation of Z-DNA and cruciforms. Both plectonemic and solenoidal supercoiling (Fig. 1.2) bring together neighbouring DNA sequences. However, only plectonemic supercoiling brings together DNA sequences which are distant in the primary structure and this may be important in stabilising the interaction of distant *cis*-acting sequences involved in the regulation of transcription and site-specific recombination (Wasserman and Cozzarelli, 1986). Furthermore, branching in plectonemically supercoiled DNA, which brings together three distinct sequences, has been proposed to favour recombination reactions which have two crossover sites and an enhancer site (Johnson *et al.*, 1987; Kanaar *et al.*, 1989). Solenoidal supercoiling results in a striking compaction of the DNA and this type of supercoiling stabilised by DNA-histone interactions is very important in the packaging of the genetic material in the nucleus of eukaryotic cells.

1.2. TOPOISOMERASES

General introduction.

Enzymes that can change the topological state of DNA are known collectively as DNA topoisomerases (for reviews see: Cozzarelli (1980a); Cozzarelli (1980b); Drlica (1990); Gellert (1981); Hsieh (1990a); Liu (1983); Maxwell and Gellert (1986); Reece and Maxwell (1991b); Vosberg (1985); Wang (1985); Wang (1987a); Wang (1987b); Wang (1991)). Topoisomerases were first recognised in 1971 by their ability to relax closed-circular, negatively supercoiled DNA. Subsequently, extensive *in vitro* studies have shown that many of these enzymes can promote a variety of topological interconversions of DNA including the supercoiling and relaxation of DNA, the intramolecular knotting and unknotting of DNA, and the intermolecular catenation and decatenation of DNA circles. A common mechanistic feature of all these reactions is the requirement for a transient break in the DNA backbone and the passage of a section of DNA through the break, followed by resealing of the DNA. The above essential aspects of topoisomerase reactions were perceived early on in the studies of these enzymes and various mechanistic models for topoisomerase action have been proposed which embrace these ideas. These models will be discussed in later sections with respect to individual types of topoisomerases.

Topoisomerases can be classified into two main groups (termed type I and type II enzymes) according to their mode of action. Type I topoisomerases act by the transient cleavage of a single strand of DNA, while type II enzymes catalyse reactions involving transient double-stranded cleavage (Gellert, 1981). As a consequence of the extent of DNA strand cleavage, type I topoisomerases change the linking number of DNA in steps of one, while the type II enzymes catalyse linking number changes in steps of two. Experimentally, type I and type II enzymes can be distinguished by incubation of the enzyme with a purified single DNA topoisomer to determine the incremental change in

linking number (Brown and Cozzarelli, 1979; Brown and Cozzarelli, 1981; Liu *et al.*, 1980; Miller *et al.*, 1981; Mizuuchi *et al.*, 1980).

Many enzymes that normally function in DNA strand transfer reactions such as site specific recombination are also capable of topoisomerisation reactions under appropriate conditions (see Gellert (1981); Wang (1985), and references therein). The key to the topoisomerase activity of strand-transfer enzymes is their ability to transiently cleave either single-stranded or double-stranded DNA and therefore these enzymes can be considered as special cases of type I or type II topoisomerases.

Historical perspective.

Topoisomerases have been isolated from a wide variety of prokaryotic and eukaryotic cells as well as some viruses (Bauer *et al.*, 1977; Liu *et al.*, 1979), mitochondria (Fairfield *et al.*, 1979; Fairfield *et al.*, 1985), and chloroplasts (Siedlecki *et al.*, 1983). In fact, the cells of all organisms so far examined have been found to contain these enzymes. The discovery of topoisomerases dates back to 1969 when an activity capable of relaxing supercoiled DNA was reported in *E. coli* extracts (Wang, 1969). Purification of the activity showed that a single enzyme was responsible and this enzyme was termed the ω protein (now called *E. coli* DNA topoisomerase I) (Wang, 1971). A eukaryotic type I topoisomerase was found the following year in mouse cell extracts (Champoux and Dulbecco, 1972). Although both the prokaryotic and eukaryotic type I enzymes operate *via* a transient single-stranded DNA break they differ in many of their properties as will be discussed below.

In 1976, a new type of DNA topoisomerase, DNA gyrase, was discovered in *E. coli* during the course of investigations into host factors required for the site-specific integration of bacteriophage λ (Gellert *et al.*, 1976a). This enzyme was found to catalyse the negative supercoiling of a double-stranded closed-circular DNA substrate in an ATP-

dependent reaction. The mechanism of DNA supercoiling by gyrase was later found to involve the formation of transient double-stranded DNA breaks (Mizuuchi *et al.*, 1980) and thus the enzyme is a type II topoisomerase (in addition to DNA gyrase it is sometimes referred to as prokaryotic topoisomerase II). Another distinct type II topoisomerase was isolated from phage T4 in 1979 (Liu *et al.*, 1979). This was found to catalyse the relaxation of both positively and negatively supercoiled DNA. Interestingly, despite the fact that these topological changes are energetically down-hill, ATP was shown to be required by the T4 enzyme. Type II topoisomerases were first isolated from eukaryotes in 1980 (Hsieh and Brutlag, 1980) and, to date, all of these eukaryotic enzymes have been found to relax positively and negatively supercoiled DNA in an ATP-dependent manner.

In Section 1.1, the biological significance of DNA topology was considered. DNA topoisomerases are intimately involved in regulating the tertiary structure of DNA in organisms and therefore these enzymes have important roles in many areas of DNA metabolism. Some of the main biological functions of topoisomerases will be considered in Section 1.2.6, after a detailed look at the enzymes themselves.

1.2.1. Prokaryotic Type I Topoisomerases

Genetic data.

Since the discovery of the *E.coli* enzyme, many prokaryotic type I topoisomerases have been described from other bacterial species such as *Micrococcus luteus* (Kung and Wang, 1977) and *Agrobacterium tumefaciens* (Lebon *et al.*, 1978). The *E. coli* enzyme is coded for by the *topA* gene which has been cloned (Wang and Becherer, 1983) and sequenced (Tse-Dinh and Wang, 1986). The gene codes for a protein of 865 amino acids with a molecular weight of approximately 97 kDa which agrees with the estimated denatured molecular weight from SDS-polyacrylamide gel electrophoresis (SDS-PAGE) (Depew *et al.*, 1978).

The *topA* gene appears to be essential since most deletion mutants of the gene are not viable. Interestingly such mutants have only been found to survive when a mutation in one of the DNA gyrase genes is also present; the reduced gyrase activity is thought to compensate for the loss of topoisomerase I activity (DiNardo *et al.*, 1982; Pruss *et al.*, 1982) (see also Section 1.2.6). Expression of the gene is regulated by the topological state of the DNA template with higher levels of expression corresponding to greater negative supercoiling (Tse-Dinh, 1985).

Protein structure and function.

The active enzyme is a single subunit protein and requires Mg^{2+} ions for its DNA relaxation activity although there is no ATP dependence. A stable C-terminal fragment of *E. coli* topoisomerase I with a molecular weight of 14 kDa has been produced either by genetic manipulation (Zumstein and Wang, 1986) or by limited proteolytic digestion with trypsin or papain (Beran-Steed and Tse-Dinh, 1989). The fragment binds to DNA-agarose with a similar affinity as the intact protein although it is not essential for the relaxation activity of the enzyme. Mutants of topoisomerase I that lack the C-terminal region exhibit a reduced affinity for DNA and it has therefore been suggested that the C-terminal portion of topoisomerase I may confer stability to the protein-DNA complex.

Since topoisomerase I relaxes intact double-stranded supercoiled DNA by reducing the linking number in steps of one it has been proposed that the mechanism involves a single-stranded DNA cleavage (Brown and Cozzarelli, 1979). Under various conditions which denature the protein it is possible to isolate cleaved DNA which is thought to represent an intermediate in the relaxation reaction. For example, addition of alkali to complexes of topoisomerase I and single-stranded circular DNA results in the breakage of the DNA and covalent binding of the protein to the 5' end of the break-site (Depew *et al.*, 1978; Liu and Wang, 1979; Tse *et al.*, 1980). Using ^{32}P-labelled DNA in a cleavage reaction with topoisomerase I, it was found that some of the label was transferred to the protein, after

hydrolysis of the DNA, and that the label was associated with tyrosine (Tse *et al.*, 1980). In this way the covalent bond between the protein and the DNA was found to be a phosphate ester linkage between tyrosine and the 5'-phosphate of DNA. The involvement of a covalent phosphotyrosine intermediate is a universal feature of all topoisomerases (with the exception of some recombination enzymes, such as γδ resolvase (Reed and Moser, 1984) and phage Mu Gin invertase (Klippel *et al.*, 1988), where a phosphoserine is involved) and is important in conserving the free energy of the broken phosphodiester bond of DNA for the DNA resealing step. Presumably the enzyme interacts non-covalently with the 3' end of the nick site so that the nick is completely held by the protein, thus facilitating rejoining of the strand in the complete relaxation reaction (Dean and Cozzarelli, 1985). Recently, in *E. coli* topoisomerase I, the active site tyrosine has been identified as Tyr-319. Furthermore, site directed mutagenesis of this residue to a serine or a phenylalanine produced an inactive enzyme, underlining the importance of the tyrosine (Lynn and Wang, 1989).

The cleavage reaction does not show a strong sequence specificity although there is some preference for a C four nucleotides away on the 5' side of the break (Wang, 1985 and references therein). There is, however, a preference for DNA structure with single-stranded and negatively supercoiled DNA being substrates for the reaction but not relaxed double-stranded DNA (Liu and Wang, 1979). Also, in nicked double-stranded circular DNA, topoisomerase I cleavage occurs on the intact strand close to the nick (Dean and Cozzarelli, 1985). Synthetic single-standed DNA homopolymers can be cleaved by topoisomerase I (Depew *et al.*, 1978) and single-stranded oligonucleotides as small as seven bases (dA_7) are substrates (Tse-Dinh *et al.*, 1983). With dA_7 and dT_8, cleavage occurs between the fourth and fifth nucleotide from the 3' end. In the case of these small oligo's, addition of a denaturant is not required for cleavage to be detected since the region of the DNA 5' to the break is too short to be retained non-covalently (Tse-Dinh, 1986). The enzyme is still active in the covalent complex with the cleaved oligo's and

addition of DNA's possessing free 3' hydroxyls promotes an intermolecular ligation reaction with the enzyme-bound oligo's (Tse-Dinh, 1986). The DNA cleavage site on the *E. coli* enzyme has been probed with analogues of dT_8 containing single phosphorothioate substitutions in various positions (Domanico and Tse-Dinh, 1988).

E. coli topoisomerase I has been shown by atomic absorption spectroscopy to contain Zn^{2+} ions (Tse-Dinh and Beran-Steed, 1988). Three Zn^{2+} ions are thought to be present per molecule of enzyme and a structural motif has been suggested in which the Zn^{2+} ions are coordinated by four cysteines. Removal of the Zn^{2+} ions requires reversible chemical modification of the cysteine residues and the apoprotein is not active in DNA relaxation or in the cleavage of supercoiled DNA, although it can still form a non-covalent complex with DNA (Tse-Dinh, 1991). Interestingly Cd^{2+} can substitute for Zn^{2+} in reconstituting active enzyme from the apoenzyme and Cd^{2+} is bound tighter than Zn^{2+} as would be expected for metal coordination to cysteines *via* sulphur. The precise role of the Zn^{2+} ions remains to be elucidated.

E. coli topoisomerase I is specific for negatively supercoiled DNA and will not relax positively supercoiled DNA under normal circumstances (Wang, 1971). Furthermore, the rate of the relaxation reaction depends on the extent of supercoiling of the DNA and becomes very slow as the DNA becomes more relaxed such that the enzyme is not capable of completely relaxing the DNA template. Topoisomerase I binds very tightly to single-stranded DNA and consequently the addition of single-stranded DNA inhibits the relaxation of supercoiled DNA by the enzyme. The specificity for negatively supercoiled DNA probably reflects a requirement of the enzyme for DNA which is at least partially single-stranded; with highly negatively supercoiled DNA, the free energy associated with the linking number deficit destabilises the helix sufficiently to form a single-stranded region when topoisomerase I binds (Liu and Wang, 1979). Interestingly, many sites of cleavage by a topoisomerase I in a negatively supercoiled plasmid have also been found to

be sites for nuclease S1, a nuclease specific for single-stranded regions of DNA (Shishido *et al.*, 1983). The requirement for single-stranded regions of DNA has been elegantly demonstrated by the finding that topoisomerase I will relax positively supercoiled DNA containing a small deletion in one strand such that a single-stranded loop is present (Kirkegaard and Wang, 1985).

In addition to its relaxation activity, topoisomerase I from prokaryotes can perform several other topological interconversions of DNA. These include the intertwining and complete renaturation of two complementary single-stranded DNA circles (Kirkegaard and Wang, 1978), the catenation and decatenation of duplex DNA circles providing that one of the molecules contains a single-strand break (Tse and Wang, 1980), and the knotting and unknotting of single-stranded circles (Liu *et al.*, 1976) and duplex circles containing a single-strand break (Brown and Cozzarelli, 1981).

Mechanism of the relaxation reaction.

Two different mechanisms have been proposed to explain the action of topoisomerase I. In one mechanism, the end of the broken strand that is not covalently bound to the enzyme is free to rotate about the unbroken strand thus relaxing the DNA (Wang, 1971). This free rotation model was favoured until the discovery of the DNA catenation and knotting reactions of topoisomerase I described above. A new mechanism was suggested to explain all the reactions of topoisomerase I; in this model, known as the enzyme-bridging mechanism, the enzyme is attached to both ends of the broken strand with one end attached *via* the covalent phosphotyrosine bond and the other end held in place non-covalently. The unbroken DNA strand is passed through the enzyme stabilised gate in its complementary strand and the break is then resealed after strand passage, relaxing the DNA by a change in linking number of one (Brown and Cozzarelli, 1981). This model can easily accommodate the catenation and knotting reactions where the DNA translocated through the gap comes from a separate molecule (Dean and Cozzarelli, 1985).

Experimental data tends to support the enzyme-bridging model. For example, using high salt and only moderately negatively supercoiled DNA to make the enzyme function distributively, topoisomerase I was found to change the linking number of a single topoisomer by one (Brown and Cozzarelli, 1981). While this favours the enzyme bridging model it does not exclude a free rotation model where the free end is very efficiently recaptured after one turn. The fact that spontaneous breakage of single-stranded or nicked DNA's is not observed in the absence of denaturants (except with short oligo's) with topoisomerase I suggests that the enzyme interacts with both ends of the broken strand. In summary, therefore, the enzyme bridging model involving strand passage is the most likely mechanism for prokaryotic topoisomerase I, although a model involving some kind of strand rotation cannot be excluded.

E. coli topoisomerase III: another prokaryotic type I enzyme.

In topA deletion mutants of *E. coli* a weak residual topoisomerase I activity was observed which led to the isolation of another topoisomerase in addition to topoisomerase I (Pastorcic, 1982). Known rather confusingly as *E. coli* topoisomerase III (despite being a type I enzyme), it has been subsequently purified (Srivenugopal *et al.*, 1984), and the gene has been cloned and sequenced (Digate and Marians, 1989). The gene, termed the *topB* gene (the *topA* gene coding for *E. coli* topoisomerase I), codes for a protein of molecular weight ~70kDa. Although smaller than *topA*, the *topB* gene shows significant homology to the former. Most of the homology is concentrated in the middle of both proteins, with 24% identity and 48% similarity over a stretch of 308 amino acids which includes the active site tyrosine of topoisomerase I. There is also a similar level of homology between *E. coli* topoisomerase III and the gene product of TOP3 in the yeast *Saccharomyces cerevisiae* (Yanagida and Sternglanz, 1990) (see Section 1.2.2). Many of the enzymatic properties of topoisomerase III are similar to those of topoisomerase I such the the Mg^{2+} dependent relaxation of negative but not positively supercoiled DNA, and the preference for binding to single-stranded DNA. However, there are also significant

differences. For example, it appears that, unlike topoisomerase I, topoisomerase III is not essential for the growth of *E. coli* cells since a mutant with a deletion in the *topB* gene is still viable. Also it has been found that topoisomerase III is considerably more efficient at promoting decatenation *in vitro* than topoisomerase I, which has led to the suggestion that, *in vivo*, topoisomerase III may be primarily involved in the decatenation of daughter DNA circles after replication (DiGate and Marians, 1988).

Reverse gyrase: a type I enzyme that introduces positive supercoils into DNA.

Reverse gyrase was first isolated from the thermophilic archaebacterium *Sulfolobus* in 1984 (Kikuchi and Asai, 1984; Mirambeau *et al.*, 1984). It was found to be an ATP-dependent topoisomerase active only at high temperatures (between about 55°C and 95°C) which had the novel property of catalysing the introduction of positive supercoils into DNA as well as relaxing negatively supercoiled DNA. Originally described as a type II enzyme, it has subsequently been shown to operate by a type I mechanism (Nakasu and Kikuchi, 1985). Purification and structural studies of the enzyme have revealed it to be a monomer of molecular weight 120-128 kDa (Nadal *et al.*, 1988; Nakasu and Kikuchi, 1985). The ATPase of reverse gyrase is activated by DNA and this activation is apparently unaffected by the topological state of the DNA although single-stranded DNA is a better effector than double-stranded DNA (Shibata *et al.*, 1987). Single-stranded DNA is also a potent inhibitor of the topoisomerase activity of the enzyme on double-stranded DNA.

The role of reverse gyrase in archaebacteria remains to be discovered. It is not known with certainty whether the genome of *Sulfolobus* is positively supercoiled *in vivo* as a result of the activity of reverse gyrase. However, the DNA of a virus-like particle isolated from *Sulfolobus acidocaldarius* has been found to be in a positive superhelical state and, therefore, it has been suggested that the whole genome of this archaebacterium may be positively supercoiled (Nadal *et al.*, 1986). One possible advantage to

thermophilic organisms in having their DNA positively supercoiled is that this tightens up the helical pitch and therefore prevents denaturation of the double helix due to the extreme conditions. Thus the function of reverse gyrase may be to maintain the DNA of thermophilic archaebacteria in a positively supercoiled form (Kikuchi and Asai, 1984).

1.2.2. Eukaryotic Type I Topoisomerases

Protein structure and function.

Originally termed the DNA untwisting enzyme, the first eukaryotic type I topoisomerase was discovered in mouse cell extracts in 1972 (Champoux and Dulbecco, 1972). Type I topoisomerases have since been found in a variety of eukaryotes including *Drosophila* (Baase and Wang, 1974), HeLa cells (Liu and Miller, 1981), avian erythrocytes (Trask and Muller, 1983), yeast (Goto *et al.*, 1984), and humans (Vosberg *et al.*, 1975). The enzymes appear to be monomers in solution with molecular weights around 100kDa (Wang, 1985). Unlike their prokaryotic counterparts, the eukaryotic type I topoisomerases can relax both negatively and positively supercoiled DNA in a reaction that does not require Mg^{2+} or ATP (Champoux and Dulbecco, 1972). Although there are some similarities between the type I topoisomerases from prokaryotic and eukaryotic sources, these enzymes are fundamentally different and appear not to be evolutionarily related (D'Arpa *et al.*, 1988; Tse-Dinh and Wang, 1986).

Eukaryotic topoisomerase I has been found to give DNA strand breaks in double-stranded DNA after treatment with SDS, alkali, or low pH. Unlike the prokaryotic enzymes, there is no preference for supercoiled DNA, and relaxed DNA is also a substrate (Champoux, 1977b). Similar DNA cleavage is also observed with single-stranded DNA as a substrate (Been and Champoux, 1980; Prell and Vosberg, 1980). Interestingly, the eukaryotic type I topoisomerases become covalently attached to the 3' end of the broken DNA strand *via* a phosphotyrosine linkage (Champoux, 1978) rather than the 5' end as is the case with the prokaryotic enzymes. There are further differences in the cleavage reaction of

the two classes of type I enzyme; whereas the prokaryotic enzymes cannot cleave DNA without the addition of a denaturant (except with short oligo's), the eukaryotic enzymes can, under certain conditions, give rise to spontaneous strand breaks. For example, cleavage of single-stranded DNA can occur in low salt (Been and Champoux, 1980; Prell and Vosberg, 1980). Moreover, it has been demonstrated that the preferred cleavage sites occur in regions where the single-stranded DNA can form base-pairs suggesting that the enzyme interacts with a duplex region of DNA (Been and Champoux, 1984). The enzyme covalently bound to the 3'end of the DNA has been shown still to be active since addition of salt or Mg^{2+} results in recircularisation of the DNA (Been and Champoux, 1981). Furthermore, in the same way that short oligo's bound to prokaryotic topoisomerase I can be religated to different DNA molecules, the DNA-protein complexes formed in the breakage reaction of eukaryotic topoisomerase I can catalyse the joining of the broken strand to the end of a different DNA molecule containing a 5'-hydroxyl.

The active site tyrosine has been determined to be Tyr-727 for the topoisomerase I in the yeast *Saccharomyces cerevisiae* (Lynn *et al.*, 1989). Based on sequence homologies the active site tyrosines in *S. pombe* topoisomerase I and the human enzyme have been deduced to be Tyr 771 and Tyr 773 respectively. Thus it appears that the active site tyrosine is close to the C-terminal end of the eukaryotic topoisomerase I which contrasts to the prokaryotic enzyme where the tyrosine is located more in the middle of the protein sequence (Lynn *et al.*, 1989).

The eukaryotic type I topoisomerases tend to exhibit a slightly higher degree of sequence specificity in their DNA cleavage sites than the prokaryotic enzymes and a limited consensus sequence has been proposed (Champoux, 1990) as shown below:

-4 -3 -2 -1

5'-(A or T)-(G or C)-(A or T)-T-3'

The 3'-T residue at the -1 position is the nucleotide to which the enzyme is attached. There is no obvious preference for bases 3' to the break site. This consensus is not absolute for all eukaryotic type I enzymes and, in addition, the position of a particular cleavage site on the DNA seems to be important. The basis for the observed weak cleavage site preference is not understood and it does not always correlate with the strength of binding of the enzyme to the DNA. It has been suggested that the lack of a strong DNA sequence specificity in both prokaryotic and eukaryotic topoisomerase I has been selected for by evolution so as not to restrict access of these enzymes to the DNA (Champoux, 1990).

As already pointed out, one of the striking differences between the eukaryotic and prokaryotic type I topoisomerases is the ability of the former to catalyse the relaxation of both negatively and positively supercoiled DNA (Champoux and Dulbecco, 1972). (Indeed this is the basis for the use of a eukaryotic topoisomerase I in the preparation of a family of topoisomers of various linking numbers in Section 2.20). Furthermore, the eukaryotic enzyme is able to relax the DNA completely (Pulleyblank *et al.*, 1975). The enzyme does not bind strongly to single-stranded DNA which does not therefore inhibit the topoisomerisation reaction.

In addition to their relaxation activity, eukaryotic type I topoisomerases can promote several other DNA topological interconversions characteristic also of prokaryotic type I enzymes. These reactions include the intertwining and complete renaturation of two complementary single-stranded DNA circles (Champoux, 1977a), and the catenation and decatenation of duplex DNA circles providing that one of the molecules contains a single-strand break (Brown and Cozzarelli, 1981). Unlike the prokaryotic enzymes, knotting of single-stranded DNA circles or double-stranded nicked or gapped circular DNA has not been demonstrated with eukaryotic topoisomerase I (Champoux, 1990).

Eukaryotic type I topoisomerases have been found to be subject to covalent modifications that affect their DNA relaxing activities (reviewed in Higgins *et al.*, 1990). Several type I enzymes have been found to be more active when phosphorylated by a protein kinase and, in the case of a topoisomerase I from *Xenopus* ovaries, the activity appears to be dependent on enzyme phosphorylation (Kaiserman *et al.*, 1988). It is not known how important phosphorylation is *in vivo* but the findings of Bjornsti and Wang (1987) that yeast topoisomerase I can be cloned and expressed in *E. coli* implies that phosphorylation is not essential for all eukaryotic type I topoisomerases. Calf-thymus DNA topoisomerase I has been found to be a good substrate for poly(ADP-ribose) synthetase which covalently attaches a poly(ADP-ribose) chain to the topoisomerase. This modification inhibits DNA relaxation by the enzyme (Ferro and Olivera, 1984) probably by decreasing the ability of the enzyme to bind to DNA; each ADP-ribose unit added to the chain on the enzyme has two negative charges and therefore decreases the affinity of the protein for DNA by electrostatic repulsion (Higgins *et al.*, 1990). Interestingly, poly(ADP-ribose) synthetase is activated by DNA which contains single or double-strand breaks, and it has been suggested that the role of poly(ADP-ribosylation) *in vivo* is to protect nicked or single strand gapped DNA produced by DNA damage or during replication from breakage by topoisomerase I (Ferro and Olivera, 1984).

Eukaryotic type I topoisomerases have been identified as the primary target of the antitumour plant alkaloid, camptothecin (reviewed in Liu, 1990). The drug appears to bind to the topoisomerase-DNA complex and inhibits reclosure of the DNA in the relaxation reaction (Hsiang *et al.*, 1985). It has been suggested that the main effects of camptothecin *in vivo* are the inhibition of DNA and RNA synthesis by blocking the progress of the replication fork and RNA polymerase respectively (Hsiang *et al.*, 1989).

Mechanism of the relaxation reaction.

The two possible mechanisms for type I topoisomerases were discussed for the prokaryotic enzymes in the previous section and it was concluded that these enzymes probably operate *via* the enzyme-bridging model and not *via* free strand rotation. For the eukaryotic type I enzymes, the free rotation model cannot be discounted. While it seems attractive to postulate a similar mode of action for all type I topoisomerases there are clearly differences in the properties of the enzymes from prokaryotic and eukaryotic sources. Champoux (1990) has argued in favour of a free rotation model for eukaryotic topoisomerase I enzymes on the basis of the following points. Firstly, there is no evidence that these enzymes interact with the end of the broken strand that is not covalently bound to the active site tyrosine. Secondly, the failure to observe DNA knotting in single-stranded or nicked duplex DNA circles is compatible with the free rotation model. Thirdly, it is possible that the catenation of nicked duplex DNA molecules can occur without a strand-passage mechanism; the enzyme has been shown to spontaneously break nicked duplex DNA circles in the strand opposite the pre-existing nick to generate linear molecules (McCoubrey and Champoux, 1986), and recircularisation of the DNA under conditions which favour DNA aggregation (which are required for the catenation reaction) could entrap other DNA circles to produce catenanes. It is possible, however, that type I enzymes all operate *via* an enzyme-bridging mechanism which differs in many details for the prokaryotic and eukaryotic enzymes, such as the level of interaction of the protein with the non-covalently bound end of the DNA, and the degree of coupling of the strand passage and religation events. It is interesting that, despite the obvious differences between prokaryotic and eukaryotic type I topoisomerases, yeast topoisomerase I will complement a lethal mutant of topoisomerase I in *E. coli* (Bjornsti and Wang, 1987). Thus it appears that the two enzymes can perform the same function in a prokaryotic environment.

Yeast topoisomerase III: another eukaryotic type I enzyme.

Recently a gene, *TOP3*, has been identified in *S. cerevisiae* that probably encodes a second type I topoisomerase which has been termed DNA topoisomerase III (Wallis *et al.*, 1989). Mutations in this gene increase recombination between short repetitive sequences, termed δ sequences, and give a reduction in growth rate. Sequencing of the gene has revealed an open reading frame coding for a protein of 656 amino acids that shows good homology with *E. coli* DNA topoisomerase I but not with any eukaryotic topoisomerase. A three-way comparison of the *TOP3* gene product and *E. coli* topoisomerase I and III has revealed that the proteins are all roughly equally related (Yanagida and Sternglanz, 1990). To date, the gene product, yeast topoisomerase III, has not been detected and therefore the *in vivo* role of the enzyme awaits clarification.

1.2.3. DNA Gyrase (Prokaryotic Type II Topoisomerase)

Introduction.

Since its discovery in *E. coli* in 1976 (Gellert *et al.*, 1976a), DNA gyrase has been identified in many other prokaryotes, examples of which are given in Table 1.1. The enzyme is a type II topoisomerase that catalyses the negative supercoiling of closed-circular DNA by coupling this reaction to the hydrolysis of ATP (for a recent review see Reece and Maxwell, 1991b). In addition to the supercoiling reaction, gyrase has been shown to promote several other topological interconversions of DNA such as the nucleotide-independent relaxation of negatively supercoiled DNA (Gellert *et al.*, 1977; Sugino *et al.*, 1977), the catenation and decatenation of two duplex circles, and the knotting and unknotting of duplex DNA (Kreuzer and Cozzarelli, 1980; Mizuuchi *et al.*, 1980). These reactions will be discussed in detail later on but it is relevant to note here that it is likely that all of the above reactions are a consequence of the same mechanism occurring with different substrates or under different conditions.

Table 1.1. Characteristics of DNA gyrase genes from different organisms (based on Reece and Maxwell, 1991b).

Organism	Gram type	Gene	Length of gene (bp)	Distance between genes (bp)	Amino acids in protein	Size of protein (kDa)	Reference
Escherichia	-	*gyrA*	2625	~1.5 X 10^6	875	97	i
coli		*gyrB*	2412		804	90	ii
Citrobacter	-	*gyrA*				107	iii
freundii		*gyrB*				96	
Pseudomonas	-	*gyrA*				~400[a]	iv
aeruginosa		*gyrB*					
Klebsiella	-	*gyrA*	2628		876	97	v
pneumoniae		*gyrB*					
Borrelia	-	*gyrA*	2430	14	810	90	vi
burgdorferi		*gyrB*	1917		639	71	
Mycoplasma	-	*gyrA*		1 bp overlap			vii
pneumoniae		*gyrB*	1953		650	72	
Haloferax	-	*gyrA*		1			viii
		gyrB	1920		640	71	
Bacillus subtilis	+	*gyrA*	2463	214	821	92	ix
		gyrB	1914		638	71	
Micrococcus	+	*gyrA*				115	x
luteus		*gyrB*				97	
Staphylococcus	+	*gyrA*	2667	39	889	100	xi
aureus		*gyrB*					xii
Streptomyces	+	*gyrA*		>3000			xiii
sphaeroides		*gyrB*				79[b]	

Notes:

[a]Molecular weight of intact gyrase complex

[b]Resistance gene cloned

References:

i. Swanberg and Wang (1987)
ii. Yamagishi *et al.* (1986)
iii. Aoyama *et al.* (1988)
iv. Miller and Scurlock (1983)
v. Dimri and Das (1990)
vi. W.M. Huang (unpublished data)
vii. Colman *et al.* (1990)
viii. Holmes and Dyall-Smith (1991)
ix. Moriya *et al.* (1985)
x. Liu and Wang (1978b)
xi L.M. Fisher (unpublished data)
xii. Hopewell *et al.* (1990)
xiii. Thiara and Cundliffe (1988)

Genetic data.

Gyrase is composed of two proteins, GyrA and GyrB. Before the discovery of gyrase, the two genes that encode the GyrA and GyrB proteins had been already identified as genetic loci determining resistance to the DNA synthesis inhibitors, nalidixic acid and coumermycin, and they were known therefore as *nalA* and *cou*, respectively. With the discovery that *nalA* coded for the GyrA protein and *cou* encoded the GyrB protein, the genes have been renamed *gyrA* and *gyrB*, accordingly.

The gyrase genes from several different organisms have been identified and in some cases the genes have been sequenced (see Table 1.1). In many cases the *gyrA* and *gyrB* genes are close to each other in the genome, with the notable exception of the *E. coli* genes which are separated from each other by over a megabase. The *gyrA* and *gyrB* genes in *E. coli* have been found to encode proteins of 875 and 804 amino acids with molecular weights of 97 and 90 kDa respectively, which is in agreement with the predicted molecular weights from SDS-polyacylamide gels (Mizuuchi *et al.*, 1978). The *E. coli* gyrase proteins have been purified to near homogeneity (Higgins *et al.*, 1978) and both the genes have been cloned into various plasmid vectors to allow their over-production (Hallett *et al.*, 1990; Horowitz and Wang, 1987; Mizuuchi *et al.*, 1984).

Structure of the protein and its complex with DNA.

Biochemical evidence.

Gyrase is thought to be active as a tetrameric A_2B_2 complex. Early evidence in favour of such a complex was obtained from an experiment where a gyrase-DNA complex, isolated from a mixture of gyrase proteins and DNA by gel filtration, was found to contain approximately equal amounts of GyrA and GyrB (Sugino *et al.*, 1980). At around the same time, experiments involving sedimentation analysis of *M. luteus* gyrase complexed with DNA fragments of about 140 bp showed that a particle of 470 kDa was formed which suggests that an A_2B_2 complex is bound to the DNA (Klevan and Wang, 1980).

The complex was found to contain roughly equal proportions of A and B proteins by SDS-PAGE. Cross-linking experiments on the gyrase-DNA complexes using dimethyl suberimidate gave species of molecular weights 420 kDa, 330 kDa, and 230 kDa as determined by SDS-PAGE. These species were tentatively assigned as A_2B_2, A_2B, and A_2 complexes respectively; cross-linking of the purified A protein yielded the 230 kDa species, while the purified B protein gave no cross-linked products (Klevan and Wang, 1980). Recently, a molecular weight of 353 kDa for gyrase from *E. coli* has been calculated from small angle neutron scattering experiments (Krueger *et al.*, 1990). This value again suggests that an A_2B_2 complex is prevalent; the difference between apparent molecular weights of the *E. coli* enzyme complex and that of *M. luteus* is consistent with the different apparent sizes of the A and B subunits from these species as shown in Table 1.1. Despite these apparent different sizes, the A and B proteins from *E. coli* and *M. luteus* can be mixed to give active chimeric gyrases (Brown *et al.*, 1979).

The nature of the gyrase-DNA complex was first investigated by Liu and Wang (1978b). They incubated *M. luteus* DNA gyrase with nicked-circular DNA in the absence of ATP and found that, after sealing with DNA ligase, the DNA was positively supercoiled. This suggested that the DNA was wrapped around gyrase in a positive superhelical sense; specifically a positive linking difference of between 0.4 to 0.6 was introduced into the DNA per gyrase molecule. More recent experiments on the *E. coli* enzyme have given a positive linking difference of 0.8 per gyrase molecule (Reece, 1990).

Supporting evidence that DNA wraps around gyrase came from digestion of gyrase-DNA complexes (formed with nicked-circular DNA and enzyme from either *E. coli* or *M. luteus*) with staphylococcal nuclease and pancreatic DNase I (Liu and Wang, 1978a). It was found that gyrase protected a region of about 140 bp from digestion with the staphylococcal nuclease. Digestion with DNase I gave a family of single-stranded DNA segments differing in length by about 10 bp. Both the length of the nuclease-resistant

DNA segment and the periodicity of the enhanced DNase I sites imply that the DNA is wrapped around the enzyme.

A general picture of the topography of gyrase-DNA complexes has emerged from further nuclease protection experiments with short DNA molecules (Fisher *et al.*, 1981; Kirkegaard and Wang, 1981; Morrison and Cozzarelli, 1981; Rau *et al.*, 1987). These experiments are consistent with a model in which gyrase binds to, and protects, a region of DNA of 100-155 bp. A central region of 40-50 bp, containing the site of DNA cleavage, is most strongly protected, and the DNA flanking this region shows sites of enhanced sensitivity to DNase I at regular intervals of 10-11 bp characteristic of DNA bound to a protein surface. Interestingly, gyrase apparently affords no protection towards methylation of the DNA by dimethyl sulphate which suggests that the entire DNA segment that is wrapped around the protein is accessible to solvent (Kirkegaard and Wang, 1981).

The gyrase-DNA complex is very stable and, at 23°C a half-life of 60-70 hours has been reported (Higgins and Cozzarelli, 1982). Relaxed or linear DNA appears to be bound more strongly than supercoiled DNA as determined by retention of gyrase-DNA complexes on nitrocellulose membranes (Higgins and Cozzarelli, 1982). It appears that single-stranded DNA is not bound by gyrase (Maxwell and Gellert, 1986). Maxwell and Gellert (1984) have shown that the ability of gyrase to bind to linear DNA depends on the length of the DNA fragment. They showed that gyrase will form filter-stable complexes with DNA's of 117 bp or larger but will only form a complex with a 55 bp fragment at high DNA concentrations. The binding curve for gyrase and the 55 bp fragment was consistent with at least two DNA molecules binding to gyrase in a cooperative manner. Therefore, gyrase may contain two, or more, DNA binding sites (Maxwell and Gellert, 1984; Maxwell *et al.*, 1986).

Although no high resolution X-ray structure for the A_2B_2 complex exists, there is good evidence for both subunits being composed of discrete folded domains (see Fig. 1.3). The first indications of such a domain structure came from the observation that a 50 kDa protein with some similarities to GyrB was present in cell extracts containing gyrase. This protein (termed B' or ν) was purified and found to form a complex with GyrA which could not supercoil DNA but had the ability to relax both negative and positive supercoils (Brown *et al.*, 1979; Gellert *et al.*, 1979). Sequencing of GyrB has revealed that B' is a C-terminal fragment of GyrB extending from residue 394 to the C-terminus (Adachi *et al.*, 1987). These findings suggested that the ATPase activity of the B protein resides in the N-terminal part of the protein, a hypothesis which has been confirmed by the cloning of the N-terminal GyrB fragment as a direct gene product (Jackson *et al.*, 1991) and the demonstration that it has a novobiocin-sensitive ATPase activity (see ATPase section later on). Thus the N- and C-terminal halves of the GyrB protein probably represent domains of the protein.

The domain structure of the gyrase A protein has been examined by limited proteolysis. It was found that treatment of GyrA with either trypsin or chymotrypsin generates two fragments of molecular weights 64 kDa and 33 kDa which are relatively stable to further digestion (Reece, 1990; Reece and Maxwell, 1989). The 64 kDa fragment was found to support a low rate of DNA supercoiling in the presence of GyrB. It was also found to support quinolone-directed DNA cleavage as efficiently as the intact A protein. The 33 kDa fragment did not support any of the reactions of gyrase but was found to enhance the supercoiling activity of the 64 kDa protein (Reece and Maxwell, 1989; Reece and Maxwell, 1991a). Both the 64 kDa and 33 kDa proteins have been expressed as gene products (Reece and Maxwell, 1991a; Reece and Maxwell, 1991c). The 33 kDa fragment, on its own, has been shown to bind DNA. Unlike the intact A_2B_2 enzyme or GyrA alone, the binding of DNA by the 33 kDa fragment does not require Mg^{2+} ions. It has been proposed that the 64 kDa protein represents the DNA breakage-reunion domain

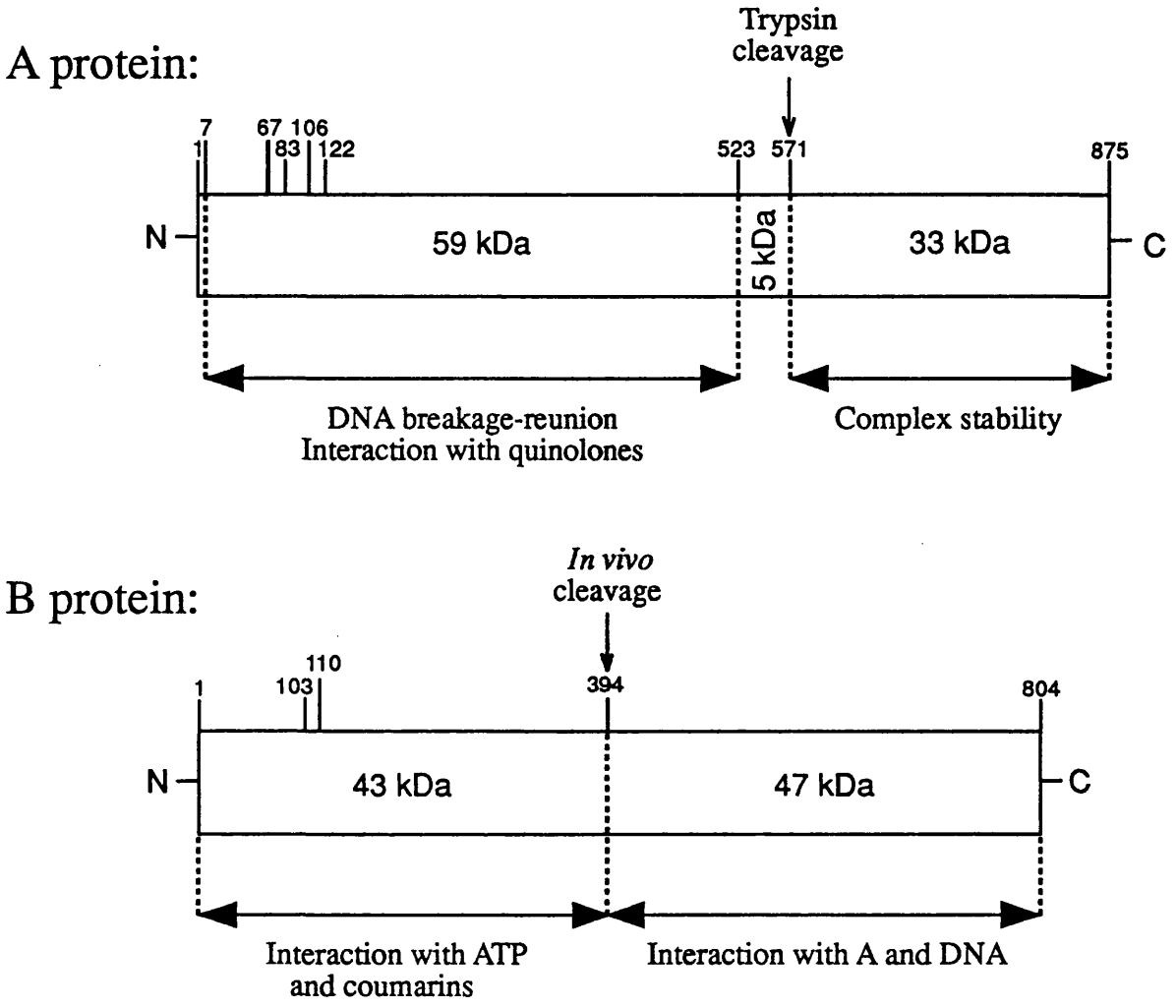

Figure 1.3. Proposed domain organisation of *E. coli* DNA gyrase (based on Reece and Maxwell, 1991b).

and the 33 kDa protein represents a non-specific DNA-binding domain which contributes to the wrapping of DNA around gyrase (Reece and Maxwell, 1989; Reece and Maxwell, 1991a).

Further evidence for the existence of structural domains within the gyrase proteins has been obtained from differential scanning microcalorimetry which measures the heat required to unfold a protein. Both the gyrase A and B proteins show two thermal unfolding transitions which correspond to the unfolding of individual domains and have been assigned by comparison with the thermal unfolding of the individually expressed domains described above (A. P. Jackson, R. J. Reece, A. Maxwell, P. M. Cullis, personal communication).

Low resolution biophysical approaches.

A number of groups have analysed gyrase and its DNA complex by electron microscopy (Kirchhausen *et al.*, 1985; Lother *et al.*, 1984; Maxwell *et al.*, 1989; Moore *et al.*, 1983; Rau *et al.*, 1987). These experiments have indicated that the gyrase tetramer is a roughly spherical particle with a diameter of approximately 150-250 Å. At high magnification, these particles have been interpreted as having a heart-shaped structure with the A subunits forming the upper lobes of the heart. Estimates of the amount of DNA associated with the protein vary between about 100 bp to 160 bp (Kirchhausen *et al.*, 1985; Maxwell *et al.*, 1989). This is in reasonable agreement with the nuclease protection data described above. Some caution should be applied in the interpretation of electron microscopy data since the size of the gyrase particles are close to the limit of resolution. For example the heart-shaped structure for gyrase only becomes apparent after image processing.

Complexes between gyrase and linear DNA fragments, ranging in size from 127 to 256 bp, have been analysed by transient electric dichroism (Rau *et al.*, 1987). This technique

can monitor the three-dimensional structure of DNA and its complexes. These experiments suggest that a single turn of DNA is wrapped around the enzyme with the entry and exit points close together. The angle between the DNA tails emerging from the complex appears to be about 120°. In the presence of the non-hydrolysable ATP analogue ADPNP (which is known to support limited DNA supercoiling by gyrase; see ATPase section) a change in the dichroism of the complexes with 172 and 207 bp DNA fragments were observed while no dichroism change was seen for a complex with a 127 bp DNA fragment. This was interpreted in terms of a conformational change occurring on nucleotide binding which results in the DNA tails becoming wrapped around the protein (Rau *et al.*, 1987).

Small angle neutron scattering and dynamic light scattering has indicated that the gyrase tetramer is a flattened sphere with a diameter of about 175 Å and a thickness of about 50 Å which could appear heart-shaped when viewed from certain angles (Krueger *et al.*, 1990). The size and shape of the particle does not appear to change significantly on binding DNA and it has therefore been suggested that the wrapped DNA may be somewhat embedded in the protein. The measured radius of gyration of the gyrase tetramer was found to be about 65 Å which is bigger than that expected for a globular protein of 400 kDa (~43 Å). This difference suggests that gyrase may contain cavities or channels within its structure that are accessible to solvent (Krueger *et al.*, 1990). The existence of such channels could provide a route for the passage of a segment of DNA through part of the protein structure during the supercoiling reaction.

Crystallography.

The first crystals of gyrase to be reported were two-dimensional crystals of the B protein grown on a lipid monolayer to which novobiocin was bound (Lebeau *et al.*, 1990). However, these crystals only diffracted to 27 Å resolution and little structural information was obtained. Crystallisation of fragments of the A and B proteins has been more

successful (Jackson *et al.*, 1991; Reece *et al.*, 1990). The 64 kDa N-terminal fragment of the GyrA protein, comprising the breakage-reunion domain of gyrase (see above), has been crystallised and the crystals have been found to diffract to 4.5 Å resolution (Reece *et al.*, 1990). In addition, the 43 kDa N-terminal fragment of GyrB, comprising the ATP binding site of gyrase, has been crystallised in the presence of ADPNP and the crystals have been found to diffract to high resolution (Jackson *et al.*, 1991; Wigley *et al.*, 1991). The structure of this protein fragment has been solved at 2.5 Å resolution (Wigley *et al.*, 1991) and is a dimer with one molecule of ADPNP bound to each monomer (Fig. 1.4). Within each 43 kDa monomer there appears to be two domains: an N-terminal domain (domain 1, comprising residues 2-220) which contains the bound ADPNP, and a C-terminal domain (domain 2, comprising residues 221-392). Most of the contacts between the two protein molecules in the dimer are formed by the N-terminal domains. One of the most notable features of this interaction is an N-terminal arm which reaches across from one monomer to interact with the other protein molecule of the dimer. Interestingly, one of these contacts involves Tyr 5 on the arm interacting with the 2' hydroxyl of the ribose ring of the nucleotide bound to the other monomer. The C-terminal domains form the sides of a hole through the protein dimer which is approximately 20 Å wide. Every arginine residue in domain 2 protrudes into this hole which may be involved in binding to a section of DNA translocated through gyrase during DNA supercoiling (Wigley *et al.*, 1991).

It may be possible, in future, to crystallise the C-terminal domains of the A and B proteins. If structures can be determined for these fragments together with the N-terminal domain of the A protein, then it may be possible to piece together the structure of the intact gyrase tetramer.

Figure 1.4. Diagram of the crystal structure of the N-terminal fragment of the gyrase B protein containing bound ADPNP based on the coordinates of Wigley *et al* (1991). The figure shows the C_α-backbone of the protein in a ribbon diagram emphasising the α-helices and β-sheets. The two identical subunits are shown in red and yellow respectively and space-filling representations of the bound ADPNP molecules are shown in pink and blue. Each subunit consists of two domains; the N-terminal domain (domain 1) is shown in the bottom half of the figure while the C-terminal domain (domain 2) is towards the top of the figure; this orientation of the structure has been chosen to facilitate correlation of this protein fragment to the overall gyrase structure modelled in Fig. 1.5. The figure was generated on computer graphics by Mike Sutcliffe, Biological NMR Centre, this University.

A model for the gyrase-DNA complex.

A model for the gyrase-DNA complex based on the various lines of evidence reviewed above has been suggested by (Reece and Maxwell, 1991b) and is shown in Fig. 1.5. The model emphasises the wrapping of the DNA around the protein, the presence of solvent-filled channels, and the domain organisation of the proteins. The overall shape of the gyrase particle is based on Krueger *et al.* (1990), and the B protein is depicted as bean-shaped according to Lebeau *et al.* (1990). The shape of the A protein and the individual domains within both proteins is arbitrary.

The DNA cleavage site of the enzyme is shown in the centre of the wrapped DNA. It is known that gyrase cleaves both strands of DNA with a four-base stagger between the single-stranded breaks, and that tyrosine 122 in the A protein becomes covalently joined to the 5' end of the strand breaks (see DNA cleavage section). If the wrapped DNA is in the B form, with a helical pitch of about 10.5 bp per turn, then the cleavage of the two strands will occur roughly on the same side of the double helix as shown in the figure.

Reactions of gyrase.

DNA supercoiling and relaxation.

The DNA supercoiling reaction requires ATP and a divalent cation (usually Mg^{2+} but see Chapter 5). In addition to its requirement for ATP hydrolysis, the Mg^{2+} is required for DNA-binding. The supercoiling reaction is also stimulated by spermidine (Gellert *et al.*, 1976a). Incubation of gyrase with a single purified DNA topoisomer has indicated that the enzyme alters the linking number in steps of two, identifying gyrase as a type II topoisomerase (Brown and Cozzarelli, 1979; Mizuuchi *et al.*, 1980). Mechanistically this has been interpreted in terms of the translocation of a DNA segment through a double-stranded DNA break.

Gyrase can negatively supercoil relaxed DNA in a processive manner, i.e. it can perform several catalytic cycles without dissociating from the DNA (as evidenced on an agarose gel by the appearance of fully supercoiled products in the presence of mainly fully relaxed DNA) (Gellert *et al.*, 1976a; Morrison *et al.*, 1980). Under conditions of high salt, which favour protein dissociation from DNA, the supercoiling reaction appears much more distributive. The turnover number for negative supercoiling by gyrase has been estimated to be about one per second (Higgins *et al.*, 1978).

pBR322 isolated from *E. coli* cells is found to have a specific linking difference of about -0.06 which corresponds to a linking number deficit of 25. However, the maximum specific linking difference achievable by gyrase is -0.11 which corresponds to a linking number deficit of 46 or 47 for pBR322 (Bates and Maxwell, 1989; Gellert *et al.*, 1976a; Westerhoff *et al.*, 1988). The *in vivo* level of supercoiling may reflect the antagonistic actions of topoisomerase I and gyrase (Sternglanz *et al.*, 1981).

The non-hydrolysable ATP analogue ADPNP is a potent inhibitor of ATP-dependent negative supercoiling by gyrase. In addition it can support limited DNA supercoiling by gyrase; incubation of relaxed DNA with high levels of gyrase in the presence of ADPNP gives a ΔLk of -0.6 per gyrase tetramer (Sugino *et al.*, 1978). This suggests that nucleotide binding to gyrase is sufficient to allow one supercoiling event but that hydrolysis of ATP is required for multiple enzyme turnover. This would predict that the supercoiling by ADPNP should be stoichiometric to the amount of enzyme present (i.e. a ΔLk of -2 per gyrase tetramer should be seen). The fact that the observed supercoiling is less than that expected may be due to a proportion of inactive enzyme (see Appendix I) or to a degree of uncoupling between nucleotide binding and DNA strand-passage.

In the absence of ATP, but in the presence of Mg^{2+}, gyrase relaxes negatively supercoiled DNA but not positively supercoiled DNA. The relaxation reaction is less

efficient than DNA supercoiling with about 20-40 times as much enzyme being required for a comparable rate (Gellert *et al.*, 1979; Higgins *et al.*, 1978). Relaxation of positive supercoils requires ATP and is thought to be mechanistically analogous to negative supercoiling. Interestingly, ADPNP will support catalytic relaxation of positive supercoils (Gellert *et al.*, 1980). Since relaxation of negatively supercoiled DNA is nucleotide-independent but relaxation of positive supercoils is nucleotide-dependent, nucleotide binding may determine the direction of the strand-passage reaction possibly by stabilising an appropriate conformation of the enzyme (see also discussion of energy transduction in gyrase in Section 1.3).

Catenation, decatenation, knotting and unknotting of DNA.

Gyrase can catalyse the formation and resolution of DNA catenanes and can knot and unknot duplex DNA circles (Kreuzer and Cozzarelli, 1980; Mizuuchi *et al.*, 1980). These reactions require ATP although no such requirement would be predicted on energetic grounds. Apparently ADPNP will not support gyrase-catalysed decatenation (R. J. Reece, P. Hallett, and A. Maxwell, personal communication), and it is possible that these reactions proceed *via* a mechanism similar to supercoiling where ATP hydrolysis ensures efficient strand passage (except that in the reactions with catenanes and knots, the translocated strand is part of a different DNA molecule to the one wrapped around gyrase). If the reaction were to proceed *via* the relaxation pathway it may be too slow to detect (Reece and Maxwell, 1991b).

DNA cleavage.

E. coli gyrase induces the double-stranded cleavage of DNA if a reaction is carried out in the presence of a quinolone antibiotic (such as nalidixic acid, oxolinic acid, or ciprofloxacin) and if it is terminated by the addition of a protein denaturant such as SDS (Gellert *et al.*, 1977; Sugino *et al.*, 1977). Linear, relaxed, and supercoiled DNA are all substrates for cleavage (Sugino *et al.*, 1977) but the cleavage of single-stranded DNA has

not been reported which is consistent with the observation that single-stranded DNA is not bound (Maxwell and Gellert, 1986). Cleavage does not require ATP, although ATP or ADPNP can affect the efficiency of cleavage at different sites (Fisher *et al.*, 1981; Sugino *et al.*, 1978).

DNA cleavage by gyrase leads to the generation of free 3'-hydroxyl termini with the 5'-phosphoryl termini being covalently bound to the A protein *via* a tyrosine residue (Sugino *et al.*, 1980; Tse *et al.*, 1980). The specific tyrosine involved has been identified as Tyr 122 by using uniformly radiolabelled DNA in a cleavage reaction, followed by proteolytic digestion of the protein and sequencing of the labelled peptides (Horowitz and Wang, 1987).

The site of DNA cleavage generally occurs near the centre of the region protected from nuclease attack (Fisher *et al.*, 1981; Kirkegaard and Wang, 1981; Morrison and Cozzarelli, 1981). The DNA sequence specificity of oxolinic acid-directed cleavage by gyrase of pBR322 *in vivo* has been examined (Lockshon and Morris, 1985). From a comparison of 19 different cleavage sites within the plasmid, a consensus sequence was proposed as shown below:

$$5'\text{-RNNNRNRT}\underset{(G)}{\overset{}{\vdots}}\text{GRYC}\overset{T}{\underset{G}{}}\text{YNYNGNY-3'}\quad\quad(T)$$

N represents any nucleotide, R is a purine, and Y is a pyrimidine. The line indicates the position of cleavage (i.e. between the 8^{th} and 9^{th} positions). T and G at the 13^{th} position are equally preferred and the G and T in brackets are preferred secondarily to the nucleotides in the sequence at these positions. Although the above consensus sequence has many degeneracies, there is some indication of dyad symmetry about an axis midway between the cleavage sites in opposite strands and this consensus sequence is generally

consistent with cleavage sites mapped *in vitro* (Fisher *et al.*, 1981; Kirkegaard and Wang, 1981; Morrison and Cozzarelli, 1979). The major site of quinolone-induced cleavage in pBR322 has been studied in detail (Fisher *et al.*, 1986) and the sequence is shown below:

5'-GGCTGGAT ⋮ GGCCTTCCCCAT-3'
990

It has been shown that mutations at this site can reduce or abolish the cleavage activity. Furthermore, it has been shown that a 34 bp linear fragment containing this cleavage site is not a substrate for the reaction but becomes a substrate if the sequence is extended by 85 bp in either direction. Thus it appears that a certain amount of flanking sequence is required for cleavage to occur and this may reflect the length of DNA required to form a gyrase-DNA complex (Maxwell and Gellert, 1984). In a separate investigation of the gyrase cleavage reaction, a family of linear 147 bp DNA fragments was prepared containing the preferred gyrase cleavage site from pBR322 in different positions (Dobbs *et al.*, in press). It was found that the same cleavage sequence was preferred regardless of its position within the DNA fragment even when the cleavage site was very close to either end of the DNA (i.e. 15 or 16 bp from either end). Thus it would seem that significant flanking sequence is only required on one side of the cleavage site.

In vivo treatment of *E. coli* cells with oxolinic acid and subsequent addition of SDS leads to the formation of DNA fragments of approximately 100 kb (Bejar and Bouche, 1984; Snyder and Drlica, 1979). This gives about 50 major cleavage sites in the whole *E. coli* genome which corresponds to about one cleavage site per topological domain within the chromosome (Snyder and Drlica, 1979). A large number of weaker sites also exist; for example, in a 10 kb region of the chromosome, 24 cleavage sites were found. Projected over the entire genome this would give over 10,000 cleavage sites of which less than 0.5% have been identified as major cleavage sites (Franco and Drlica, 1988). One explanation for observed frequencies of major and minor cleavage sites, assuming that

Figure 1.5. Proposed structure of the gyrase-DNA complex based on Reece and Maxwell (1991b). In part (a), the DNA is shown as a shaded loop wrapped around the A_2B_2 gyrase complex. The two GyrA proteins are in the upper part of the model and the GyrB proteins are in the lower part; the amino and carboxy domains of these proteins are indicated by -N and -C. The black dots represent the sites of covalent attachment of the DNA to the protein during DNA cleavage. In part (b), a transverse view of the model in part (a) is shown.

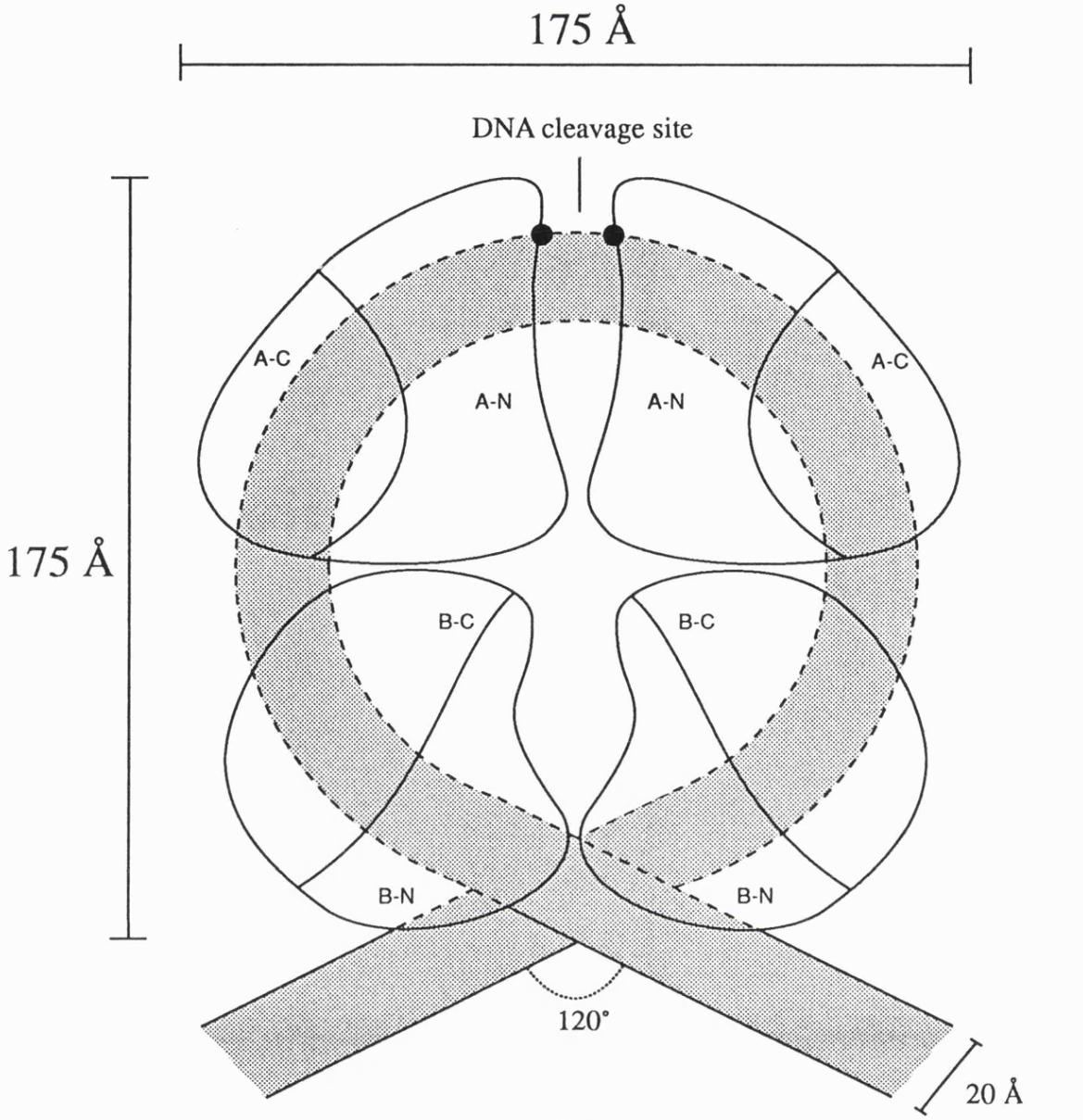
175 Å
DNA cleavage site
175 Å
A-C
A-N
A-N
A-C
B-C
B-C
B-N
B-N
120°
20 Å

(a)

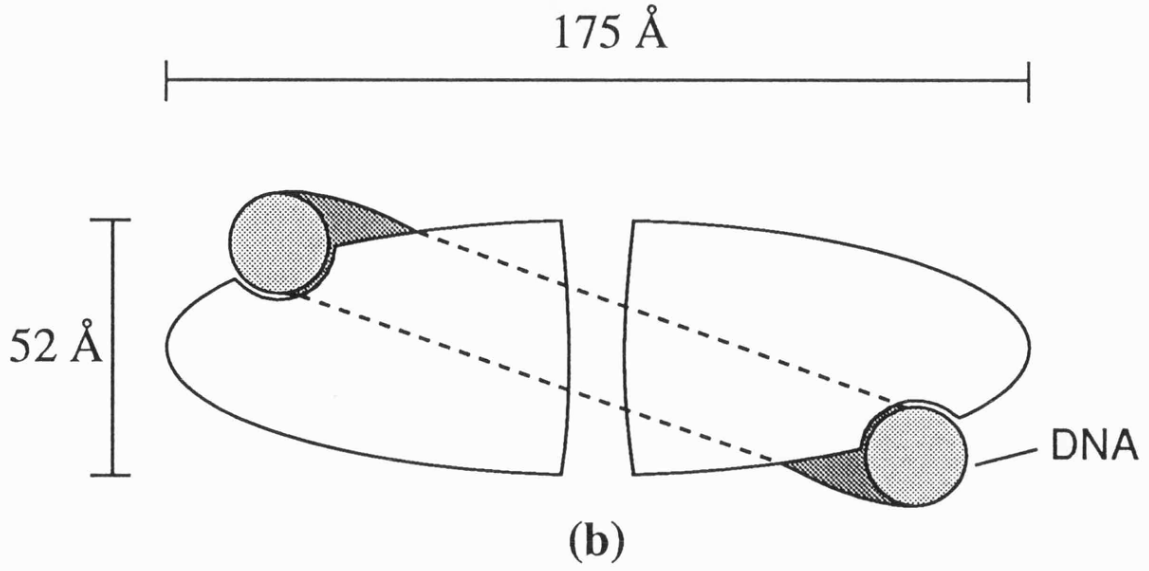
175 Å
52 Å
DNA

(b)

they represent most of the places where gyrase interacts with the DNA, is that a small number of specific strong interaction sites are used by gyrase to maintain the overall superhelical tension in the chromosome, and the weaker dispersed sites allow gyrase to provide the localised swivelling needed for DNA transcription and replication (Drlica and Coughlin, 1989) (see Section 1.2.6).

The chemical structure of some of the more common quinolones is shown in Fig. 1.6. (a). In addition to causing DNA cleavage to occur after treatment with SDS, the quinolones are potent inhibitors of both DNA supercoiling and relaxation (Gellert *et al.*, 1977). Their mode of action in causing cleavage is not fully understood but it has generally been assumed that quinolone-directed cleavage occurs at the same sites as the DNA breakage involved in the normal supercoiling reaction of gyrase; the effect of quinolones appears to prevent (or retard) the DNA reclosure step (Liu, 1990). In the supercoiling reaction, the mechanism of DNA reclosure following cleavage is not known since there is no experimental evidence to suggest how this reaction occurs. However, if samples are briefly heated to 80°C before the addition of SDS in a quinolone-directed cleavage reaction, the supercoiled substrate remains intact which suggests that either cleavage occurs only after SDS addition, or, more probably, that the broken DNA ends are more efficiently resealed prior to protein-DNA dissociation.

Although the intracellular target of the quinolones is identified to be DNA gyrase by various quinolone-resistant mutations in *gyrA* (and occasionally in *gyrB*), *in vitro* studies have implicated single-stranded DNA as the preferential binding site of the quinolones (Shen and Pernet, 1985). Further studies suggest that DNA is indeed recognised by the quinolones but that a gyrase-DNA complex is the target of the drugs (Shen *et al.*, 1989a; Shen *et al.*, 1989b). A model for the mechanism of gyrase inhibition by quinolones has been proposed based on the above experiments (Shen *et al.*, 1989c). In the model gyrase binds to relaxed double-stranded DNA and cleaves both strands with the usual four base

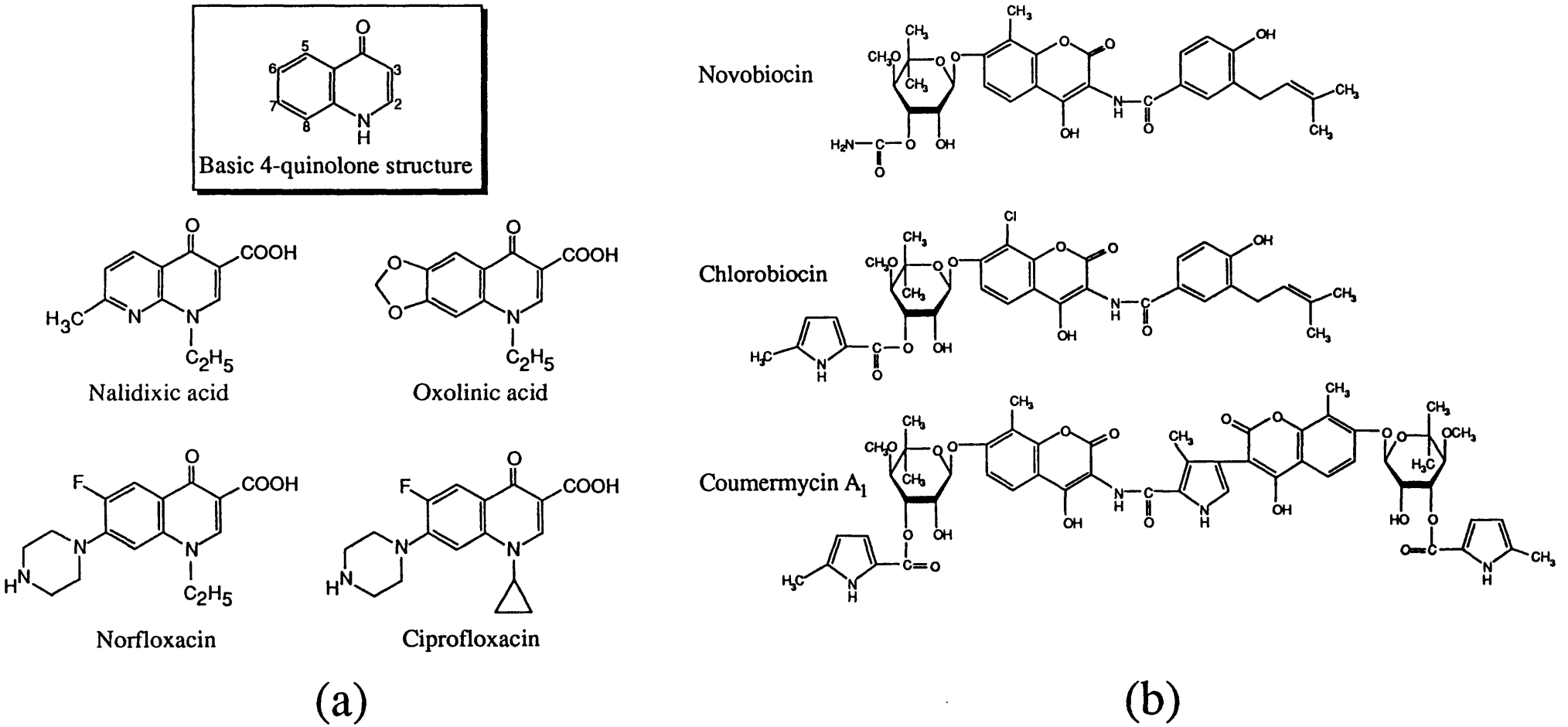

Figure 1.6. The structures of the quinolone and coumarin gyrase inhibitors. (a) shows the structures of some of the common quinolone drugs. (b) shows the structures of some of the common coumarin drugs.

stagger. As the cleaved DNA strands are separated, to allow the strand passage event to occur, single-stranded DNA is exposed and forms the quinolone binding site. On each single-stranded piece of DNA, two drug molecules, associated with each other by ring stacking, are proposed to interact *via* hydrogen bonds to two exposed bases. These two drug molecules on opposing DNA strands interact hydrophobically to form a tetramer which effectively blocks the resealing of the DNA and locks the cleaved gyrase-DNA complex in place. Although this model is speculative, it does at least provide a hypothesis which can be tested experimentally.

How the inhibition of gyrase by quinolones causes cell death is not fully understood but one hypothesis suggests that the quinolone-gyrase-DNA complex inhibits DNA transcription and replication by blocking the passage of RNA polymerase and the replication fork respectively (Liu, 1990).

ATPase activity.

The ATPase activity of gyrase is greatly stimulated by linear, nicked-circular, and relaxed double-stranded DNA (Maxwell and Gellert, 1984; Mizuuchi *et al.*, 1978). The number of superhelical turns introduced into an initially relaxed circular DNA substrate has been calculated to be approximately equal to the number of ATP molecules hydrolysed by gyrase (Sugino and Cozzarelli, 1980) which suggests that, in the initial stage of the supercoiling reaction, two molecules of ATP are hydrolysed per round of supercoiling. However, ATP hydrolysis continues after the DNA is fully supercoiled which suggests that significant slip in the coupling of ATP hydrolysis to DNA strand passage can occur (Sugino and Cozzarelli, 1980). Analysis of such ATPase slip at high specific linking differences is complicated by the presence of nicked circular DNA, usually present in supercoiled DNA preparations, which may allow the enzyme to idle and wastefully hydrolyse ATP.

The gyrase B protein alone has been shown to possess a low intrinsic ATPase activity which is greatly stimulated when GyrA and DNA are added (Maxwell and Gellert, 1984). Evidence that this protein contains the ATP binding site came originally from the covalent labelling of the active site with the 2',3'-dialdehyde derivative of (α-^{32}P)ATP and the demonstration that the B protein retained the radioactivity (Mizuuchi *et al.*, 1978). More recently, affinity labelling experiments using the reactive ATP analogue, pyridoxal 5'-diphospho-5'-adenosine, have confirmed that each GyrB protein contains one ATP binding site and have suggested that Lys 103 and Lys 110 may be involved in ATP binding (Tamura and Gellert, 1990). Furthermore, crystallographic studies have confirmed that ATP is bound by the N-teminal portion of the B protein (see above) (Wigley *et al.*, 1991).

Analysis of the DNA-dependence of the gyrase ATPase reaction has shown that the stimulation of the ATPase activity is dependent on the length of the DNA but largely independent of the DNA sequence (Maxwell and Gellert, 1984). DNA molecules of 100 bp or more were found to be effective cofactors for the ATPase reaction but those of 70 bp or less were found only to stimulate the ATPase at very high concentrations. For the DNA fragments of less than 70 bp, the dependence of the ATPase on DNA concentration was found to be sigmoidal which was interpreted in terms of gyrase having at least two DNA-binding sites required for stimulation of the ATPase (Maxwell and Gellert, 1984; Maxwell *et al.*, 1986).

The kinetics of ATP hydrolysis by gyrase have been studied by several groups using steady-state methods. The B protein on its own has been found to have a K_M for ATP of 1.7mM and a turnover number of about 1/s (Staudenbauer and Orr, 1981). In the presence of the A protein and DNA, the K_M appears to be 0.3-0.5 mM with the turnover remaining unchanged at about 1/s (Maxwell and Gellert, 1984; Staudenbauer and Orr, 1981; Sugino *et al.*, 1978; Sugino *et al.*, 1980); the exact value may depend on the DNA

used (Maxwell and Gellert, 1984) or on the protein preparation. A number of nucleotides have been reported to be competitive inhibitors of the ATPase reaction such as ADPNP, ADP, and AMP (Sugino and Cozzarelli, 1980). However, it has been found that the inhibition by ADP deviates markedly from Michaelis-Menten kinetics (Maxwell *et al.*, 1986) and this inhibition can be modelled to a scheme involving the binding of two ATP molecules to each gyrase tetramer prior to hydrolysis. Recently, evidence for cooperativity between the two nucleotide binding sites in gyrase has been obtained from experiments on the binding of ADPNP (Tamura *et al.*, 1992). It was found that ADPNP binds very slowly to gyrase in the absence of ATP but that ATP can accelerate the rate of ADPNP binding by over 15-fold. This suggests that there is positive cooperativity in nucleotide binding to the two gyrase subunits. Such data must cast doubt upon the significance of the steady-state parameters described above.

A class of antimicrobial agents known as the coumarins (see Fig. 1.6. (b)) have been shown to inhibit supercoiling by gyrase (Gellert *et al.*, 1976a; Gellert *et al.*, 1976b) but relaxation of supercoiled DNA is unaffected by the coumarins (Gellert *et al.*, 1977). It has been shown that the coumarin, novobiocin, specifically inhibits the binding of a 2',3'-dialdehyde derivative of ATP to gyrase (Mizuuchi *et al.*, 1978). In addition, steady-state kinetic experiments have shown that novobiocin and coumermycin A_1 (Fig. 1.6. (b)) are potent inhibitors of ATP hydrolysis by gyrase with the inhibition appearing to be competitive (Sugino and Cozzarelli, 1980; Sugino *et al.*, 1977). That the inhibition appears to be competitive is somewhat surprising since the drugs do not share much structural similarity to ATP. Several spontaneous coumarin-resistance mutations have been mapped to the GyrB protein (Contreras and Maxwell, 1992; del Castillo *et al.*, 1991; Holmes and Dyall-Smith, 1991). The most common mutation is at Arg 136. Proteins bearing mutations at this position have been found to have reduced supercoiling and ATPase activities *in vitro* and *in vivo* in addition to enhanced resistance to coumarin drugs (Contreras and Maxwell, 1992). From the crystal structure of the N-terminal fragment of

GyrB, Arg 136 does not appear to be directly involved in interacting with ATP although it forms a hydrogen bonding interaction with the main chain carbonyl of Tyr 5, on the N-terminal arm of the opposing monomer, which does interact with ATP (see crystallography section above).

Studies on coumarin inhibition of the intrinsic ATPase of the N-terminal fragment of GyrB have shown that novobiocin binds with a stoichiometry of two molecules to one protein dimer, and that coumermycin binds with a stoichiometry of one to one (J.A. Ali, A.P. Jackson, A.J. Howells, and A. Maxwell, personal communication). This is consistent with the chemical structures of these drugs in that coumermycin resembles a dimer of novobiocin.

Mechanism of DNA supercoiling by gyrase.

The mechanism of gyrase-catalysed supercoiling has intrigued investigators since the discovery of gyrase. Many models have been proposed to account for this remarkable reaction (see Maxwell and Gellert (1986); Reece and Maxwell (1991b) for reviews). Any model must take into account the following features:

(1) approximately 120 bp of DNA is wrapped around the enzyme in a single turn with a positive superhelical sense;

(2) the wrapped DNA is cleaved in both strands and the 5'-phosphoryl termini of the DNA are covalently attached to the A protein;

(3) the linking number of the DNA is changed in steps of two;

(4) gyrase is able to supercoil, relax, knot, unknot, catenate, and decatenate closed-circular duplex DNA.

The above requirements are satisfied by a mechanism involving the passage of a double-stranded DNA segment through a transient double-stranded break which is then resealed

(Wang, 1982). This type of DNA translocation mechanism gives rise to two further mechanistic considerations. Firstly, since both DNA strands are broken, the cleaved complex must be stabilised by the protein so that the broken DNA ends cannot rotate with respect to each other which would lead to complete relaxation of the DNA. While stabilising the cleaved DNA, the protein must allow the translocated DNA segment to pass through the DNA gap and into at least part of its structure. Secondly, the translocated DNA segment could, in principle, be part of the region wrapped around the enzyme or it could come from a more distant part of the sequence. It has been shown that gyrase can supercoil DNA circles as small as 174 bp which suggests that the translocated DNA segment can, at least in some cases, be close to (or part of) the wrap (Bates and Maxwell, 1989). In contrast, catenation and decatenation reactions are most easily explained in terms of a distant part of the DNA (in these cases a segment from a completely different molecule) being translocated. It is likely, therefore, that the translocated DNA can be either part of (or close to) the wrap or a more distant segment depending on the reaction conditions.

One model for gyrase-catalysed DNA supercoiling based on that of Reece and Maxwell (1991b), and similar to the "molecular gate" model proposed by Wang (1982), is shown in Fig. 1.7. For simplicity, gyrase is represented simply as a flattened sphere; further details of the protein structure have already been shown in the model of Fig. 1.5. Gyrase is shown initially bound to relaxed closed-circular DNA with approximately 120 bp of the DNA wrapped around the protein in a positive superhelical sense. This necessitates the formation of a negative writhe elsewhere in the molecule to relieve the strain generated by the positive writhe. Gyrase then cleaves the wrapped DNA in both strands and the 5'-ends of the broken strands become covalently attached to the A subunits of gyrase *via* phosphate ester linkages with Tyr 122. In addition to these covalent bonds holding the 5'-ends of the broken strands to the protein, the 3'-ends of the broken DNA must also be held in place *via* non-covalent interactions with the protein. Such interactions stabilise the

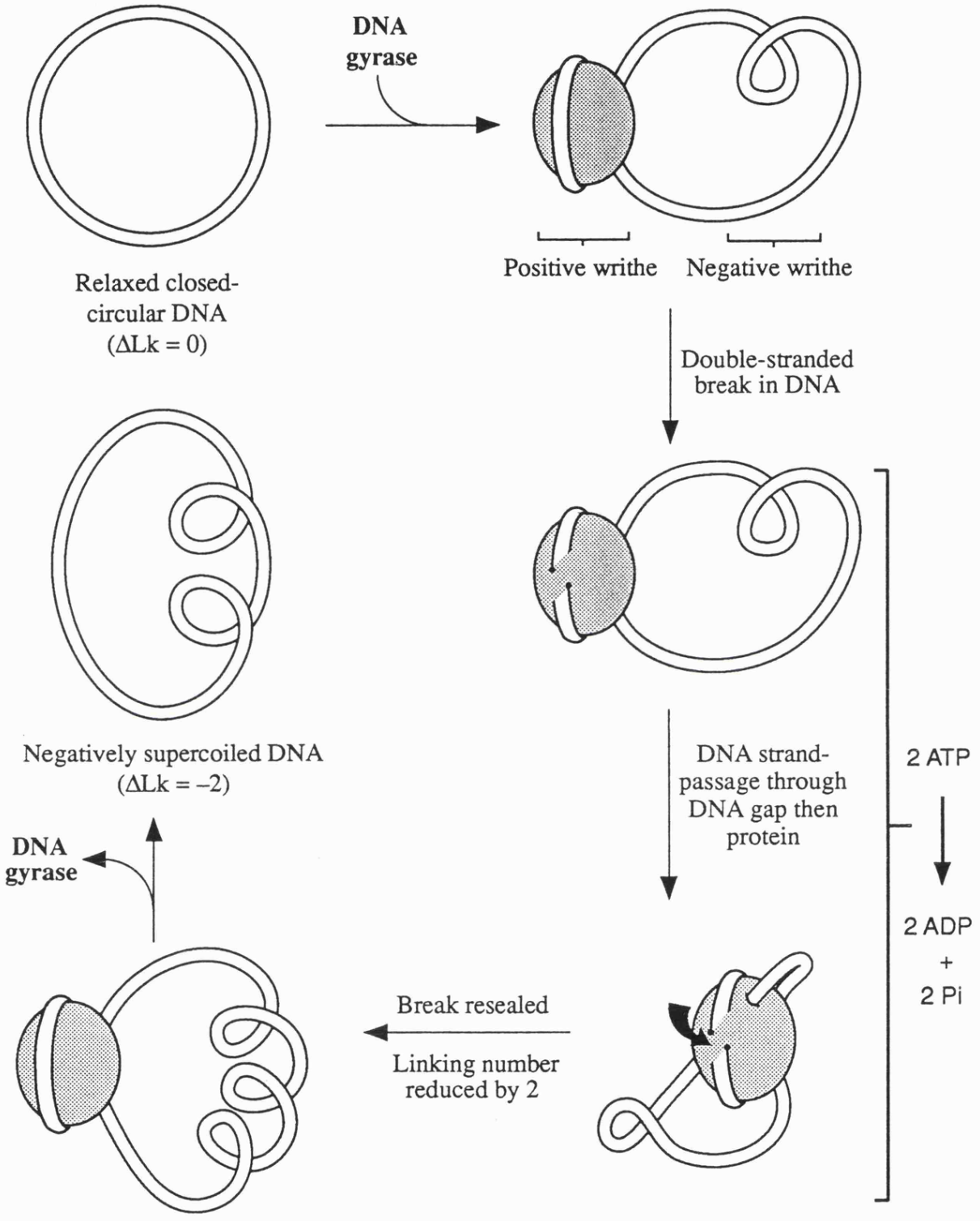

Figure 1.7. A proposed mechanism for negative supercoiling by DNA gyrase. Please see text for explanation.

break site and will not allow the DNA to untwist and relieve the strain the of the negative writhe elsewhere in the circle. DNA strand passage can occur through the break site and also through at least part of the protein structure; inter-subunit channels within the protein structure may facilitate this process (Fig. 1.5). In the model the translocated DNA is shown to be close to the wrapped DNA, and after passage through the gap it may be stabilised within the protein. One possibility is that ATP hydrolysis allows the release of the translocated DNA from the opposite side of the protein complex to the breakage-reunion site (i.e. *via* a channel between the B subunits; Fig. 1.5). This would result in the vectorial passage of the translocated DNA through the gyrase complex and would presumably require large conformational changes (see the discussion of energy transduction in gyrase in Section 1.3). Further investigations may shed light on the details of the DNA translocation mechanism.

The passage of the translocated double-stranded DNA through the double-stranded DNA break reduces the linking number of the DNA by two which is realised when the translocated DNA is released from the interior of the protein (this reduction in linking number is shown in the structure in the bottom left of Fig. 1.7). There are now two possible pathways. Firstly, the DNA break could be resealed and the gyrase dissociate from the DNA as shown in the figure. This would result in distributive supercoiling since the gyrase would have to bind to DNA again in order to catalyse further supercoiling. Secondly, the DNA break may or may not be resealed and the gyrase remains bound to the DNA, ready to perform further reaction cycles. This would result in processive supercoiling which is often observed with gyrase. If the DNA break were not resealed between cycles, gyrase would remain covalently attached to the DNA and another DNA strand passage event could take place. If the break is resealed after each reaction cycle then the DNA must be broken again before another strand passage event can occur. At present, it is not known whether DNA translocation through the protein is coupled to resealing of the DNA break.

break site and will not allow the DNA to untwist and relieve the strain the of the negative writhe elsewhere in the circle. DNA strand passage can occur through the break site and also through at least part of the protein structure; inter-subunit channels within the protein structure may facilitate this process (Fig. 1.5). In the model the translocated DNA is shown to be close to the wrapped DNA, and after passage through the gap it may be stabilised within the protein. One possibility is that ATP hydrolysis allows the release of the translocated DNA from the opposite side of the protein complex to the breakage-reunion site (i.e. *via* a channel between the B subunits; Fig. 1.5). This would result in the vectorial passage of the translocated DNA through the gyrase complex and would presumably require large conformational changes (see the discussion of energy transduction in gyrase in Section 1.3). Further investigations may shed light on the details of the DNA translocation mechanism.

The passage of the translocated double-stranded DNA through the double-stranded DNA break reduces the linking number of the DNA by two which is realised when the translocated DNA is released from the interior of the protein (this reduction in linking number is shown in the structure in the bottom left of Fig. 1.7). There are now two possible pathways. Firstly, the DNA break could be resealed and the gyrase dissociate from the DNA as shown in the figure. This would result in distributive supercoiling since the gyrase would have to bind to DNA again in order to catalyse further supercoiling. Secondly, the DNA break may or may not be resealed and the gyrase remains bound to the DNA, ready to perform further reaction cycles. This would result in processive supercoiling which is often observed with gyrase. If the DNA break were not resealed between cycles, gyrase would remain covalently attached to the DNA and another DNA strand passage event could take place. If the break is resealed after each reaction cycle then the DNA must be broken again before another strand passage event can occur. At present, it is not known whether DNA translocation through the protein is coupled to resealing of the DNA break.

At some point in the cycle two ATP molecules are hydrolysed but it is not known how the energy associated with this reaction is coupled to the supercoiling reaction. This aspect is discussed in Section 1.3.

1.2.4. Eukaryotic Type II Topoisomerases

Eukaryotic type II topoisomerases have been identified from a number of different sources including *Drosophila* embryos (Hsieh and Brutlag, 1980), HeLa cells (Miller *et al.*, 1981), yeast cells (Goto *et al.*, 1984), and calf thymus (Darby and Vosberg, 1985). The enzymes from different sources all appear to be related to each other at both the functional and structural level. They are all ATP-dependent enzymes and catalyse the relaxation of negative and positive supercoils as well as the knotting, unknotting, catenation, and decatenation of closed-circular double-stranded DNA (see Hsieh (1990b) for review). Structural studies have revealed that the enzymes exist as homotypic dimers with subunit molecular masses around 170 kDa.

Eukaryotic type II topoisomerases differ from their prokaryotic counterparts in that they are unable to supercoil DNA yet they require ATP for their relaxation activity. The ATP-dependent DNA relaxation reaction has been studied in the *Drosophila* enzyme (Osheroff *et al.*, 1983). It has been found that, in contrast to the ATP-independent relaxation of negatively supercoiled DNA by bacterial DNA gyrase, the eukaryotic type II topoisomerase appears to relax DNA in a processive manner. The ATPase of the enzyme is greatly stimulated by DNA with supercoiled DNA being a more efficient cofactor than relaxed or linear DNA; the same pattern is found in the DNA-binding affinity of the enzyme. Experiments with ADPNP and $ATP_{\gamma}S$ have shown that these nucleotides promote a single round of DNA relaxation (a change in linking number of 2) per enzyme molecule present. This suggests that nucleotide binding is sufficient for strand passage while enzyme turnover requires nucleotide hydrolysis: a result similar to gyrase-catalysed DNA supercoiling. An estimate of the number of ATP molecules hydrolysed per

supercoil removed gave a value of 4. However, the significance of this is uncertain since the relaxation reaction is energetically "down-hill" and also the hydrolysis of ATP continues after full relaxation has occurred. The coumarin drugs which inhibit gyrase-catalysed ATP hydrolysis also show a weak inhibition of the eukaryotic type II topoisomerases although much higher levels of the drugs are required (Hsieh and Brutlag, 1980; Osheroff *et al.*, 1983).

DNA sequencing has revealed interesting homologies between the genes encoding eukaryotic type II enzymes and DNA gyrase. It appears that the polypeptide of eukaryotic enzymes has three distinct regions: an amino-terminal region with homology to the B subunit of DNA gyrase, a central region with homology to the A subunit of gyrase, and a carboxy-terminal region characterised by clusters of charged amino acids (Lynn *et al.*, 1986; Uemura *et al.*, 1986; Wyckoff *et al.*, 1989). Thus it is likely that the N-terminal portion of the eukaryotic type II topoisomerases contains the ATP binding site and the middle region of the protein contains the DNA breakage and reunion activity. A role for the C-terminal region is unclear since it is not essential for catalytic activity (Lindsley and Wang, 1991).

Recently the domain structure of the yeast topoisomerase II has been probed by limited proteolysis and found to consist of at least four domains (Lindsley and Wang, 1991). These domains may be similar to those proposed for gyrase (Reece, 1990). Furthermore, Lindsley and Wang (1991) have showed that the proteolytic cleavage of yeast topoisomerase II is altered by the binding of ADPNP or $ATP_{\gamma}S$, suggesting that nucleotide binding gives rise to allosteric interdomain movements in the enzyme.

Eukaryotic type II topoisomerases induce double-stranded breakage of DNA if the reactions are terminated with a protein denaturant such as SDS (Sander and Hsieh, 1983). The structure of the DNA at the cleavage site is the same as that induced by DNA gyrase:

i.e. a double-strand break staggered by four nucleotides in each strand with the 5'-ends of the break site covalently linked to the enzyme (Sander and Hsieh, 1983). The attacking nucleophile of the enzyme has been found to be Tyr 783 in *S. cerevisiae* (Worland and Wang, 1989).

The DNA cleavage reaction has been used to analyse the DNA sequence preference of the eukaryotic type II topoisomerases although no unified consensus has emerged with some differences being apparent among different species. DNase I footprinting of a *Drosophila* topoisomerase II-DNA complex containing a preferred cleavage site has revealed that the enzyme protects about 20-30 bp with the cleavage site occurring in the middle of the protected region (Lee *et al.*, 1989). There was no evidence for DNase I sensitive sites spaced at intervals of ~10 nucleotides which suggests that the DNA is not wrapped around the enzyme as it is for gyrase. It was suggested that the lack of DNA wrapping may be the reason why eukaryotic type II topoisomerases are unable to supercoil DNA.

A number of anti-tumour drugs have been found to be inhibitors of eukaryotic type II topoisomerases. These include DNA intercalators such as the acridine, 4'-(9-acridinylamino) methansulphon-m-aniside (m-AMSA), and non-intercalators such as etoposide (VP-16) (see Liu, 1990). Despite intensive study their mode of action is not completely understood. However, one possibility is that they interfere with the DNA reunion step in the relaxation mechanism of eukaryotic topoisomerase II perhaps by binding to the DNA at the DNA-protein gapped complex displacing the free 3'-ends so that resealing of the DNA strands cannot occur (Liu, 1990).

1.2.5. Viral Topoisomerases

Most viruses recruit the host's topoisomerases for their own purposes. However, two of the more complex double-stranded DNA viruses have been found to encode their own topoisomerases. The bacteriophage T4 and its relatives encode a type II ATP-dependent

topoisomerase with similarities to eukaryotic topoisomerase II, while vaccinia, a poxvirus, encodes a type I enzyme (see Huang (1990) for a review).

The T4 topoisomerase is a multisubunit complex coded for by three genes known as gene 39, 52, and 60 which encode polypeptides of about 60 kDa, 50 kDa, and 18 kDa respectively (Huang, 1990). The native enzyme has a Stokes radius of ~60 Å as determined by gel filtration which corresponds to a globular protein of ~300 kDa which would be consistent with a complex involving at least two copies of each of the subunits.

Similar to eukaryotic topoisomerase II, the viral enzyme relaxes both negative and positive supercoils in an ATP dependent manner as well as catalysing the catenation, decatenation, knotting, and unknotting of duplex circles under the appropriate conditions. The ATPase activity of the enzyme has been shown to be stimulated by DNA with both double-stranded and single-stranded DNA being effective cofactors (Huang, 1990). It has been suggested that, like other type II enzymes, nucleotide binding allows DNA strand passage but that nucleotide hydrolysis is required for enzyme turnover since $ATP_{\gamma}S$ supports limited DNA relaxation roughly stoichiometric to the amount of enzyme present (Liu *et al.*, 1979). An estimation of the stoichiometry of ATP's hydrolysed to DNA relaxation has yielded a value of between 1 and 2 ATP's hydrolysed per supercoil relaxed although this is subject to the same uncertainties discussed for the eukaryotic topoisomerase II.

Addition of a protein denaturant such as SDS reveals double-stranded DNA cleavage by the viral enzyme with the 5'-ends of the newly broken strands covalently linked to the protein in a similar way to that observed for the eukaryotic topoisomerase II. It has been found that a tyrosine residue on the T4 gene 52 protein is the amino acid that becomes covalently bound to the DNA which identifies this subunit as the breakage-reunion protein (Rowe *et al.*, 1984). Quinolone drugs such as oxolinic acid have been found to

inhibit the relaxation activity of T4 topoisomerase and enhance the DNA cleavage reaction although much higher concentrations of the drug are required than for DNA gyrase. The quinolones have been used to determine the sequence preference for DNA cleavage by the enzyme but although the cleavage pattern is clearly non-random, no unified consensus sequence has emerged.

The T4 topoisomerase genes have been cloned and sequenced (Huang, 1986a; Huang, 1986b; Huang *et al.*, 1988). Gene 39 encodes a protein of 519 amino acids, gene 52 encodes a protein of 441 amino acids, and gene 60 encodes a protein of 160 amino acids. The sequences of these genes have revealed marked homology with eukaryotic topoisomerase II and DNA gyrase. Specifically, T4 gene 39 aligns with the N-terminal portion of *gyrB* and the N-terminal portion of *TOP2*, the T4 gene 60 aligns with the C-terminal portion of *gyrB* and an equivalent region on *TOP2*, and the T4 gene 52 can be aligned to the N-terminal portion of *gyrA* and a central region in *TOP2*. Thus it is likely that the T4 gene 39 protein is responsible for ATP hydrolysis, and the T4 gene 52 protein performs the DNA breakage-reunion activity. Support for this hypothesis has come from studies of the individual proteins (Huang, 1990). The gene 39 protein, which is a monomer in solution, has been found to possess a weak ATPase activity, while the gene 52 protein, which is a dimer in solution, can perform a non-catalytic DNA relaxation reaction presumably *via* DNA breakage and reunion. The gene 60 protein has been found to possess no activity on its own but can form large aggregates. All three proteins are required to reconstitute a catalytically active enzyme and it has been suggested that the role of the gene 60 protein is to hold the other two proteins together *via* protein-protein interactions (Huang, 1990).

Why the bacteriophage T4 has acquired its own distinct topoisomerase is not known, but studies on phage bearing mutations in one or more of the topoisomerase genes suggest

that the enzyme is essential in the initiation of the replication of the phage DNA (Huang, 1990).

Vaccinia virus is a relatively complex DNA virus with a genome size of 185 kb. The topoisomerase activity in this virus was discovered in 1977 (Bauer *et al.*, 1977). The enzyme has since been purified and its properties have been investigated (Foglesong and Bauer, 1984; Shaffer and Traktman, 1987). It is a type I topoisomerase with a single polypeptide of ~32 kDa. Many of the enzyme's properties are similar to eukaryotic type I topoisomerases; for example, it relaxes both positively and negatively supercoiled DNA, and becomes covalently bound to the 3'-end of the broken DNA strand after DNA cleavage. Unexpectedly, it appears to be inhibited by coumarin drugs despite the lack of a requirement for ATP (Shaffer and Traktman, 1987). The vaccinia topoisomerase gene has been sequenced and found to encode a protein of 314 amino acids (Shuman and Moss, 1987) which has reasonable homology to eukaryotic topoisomerase I but not with the prokaryotic enzyme (Lynn *et al.*, 1989).

1.2.6. *In vivo* Roles of Topoisomerases

General maintainance of superhelical tension

As enzymes that can alter the topology of DNA, topoisomerases are important in many aspects of DNA metabolism. The genome of most organisms (with the possible exception of the archaebacteria which possess reverse gyrase) is maintained in a negatively supercoiled state. In eukaryotes, the DNA is wrapped around histones in a left-handed (negative superhelical) fashion and the compensatory positive supercoiling that occurs in the free DNA is relaxed by type I and type II topoisomerases to generate negatively supercoiled DNA stabilised on the histones. In prokaryotes, while histone-like proteins have been identified, DNA gyrase may be the dominant factor responsible for the generation of negative superhelical tension. The extent of this negative supercoiling may, in fact, be controlled by the diametrically opposed activities of topoisomerase I and DNA

gyrase; lethal mutations in the *E. coli topA* gene encoding topoisomerase I are compensated for by mutations in *gyrA* or *gyrB* which reduce DNA gyrase activity (DiNardo *et al.*, 1982; Pruss *et al.*, 1982). Moreover, the expression of the *topA* and gyrase genes are sensitive to the topological state of the chromosome: the expression of the gyrase genes is increased by a reduction in negative supercoiling whereas the expression of *topA* is decreased (Menzel and Gellert, 1983; Tse-Dinh, 1985). This may represent a homeostatic mechanism for the control of DNA supercoiling within the cell.

Some aspects of the biological importance of negative DNA supercoiling has already been considered (see Section 1.1). In addition to their general role in maintaining superhelical tension, topoisomerases have been implicated in specific reactions involving DNA such as transcription and replication.

Transcription generates supercoiled domains.

Negative supercoiling of DNA facilitates DNA strand separation as is required for the initiation of transcription. Thus negative supercoiling would be expected to enhance gene expression. However, this is not always the case as is seen, for example, with the gyrase genes described above; correct promoter recognition by RNA polymerase seems to be influenced by the topology of the DNA in a way that varies depending on the particular gene.

Recently considerable evidence has accumulated which suggests that transcription can affect the supercoiling of the DNA template (reviewed in Drlica (1990); Wang (1991); Wang and Liu (1990)). In 1983, it was found that inhibition of DNA gyrase in *E. coli* harbouring pBR322 caused the plasmid to become positively supercoiled (Lockshon and Morris, 1983). Subsequently, it was found that pBR322 isolated from *E. coli topA* mutants was much more negatively supercoiled than the same plasmid isolated from normal strains (Pruss, 1985). Furthermore, it was shown that the unusually high

negative supercoiling of pBR322 in the *topA* mutants was dependent on the transcription of the *tet* gene in the plasmid (Pruss *et al.*, 1986). A model to explain these results was proposed by Liu and Wang (1987) which suggested that transcription may generate supercoiled domains (see Fig. 1.8). As RNA polymerase tracks along the DNA template, transcribing a particular gene, it must follow the helical path of the DNA strands which could be accomplished by rotation of the transcription complex around the DNA axis. However, Liu and Wang argued that the transcription complex, consisting of RNA polymerase, the nascent mRNA, and possibly ribosomes translating the message in a coupled manner, may be restricted from rotating around the DNA axis because of the high frictional drag in the cellular mileau. Instead they proposed that the DNA would turn about its own axis with positively supercoiled DNA being generated ahead of the transcription ensemble and negatively supercoiled DNA being generated behind the complex. In many DNA molecules in prokaryotes and eukaryotes, discrete topological domains probably exist as a result of attachments to cellular structures such as membranes or the nuclear matrix in eukaryotes. The existence of such topological regions may prevent the oppositely supercoiled domains generated by transcription from cancelling one another out, and topoisomerases may function to relax these supercoiled domains ahead of and behind the transcription ensemble. In prokaryotes, topoisomerase I can only relax negatively supercoiled DNA and gyrase can only relax positively supercoiled DNA (at the ATP levels prevalent in the cell), and so the activities of these two topoisomerases are directed to the oppositely supercoiled domains generated by transcription. In a plasmid containing two genes in opposite directions (such as the *tet* and *bla* genes of pBR322) the transcriptional supercoiled domains will reinforce each other. Inhibition of gyrase should abolish the relaxation of positively supercoiled domains and therefore lead to positively supercoiled plasmid while inhibition of topoisomerase I should lead to enhanced negative supercoiling of the plasmid. This explains the results of Lockshon and Morris (1983) and Pruss *et al.* (1986) described above. Further support for the twin supercoiled domain model has come from

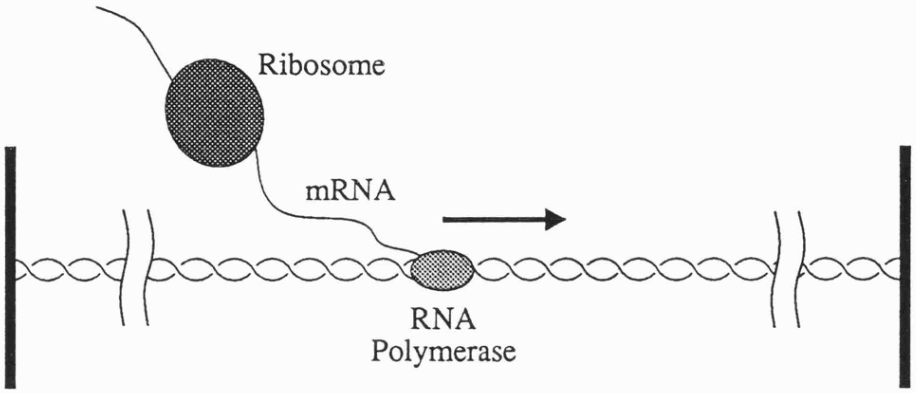

(a)

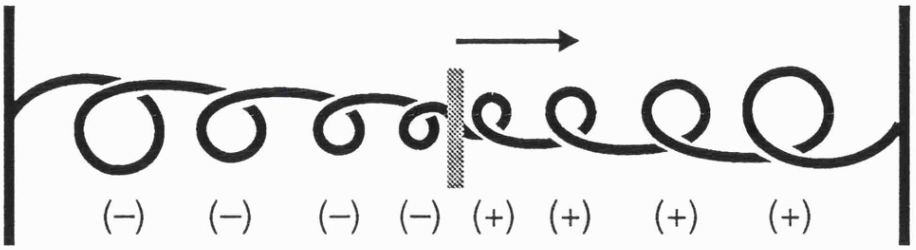

(b)

Figure 1.8. Formation of twin domains of supercoiling by transcription elongation. (a) shows the transcription complex with RNA polymerase transcribing a topologically isolated domain of DNA into mRNA, to which ribosomes become attached. (b) shows how relative movement of the transcription complex (represented by the shaded bar) along the DNA results in positively supercoiled DNA ahead of the transcription complex and negatively supercoiled DNA behind the complex.

experiments which showed that in derivatives of pBR322 in *E. coli* inversion of the *tet* gene reduced the positive supercoiling resulting from inactivation of gyrase and also reduced the excess negative supercoiling resulting from topoisomerase I inhibition (Wu *et al.*, 1988).

It has been harder to test the twin supercoiled domain model in eukaryotes since both topoisomerase I and topoisomerase II can relax negative and positive supercoils with the consequence that the inhibition of one type does not lead to differential relaxation of the supercoiled domains. However, experiments on yeast have suggested that the twin supercoiled domain model is equally applicable to eukaryotes as it is to prokaryotes (Giaever and Wang, 1988). It was found that a yeast plasmid became positively supercoiled in cells where topoisomerase I and II were inactivated and *E. coli* topoisomerase I was expressed. Thus one of the major roles of topoisomerases in both prokaryotes and eukaryotes may be in the dissipation and control of transcriptionally generated supercoiled domains.

Roles of topoisomerases in DNA replication.

Initiation of DNA replication involves unwinding of the DNA at the origin and is therefore facilitated by negative DNA supercoiling; in bacteria, DNA gyrase appears to be required in the initiation of DNA replication presumably because of its general role in negative supercoiling (Gellert, 1981; Wang, 1985). This is supported by studies on a cell-free DNA replication system, composed of bacteriophage λ and *E. coli* replication proteins, where initiation of replication occurred in the absence of gyrase if the DNA template was already supercoiled (Mensa-Wilmot *et al.*, 1989).

The elongation stage in DNA replication can be thought of as a special case of the twin supercoiled domain model in which the progress of the replication fork generates positive supercoils ahead of it, while behind the fork the separated parental strands can be thought

of as an extreme case of DNA unwinding (or negative supercoiling) (Wang, 1991). In prokaryotes, DNA gyrase would be expected to remove the positive supercoils generated ahead of the replication fork in order to facilitate its progress although there is no direct evidence for this *in vivo*. It has been shown in the cell-free replication system described above that replication initiated in the absence of gyrase was blocked early on in the elongation stage by the accumulation of torsional stress in the DNA consistent with the requirement for gyrase-mediated relaxation of positive supercoils (Mensa-Wilmot *et al.*, 1989).

In eukaryotes, either topoisomerase I or topoisomerase II can remove positive supercoils, and experiments on yeast DNA replication have shown that only when both topoisomerases are inactivated is there a reduction in the elongation of replication (Kim and Wang, 1989).

When two replication forks converge at the end of DNA replication, the unwinding of the parental DNA strands may lag behind the completion of the progeny strand synthesis in which case, after ligation of the newly formed strands by ligase, catenated double-stranded DNA molecules are formed (see Fig. 1.9). Clearly decatenation is required before cell division can successfully occur, and this decatenation would require the action of a type II topoisomerase. In *E. coli*, mutations in gyrase have been found to prevent segregation of daughter chromosomes suggesting that the decatenation activity of this enzyme is important in the termination of DNA replication (Steck and Drlica, 1984). Recently, two genes encoding a new topoisomerase, topoisomerase IV, have been identified in *E. coli* on the basis of mutations that prevent proper chromosome segregation. The genes are known as *parC* and *parE* and have been found to possess homology to *gyrA* and *gyrB* respectively, although crude cell lysates of overproduced ParC and ParE proteins showed a high DNA relaxing activity in contrast to the supercoiling activity of gyrase (Kato *et al.*, 1990). Thus both gyrase and topoisomerase

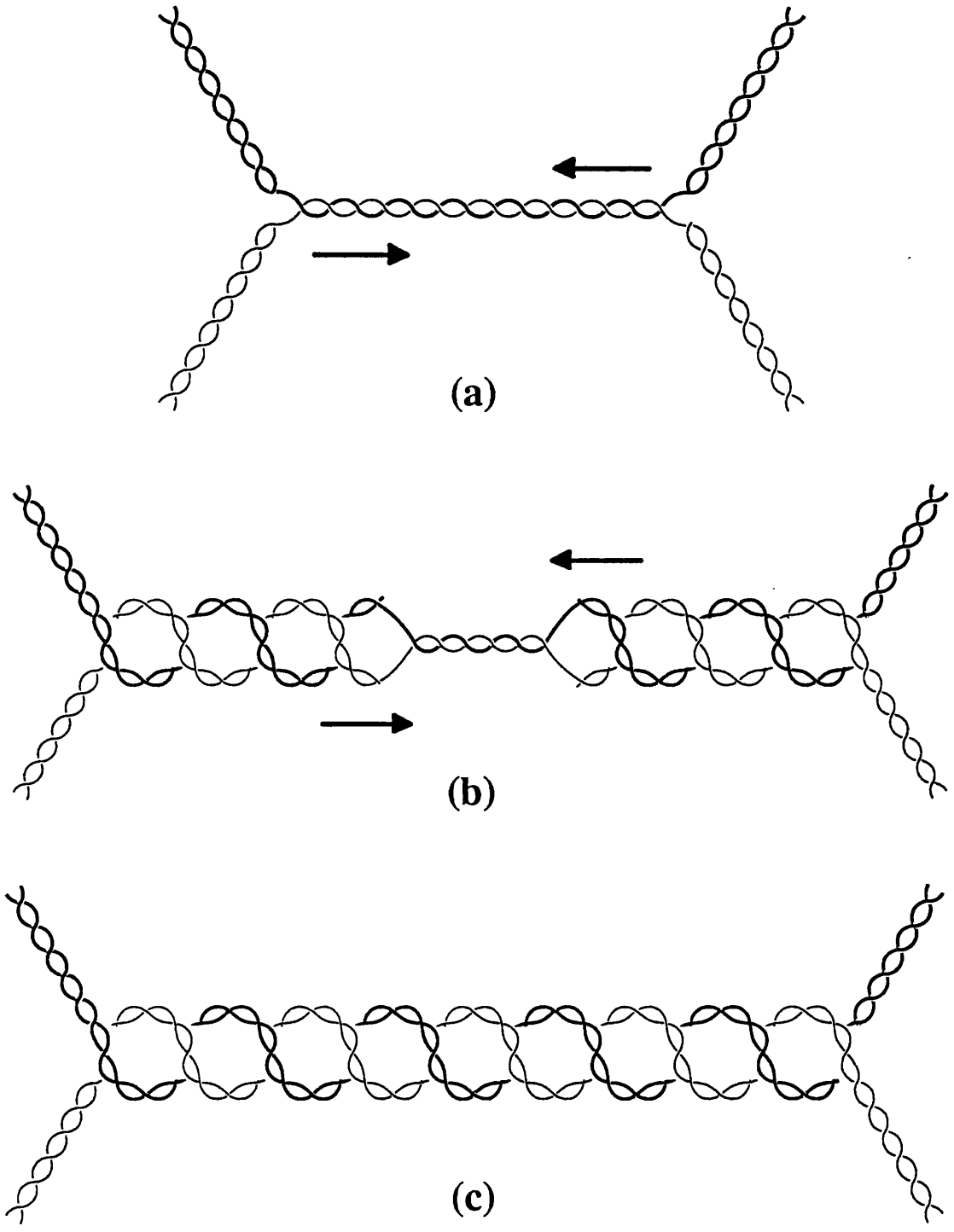

Figure 1.9. Formation of catenated DNA at termination of replication. (a) shows two replication forks converging at the end of replication. (b) shows the replication forks at a more advanced stage. At this stage, if synthesis of the progeny strands proceeds faster than the unwinding of the duplex ahead of the transcription forks, then catenated duplex DNA molecules result (as in (c)) after sealing of the strands by DNA ligase. Alternatively, if synthesis of the progeny strands is sufficiently slow, the structure in (b) may be decatenated *via* the action of either a type I or type II topoisomerase to yield separated gapped daughter molecules which are filled in by further DNA synthesis.

IV seem to be essential for chromosome segregation at the end of replication; why two type II enzymes are required is not clear.

In yeast expressing a temperature-sensitive topoisomerase II mutant, DNA catenanes were found to accumulate at the non-permissive temperature suggesting that segregation of daughter replicons requires topoisomerase II in eukaryotes (DiNardo *et al.*, 1984).

The pathway for the termination of DNA replication shown in Fig. 1.9 is not the only possible pathway; if untwisting of the parental DNA strands is fast compared to completion of progeny strand synthesis, then gapped interlinked DNA molecules may result which could be separated *via* the action of either type I or type II topoisomerases. Interestingly, it has been demonstrated that *E. coli* topoisomerase I is able to decatenate daughter molecules in an *in vitro* pBR322 replication system when the enzyme is present at high concentration (Minden and Marians, 1986). It has also been speculated that *E. coli* topoisomerase III may be involved in chromosome segregation (DiGate and Marians, 1988).

A possible structural role for gyrase in maintaining the 50 or so topological domains in the *E. coli* genome was considered in the discussion of DNA cleavage by gyrase in Section 1.2.3. It has been proposed that eukaryotic topoisomerase II may also have a structural role in the organisation of the chromosome since immunomicroscopy has implicated topoisomerase II as a major component of the chromosome scaffold (Earnshaw *et al.*, 1985; Earnshaw and Heck, 1985). Further characterisation of the *in vivo* locations of topoisomerases may yield more insights into their functions.

1.3. BIOLOGICAL ENERGY COUPLING

The ubiquitous use of ATP as a carrier of free energy.

Living organisms require a continual input of free energy for three main purposes: the performance of mechanical work *via* muscle contraction and other cellular movements, the active transport of molecules and ions, and the biosynthesis of macromolecules from simple precursors. The energy source can vary; chemotrophs obtain free energy from the oxidation of foodstuffs while phototrophs obtain it directly from light. But a unifying feature of all organisms is the generation of ATP as a carrier of free energy. The central role of this nucleotide in many biological processes is shown in Fig. 1.10.

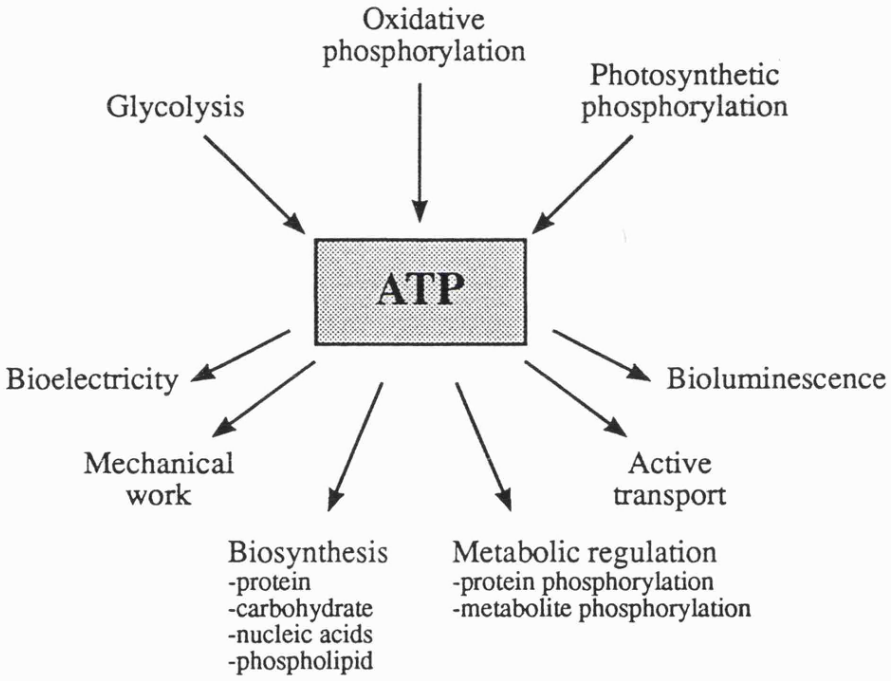

Figure 1.10. The biological roles of ATP; its formation and utilisation in cells (based on Cohn, 1991).

What features of ATP contribute to its widespread adoption in energy transfer? As discussed by Westheimer (1987) in his paper entitled, "Why nature chose phosphates", the two most important properties of ATP are its kinetic stability and its thermodynamic

instability. ATP is negatively charged at physiological pH (the first pK_a is ~2) and this ensures that the molecules are retained in the cytoplasm of cells since they are unable to cross the lipid membranes. The negative charges at physiological pH also make the phosphoanhydride bonds of ATP less susceptible to attack by nucleophiles, thus imparting kinetic stability in the absence of activation by enzymes. Finally, the negative charge of ATP is important in its interactions with positively charged ligands, such as metal ions and some amino-acid residues of proteins. The thermodynamic instability of ATP is due to the greater relative stability of ADP and P_i; three main factors are responsible. Firstly, at physiological pH, the cleavage of the β-γ bond of ATP relieves charge repulsion. Secondly, the formation of P_i is particularly favourable owing to its resonance stabilisation. Thirdly, the extent of solvation increases on forming the product anions.

Mechanisms of free energy transduction in biological systems.

It is apparent from Fig 1.10 above that the free energy stored as ATP can be used to drive chemical reactions (eg. in biosynthesis and metabolic regulation) and to perform work (eg. mechanical work and active transport). In the latter case, the reactions are mediated by enzymes that operate in coupled vectorial processes essentially like energy transducing machines. Energy coupling systems that drive mechanical work are important in muscle contraction, ciliary movement, cell division, cytoplasmic streaming in plants, DNA replication (eg. DNA helicase), and DNA supercoiling (DNA gyrase); examples involved in active transport are the Na^+-K^+ATPase and the Ca^{2+} ATPases of the sarcoplasmic reticulum and plasma membrane. While all of the above examples of free energy transduction systems use ATP as an energy source, this is not universally the case; for example, the Ca^{2+} pump in the inner membrane of mitochondria couples an electrochemical proton gradient to the influx of Ca^{2+} against a concentration gradient, and the synthesis of ATP in mitochondria, bacteria, and chloroplasts by ATP synthases involves the coupling of a proton gradient to the formation of ATP from ADP and P_i.

As a background to how DNA gyrase may couple the free energy of ATP hydrolysis to DNA supercoiling, it is useful to consider the detailed mechanisms of free energy transduction in other biological systems. Two particularly well characterised examples are muscle contraction and Ca^{2+} transport by the sarcoplasmic reticulum and I shall concentrate on these before turning to DNA gyrase. Much of the following discussion is based on Eisenberg and Hill (1985).

Mechanism of energy transduction in muscle contraction.

Skeletal muscle is composed of many muscle fibres which are, in turn, composed of myofibrils. Under the electron microscope, myofibrils can be seen to consist of interdigitating thin and thick filaments composed of actin and myosin respectively. (For a more detailed description of the anatomy of muscle see Bagshaw, 1982; Stryer, 1988). During contraction these filaments are thought to slide past each other. This process is mediated by cross-bridges that extend from the myosin filament and cyclically interact with the actin filament as ATP is hydrolysed (Fig. 1.11 (a)).

Actin and myosin are polymeric structures as shown in Fig. 1.11 (b). Each globular actin monomer is composed of a single polypeptide of molecular weight 43kDa. Myosin monomers are comprised of two heavy chains, each with a molecular weight of 200kDa, and four light chains with molecular weights of approximately 20kDa. These polypeptide chains fold into three separate domains which have distinct functions; the subfragment-1 domain (S1) forms two globular cross-bridges to actin ; the light meromyosin domain (LMM) is involved in aggregation of myosin monomers to form filaments; the subfragment-2 domain (S2) provides a flexible connection between the myosin filament and the cross-bridges. It is thought that the two cross-bridges associated with each myosin molecule are identical and function independently.

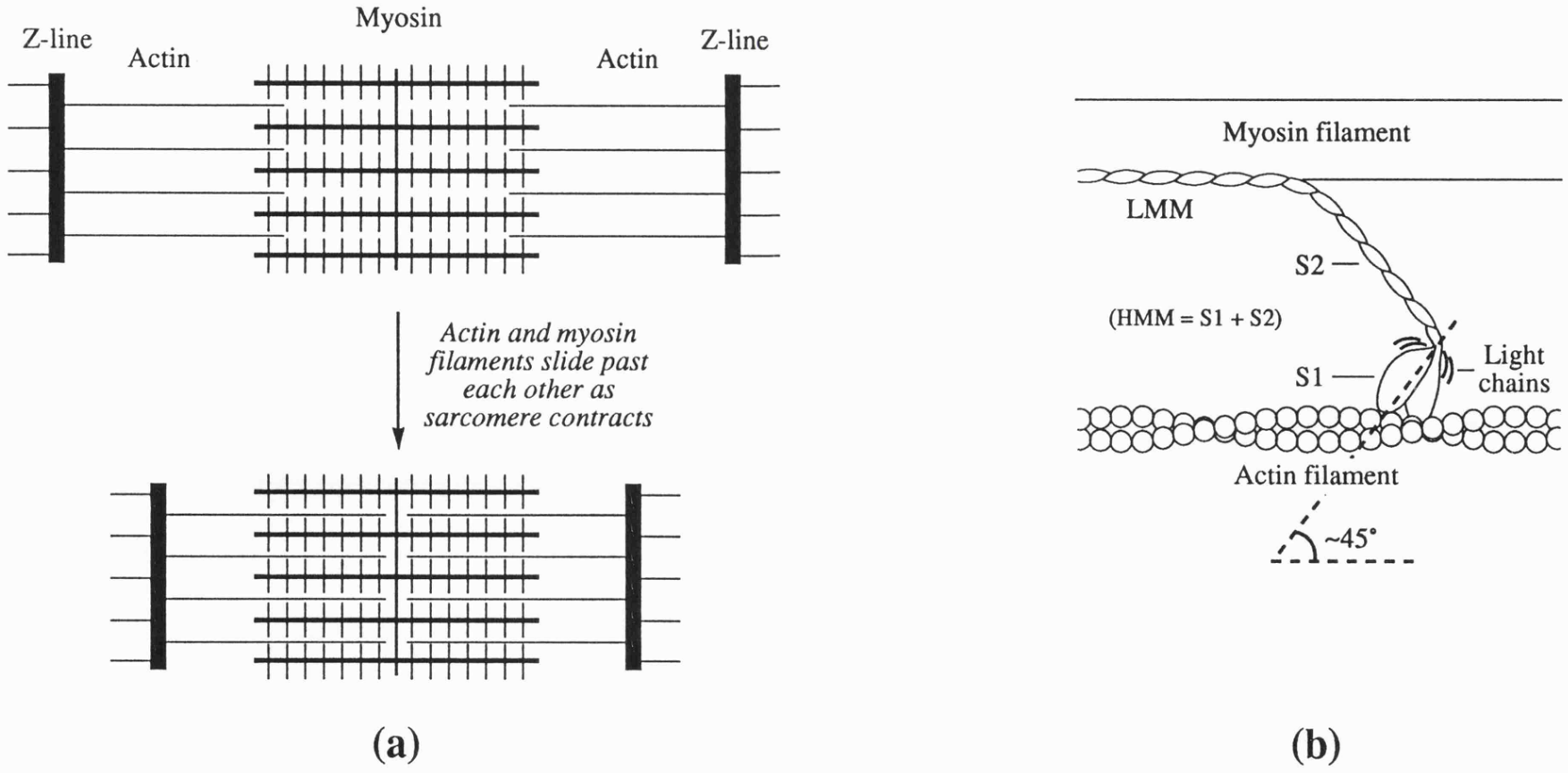

Figure 1.11. (a) Diagram of a single segment (sarcomere) of a muscle fibre as it contracts. Contraction of many segments in concert leads to shortening of the whole muscle. (b) Diagram of a myosin molecule bound to an actin filament in the absence of ATP. Both the myosin and actin filaments are polymeric structures; each circle in the actin filament represents an actin monomer. Only one myosin molecule is shown in the figure; in vertebrate skeletal muscle there is one myosin cross-bridge for every two actin monomers. During contraction, the actin filament moves to the left relative to the myosin filament.

In the absence of ATP, the myosin cross-bridges appear to bind to actin at an angle of about 45°, forming a tight complex corresponding to the rigor state of muscle. The cross-bridges in relaxed muscle, however, appear to be mostly detached from actin and are at an angle of about 90° to the actin filament. This has led to the concept that the cross-bridges go through oar-like cycles as they push the actin filament past the myosin filament, first binding to the actin filament in the 90° state, then transforming to the 45° state as they drive the movement of the actin filament, and finally detaching and returning to the 90° state ready for another cycle.

How then is this cycle driven by ATP hydrolysis? One model is shown in Fig. 1.12. Part (a) of this figure shows the kinetic model for ATP hydrolysis proposed by Stein *et al.* (1979). In each cycle of ATP hydrolysis, myosin alternates between two conformations, a weak-binding conformation and a strong-binding conformation. The binding of ATP transforms the myosin from the strong-binding conformation to the weak-binding conformation. Several kinetic steps (hydrolysis and a rate-limiting step) occur while the myosin is in the weak-binding conformation with the free and actin-bound states in rapid equilibrium. Release of P_i eventually transforms the myosin back into the strong-binding conformation.

While there is some conflict as to whether there is a separate ATP hydrolysis step and rate-limiting step or whether ATP hydrolysis, itself, is rate-limiting (Rosenfeld and Taylor, 1984), the main features of this scheme are generally accepted (Eisenberg and Hill, 1985). Thus, ATP hydrolysis can occur while myosin S1 is bound to actin and S1 alternates between a strong-binding and weak-binding conformation during the ATPase cycle.

Eisenberg and Greene (1980) developed a model for the action of the myosin cross-bridges in muscle contraction based on the above ATPase scheme (Fig. 1.12 (b)). They

Figure 1.12. Model for the mechanism of muscle contraction. (a) Kinetic cycle of S1 ATPase according to Stein et al. (1979). The bold arrows show the predominant pathway. The dashed arrows show the very slow rate-limiting step in the absence of actin. The relative lengths of the forward and reverse arrows indicate qualitatively the free energy change across a reaction. (b) Cross-bridge model according to Eisenberg and Greene (1980). The myosin cross-bridges are shown schematically simply as single headed arrows. Also the 45° and 90° conformations are highly schematic and the detailed structural changes that probably occur in the cross-bridges are not addressed.

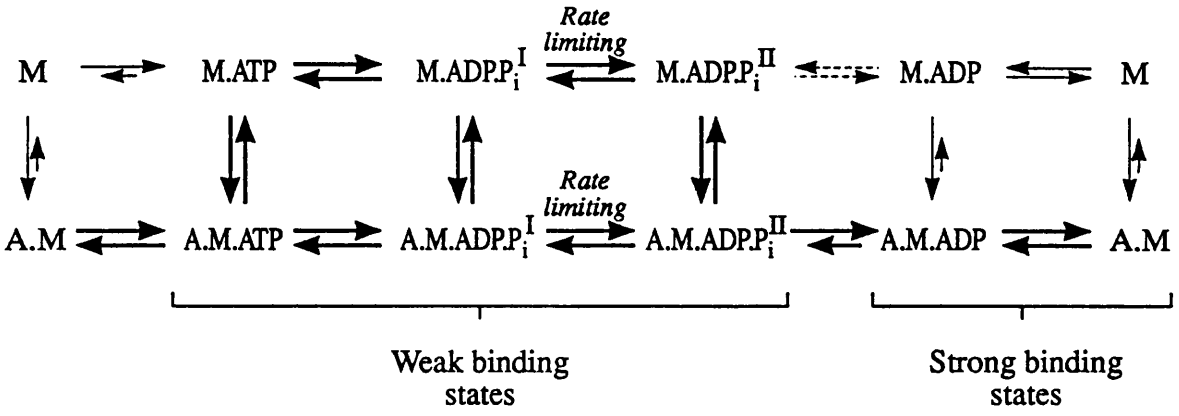
M
M.ATP
M.ADP.P$_i^I$
Rate limiting
M.ADP.P$_i^{II}$
M.ADP
M
A.M
A.M.ATP
A.M.ADP.P$_i^I$
Rate limiting
A.M.ADP.P$_i^{II}$
A.M.ADP
A.M
Weak binding states
Strong binding states

(a)

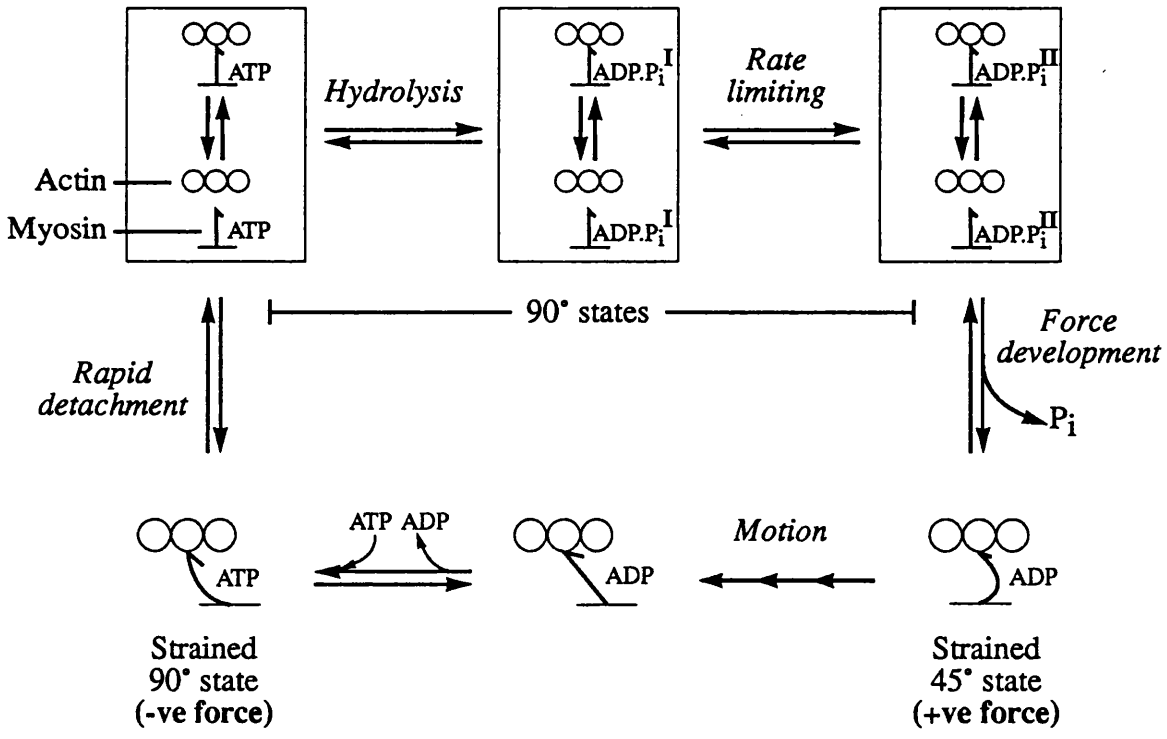
ATP
Hydrolysis
ADP.P$_i^I$
Rate limiting
ADP.P$_i^{II}$
Actin
Myosin
ATP
ADP.P$_i^I$
ADP.P$_i^{II}$
90° states
Rapid detachment
Force development
P$_i$
ATP
ATP ADP
ADP
Motion
ADP
Strained 90° state (-ve force)
Strained 45° state (+ve force)

(b)

assumed that the weak-binding states of the cross-bridges are in the 90° conformation while the strong-binding states are in the 45° conformation.

Considering the species in the top left-hand corner of Fig. 1.12 (b), this is in the weak-binding 90° conformation with ATP bound. In the same way as in the kinetic scheme of part (a), the free and actin-bound cross-bridges are in rapid equilibrium. ATP hydrolysis and a rate-limiting step occur while the myosin cross-bridge is in the weak-binding 90° conformation as also implied by the kinetic scheme. P_i release from the cross-bridge into solution now occurs, accompanied by a conformational change of the cross-bridge to the 45° strong-binding state. In muscle, the cross-bridge is not free to assume the 45° conformation since it is tightly bound to actin and, instead, the cross-bridge becomes strained. This creates a positive force on the actin filament; when a sufficient number of cross-bridges have developed this ATP-induced strain, the actin filament can slide past the myosin filament. As the actin filament slides, the strain in the cross-bridges is relieved and they drop to a lower free energy level. Finally ADP release from the relaxed 45° conformation allows ATP to bind and induce the 90° weak-binding state. It is assumed that the release of ADP from muscle is much slower than it is with S1 in solution, until the work stroke is completed, so that the cross-bridge remains in the strong-binding state until all the strain is translated into movement of the actin filament. Just as the formation of the 45° state on P_i release developed positive force on the actin filament, the formation of the 90° state on binding ATP develops a negative force. Crucially, however, the 90° state only binds actin weakly, and can rapidly detach from actin before the negative force can reverse the work already done in the cross-bridge cycle.

The above model is supported by studies with ADPNP which have shown that this ATP analogue actually causes a muscle fibre to lengthen slightly. This can be rationalised by reference to Fig. 1.12 (b) as follows: ADPNP would enter the cycle at the same place as

ATP but, since it cannot be hydrolysed, the cross-bridges will be trapped in the strained 90° state and, eventually, the negative force will be realised as a slight increase in the length of the muscle fibre. There is also a body of evidence to favour the existence of different cross-bridge conformations in the weak and strong-binding states (Eisenberg and Hill, 1985).

Mechanism of energy transduction in the sarcoplasmic reticulum ATPase.

The sarcoplasmic reticulum forms a network of channels in muscle cells and serves as an intracellular store of Ca^{2+}. The sarcoplasmic reticulum ATPase is responsible for pumping Ca^{2+} from the cytosol into the sarcoplasmic reticulum. A high concentration of Ca^{2+} in the sarcoplasmic reticulum is important in the action of muscle; when a nerve impulse depolarises the muscle cell membrane, Ca^{2+} is released from the sarcoplasmic reticulum into the cytosol which stimulates the muscle to contract. Since the sarcoplasmic reticulum ATPase is the major protein in the reticulum membrane, it is relatively easy to purify, and consequently its properties have been studied in detail. Furthermore, it can be incorporated into vesicles which facilitates energy coupling studies.

The mechanism of this active transport enzyme (Fig. 1.13) has several features in common with myosin action. For example, both enzymes exist in two conformations, one of which binds ligand weakly, and one of which binds ligand strongly. In the case of myosin, the ligand is actin and the two conformations are the 45° and 90° species; in the case of the sarcoplasmic reticulum ATPase, the ligand is Ca^{2+} and the two conformations are either open to the inside of the cell (*inside* conformation), or open to the outside of the cell (*outside* conformation).

Considering the active transport cycle from the top-left, it begins with the enzyme in the strong-binding *inside* conformation. Ca^{2+} ions bind tightly to the enzyme and the enzyme is then phosphorylated by ATP to give an acyl phosphate intermediate. This

Figure 1.13. Model for the active transport of Ca^{2+} by the sarcoplasmic reticulum ATPase (deMeis and Vianna, 1979). (a) Kinetic cycle. The bold arrows show the predominant pathway. Dashed arrows indicate steps that are very slow and the relative lengths of forward and reverse arrows show qualitatively the free energy change across a reaction. E represents the strong-binding *inside* conformation and E* represents the weak-binding *outside* conformation. E-P represents the covalent acyl phosphate intermediate. For simplicity the model shows one Ca^{2+} ion transported per ATP hydrolysed when in reality the stoichiometry is two Ca^{2+} per ATP. (b) Schematic representation of the Ca^{2+} transport cycle based on the kinetic cycle in (a).

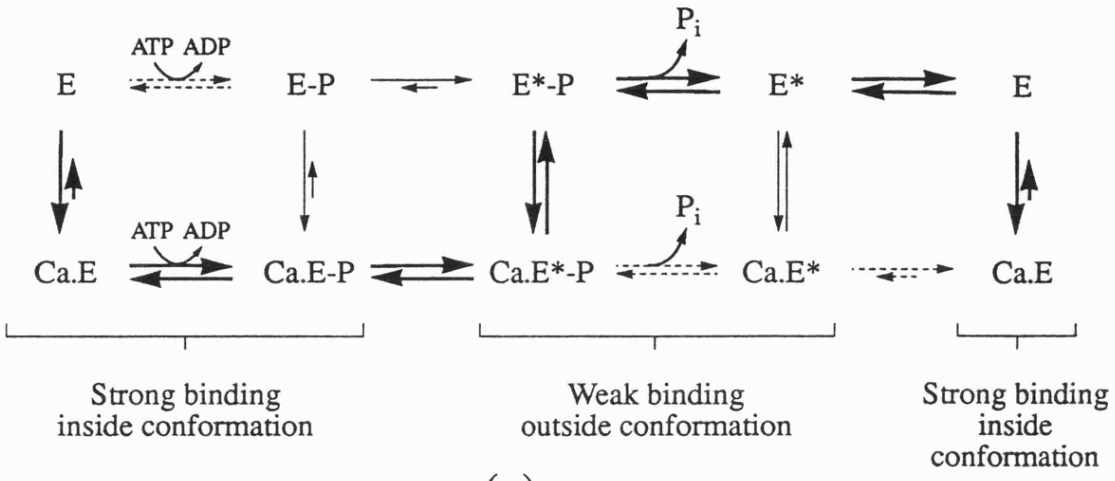
E
ATP ADP
E-P
E*-P
Pi
E*
E
Ca.E
ATP ADP
Ca.E-P
Ca.E*-P
Pi
Ca.E*
Ca.E
Strong binding
inside conformation
Weak binding
outside conformation
Strong binding
inside
conformation

(a)

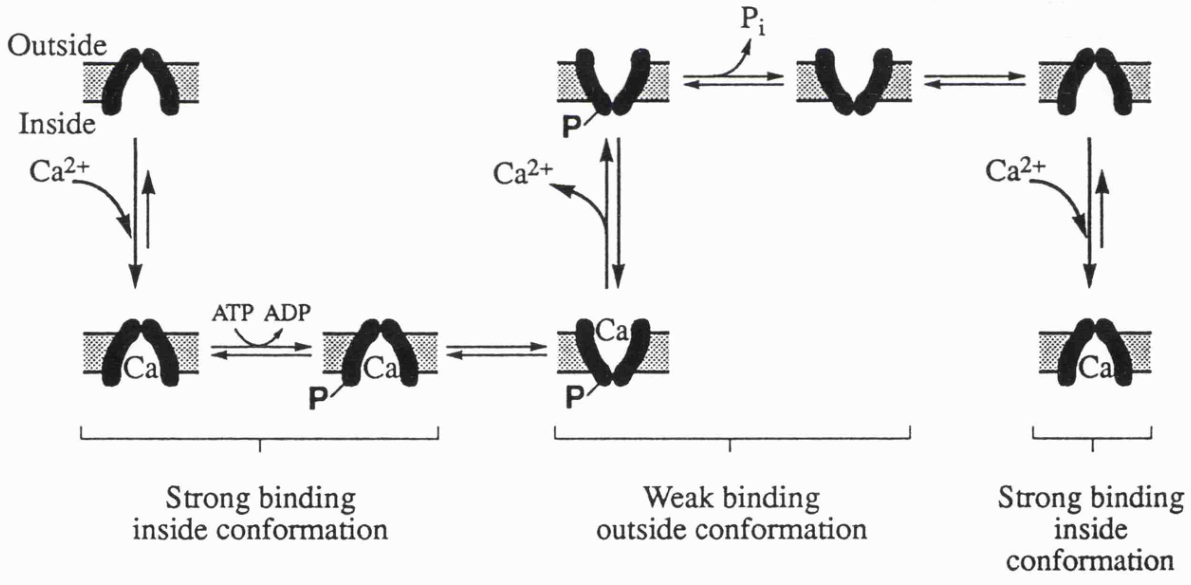
Outside
Inside
Ca2+
ATP ADP
Ca
P
Pi
Ca2+
Ca
P
Ca2+
Ca
Strong binding
inside conformation
Weak binding
outside conformation
Strong binding
inside
conformation

(b)

promotes a transformation of the enzyme to the weak-binding *outside* conformation and the weakly bound Ca^{2+} can now be released. The acyl phosphate is now hydrolysed and P_i is released from the enzyme which induces it to return to the strong-binding *inside* conformation ready for another cycle.

The importance of binding energy.

The mechanisms of energy transduction in the sarcoplasmic reticulum ATPase and in myosin have three main common themes:

(1) Ligand (eg. Ca^{2+} or actin) binds to the enzyme with a strong binding energy. In the cross-bridge cycle this allows the cross-bridge to exert significant force without detaching from actin, while in the transport cycle it allows Ca^{2+} to bind to the enzyme despite its low concentration inside the cell. In both these enzymes the strong-binding state occurs when ATP is not bound.

(2) At some point in the cycle, the enzyme undergoes a major conformational change that alters the physical position of the ligand.

(3) During the cycle, the binding constant of the ligand decreases, which allows the ligand to detach from the enzyme.

In myosin, the binding energy of ATP allows the structural change to take place and also provides the energy required to dissociate the strongly bound actin. ATP is now strongly bound instead of actin and the strong non-covalent bonds between ATP and myosin must be broken to complete the energy transduction cycle. This is achieved by first hydrolysing the ATP to ADP and P_i with little overall change in free energy. The ADP and P_i, however, can now readily dissociate from the enzyme back to solution since this is energetically favourable.

In the active transport enzyme, ATP binding does not directly supply the free energy to weaken the binding of Ca^{2+}; rather it phosphorylates the enzyme, and strong non-covalent interactions with the acyl phosphate intermediate allow the the enzyme to undergo a conformational change which has a greatly reduced affinity for Ca^{2+}. Hydrolysis of the acyl phosphate and release of P_i into solution allows the enzyme to regain its strong-binding conformation ready for a new cycle. Interestingly, it has been shown that the Ca^{2+} gradient produced by the Ca^{2+} pump is the same when either ATP or $ATP_{\beta}S$ is used as the free energy source. This was surprising because the free energy of hydrolysis of the thionucleotide has been found to be approximately 10.5kJ/mol more exergonic than ATP. It is possible therefore that the dominant factor controlling the extent of the Ca^{2+} gradient produced is the free energy of hydrolysis of the acyl phosphate intermediate. This hypothesis is discussed further in Chapter 7 in relation to DNA gyrase.

A unifying feature of the above enzymes emerges. This is, that by binding tightly to an enzyme, a ligand (like an acyl phosphate group or ATP) can cause both a structural change and the detachment of another bound ligand at some point in a free energy transduction cycle, and then itself can be easily released from the enzyme at another point in the cycle after it is chemically changed to a form that is more stable in solution.

This principle is also applicable to energy coupling systems where the free energy is provided by an ion gradient such as the ATP synthases (Boyer, 1989). Here ATP is synthesised from ADP and P_i by coupling this reaction to a proton gradient across a membrane. Firstly, ADP and P_i bind to the enzyme and ATP is formed with virtually no change in free energy. Next, a proton, acting as a typical ligand (like ATP or the acyl phosphate in the muscle and active transport examples respectively), binds weakly to the enzyme from the side of the membrane where it is at high concentration. The enzyme then undergoes a conformational change which makes the proton accessible to the other

side of the membrane at the same time as increasing its binding affinity to the enzyme. This latter effect decreases the strength of binding of the the newly synthesised ATP which can then dissociate into solution. Release of the strongly bound proton, to complete the cycle, can occur without the requirement of an enzyme conformational change, since it is released on the side of the membrane where it is at low concentration.

Energy transduction in DNA gyrase.

From the discussion of the structural aspects of gyrase catalysed DNA supercoiling in Section 1.2, a mechanism for free energy transduction in gyrase can be advanced. ATP binds to the enzyme and the binding energy allows a conformational change to take place. From studies on the 43kDa fragment of GyrB (described in Section 1.2), it is likely that the B subunits come together on binding ATP. This movement may be transmitted to the A proteins which could move apart opening up a channel between them. It is assumed that the DNA wrapped around gyrase is already cleaved and covalently bound to tyrosines 122 in the A proteins before the ATP-induced conformational change can take place. Part of the DNA (termed the passage helix by Corbett *et al.*, 1992) can now pass through the double-stranded break in the wrapped DNA and into the channel between the A subunits. The passage helix is then presumably bound non-covalently within the protein either between the A subunits or part of the B proteins; the hole seen in the crystal structure of the 43kDa protein suggests that the passage helix could be bound in this part of the complex. (With ADPNP the reaction is trapped in this state and thus, after resealing of the double strand gap in the wrapped DNA and removal of the protein, negative DNA supercoiling stoichiometric to the amount of enzyme is revealed). Hydrolysis of ATP now occurs. This hydrolysis *per se* does not involve a large change in free energy (i.e. the "on" enzyme equilibrium may be close to unity) but the dissociation of the products ADP and P_i into solution is an exergonic process. The free energy associated with this step is used to drive the formation of a different protein conformation where the B subunits separate and the passage helix becomes less tightly bound inside the protein and

can leave through newly formed channel between the B subunits. The key energetic events in this scheme are:

(1) the free energy of ATP binding promotes an enzyme conformational change that allows the passage helix to enter the protein structure *via* a channel between the A subunits;

(2) the free energy associated with binding of the passage helix in the protein stabilises this translocated strand and may further stabilise the new enzyme conformation;

(3) the free energy of dissociation of ADP and P_i into solution promotes the return of the enzyme to its original conformation and the release of the passage helix from between the B subunits of the protein complex.

Thus the process hinges on the stabilisation of an otherwise unfavourable enzyme conformation by ATP binding. In order to be acceptable the model must account for the ATP independent relaxation of cccDNA. This can be explained by assuming that DNA relaxation occurs essentially by a reverse of the supercoiling cycle (as was discussed in Section 1.2). Hence, translocation of a passage helix into the protein through the open channel between the B subunits allows the DNA to bind to its site inside the protein and stabilise the unfavourable protein conformation with the gate between the B subunits closed. Release of the passage helix through the channel between the A subunits and through the double stand gap in the wrapped DNA is favourable since this relaxes the DNA. The model also explains the strict directionality of the supercoiling reaction in the presence of ATP even when the overall thermodynamic requirement for free energy is removed such as the nucleotide dependent relaxation of positive supercoiling; ATP (or ADPNP) binding is required to open up the gap between the A subunits to allow the passage helix to enter the protein. In the case of ADPNP-catalysed relaxation of positive

supercoiling (Gellert *et al.*, 1980), the requirement for ATP hydrolysis and the free energy of ADP and P_i release is replaced by the free energy of DNA relaxation and hence nucleotide binding is sufficient for enzyme turnover.

There are parallels with the model for energy coupling in gyrase and the models for muscle and the Ca^{2+} active transport enzyme. For example, the free energy of cofactor binding (ATP for muscle and gyrase; P_i for the Ca^{2+} pump) is important in all three cases. However, whereas ATP hydrolysis and P_i release promotes strong binding of myosin to actin, ATP hydrolysis and product release favour dissociation of the passage helix from the interior of the gyrase complex. In this respect gyrase may resemble kinesin and the elongation factor Tu where nucleotide hydrolysis favours ligand detachment.

Although this model is speculative, it is consistent with mechanistic studies on gyrase-catalysed DNA supercoiling discussed in Section 1.2; more work is required for a detailed understanding of the mechanistic events in gyrase-catalysed DNA supercoiling.

1.4. NUCLEOSIDE PHOSPHOROTHIOATES

Nucleoside phosphorothioates, where a sulphur atom replaces a non-bridging phosphate oxygen, have been widely used to investigate the mechanisms of many enzymes catalysing reactions at phosphoryl centres (for reviews see Cohn (1982); Cullis (1988); Eckstein (1985); Frey (1989); Knowles (1980)). Incorporation of a sulphur atom into a prochiral phosphoryl centre generates chirality at the particular phosphorous and this has been exploited in the determination of the stereochemical course of a number of enzymes including nucleases, phosphodiesterases, phosphokinases, and phosphatases (see also Chapter 3). In addition, chiral nucleoside phosphorothioates have been successfully used as to probe the nucleotide binding sites of many enzymes such as kinases and

kinases and phosphatases and to characterise the type of metal-nucleotide complex handled by a particular enzyme (see also Chapters 4 and 5).

Structural aspects of nucleoside phosphorothioates

In rationalising how nucleoside phosphorothioates interact with enzymes it is important to consider their chemical structure. The localisation of charge in nucleoside phosphorothioates has been the subject of much debate. In early publications in the 70's and early 80's the thiophosphate anion was assumed to have a phosphorus-sulphur bond order of 2 with the negative charge localised on oxygen. Thus phosphate monoesters (1a) and diesters (1b) were represented as shown below.

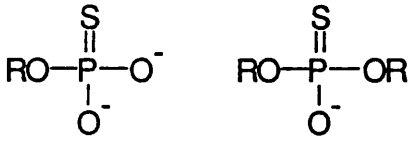

(1a) (1b)

This assumption was based partly on the greater electronegativity of oxygen compared to sulphur and partly on the crystal structure of the triethylammonium salt of uridine 2',3'-O,O-cyclophosphorothioate (2) (Saenger and Eckstein, 1970).

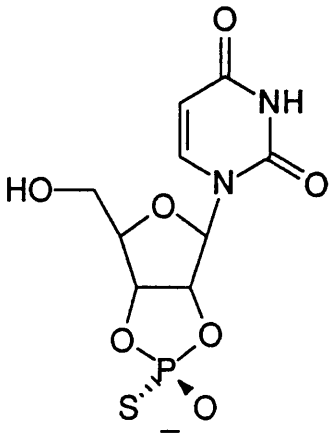

(2)

In this structure the triethylammonium counter ion formed an H-bond to the exocyclic oxygen. The exocyclic P-O bond length was found to be 1.48 Å and the P-S bond length was found to be 1.95 Å, while the endocyclic P-O bonds were found to be 1.58 Å and 1.61 Å. A P-O bond order of 1 and a P-S bond order of 2 was assigned from comparisons with bond lengths of other molecules. However, recent consensus bond lengths (shown in Table 1.2) are not consistent with the above assignments and, instead, suggest a mesomeric state. Some caution should be applied in interpreting crystal structure information since the interaction with the counter ion as well as crystal packing effects could distort the bond lengths and thus a different structure may be prevalent in solution.

Table 1.2. Reference bond lengths[a]

Bond	P-O	P=O	P-S	P=S
Length (Å)	1.56	1.45	2.10	1.92

[a]Liang and Allen (1987)

A critical appraisal of bonding in phosphorothioates was made by Frey and Sammons (1985) who concluded that charge is localised on sulphur and that the P-S bond order is very close to 1 in mono-, di-, and trianions. Their argument was based on data from a variety of solution techniques including ^{18}O-induced upfield shifts in ^{31}P-NMR, ^{17}O NMR chemical shifts, ^{31}P-^{17}O coupling constants, and vibrational spectroscopy. Subsequent observations of an ^{36}S-induced perturbation of the ^{31}P-NMR chemical shift in an O,O-dialkyl phosphorothioate monoanion (3) were consistent with a P-S single bond (Frey *et al.*, 1986).

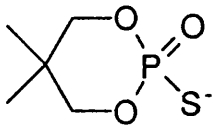

(3)

Ab initio electronic structure calculations on phosphoric and thiophosphoric acid have been used to test the hypothesis of Frey and Sammons (Liang and Allen, 1987). The lack of P-S double bonds was confirmed and in the trianion a P-S single bond with unit charge on sulphur was computed. However, on progressing to the monoanion, the charge on sulphur was found to decrease towards a mesomeric state. It is important to note that these calculations apply to the gas phase and do not necessarily model the structures in solution.

Thiophosphoric acids and esters are more acidic than the corresponding phosphoric acids and esters. For example the pK_a values of thiophosphoric acid are 1.67, 5.40, and 10.14, compared to 2.1, 7.2, and 12.3 for phosphoric acid (Frey and Sammons, 1985, and references therein). This is consistent with the arguments above and reflects the greater stability of negative charges on sulphur than on oxygen and is probably due to the larger size and greater polarisability of sulphur which gives lower charge densities than in oxyanions.

Considering all of the evidence, phosphorothioate anions are probably best represented with a negative charge localised on sulphur and a P-S bond order of 1, and this convention shall be used throughout this thesis. It is recognised however that some delocalisation of charge from sulphur may be significant in thiophosphate diesters such as $ATP_{\alpha}S$ and $ATP_{\beta}S$.

1.5. AIMS OF THIS PROJECT

It is clear from Section 1.2.6 that topoisomerases play a vital role in several cellular processes in both prokaryotic and eukaryotic organisms. There is evidence for evolutionary relationships between several topoisomerases and, while there are clear differences among separate classes of the enzymes, it is not unreasonable to expect that they may have common themes in their mechanisms.

DNA gyrase is unique amongst the topoisomerases in its ability to couple the free energy of ATP hydrolysis to the introduction of negative supercoils into DNA (although reverse gyrase appears to be able to couple ATP hydrolysis to the introduction of positive DNA supercoils). The mechanism proposed for gyrase-catalysed DNA supercoiling in Fig. 1.7 identifies a number of key mechanistic events about which little is known. For example, the strand passage reaction is thought to require the movement of a segment of the DNA through at least part of the protein and the way that this occurs is not understood at present. In addition, interaction of ATP with the enzyme, and the way in which its hydrolysis is coupled to the DNA strand passage reaction remains to be clarified.

In this work it was proposed to investigate various aspects of the interaction of ATP with gyrase, predominantly by the use of the phosphorothioate analogues of ATP shown in Fig. 1.14. (In a parallel project aspects of the interaction of gyrase with DNA were investigated by the use of DNA labelled specifically with phosphorothioate linkages; eg. see Dobbs *et al.* 1992). By analogy with work done on other phosphoryl transfer enzymes using nucleoside phosphorothioates, it was hoped that information on the following aspects of gyrase could be obtained:

(1) the configuration of the active metal-nucleotide complex handled by the enzyme (Chapters 4 and 5);

(2) the stereochemical course of the ATPase reaction catalysed by gyrase (whether or not a phosphoenzyme is involved in the reaction; Chapter 3);

(3) the coupling of the ATP hydrolysis reaction to DNA supercoiling (Chapters 4 and 6).

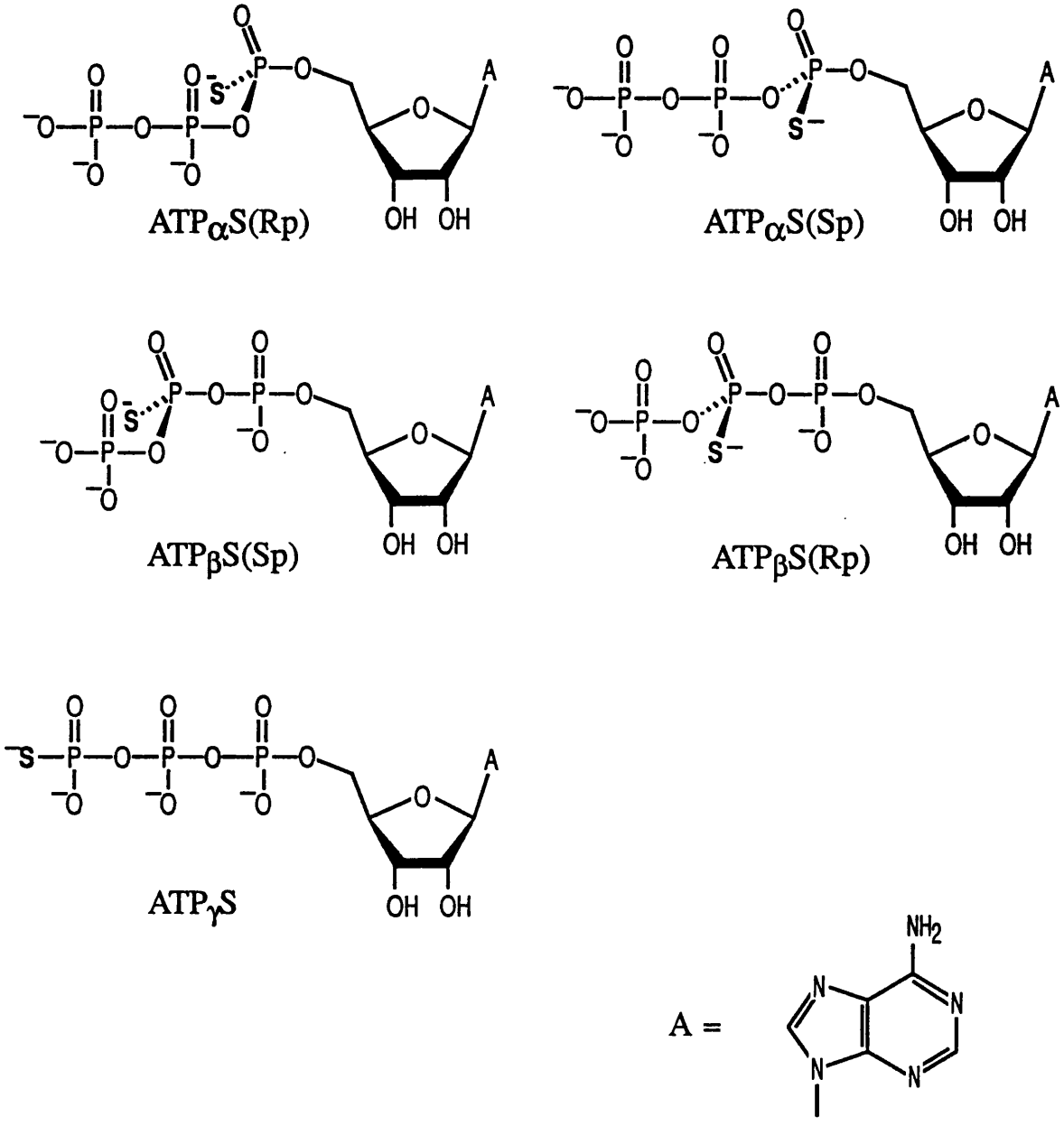

Figure 1.14. Diagramatic representation of the structures of the phosphorothioate ATP analogues used in this study. For $ATP_{\alpha}S$ and $ATP_{\beta}S$ the sulphur atom generates chirality at the particular phosphoryl centre; since ATP possesses other chiral centres on the ribose ring, these phosphorothioate molecules are diastereoisomers.

Chapter 2

Materials and Methods

2.1. Solvents.

All water used was deionised and filtered via a Milli Q system. Solvents were distilled according to the methods of Perrin and Armarego (1988).

Acetonitrile and dichloromethane were distilled from calcium hydride and then stored over 4Å molecular sieves. N,N-Dimethylformamide (DMF) was stirred with barium oxide and distilled under reduced pressure (15mmHg). It was stored over 4Å molecular sieves. Dioxane was passed through an alumina column and distilled from sodium and benzophenone. Pyridine and triethylamine were refluxed over potassium hydroxide pellets followed by distillation. Solvents were stored over 4Å molecular sieves. Diethyl ether (ether) was dried over sodium wire and refluxed with lithium aluminium hydride followed by distillation and storage over 4Å molecular sieves. Chloroform was shaken with half its volume of water 4 or 5 times and dried for 24 hours with anhydrous calcium chloride before distillation.

2.2. Syntheses

2.2.1. Preparation of trisodium thiophosphate.

The trisodium salt of inorganic thiophosphate was synthesised based on the methods of Akerfeldt (1960); Arnold (1986). Sodium hydroxide pellets (54g; 1.35mol) were dissolved in 250ml water and thiophosphoryl chloride (17.5ml; 0.17mol), freshly distilled under nitrogen at reduced pressure (20mmHg), was added. The mixture was stirred at 80°C for 30 min., following the reaction by ^{31}P-NMR. The slightly yellow solution was kept in a fridge at 4°C overnight during which time a white precipitate formed. This was collected by filtration and washed with 100ml water/ethanol (1:1 ($^{v}/_{v}$)). The precipitate was dissolved in 200ml water at 50°C and reprecipitated by slow addition of methanol (100ml) under constant rapid stirring. The solution was cooled under tap water, filtered, and the resulting white crystals were washed with ethanol (50ml). The product was made anhydrous by stirring in methanol (200ml) for 90 min.,

filtering, and extensive drying *in vacuo* at 80°C. A white powder was obtained (24.63g; 0.137mol; 81%).

^{31}P-NMR δ(36.5MHz, D_2O) +32.0 ppm (s).

2.2.2. Preparation of S-2 carbamoylethylthiophosphate.

The disodium salt of S-2 carbamoylethylthiophosphate was synthesised according to Cook (1970). A solution of trisodium thiophosphate (8.8g; 0.5mol) in water (75ml) was treated with 3-chloro-propionamide (8g; 0.084mol) in DMF (15ml) for 24 hours at room temperature. The solution was filtered and ethanol was added with stirring to the filtrate. A white precipitate formed which was filtered, washed with ethanol, and dried in a desiccator (7.33g; 0.032moles; 64%).

^{31}P-NMR δ(36.5MHz, D_2O) +16.2 ppm (s).
^{1}H-NMR δ(90MHz, D_2O) +2.8 (multiplet).

2.2.3. Preparation of S-2-carbamoylethylthiophosphate (tri-*n*-butyl-ammonium salt).

The sodium salt of S-2-carbamoylethylthiophosphate (0.916g; 4mmol) was dissolved in water and added to approximately 50ml Dowex-50 in the pyridinium form. The solution was filtered and water was removed by evaporation. The residue was dissolved in methanol containing tri-*n*-butylamine (950µl; 4mmol). After removal of the methanol the product was dried by three successive evaporations of 5ml aliquots of dry pyridine.

2.2.4. Preparation of adenosine 5'-O-(2-thiodiphosphate),(ADPβS).

The triethylammonium salt of adenosine 5'-O-(2-thiodiphosphate) was synthesised following the procedure of Goody and Eckstein (1971). Adenosine 5'-phosphate (free acid; 174mg; 0.5mmol) was added to dry methanol (2.5ml) and tri-*n*-octylamine (220µl;

0.5mmol) and the mixture was gently warmed until a solution was obtained. The solvent was removed by evaporation with dry DMF (4 x 3ml). Dry dioxane (4ml) was added to the residue, followed by dry DMF (600µl). Diphenylphosphorochloridate (150µl; 0.72mmol) and tri-n-butylamine (150µl) were then added. A white precipitate was formed which redissolved on stirring. After 3 hours at room temperature the solvent was removed by evaporation and dry ether (25ml) was added to the residual yellow gum. The mixture was kept at 4°C for 30 min. after which time the ether was removed by decantation. The remaining solid was freed of volatiles by evaporation of dry dioxane (3ml) to yield a yellow gum. A solution of the tri-*n*-butylammonium salt of S-2-carbamoylethylthiophosphate (1mmol) in dry pyridine (3ml) was added to the activated adenosine 5'-phosphate species and the solution was left at room temperature for 3 hours for a precipitate to form. Pyridine was removed by evaporation and 0.2M sodium hydroxide (40ml) was added. The cloudy suspension was heated at 100°C for 10 min. After cooling, the mixture was neutralised by passage through Dowex-50 (pyridinium form) and treated with 2-mercaptoethanol (200µl). The solution was filtered and the filtrate was applied to a DEAE-Sephadex A25 column (1.5cm x 80cm) and eluted with a linear gradient (100mM-600mM; 1.5L+1.5L) of triethylammonium bicarbonate (TEAB) buffer at pH 7.6. The product eluted at approximately 460mM TEAB indicative of a species with 2-4 charges. After removal of TEAB with methanol, the ADPβS was obtained as a slightly yellow gum which was dissolved in water and stored at -20°C.

^{31}P-NMR δ(36.5MHz, D_2O) -11.7 (d, J = 35Hz; P_α); +32.85 (d, J = 31Hz; P_β).

2.2.5. Preparation of the diastereoisomers of adenosine 5'-O-(2-thiotriphosphate), ($ATP_\beta S$).

The pure Rp and Sp epimers of $ATP_\beta S$ were prepared from $ADP_\beta S$ by exploiting the stereospecificity of kinase action at prochiral centres using high-energy phosphorylating agents. Procedures were based on those reported by Eckstein and Goody (1976).

2.2.5a. Preparation of the Sp epimer of adenosine 5'-O-(2-thiotriphosphate), ($ATP_\beta S(Sp)$).

Pyruvate kinase was used to give predominantly the Sp epimer of $ATP_\beta S$ while hexokinase was used to degrade contaminating amounts of the Rp epimer. The reaction conditions for the pyruvate kinase catalysed reaction were as follows: 50mM Tris.HCl (pH 8.0), 200mM KCl, 1mM DTT, 4mM $MgCl_2$, 2mM ADPβS, 2.2mM PEP, 0.7mg pyruvate kinase (350 units), water to a final volume of 27ml. The reaction was incubated at 25°C for 4 hours and progress was monitored by TLC. After 4 hours the reaction was stopped by extraction with an equal volume of chloroform/isoamyl alcohol and the aqueous layer was loaded onto a DEAE-Sephadex column and eluted with TEAB in the usual way. A small amount of the reaction mixture was retained for analysis by HPLC. The isolated $ATP_\beta S$ contained significant amounts of the Rp epimer. This was degraded to $ADP_\beta S$ using the following conditions: 50mM Tris.HCl (pH 8.0), 100mM KCl, 1mM DTT, 4mM $MgCl_2$, 1mM $ATP_\beta S(Sp)$, 1mM glucose, hexokinase (400µl; 250 units), water to a final volume of 25ml. Aliquots were removed at various times and extracted with an equal volume of chloroform/isoamyl alcohol before analysis by HPLC to monitor the reaction. The reaction was stopped by passage through Chelex 100 (Sigma) and the pure $ATP_\beta S(Sp)$ was purified by ion-exchange. After removal of triethylammonium bicarbonate, an aqueous solution of the triethylammonium salt of $ATP_\beta S(Sp)$ was stored at -20°C.

$ATP_\beta S(Sp)$: ^{31}P-NMR δ(121.5 MHz, D_2O) -12.20 (d, J = 27Hz; P_α), +28.59 (overlapping dd; P_β), -6.89 (d, J = 28Hz; P_γ).

2.2.5b. Preparation of the Rp epimer of adenosine 5'-O-(2-thiotriphosphate), ($ATP_\beta S(Rp)$).

Acetate kinase was used to give almost entirely the Rp epimer while any Sp contaminant was degraded with myosin S1 fragment (gift of Richard Ankrett, Dept. of Biochemistry,

this University). The reaction conditions for the acetate kinase catalysed reaction were: 50mM Tris.HCl (pH 8.0), 7.2mM $MgCl_2$, 1mM DTT, 3.6mM $ADP_{\beta}S$, 30mM acetyl phosphate, acetate kinase (400units). The reaction was incubated at 25°C for 4 hours monitoring the reaction by TLC and the reaction was stopped by extracting with an equal volume of chloroform/isoamyl alcohol. The $ATP_{\beta}S$ was purified by ion-exchange chromatography as described for the Sp epimer and a small amount of the reaction mixture was analysed by HPLC as also previously described. Any contaminating $ATP_{\beta}S$(Sp) was removed using the following conditions: 50mM Tris.HCl (pH 8.0), 4mM $MgCl_2$, 1mM DTT, 1mM ATPβS(Rp), myosin S1 (4 units). Aliquots were removed at various times and extracted with an equal volume of chloroform/isoamyl alcohol before analysis by HPLC to monitor the reaction. The reaction was stopped by passage through Chelex 100 (Sigma) and the pure $ATP_{\beta}S$(Rp) was purified by ion-exchange. After removal of triethylammonium bicarbonate, an aqueous solution of the triethylammonium salt of $ATP_{\beta}S$(Rp) was stored at -20°C.

$ATP_{\beta}S$(Rp): ^{31}P-NMR δ(121.5 MHz, D_2O) -12.19 (d, J = 26Hz; P_{α}), +28.54 (overlapping dd; P_{β}), -6.93 (d, J = 28Hz; P_{γ}).

2.2.6. Preparation of adenosine 5'-O-(1-thiotriphosphate), ($ATP_{\alpha}S$).

$ATP_{\alpha}S$ was synthesised as a racemic mixture by the method of Ludwig and Eckstein (1989). 2',3'-diacetyl adenosine (0.352g; 1mmol) was dissolved in dry pyridine (20ml) and evaporated to dryness. The residue was further dried over phosphorous pentoxide under vacuum for 1 hour. Argon was introduced into the reaction flask which was sealed with a rubber septum. A small positive pressure of argon was maintained in the reaction vessel by connecting an argon-filled balloon. Dry pyridine (1.0ml) was injected through the septum followed by dry dioxane (3.0ml). A freshly prepared 1M solution of 2-chloro-4H-1,3,2-benzodioxaphosphorin-4-one (salicyl phosphorochloridite) in dry dioxane (1.1ml; 1.1μmol), was injected into the stirred solution of the nucleoside and a

white precipitate was formed. After 10 min. a well-vortexed mixture of a 0.5M solution of bis (tri-*n*-butylammonium) pyrophosphate in dry pyridine (3.0ml) and tri-n-butylamine (1.0ml) was injected.

The pyrophosphate salt was prepared according to the procedure of Moffat (1964) as follows. Tetrasodium pyrophosphate decahydrate (2.23g; 5mmol) was dissolved in water (50ml). This was passed through a column of Dowex 50WX8 in the protonated form. The column was washed with water and the eluate dropped directly into a cooled (ice-water) and stirred solution of tri-*n*-butylamine (2.38ml; 10mmol) in ethanol (20ml). The column was washed until the pH of the eluate increased to 5.0 (approximately 70ml water). The ethanol/ water solution was evaporated to dryness and re-evaporated twice with ethanol and finally with anhydrous DMF (30ml). The residue was dissolved and diluted to 10ml DMF. This slightly yellow solution was stirred over 4 Å molecular sieves.

On addition of the bis (tri-n-butylammonium) salt to the nucleotide, the white precipitate immediately dissolved and, after 10 min., a suspension of sulphur (64mg; 2mmol) in DMF (2.0ml), followed by a further 1.0ml aliquot of DMF (to ensure complete transfer of sulphur), was injected. The reaction was stirred for 10 min. and the septum was removed. Water (50ml) was added and after 30 min. the reaction mixture was evaporated to dryness yielding an orange gum. This was dissolved in concentrated ammonia (200ml) and ammonolysis was carried out for 5 hours at 25°C. The reaction mixture was evaporated to dryness, and the residue was dissolved in water (50ml) and applied to a DEAE-Sephadex A25 column (2.5cm x 60cm) which was eluted with a linear gradient of TEAB (0.2M-1.0M; 1.5L+1.5L). The product eluted at 650mM TEAB (690μmoles; 69%) After removal of TEAB in the usual way the $ATP_{\alpha}S$ was stored as a 220mM aqueous solution at -20°C.

^{31}P-NMR δ(24.3MHz, D_2O) +44.9 (d, J = 34Hz; P_α), -23.4 (overlapping dd, J = 19Hz; P_β), -9.1 (d, J = 19Hz; P_γ).

TLC (PEI-cellulose): Rf = 0.13

2.2.7. Preparation of pure diastereoisomers of $ATP_\alpha S$.

The Rp and Sp epimers of $ATP_\alpha S$ were prepared from a racemic mixture by preparative reverse phase HPLC (see Section 2.6). A maximum of 5μmoles of $ATP_\alpha S$ was loaded onto the column which was eluted with a linear gradient of acetonitrile with the Sp epimer eluting before Rp. Fractions (1ml) were collected and the A_{260} of each was verified on a spectrophotometer before fractions corresponding to single peaks on the chromatogram were pooled. These were then concentrated on a rotary evaporator, treated with methanol to remove TEAB, and stored at -20°C as aqueous solutions. The isomeric purity of the samples was confirmed by analytical reverse phase HPLC.

$ATP_\alpha S$(Sp): ^{31}P-NMR δ(121.5 MHz, D_2O) +42.75 (d, J = 28Hz; P_α), -23.11 (overlapping dd; P_β), -6.20 (d, J = 20Hz; P_γ).

$ATP_\alpha S$(Rp): ^{31}P-NMR δ(121.5 MHz, D_2O) +42.44 (d, J = 28Hz; P_α), -23.13 (overlapping dd; P_β), -6.19 (d, J = 20Hz; P_γ).

2.2.8. Preparation of 2'(3')-O-(N-methyl)anthraniloyl adenosine 5' triphosphate (mantATP).

The disodium salt hydrate of adenosine 5' triphosphate (ATP; 2mmol; 1.10g) was dissolved in water (20ml) at 38°C. The pH was adjusted to 9.6 with 1M NaOH. N-methylisatoic anhydride (3mmol; 0.531g) was added to this solution with continuous stirring and the pH was maintained at 9.6 by titration with 1M NaOH. After 4 hours the pH was adjusted to 7 with 1M HCl. Solid unreacted N-methylisatoic anhydride was removed by filtration and the solution was loaded onto a column of Sephadex LH20 (140

cm^3). The column was eluted with water at a flow rate of 50ml/hour and 5ml fractions were collected. The product was identified by TLC using silica plates developed in propan-1-ol/ ammonium hydroxide/ water (6:3:1 (v/v)) and 0.5mg/ml EDTA. Fractions 24-28 gave single spots (Rf 0.22). These were pooled and further purified by ion-exchange chromatography using Sephadex A25. The product was obtained as a clear gum with a blue fluorescence (221μmoles; 11%). The absorption spectrum gave maxima at 255nm (corresponding to the adenosine moeity) and 354nm (corresponding to the mant group).

^{31}P δ(24.3MHz, D_2O) -10.6 (d, J = 24 Hz), -21.1 (overlapping dd; J = 22 Hz), -5.4 (d; J = 19 Hz)

2.3. NMR spectra.

Routine ^{31}P-NMR spectra were recorded on a Jeol FX60 machine operating at 24.3 MHz and on a multiprobe Jeol FX90Q machine operating at 36.5 MHz. An external D_2O lock was used and chemical shifts were related to 85% H_3PO_4. High field ^{31}P spectra were recorded on Bruker AM300 and AM500 machines operating at 121.5 MHz and 202.5 MHz respectively. Routine ^1H-NMR spectra were recorded on a Varian EM-390 machine operating at 90MHz.

2.4. Anion-exchange chromatography using DEAE-Sephadex A25 resin.

Diethylaminoethyl (DEAE) Sephadex provides a convenient support for the separation of negatively charged molecules. 1M TEAB buffer was prepared by bubbling CO_2 (produced from dry ice) through a 1M solution of freshly distilled triethylamine until the pH was approximately 7.6. The buffer was stored at 4°C for up to 3 months. Approximately 20g DEAE-Sephadex A25 (Pharmacia) was activated from powder by treatment overnight with 1M NH_4HCO_3. The swelled resin was then washed thoroughly with water and stored in a sealed beaker at 4°C in a fridge. A suitably sized glass column

was filled with resin which was packed and equilibrated with water. The sample was loaded onto the column via a peristaltic pump (LKB) and eluted with approximately 20 column volumes of a linear concentration gradient of TEAB. The eluate was monitored spectroscopically at 260nm and collected in a fraction collector. Used Sephadex was regenerated by treatment with 1M NH_4HCO_3 followed by water.

2.5. Thin-layer chromatography (TLC).

Nucleotides were analysed on both silica and PEI-cellulose TLC plates. For silica plates highly polar solvent systems are required since nucleotides are themselves very polar molecules. The system used consisted of ethanol/ammonium acetate (7:3). Precoated silica plates of 0.2mm thickness on aluminium were used (60F-254; Merck & Co.). PEI-cellulose TLC plates generally gave better separations than silica plates and were developed in 0.75M KH_2PO_4 (pH 3.4).

2.6. High Performance Liquid Chromatography (HPLC).

Reverse phase HPLC was used both analytically and preparatively to separate mixtures of nucleotides. Separations were performed on either a Shimadzu LC-4A fitted with a Shimadzu CR2 AX chart recorder or a Hewlett-Packard HP1090 dual pump machine with an automatic injector. For analytical separations a 5µm ODS-hypersil 25mm x 4.6mm C_{18} reverse phase column (FSA chromatography) was used while a larger column (25mm x 10mm) was used for preparative purposes. Conditions were based on those reported by Lazewska and Granowski (1990); Ludwig and Eckstein (1989); Marquetant and Goody (1983). The column was equilibrated with 100mM TEAB (pH 7.6) at a flow rate of 1.5-2.0ml/min. or 4ml/min. for the analytical or preparative column respectively. Between 12nmoles (analytical column) and 5µmoles (preparative column) of nucleotide in 24µl to 500µl was injected via a rheodyne onto the column and eluted with a linear gradient of acetonitrile. The gradients used varied for different experiments up to 20% acetonitrile. For the separation of the diastereoisomers of $ATP_{\beta}S$ 20mM

$MgCl_2$ was included in the TEAB buffer. It was important not to exceed 20% acetonitrile in the $MgCl_2$ experiments because $MgCl_2$ was insoluble at high acetonitrile concentrations.

2.7. Bacterial growth media.

All media for the growth of bacteria were prepared and sterilised using standard microbiological techniques. For plate media 15g/L of agar (Oxoid code L11) were added to each of the recipes.

Luria-Bertani (LB) medium.

Tryptone (Difco)	10.0g
Yeast extract (Difco)	5.0g
NaCl	10.0g
Water to 1L	

Super broth medium.

This broth gives yields of DNA much greater than those obtained with LB broth.

Tryptone (Difco)	12.0g
Yeast extract (Difco)	24.0g
Glycerol	8.0ml
Water to 900ml	

Phosphate buffer solution:

KH_2PO_4	0.17M
K_2HPO_4	0.72M
Water to 100ml	

The two above solutions were autoclaved separately and combined when cool.

2.8. Antibiotics in growth media.

Antibiotic	Stock concentration	Concentration used
Ampicillin (Na salt)	50mg/ml	50-100μg/ml
Tetracycline (hydrochloride)	15mg/ml freshly made.	15μg/ml

2.9. Plasmids used in this study.

pBR322 (4361bp)

A multi-purpose cloning vector carrying the genes for ampicillin and tetracycline resistance (Bolivar *et al.*, 1977).

pAG111 (7.2kb)

A plasmid based on pTTQ18 harbouring the *gyrB* gene under the control of the tac promotor (Hallett *et al.*, 1990).

pAJ1 (7.2kb)

Based on pAG111 with a stop codon engineered into the *gyrB* gene to produce a 43kDa truncated protein corresponding to the N-terminal domain of the gyrase B protein (Jackson *et al.*, 1991).

2.10. Removal of proteins from nucleic acid solutions by extraction with phenol:chloroform.

Proteins were removed from samples of nucleic acids by extraction with an equal volume of phenol/chloroform/isoamyl alcohol (25:24:1) equilibrated with TE (10mM Tris.HCl (pH 7.5), 1mM EDTA). 8-hydroxyquinoline (0.1%) was also added to the phenol/chloroform/isoamyl alcohol solution as an antioxidant and weak chelator of metal ions. This gives the phenol mixture a straw-coloured appearance. Most phenol extractions were carried out on a small scale in 1.5ml Eppendorf tubes. Equal volumes of sample and phenol/chloroform/isoamyl alcohol were vortexed thoroughly and the phases separated by centrifugation at 12,000 rpm for 2 min. The upper aqueous phase was

transferred to a fresh tube taking care to avoid carry over of protein from the interface or phenol. Occasionally, to achieve the best recovery, the organic phase was back extracted with an equal volume of TE and this was combined with the first extraction. An equal volume of chloroform/isoamyl alcohol (24:1) was added to extract the phenol and the aqueous layer was transferred to a fresh tube after centrifugation at 12,000 rpm for 2 min.

2.11. Ethanol precipitation of nucleic acids.

This rapid method for concentrating DNA samples was generally performed on a small scale in 1.5ml Eppendorf tubes. Sterile 3M sodium acetate was added to aqueous solutions of nucleic acids to give a final concentration of 0.3M. 3 volumes of ice-cold 100% ethanol were added and the tubes were mixed well and left on dry ice for 15 min. to precipitate fully. The precipitate was recovered by centrifugation at 12,000 rpm for 10 min. at 4°C and then washed with 70% ethanol to remove salt. After further centrifugation for 2 min. at 4°C, the DNA was dried under vacuum using a Gyrovap (Howe) or a lyophiliser (Edwards Modulyo). The DNA was resuspended in a suitable volume of sterile TE and stored at 4°C.

2.12. Determination of the concentration of DNA in solution.

The concentration of a DNA sample was determined spectrophotometrically using a suitable dilution of the sample in TE and measuring its A_{260}. An absorbance of 1 corresponds to a concentration of approximately 50µg/ml for double-stranded DNA and 40µg/ml for single stranded DNA. The purity of the DNA sample was estimated from the ratio of A_{260}/A_{280} where a value of 1.8 indicates pure DNA and a value of 2.0 corresponds to pure RNA. In the presence of contaminating protein or phenol the ratios above are reduced.

2.13. Protein concentration determination.

Protein concentrations in solution were determined by the method of Bradford (1976). An appropriate volume of the protein solution was diluted into 100µl total of Enzyme Buffer (50mM Tris.HCl (pH 7.5), 100mM KCl, 10% ($^{w}/_{v}$) glycerol, 5mM DTT, 1mM EDTA), and 1ml of Bradford Reagent was added. The Bradford Reagent reagent was prepared by dissolving 100mg of Coomassie Brilliant Blue G-250 (Serva) in 50ml 95% ethanol. To this solution was added 100ml 85% ($^{w}/_{v}$) phosphoric acid and the resulting solution was made up to a final volume of 1L with distilled water. This solution was filtered through Whatman no.1 filter paper. Absorbance at A_{595} was determined after incubation at room temperature for 5 min. and compared to a standard curve constructed with bovine serum albumin.

2.14. Preparation of cell extracts using a French press.

All components of the French press were thoroughly cooled in ice before use. An aliquot of cells in Tris/Sucrose was thawed and the following were added: DTT to 2mM, EDTA to 20mM, and KCl to 100mM. The cells were passed two or three times through the press which was kept at a pressure of between 8,000 to 12,000 psi. Cell debris was removed by centrifugation at 35,000 rpm in a Beckman VTi 50 rotor for 1 hour at 2°C. The supernatant was transferred to a sterile Falcon tube and either quick-frozen in liquid nitrogen for storage at -70°C or purified further directly.

2.15. Preparation of cell extracts by sonication.

Sonication was used to prepare small scale cell extracts for quick analysis. Harvested cells were resuspended in approximately 250µl Enzyme Buffer (50mM Tris.HCl (pH 7.5), 100mM KCl, 10% ($^{w}/_{v}$) glycerol, 5mM DTT, 1mM EDTA) and disrupted by two 20s bursts of sonication in an MSE 150W ultrasonic disintegrator set at amplitude 7 and medium power, using a precooled 3mm stainless steel probe. Cell debris was removed by centrifugation at 12,000 rpm for 2 min. at 4°C and the supernatants collected.

2.16. Gel Electrophoresis.

Electrophoresis through agarose or polyacrylamide gels was used to separate and identify DNA fragments and proteins. Both types of gel consist of a complex matrix of polymers through which the macromolecule migrates under an applied electric field by virtue of its charge at the ambient pH.

2.16.1. Agarose gel electrophoresis of DNA.

Agarose (Miles), at a concentration of 0.8-1.0% ($^{w}/_{v}$) depending on the experiment, was melted in TAE (40mM Tris acetate, 2mM EDTA) and poured into a suitable purpose-built former (25-100ml capacity). Once set, the gel was transferred to a horizontal gel electrophoresis tank and submerged in TAE buffer. DNA samples were loaded and electrophoresed until the bromophenol blue dye present in the samples neared the end of the gel. The DNA was then stained for 10 min. in a solution of ethidium bromide (2μg/ml) in TAE buffer and then destained in TAE prior to visualisation of the DNA with a transilluminator operating at 302nm. Gels were photographed using Kodak TMAX 5" x 4" professional film which was developed in Kodak D-19 developer and fixed with Kodak FX-40 fixer for 5 min.

2.16.2 Resolution of negatively supercoiled topoisomers.

On normal agarose gels supercoiled DNA has a greater mobility than relaxed DNA. The supercoiled band actually consists of many topoisomers which are not resolved. In the presence of the intercalating agent, chloroquine, these topoisomers can be revealed. Chloroquine exerts its effect by intercalating between the DNA bases and consequently decreasing the twist of the DNA. Since the linking number remains unchanged there is a compensating increase in the writhe of the DNA. Thus negatively supercoiled DNA is made more positively supercoiled and the magnitude of this effect is proportional to the concentration of chloroquine until the DNA is saturated with the intercalator.

0.8% Agarose gels were made up in TPE buffer (40mM Tris base, 30mM sodium dihydrogen phosphate, 0.5mM EDTA) in the presence of various concentrations of chloroquine (3-90μg/ml) and were electrophoresed in TPE buffer (containing the same concentration of chloroquine) which was recirculated. Gels were run as far as possible for optimum topoisomer separation and destained by 3 x 60 min. immersions in fresh 1L TPE buffer before staining with ethidium bromide and photography.

2.16.3. Gel retardation Assays.

The binding of protein to DNA fragments can often be followed by gel electrophoresis (Garner and Revzin, 1986). A stable protein-DNA complex can be distinguished from free DNA by its different electrophoretic mobility. The binding of gyrase to a 172bp DNA fragment (containing the preferred gyrase DNA binding site of the sea urchin 5S rRNA gene (Rau *et al.*, 1987; Simpson *et al.*, 1985)) was performed essentially as described by Maxwell and Gellert (1984). DNA gyrase was incubated for 60 min. at 25°C with the 172bp DNA fragment in 50mM Tris.HCl (pH 7.5), 55mM KCl, 4mM $MgCl_2$, 5mM DTT, 5% glycerol, 0.36mg/ml BSA. The reactions were then electrophoresed through a 5% polyacrylamide Tris-borate-$MgCl_2$ (TBM) native gel in TBM buffer (90mM Tris.HCl (pH 7.5), 90mM boric acid, 5mM $MgCl_2$) using a BioRad MiniProtean II mini-gel system. Gels contained 5% Acrylamide (29:1 Acryl:bis), 90mM Tris.HCl (pH 7.5), 90mM boric acid, 5mM $MgCl_2$, 0.1% ($^{w}/_{v}$) AMPS, 0.1% ($^{v}/_{v}$) TEMED and were poured between two glass plates separated by 0.75mm. Gels were prerun at 25mA for 30 min. before loading the binding reaction mixtures. These were loaded without the addition of dye as this disrupts the protein-DNA complex. Dye was loaded into separate wells to indicate the progress of samples on the gel. After electrophoresis the gels were stained with ethidium bromide to show the DNA or silver to show both the protein and the DNA.

2.16.4. Silver staining of polyacrylamide gels.

All manipulations were carried out in a siliconised evaporating dish on a briskly rotating table. Fixing solution was contained 40% methanol, 5% acetic acid. Staining solution was prepared with 12 ml 0.36% ($^{w}/_{v}$) NaOH, 1 ml concentrated ammonia solution, 0.5 g silver nitrate, 50 ml 20% ($^{v}/_{v}$) ethanol. If the brown colour persisted more ammonia solution was added dropwise until clear. Developing solution was prepared with 250 ml water, 1.25 ml 1% ($^{w}/_{v}$) citric acid, 125 µl 40% ($^{w}/_{v}$) formaldehyde. The gel was fixed for at least 15 min. in 100ml fixing solution and then washed 3 times with 100ml water for 10 min. Half of the staining solution (preincubated at 37°C) was added and left for 10 min. This was repeated for the remaining staining solution, and the gel was then washed with 3 treatments of water. The gel was then developed with 50-100ml aliquots of developing solution until a satisfactory image was obtained which was fixed with 100ml of fixing solution. Gels were photographed using a blue Wratten 47 filter.

2.16.5. Polyacrylamide gel electrophoresis of proteins (SDS-PAGE).

Proteins were analysed on 12.5% discontinuous polyacrylamide gels containing 0.1% ($^{w}/_{v}$) SDS with a 4% polyacrylamide stacking gel (Laemmli, 1970), using a Mini Protean II gel system (BioRad) according to the methods of Hames (1981). Generally 0.75mm thick gels were employed. A 3ml separating gel (pH 8.8) was poured between clean glass plates in a casting stand and left to fully polymerise. 1.5ml of stacking gel was overlayed on the separating gel and a sample comb was inserted. The prepared polyacrylamide gel was held vertically in place in an electrophoresis tank which was filled with 500ml SDS Running Buffer (25mM Tris, 192mM glycine, 01%($^{w}/_{v}$) SDS). The separating and stacking gels were made up as shown in the following table:

	12.5% Separating Gel (ml)	4% Stacking Gel (ml)
30% Acrylamide (37.5:1 Acryl: Bisacryl)	4.0	1.35
1M Tris.HCl (pH 8.8)	3.75	-
1M Tris.HCl (pH 6.8)	-	1.25
10% SDS	0.1	0.1
10% AMPS	0.05	0.05
Water	2.1	7.35
TEMED	0.01	0.01

Protein samples were prepared by adding an equal volume of Sample Application Buffer (125mM Tris.HCl (pH 6.8), 4% SDS, 20% ($^{w}/_{v}$) glycerol, 10% β-mercaptoethanol, 0.002% bromophenol blue) and placing in a boiling water bath for 5 min. Gels were run at 200V for 45 min. and stained for 30 min. in 30% ($^{v}/_{v}$) methanol, 0.01% ($^{w}/_{v}$) Coomassie Brilliant Blue R (Sigma), 12% ($^{w}/_{v}$) trichloroacetic acid, 10% ($^{w}/_{v}$) sulfosalicylic acid (Sigma). The gel was destained for several hours in 7.5% acetic acid, 5% ethanol. Gels were photographed using Kodak Tmax 100 4" x 5" film.

2.17. Isolation of plasmid DNA

Plasmid DNA was isolated by the method of Birnboim and Doily (1979), either on a small analytical scale or a large scale for the preparation of milligram quantities used in assays. Plasmids isolated on the large scale method were purified by equilibrium gradient centrifugation in caesium chloride and ethidium bromide (Radloff *et al.*, 1967).

2.17.1. Microscale isolation of plasmid DNA by alkaline lysis

A 5ml overnight culture was grown up in a 30ml sterile universal tube in the presence of ampicillin at 50μg/ml (or other suitable antibiotic depending on the plasmid's resistance

gene). The following day, 1ml of the culture was transferred to a sterile Eppendorf tube and centrifuged at 12,000 rpm for 2 min. The supernatant was removed by aspiration using a disposable pipette tip attached to a water pump, and the pellet was resuspended in 100µl of ice-cold Solution 1 (25mM Tris.HCl (pH 8.0), 50mM sucrose, 10mM EDTA) containing 2mg/ml lysozyme, and incubated on ice for 5 min. The resulting sphaeroplasts were then lysed by addition of 200µl of Solution 2 (0.2M NaOH, 1%($^{w}/_{v}$) SDS), which was thoroughly mixed by inverting the tubes several times (but not vortexing). After incubating the tubes on ice for 5 min., 150µl of ice-cold Solution 3 (3M sodium acetate (pH 4.8)) was added and mixed well by gentle vortexing. The tubes were incubated on ice for a further 5 min. to allow chromosomal DNA to form an insoluble precipitate with the majority of proteins and high molecular weight RNA, leaving the covalently closed circular plasmid DNA in solution. The precipitate was pelletted by centrifugation at 12,000 rpm for 5 min. and the supernatant was transferred to a fresh tube. Contaminating proteins were removed by phenol extraction and the plasmid DNA was precipitated with ethanol. The DNA pellet was dried in a lyophiliser and resuspended in 20µl of sterile TE containing ribonuclease A (25µg/ml).

2.17.2. Large Scale isolation of plasmid DNA

A 5ml overnight culture of *E. coli*, containing the plasmid of interest, was inoculated into either 4 or 8 x 400ml of Super Broth in baffled conical flasks and grown at 37°C in a shaking incubator for 48 hours. The cultures were transferred to Beckman polycarbonate bottles and centrifuged at 8,000 rpm for 10min. at 4°C in a Beckman J2-21 centrifuge with a Beckman JA10 rotor. The pellets were resuspended in 48ml Solution 1. A further 12ml of Solution 1 containing 10 mg/ml lysozyme was added and the solution was incubated at room temperature for 10 min. The weakened cells were lysed by the addition of 120ml of Solution 2, thoroughly mixed by inversion, and incubated on ice for 5 min. Chromosomal DNA, proteins, and high molecular weight RNA were precipitated by neutralisation with 60ml Solution 3 and incubation on ice for 15 min. The precipitate was

pelleted by centrifugation for 10 min. at 8,000 rpm at 4°C and the supernatant was filtered through glass wool into a fresh polycarbonate bottle. Nucleic acids were precipitated by the addition of 150ml propan-2-ol and incubation at room temperature for 5 min. After centrifugation for 10 min. at 8,000 rpm at 20°C, the supernatant was removed and the pellet resuspended in 4 ml TE. The sample was accurately weighed.

At this stage the resuspended sample contained large amounts of RNA, some chromosomal DNA, and open-circular (or nicked) plasmid DNA, in addition to the required ccc plasmid DNA. The sample was made free of these contaminants by the use of ethidium bromide - CsCl density gradient centrifugation. 1.019g of ultrapure CsCl was added per gram of sample, followed by 0.11ml of ethidium bromide per gram of sample. The resulting solution had a refractive index of 1.392-1.400, and was pipetted into a Beckman polyallomer tube (39ml capacity), heat sealed, and centrifuged using a VTi50 rotor in a Beckman L5-65 ultracentrifuge at 45,000 rpm overnight. This produces a density gradient of CsCl with the downward centrifugal pull on the caesium and chloride ions being balanced by diffusion. Where a macromolecule bands in this gradient is dependent on its buoyant density. DNA has a buoyant density of about 1.7 g/cm^3 and migrates to near the middle of the gradient. Proteins have much lower buoyant densities and float to the top of the tube while RNA will pellet at the bottom. The presence of a saturating concentration of ethidium bromide allows supercoiled ccc plasmid DNA to be resolved from linear and nicked-circular DNA. Ethidium bromide binds to DNA by intercalating between adjacent base pairs, causing partial unwinding of the double helix. This unwinding results in a decrease in the buoyant density of the DNA. Supercoiled ccc DNA has much less freedom to unwind than linear or nicked-circular DNA and it is therefore able to bind much less ethidium. The buoyant density of supercoiled ccc DNA is therefore greater than linear or nicked-circular DNA.

After centrifugation, the ccc plasmid DNA was visualised under a long-wave UV light source as an intensely fluorescent band half-way down the tube. This band was removed using a sterile disposable syringe and a 20 gauge needle, and transferred to a smaller Beckman polyallomer tube (5.1ml capacity) which was filled using a balance solution of CsCl/ethidium bromide, heat sealed, and centrifuged in a VTi65.2 rotor in a Beckman L5-65 ultracentrifuge at 48,000 rpm overnight.

The ccc DNA band was removed as described above and transferred to a 30ml Corex tube. The ethidium bromide was removed by extracting 5-6 times with equal volumes of water-saturated butanol. Equal volumes of propan-2-ol and water were added and the DNA was left to precipitate at room temperature for 2 hours. The precipitate was then pelleted by centrifugation at 8,000 rpm for 30 min. at 4°C using a swing-out rotor in a Sorval RC-5B centrifuge. After drying the pellet in a lyophiliser it was resuspended in a minimum volume of TE and the yield of purified plasmid was determined spectrophotometrically by its absorption at A_{260}. The DNA was stored at 4°C.

2.18. Preparation of relaxed DNA

Relaxed pBR322 for use as the standard substrate in gyrase supercoiling assays was prepared from native supercoiled plasmid according to Bates and Maxwell (1989). Purified supercoiled pBR322, was incubated in 20mM Tris.HCl (pH 8.0), 200mM NaCl, 0.25mM EDTA, 5% ($^{w}/_{v}$) glycerol, 100µg/ml BSA, 3µl chicken erythrocyte topoisomerase I (40 units/µl; gift of Anthony Maxwell, Dept. of Biochemistry, this University) at 37°C for 60 min. Relaxation was confirmed by electrophoresis on a 1% agarose gel and then purified from nicked and linear DNA by equilibrium gradient centrifugation with CsCl and ethidium bromide.

2.19. Preparation of nicked pBR322.

Nicked pBR322 was prepared from supercoiled plasmid by the action of DNase I in the presence of saturating amounts of ethidium bromide (Greenfield *et al.*, 1975). On binding to DNA, ethidium bromide causes the DNA backbone to untwist. Supercoiled DNA is topologically constrained and is less able to untwist than nicked DNA. Consequently supercoiled DNA can bind much less ethidium than nicked DNA. When supercoiled DNA is treated with DNase in the presence of ethidium bromide the first nick introduced into the DNA allows it to untwist and bind further ethidium. This is believed to drastically alter the conformation of the DNA such that it is no longer a substrate for the DNase catalysed reaction. In this way plasmids can be prepared which contain a single nick per molecule.

The reaction (total volume 6ml) contained the following: 20mM Tris.HCl (pH 7.5), 150mM NaCl, 5mM $MgCl_2$, 5mM $CaCl_2$, 0.3mg supercoiled pBR322, 4.5mg/ml ethidium bromide, 15units DNase I (Boehringer). After incubating for 60 min. at 25°C the reaction was stopped by chloroform extraction and the DNA was isolated by ethanol precipitation . The nicked DNA was purified by equilibrium density centrifugation on a CsCl/ethidium bromide gradient.

2.20. Preparation of topoisomer standards.

A series of topoisomers of different negative superhelicity was prepared by the action of a eukaryotic topoisomerase I on native supercoiled pBR322 in the presence of different amounts of ethidium bromide. Ethidium bromide binds to the DNA reducing the twist and thus increasing the writhe. Depending on the ethidium concentration, DNA with varying levels of writhe can be formed. Relaxation with a eukaryotic topoisomerase I, which can relax negative and positive supercoils (Champoux and Dulbecco, 1972), gives an apparently relaxed plasmid with ethidium bromide still bound. On extraction of the ethidium bromide and the topoisomerase, the plasmid becomes negatively supercoiled

with the superhelical density being proportional to the concentration of ethidium bromide previously present.

Reactions were performed in 100µl volumes and contained 20mM Tris.HCl (pH 8.0), 200mM NaCl, 0.25mM EDTA, 5% ($^{w}/_{v}$) glycerol, 100µg/ml BSA, 20µg/ml native-supercoiled pBR322, 1µl chick erythrocyte topoisomerase I, ethidium bromide at various concentrations (0-2.61µg/ml). The reactions were incubated at 25°C for 60 min. and the protein and ethidium were removed by phenol/chloroform extraction followed by back extraction with 10µl 2% SDS. A series of chloroquine gels were run to determine the levels of supercoiling in the different samples.

2.21. Preparation of *E. coli* DNA gyrase.

The A and B subunits of DNA gyrase were prepared separately from *E.coli* strains harbouring plasmids containing the *gyrA* or *gyrB* gene as appropriate. Throughout all stages in the purification of the proteins the temperature was kept to 4°C or below.

2.21.1. Preparation of the DNA gyrase A subunit (GyrA).

Partially purified GyrA (purified from cell extracts of *E. coli* strain RW1053 (harbouring pMK90 (Mizuuchi *et al.*, 1984)) by ammonium sulphate precipitation and DEAE-sepharose column chromatography) was a gift of Anthony Maxwell. The protein was obtained in TGED (50mM Tris.HCl (pH 7.5), 10% ($^{w}/_{v}$) glycerol, 1.0mM EDTA, 5mM DTT) and approximately 0.25M NaCl (determined by conductivity measurements). Samples were made approximately 0.15M with respect to salt concentration before anion exchange chromatography using a Mono Q 5/5 column (Pharmacia) and a Fast Protein Liquid Chromatography (FPLC) machine (Pharmacia). After equilibrating the column with TED (50mM Tris.HCl (pH 7.5), 1.0mM EDTA, 5mM DTT), the protein solution was loaded via a superloop and eluted at a flow rate of 1ml/min. with a linear gradient of 0-0.6M NaCl in TED. GyrA eluted at about 0.4M NaCl. Peak fractions (as determined

by SDS-PAGE) were pooled and dialysed overnight against Enzyme Buffer (50mM Tris.HCl (pH 7.5), 100mM KCl, 5mM DTT, 1mM EDTA, 10% ($^{w}/_{v}$) glycerol). The protein was then aliquotted, quick-frozen in liquid nitrogen, and stored at -70°C. From SDS-PAGE gels GyrA was estimated to be >95% pure.

2.21.2. Preparation of the DNA gyrase B subunit (GyrB).

E. coli strain JMtacB (JM109 containing pAG111 with the *gyrB* gene under tight control of the *tac* promoter (Hallett *et al.*, 1990)) was streaked out onto an LB agar plate containing 100µg/ml ampicillin and incubated at 37°C overnight. A single colony was inoculated into 10ml LB which was grown up overnight at 37°C and used to inoculate 200ml LB which was incubated overnight at 37°C. The 200ml culture was aseptically decanted into an 'inoculating flask' which was used to inoculate 12L of pre-sterilised LB at 37°C in an LH 2000 series 1 fermenter. A sterile air supply was connected to the inoculating flask which was, in turn, connected to the fermenter via a sterile inoculating needle. Sterile air was blown into the flask, displacing the culture into the fermenter. The culture was grown using a stirring rate of 600 rpm and a sparge rate of 15L/min. of sterile air while the pH was maintained automatically at pH 7.0 with 1M KOH.

When the A_{595} was approximately 0.5, the cells were induced by the addition of IPTG to a final concentration of 50µM. The culture was grown up until the A_{595} started to plateau ($A_{595} \approx 3.5\text{-}5.0$). The cultures were chilled on ice and then centrifuged at 5,000 rpm for 10 min. to pellet the cells. Cell pellets were resuspended in a minimum volume of Tris/Sucrose (50mM Tris.HCl (pH 7.5), 10% sucrose) and either quick-frozen in liquid nitrogen before storage at -70°C or processed further directly.

Cell extract was prepared using a French press (see 2.14) and dialysed against TGED overnight. A column of Heparin-Sepharose (Pharmacia) was washed with 3-4 column volumes 1M NaCl and equilibrated with at least 5 column volumes of TGED. The

dialysed GyrB cell extract was then loaded onto the column and recirculated for 1hour to ensure maximum protein binding to the column. The protein was eluted with a linear gradient of 0-0.5M NaCl at a flow rate of between 1-2ml/min. with GyrB eluting at approximately 0.18M NaCl. Peak fractions were identified by SDS-PAGE and pooled. The salt concentration was made < 0.1M by dilution with TED and the protein was loaded onto an FPLC Mono Q 5/5 column (Pharmacia) equilibrated in TED. Protein was eluted with a linear gradient of 0-0.6M NaCl in TED. Peak fractions were pooled, dialysed into Enzyme Buffer overnight, aliquotted, and quick-frozen in liquid nitrogen for storage at -70°C. The purity of GyrB was estimated to be > 90%.

2.22. Determination of the activities of the gyrase subunits

The activities of the individual subunits were determined from supercoiling assays. One subunit was added to the assay in excess so that an estimate of the activity of the limiting subunit could be made from serial dilutions. 1 unit of activity was defined as the amount of the limiting subunit required to convert 50% of the relaxed DNA to the supercoiled form in 1 hour at 25°C as estimated from the relative intensity of the supercoiled band on an agarose gel.

2.23. Reconstitution of DNA gyrase from its subunits.

The DNA gyrase tetramer was reconstituted from its subunits by incubating equimolar quantities of each subunit at 25°C for 30 min. in 50mM Tris.HCl (pH 7.5), 100mM KCl, 10% ($^{w}/_{v}$) glycerol, 5mM DTT, 1mM EDTA, quick-frozen and stored at -70°C. In calculating an equimolar mixture of A and B proteins the following Bradford reagent correction factors were used (M. Gellert, personal communication): GyrA: 1.43; GyrB: 0.71. The specific activity of the tetramer was determined from supercoiling assays with serial dilutions of the protein.

2.24. 43kDa fragment preparation.

E. coli strain JM109 (harbouring plasmid pAJ1) was streaked out onto a plate which was grown overnight at 37°C. A single colony was used to inoculate 10ml LB which was grown up overnight and used to inoculate 200ml LB which was grown overnight and transferred to an inoculating flask for the fermenter. The fermenter culture was grown as described for the GyrB preparation (2.21.2). A cell extract was prepared using a French press, and the 43kDa protein was purified on a Heparin-Sepharose column followed by an FPLC Mono Q step. Large scale purifications were accomplished using a High Load column (Pharmacia) in place of the Mono Q column. Using this column 50mg of protein were successfully purified in one run. The purified 43kDa protein was dialysed overnight into EB and quick-frozen for storage at -70°C.

2.25. Isolation of gyrase-DNA complexes via spun-columns.

Gyrase-DNA complexes were prepared in the absence of divalent metal ions by gel filtration of complexes preformed in the presence of Mg^{2+} ions.

DNA gyrase was incubated with relaxed pBR322 at 10µg/ml in standard supercoiling conditions minus nucleotide for 60 min. at 25°C. Spin-columns were prepared by packing Sephadex G50, equilibrated in column buffer (supercoiling buffer minus $MgCl_2$ and DTT), into 1ml disposable sterile syringes plugged with sterile glass wool. The columns were equilibrated by 5 treatments with 120µl of column buffer which was spun in a bench top centrifuge for 2 min. at 1500rpm. 120µl of the gyrase reaction mixture was then applied to each column which was spun at 1500rpm for 2 min. The eluents, containing the gyrase-DNA complexes in column buffer, were used immediately in further experiments.

2.26. ATPase assays

Three different ATPase assays were used; two measured P_i release while one measured ADP release.

2.26.1. Measurement of P_i formation using malachite green.

This assay worked by the formation of a phosphomolybdate complex with P_i which could be detected in a spectrophotometer at A_{600}-A_{650} (Chan *et al.*, 1986; Lanzetta *et al.*, 1979). In the standard assay 200µl of reaction mixture (which, for gyrase, was the same as a supercoiling assay mixture except for the DNA effector which was sometimes varied) were incubated for various times. 1ml of Malachite Green Reagent (1 volume of 4.2% ammonium molybdate in 5M HCl plus 3 volumes of 0.05% malachite green solution, incubated for 30 min. at room temperature for 30 min. and then filtered) was added to each sample. The mixture was incubated for 30 min. on ice and 40ml of 1.5% Tween 20 (polyoxyethylene sorbitan monolaurate) was added and the samples incubated for a further 15 min. at room temperature. The A_{650} was measured and compared to a standard curve constructed with stock solutions of potassium dihydrogen phosphate.

For most experiments a scaled down version of the assay in microtitre plates was used. 30µl of ATPase reaction mixture was incubated for various times (usually 5 hours) and successive two-fold dilutions were made in a microtitre plate. 150µl of Malachite Green Reagent was added to each well. The plate was incubated on ice for 30 min. and 20µl of 0.5% Tween 20 was added to each sample. After 15 min. at room temperature the plate was read at 630nm in a microtitre plate reader. An internal calibration of phosphate standards was incorporated on each plate.

2.26.2. Continuous enzyme-linked phosphate assay.

The ATPase activity of gyrase was monitored continuously by coupling the release of phosphate to the nucleoside phosphorylase catalysed phosphorolysis of 7-methyl

guanosine (m^7Guo) to 7-methylguanine (m^7Gua) (Banik and Roy, 1990). The gyrase ATPase reaction mixture was based on the supercoiling reaction conditions except that BSA was omitted. Reaction volumes were 150µl and contained, in addition to the gyrase reaction mixture components, 0.2 units nucleoside phosphorylase (Sigma) [previously dialysed into enzyme buffer and stored aliquotted at -70°C], and 60-180µM m^7Guo (Sigma). Assays were performed in fluorescence microcells and gyrase was added to initiate the reaction. The decrease in fluorescence was observed at 395nm (the excitation wavelength being 300nm) using either a Baird Atomic or an SLM 8000 fluorimeter (SLM instruments). The decrease in fluorescence with phosphate formation was calibrated with standard concentrations of potassium dihydrogen phosphate.

2.26.3. Pyruvate kinase/ lactate dehydrogenase assay for ADP formation.
The release of ADP was monitored continuously using pyruvate kinase coupled to lactate dehydrogenase and the oxidation of NADH. The gyrase reaction conditions were the same as the supercoiling reaction mixture except that the DNA effector was sometimes varied. In addition, 250µM NADH, 400mM phosphoenolpyruvate (PEP), pyruvate kinase (1.1 units), lactate dehydrogenase (1.4 units) were present and the total assay volume was 150µl in a quartz microcell. The decrease in absorbance was followed at 340nm and calibrated from the extinction coefficient of NADH (ε = 6220 at pH 7.5) and double-checked by addition of known amounts of ADP.

2.26.4. $ATP_\gamma S$ hydrolysis using ^{35}S-labelled material.
The hydrolysis of $ATP_\gamma{}^{35}S$ by gyrase to ADP and ^{35}S-labelled thiophosphate was investigated by incubating gyrase with the radioactive nucleotide for various times, separating the products on TLC, and counting in a scintillation counter. The reaction mixture for the hydrolysis reaction was the same as for the supercoiling reaction except that linear pBR322 (*Eco*RI digest) was used. Reactions were incubated at either 25°C or 37°C for up to 12 hours and then applied directly to PEI-cellulose TLC plates which were

developed in 0.75M KH_2PO_4 (pH 3.4). The TLC plates were then cut into segments and each segment was placed in a scintillation vial in 10ml of scintillation fluid (Optiscint T) which was then counted overnight in a scintillation counter.

2.27. DNA gyrase supercoiling assay.

The standard DNA supercoiling assay was based on that described by Mizuuchi *et al.* (1984) and carried out essentially as described by Bates and Maxwell (1989). The assay was performed in a 30µl reaction volume containing in addition to DNA gyrase: 35mM Tris.HCl (pH 7.5), 24mM KCl, $MgCl_2$ at 4mM above the nucleotide concentration, 1.8mM spermidine, 0.36mg/ml BSA, 9µg/ml tRNA, 6.5% ($^{w}/_{v}$) glycerol, 5mM DTT, 1.4mM ATP, 10µg/ml relaxed pBR322 DNA. The concentration of ATP or ATP analogues in certain supercoiling experiments was varied as shown in the results. Reactions were incubated at 25°C for 60 min. and 12µl of STEB stop dye (40% sucrose, 100mM Tris.HCl (pH 7.5), 1mM EDTA, 0.5mg/ml bromophenol blue) was added. Reactions were extracted with an equal volume of chloroform/isoamyl alcohol (24:1) and the DNA was electrophoresed through a 0.8% agarose gel in TAE buffer.

2.28. DNA gyrase relaxation assay.

The nucleotide-independent relaxation of negatively supercoiled DNA by gyrase (Gellert *et al.*, 1977), was assayed using similar conditions to the supercoiling assay except that native supercoiled pBR322 DNA was used instead of the relaxed form and spermidine and ATP were omitted. The standard assay involved incubating the components for 60 min. at 25°C, addition of STEB stop dye, extraction with chloroform/isoamyl alcohol, and electrophoresis as described for the supercoiling assay.

2.29. DNA gyrase DNA cleavage reaction.

Double-stranded cleavage of DNA by gyrase induced by the presence of a quinolone drug (Gellert *et al.*, 1977), was assayed using the same conditions as used for the supercoiling

assay except that alternative forms of DNA were used and ciprofloxacin at 3μg/ml was added while ATP was omitted. In some experiments on the cleavage pattern produced by gyrase the reactions were incubated for 60 min. without ciprofloxacin followed by treatment with the drug for 5 min. In all experiments 4μl of 2% SDS was added after incubation with ciprofloxacin and mixed by vortexing. 7μl of proteinase K at 10mg/ml were added followed by incubation at 37°C for 30 min. Electrophoresis through 1% agarose gels in TAE followed by staining with ethidium bromide revealed the cleaved DNA fragments.

2.30. Equilibrium experiments with arginine kinase.

The free energy of hydrolysis of ATP, $ATP_{\alpha}S$, and $ATP_{\beta}S$ were compared by investigating the relative equilibrium concentrations of the triphosphate and diphosphate of each of these nucleotides in the arginine kinase reaction. Reactions were carried out at 1mM nucleotide and 30mM nucleotide. The concentration of nucleotide was determined by A_{260}. Arginine solutions were quantitated by a PK/LDH coupled assay (see Section 2.26.3). The reaction mixture contained: 200mM Hepes pH 8.0, 10mM magnesium acetate, 100mM potassium chloride, 5mM DTT, 250mM NADH, 400mM PEP, 75units pyruvate kinase, 90 units lactate dehydrogenase, 1mM ATP, arginine kinase (0.165mg/ml; 120 units/mg), arginine. On addition of arginine there was a rapid drop in the absorbance corresponding to the concentration of arginine. Arginine kinase (Sigma) was dialysed into 200mM Hepes pH 8.0, 5mM DTT, 100mM glycine, and stored at 4°C.

The arginine kinase reactions contained 200mM Hepes, 5mM DTT, 5mM magnesium acetate, 1mM arginine, 1mM nucleotide, 10μl arginine kinase (1.65 mg/ml; 120units/mg) in a total volume of 500μl. (The reactions with 30mM nucleotide were identical except that 40mM magnesium acetate, 30mM arginine, and 50μl arginine kinase were used). At various times 100μl samples were removed and 25μl 2% SDS followed by 12μl of 10mg/ml proteinase K were added. The samples were incubated at 30°C for 30 min. and

then quick frozen and stored at -70°C until analysis by HPLC. 24µl of the samples were loaded directly onto a C_{18} reverse phase analytical column, fitted with a C_{18} guard column, and eluted with a linear gradient of acetonitrile (0 - 10% in 25 min.) in 100mM TEAB (pH 7.6). The relative concentrations of di- and trinucleotides were determined from the integrals of their peaks in the chromatograms.

Equilibrium concentrations were also determined from the integrals of peaks in ^{31}P-NMR experiments. Reactions were carried out in 5mm NMR tubes positioned inside 10mm NMR tubes containing D_2O and comprised the same as described for the 30mM nucleotide HPLC reaction in a total volume of 500µl. Spectra were obtained at 121.5 MHz in Fourier transform mode on a Bruker AM300 spectrometer with the sample temperature controlled at 30°C. Spectral parameters were: spectral width, 3600 Hz; pulse width, 10ms; aquisition time, 1.1s; pulse delay, 10s; line broadening, 1.7Hz.

2.31. Crystallisation of the gyrase 43kDa fragment.

Samples of 43kDa protein were laid down for crystallisation using the hanging drop method (Eisenberg and Hill, 1989), which allows a drop of protein solution to equilibrate by vapour diffusion with a reservoir of precipitant above which it is suspended. Equilibration occurs by distillation of water out of the drop and into the well, thereby concentrating both the protein and the precipitant in the drop towards saturation. Polyethylene glycol (PEG) was used as the precipitant. Since mixtures of PEG and protein provide a good medium for the growth of microbes (especially molds) stock solutions of PEG were passed through 0.2µm filters before use. The 43kDa protein was concentrated to 5-10mg/ml using an Amicon ultrafiltration unit with an Amicon diaflow YM30 membrane. The concentrated solution was dialysed overnight into crystallography buffer (20mM Tris.HCl (pH 7.0-8.8, depending on the pH conditions required), 5mM $MgCl_2$, 1mM DTT). The protein solution was centrifuged for 5 min. at 12,000rpm at 4°C to remove any precipitate and PEG (molecular weights used were 600; 1,000; 4,000;

6,000; 8,000; 20,000) was added to the desired concentration (usually 5%) in 1% steps to avoid precipitation. Nucleotide and other components such as salt to slow down crystallisation were added and the solution was gently mixed. 12µl drops were applied to clean plastic coverslips (Bel-Art) which were then inverted over the wells of a 24 well culture plate (Linbro, Flow Laboratories). The wells contained the precipitant at various concentrations (5-20%) in 2ml of crystallography buffer. An air-tight seal between the lip of each well and the cover slip was achieved with high vacuum grease. The culture plates were left undisturbed in an incubator at 22°C From time to time the plates were examined for the presence of crystals or precipitates using a binocular microscope (Wild M3C; Herrbrugg, Switzerland). Photographs were taken using an Olympus microscope fitted with an Olympus OM-1 camera and either Ilford FP4 black & white or Kodachrome 25/Fujikrome 100 colour slide film. Two polarising filters (Hoya), one in front of the microscope lens and the other in front of the light source, were rotated independently to provide plane polarised light.

Chapter 3

Positional Isotope Exchange and Stereochemical Investigations on the DNA Gyrase ATPase

3.1. INTRODUCTION

Two of the most basic questions that can be raised concerning the mechanism of phosphoryl transfer enzymes are:

(i) When do substrates combine and products leave the catalytic cycle (the kinetic mechanism)?

(ii) Are there any covalent intermediates formed during the reaction pathway (the chemical mechanism)?

Generally, for a complete understanding of the kinetic mechanism of an enzyme, a combination of steady state and pre-steady state kinetics is required (eg. see Fersht, 1985). In the case of gyrase-catalysed ATP hydrolysis, interpretation of steady state kinetic data is complicated by deviations from Michaelis-Menten behaviour (as already mentioned in Chapter 1). In this chapter, aspects of the kinetic mechanism of the gyrase ATPase have been addressed through the application of positional isotope exchange techniques. In addition, experiments directed towards the elucidation of the chemical mechanism of the ATPase reaction are described.

The gyrase ATPase and most other ATPases can be described by the following minimal scheme:

$$\text{ATP} + \text{E} \underset{k_{-1}}{\overset{k_1}{\rightleftharpoons}} \text{E.ATP} \underset{k_{-2}}{\overset{k_2\ (H_2O)}{\rightleftharpoons}} \text{E.ADP.P}_i \underset{k_{-3}}{\overset{k_3}{\rightleftharpoons}} \text{E} + \text{ADP} + \text{P}_i \qquad \text{(eqn. 3.1)}$$

ATP binds to the enzyme in step 1, hydrolysis of enzyme-bound ATP to bound ADP and P_i occurs in step 2, and product release occurs in step 3. If k_3 is much greater than k_{-2}, then product release occurs without further reaction. However, if k_{-2} is significant with respect to k_3, then resynthesis of bound ATP by reversal of step 2 can occur with a loss

of a P_i oxygen back to the water pool. If the P_i of the bound products complex has sufficient rotational freedom to scramble the P_i oxygens on reversal of step 2, then the water-derived oxygen incorporated in the first hydrolysis can be retained in the reformed ATP (Fig. 3.1). Clearly proton transfer steps must be implicated in this exchange process.

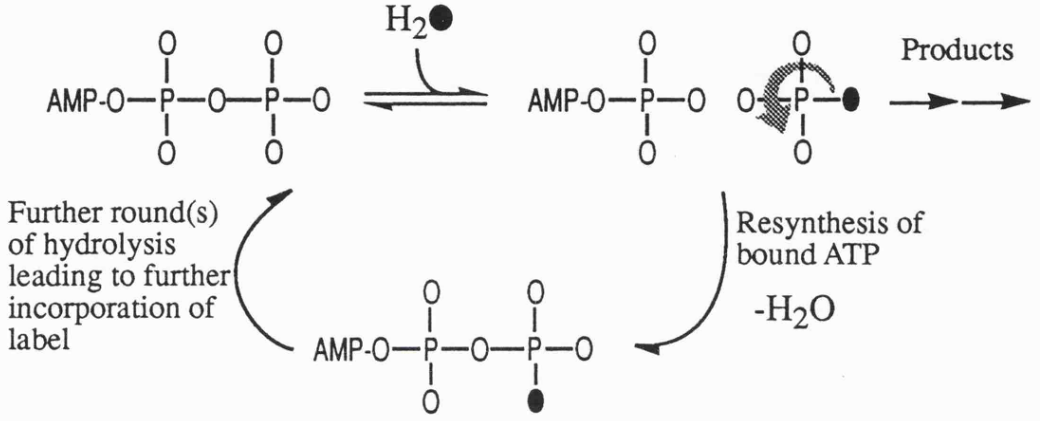

Figure 3.1. Phosphate-Water Exchange

Subsequent hydrolysis of this bound ATP will give P_i containing two water-derived oxygens and further cycles of ATP resynthesis and hydrolysis will produce P_i species with higher levels of incorporation of water-derived oxygens. If ^{18}O-labelled water is used then the incorporation of water-derived oxygens into P_i can be detected. For the simple model of equation 3.1, the ratio of k_{-2}/k_3 (known as the R value) can be calculated from the observed incorporation of ^{18}O into the released P_i. This type of exchange is a consequence of net hydrolysis and is designated *intermediate* exchange.

Other exchanges, known as *medium* exchanges, are also possible where no net chemical change is necessary. For example, incubating enzyme with ADP and P_i can result in exchange of P_i oxygens with water oxygens if the ADP and P_i are able to bind to the enzyme by reversal of step 3, undergo reversal of step 2 (with accompanying loss of a P_i oxygen to water), and then be released back to the medium in step 3. This is known as medium $P_i \rightleftharpoons$ water exchange. Exchange of γ-phosphoryl oxygens of ATP with water

can occur if ATP can bind to the enzyme in step 1, undergo hydrolysis and resynthesis in steps 2 and -2, and then dissociate from the enzyme by reversal of step 1. (i.e. medium ATP $\rightleftharpoons$ water exchange).

Oxygen isotope methods have been applied to the gyrase ATPase previously (D. Hackney, A. Maxwell, M. Gellert, unpublished manuscript). Gyrase was incubated with ATP in ^{18}O-labelled water and the product P_i was analysed for incorporation of ^{18}O after extensive ATP hydrolysis. The P_i from reaction mixture was isolated by ion exchange chromatography and derivatised to methyl, ethyl or propyl phosphate before mass spectral analysis. It was found that more than one ^{18}O was incorporated into P_i which is consistent with the on-enzyme ATP hydrolysis step (k_2) being reversible (see Fig 3.1 and Eqn. 3.1). Furthermore, taking into account statistical factors and the ^{18}O content in the water (98%), a value for the ratio of k_{-2}/k_3 was calculated. In the presence of an ATP regenerating system the R value was found to be 0.2 which increased about two-fold when no ATP regenerating system was present.

The finding that the on-enzyme hydrolysis of ATP was reversible opened the way to further analysis of the kinetic mechanism of ATP hydrolysis by similar oxygen isotope studies. Medium ATP$\rightleftharpoons^{18}O$ water exchange during net ATP hydrolysis and $P_i\rightleftharpoons^{18}O$ water exchange in the presence of ADP and P_i were very low which was interpreted as indicating that net ATP binding and net product release are essentially irreversible.

In this chapter, a complementary approach is described whereby the ATP off-rate (k_{-1}) has been analysed using ATP labelled uniquely at the β,γ-bridge position of the triphosphate chain. Thus it was planned to investigate whether any bridge to non-bridge scrambling of ^{18}O took place during net ATP hydrolysis catalysed by gyrase (Fig. 3.2). Given that the hydrolysis step (k_2 in Eqn 3.1) is reversible and making the assumption that the β-phosphoryl group of ADP possesses sufficient rotational freedom in the

enzyme-bound products complex, scrambling of ^{18}O should occur. Detection of this scrambling would then be dependent on the rate of dissociation of ATP (k_{-1}) compared to the rate of ATP hydrolysis (k_2). Thus it was anticipated that this approach would provide further information on the ATP off-rate in gyrase.

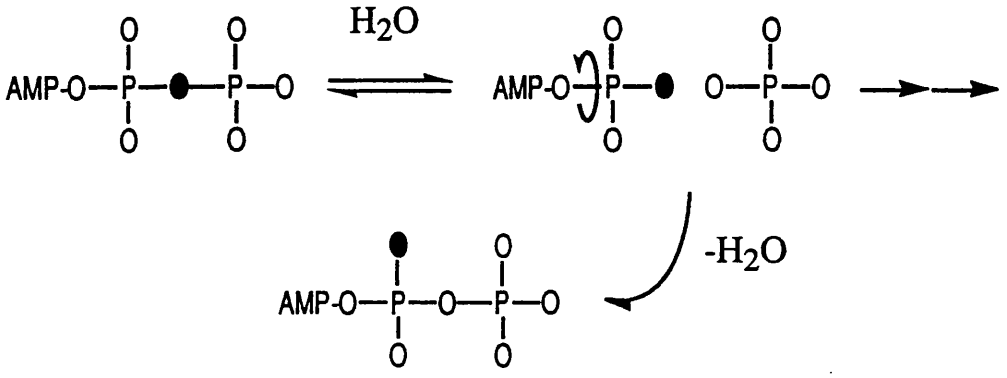

Figure 3.2. Bridge to non-bridge scrambling of ^{18}O label.

Investigations on the chemical mechanisms of phosphoryl transferases have focussed on whether a phosphoenzyme is involved in the reaction pathway and whether the reaction occurs *via* an associative (S_N2-like) or a dissociative (S_N1-like) mechanism. A number of approaches have been used to test for a phosphorylated enzyme intermediate although these have often proven inconclusive (see Cullis, 1988 for review). The most powerful and unambiguous evidence indicating the presence or absence of a phosphoenzyme intermediate comes from the determination of the stereochemical course of the reaction (i.e. whether the reaction proceeds with retention or inversion at phosphorous). Usher *et al.* (1970) pioneered the investigation of the stereochemistry of enzyme catalysed displacement reactions at phosphorous in their study of the ribonuclease A reaction. Subsequently, a wide range of phosphoryl transferases have been characterised from a stereochemical perspective and the approaches have been extensively reviewed (Cullis, 1988; Eckstein, 1985; Frey, 1982; Knowles, 1980). For the kinases, phosphoryl transfer from a mono substituted phosphate ester (such as the γ-phosphate of ATP) to an acceptor nucleophile involves a *pro-pro*-chiral substrate going to a *pro-pro*-chiral product.

Thus, in order to follow the stereochemical course of the reaction, the transferring phosphoryl group must be made chiral. Two methods have been developed based on isotopically chiral (^{16}O, ^{18}O) thiophosphate esters and (^{16}O, ^{17}O, ^{18}O) phosphate esters, together with configurational analyses of the products by ^{31}P-NMR (Buchwald *et al.*, 1982; Lowe, 1983). For phosphatases, such as ATPases, a *pro-pro*-chiral substrate is hydrolysed to a *pro-pro-pro*-chiral product (P_i) for which there is only one stereochemical approach based on chiral thiophosphate esters. Thus, in order to produce a chiral product, (γ-^{16}O, ^{18}O, S)ATP is required which is hydrolysed in ^{17}O-water to yield (^{16}O, ^{17}O, ^{18}O) chiral inorganic thiophosphate. Alternatively, (γ-^{17}O, ^{18}O, S)ATP can be prepared and hydrolysed in unlabelled water to yield chiral PS_i (Webb, 1982). The configuration of this product can then be analysed either by its enzymatic incorporation into $ATP_{\beta}S$(Sp) followed by ^{31}P-NMR (Webb and Trentham, 1980a), or by chemical derivatisation and ^{31}P-NMR (Arnold and Lowe, 1986).

The results of the stereochemical analyses of various kinases and phosphatases, using the chiral phosphate and chiral thiophosphate methodologies, are shown in Table 3.1. It can be seen that the majority of reactions proceed with inversion of configuration at phosphorous. Such inversion is generally interpreted as evidence for a single in-line nucleophilic substitution at phosphorous while retention of configuration is taken as evidence for two successive inversion steps with the involvement of a covalent phosphoenzyme intermediate. More precisely, overall inversion would accord with any odd number of in-line phosphoryl transfers whereas retention would imply an even number of transfers. However, in the absence of compelling evidence for multiple phosphoryl transfers pathways, the simplest mechanism is the most plausible. In principle, retention of configuration could also be observed if the reaction proceeded *via* an adjacent addition-elimination mechanism involving pseudorotation of the intermediate prior to the elimination step. In the same way inversion could be reconciled with a double displacement reaction mechanism involving a phosphoenzyme if an in-line displacement

Table 3.1. The stereochemical course of some of the kinases and phosphatases

Enzyme	Stereochemical course	(^{16}O,^{17}O,^{18}O) method	(^{16}O,^{18}O,S) method
Phosphokinases			
Acetate kinase	INV	(Blättler and Knowles, 1979)	
Adenosine kinase	INV		(Richard *et al.*, 1980)
Adenylate kinase	INV		(Richard and Frey, 1978)
Creatine kinase	INV	(Hansen and Knowles, 1981)	
Glucokinase	INV	(Pollard-Knight *et al.*, 1982)	
Glycerol kinase		(Blättler and Knowles, 1979)	(Blättler and Knowles, 1979; Orr *et al.*, 1978; Pluira *et al.*, 1980)
Hexokinase	INV	(Lowe and Potter, 1981)	(Blättler and Knowles, 1979; Orr *et al.*, 1978)
Nucleosidediphosphate kinase	RET		(Sheu *et al.*, 1979)
Nucleoside phosphotransferase	RET		(Richard *et al.*, 1979)
Phosphofructokinase	INV	(Jarvest *et al.*, 1981)	
Polynucleotide kinase	INV	(Jarvest and Lowe, 1981)	(Bryant *et al.*, 1981; Pluira *et al.*, 1980)
Pyruvate kinase	INV	(Lowe *et al.*, 1981)	(Blättler and Knowles, 1979; Orr *et al.*, 1978)
Ribulose phosphate kinase	INV		(Miziorki and Eckstein, 1984)
Thymidine kinase	INV	(Arnold *et al.*, 1986)	
			(^{16}O,^{17}O,^{18}O,S) method
Phosphatases			
Acid phosphatase	RET	(Saini *et al.*, 1981)	
Alkaline phosphatase	RET	(Jones *et al.*, 1978)	
Mitochondrial ATPase	INV		(Webb *et al.*, 1980)
Myosin ATPase	INV		(Webb and Trentham, 1980b)
Sarcoplasmic reticulum ATPase	RET		(Webb and Trentham, 1981)
Elongation factor G GTPase	INV		(Webb and Eccleston, 1981)
Elongation factor T GTPase	INV		(Eccleston and Webb, 1982)
p21 cHa-ras GTPase	INV		(Feuerstein *et al.*, 1989)
Thermophilic bacterium PS3 ATPase	INV		(Senter *et al.*, 1983)
Pyrophosphatase	INV		(Gonzalez *et al.*, 1984)
Glucose-6-phosphatase	RET	(Lowe and Potter, 1982)	
Snake venom 5'-nucleotidase	INV		(Tsai and Chang, 1980)

and an adjacent displacement occurred. However, there is no evidence for mechanisms involving pseudorotation in phosphoryl and nucleotidyl transferases. Furthermore, in all the cases where there is compelling evidence for a phosphoenzyme intermediate, either from kinetic approaches or from isolation, overall retention has been observed.

Thus the simplest interpretation of the stereochemical results in Table 3.1 is that individual enzyme-catalysed displacement reactions at phosphorous proceed by an associative in-line mechanism presumably involving a pentacoordinated transition state (or intermediate) with trigonal bipyramidal geometry and the in-coming and leaving groups in the apical positions. However, it is impossible to completely rule out a dissociative pathway that could still give inversion of configuration in which the initially formed metaphosphate is either tightly bound by the enzyme and prevented from tumbling in the active site or trapped by the second substrate before rotation can occur. To date, there is still some debate as to the whether the transition states in enzyme catalysed phosphoryl transfer reactions are predominantly associative or dissociative in character (eg. see Herschlag and Jencks (1987); Jones *et al.* (1991); Westheimer (1987)).

In the work described in this chapter, it was planned to investigate the feasibility of the stereochemical analysis of the gyrase ATPase by characterising the interaction of $ATP_{\gamma}S$ with the enzyme.

3.2. RESULTS

3.2.1. Positional isotope exchange (PIX) experiments with (β,γ-^{18}O) ATP

ATP specifically labelled with ^{18}O in the β,γ-bridge position was a gift of Paul Cullis (Department of Chemistry, this University). Control experiments established that this sample behaved identically to authentic ATP in gyrase supercoiling assays and ATPase assays (data not shown). ^{31}P-NMR was used to confirm that the ^{18}O isotope was present in the β,γ-bridge position. This analysis was based on the fact that ^{18}O gives rise to a small upfield shift in the ^{31}P signal of the phosphorous to which it is bonded and that the magnitude of this shift increases with increasing bond order (Cohn and Hu, 1978). The spectrum was consistent with the sample containing approximately 95% (β,γ-^{18}O) ATP, approximately 3% unlabelled ATP (which was identified by adding authentic ATP and rerecording the NMR), and approximately 2% (β-^{18}O) ATP (^{18}O in the non-bridge position of the β-phosphate).

It was planned to utilise the β,γ-^{18}O-ATP material to investigate whether scrambling of the label could be detected in the gyrase ATPase reaction as described in the introduction to this chapter. Thus gyrase was to be incubated with the labelled ATP and hydrolysis allowed to progress to approximately 50% before stopping the reaction and isolating the remaining ATP for analysis of the position of the ^{18}O label. In order to find out the length of incubation time required in the PIX experiments for extensive ATP hydrolysis (ca. 60%) to occur, gyrase was incubated with unlabelled ATP and DNA in the standard reaction buffer (Section 2.26.1) and aliquots were removed at intervals and assayed for P_i formation by the malachite green procedure (Section 2.26.1). The results of this analysis are shown in Fig 3.3. It can be seen that initially the rate of P_i formation was nearly linear but slowed considerably with time. This probably reflected the depletion of ATP and inhibition by the resulting ADP. The possibility that the decrease in the rate of the ATPase with time was due to denaturation of the gyrase was eliminated by the addition of

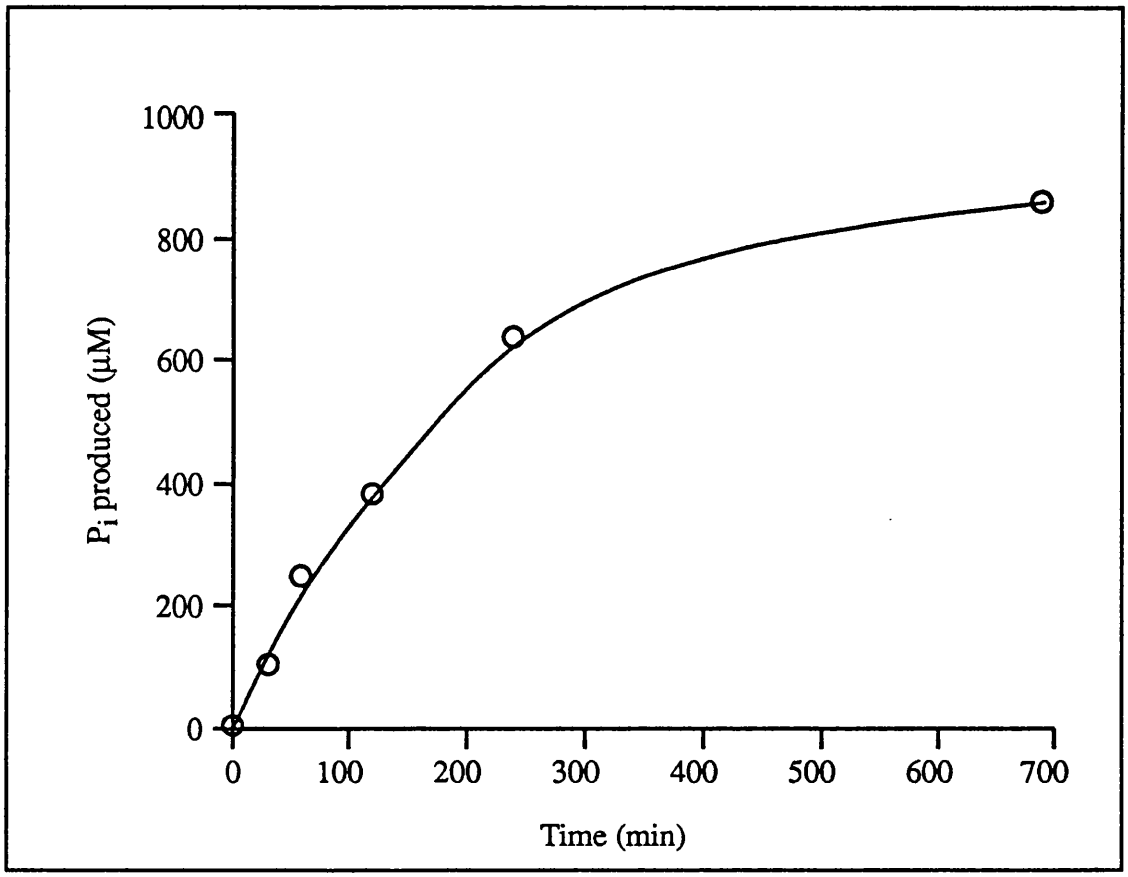

Figure 3.3. ATP hydrolysis (as determined by P_i formation) by gyrase over a long time course. P_i formation was determined by the malachite green procedure (Section 2.26.1) in microtitre plates. Gyrase (75nM) was incubated at 25°C with an initial concentration of ATP of 1.4mM and a linear 172 bp DNA fragment (90nM) in the standard ATPase reaction mixture (total volume = 300μl). At various times 30μl were removed and assayed for the presence of P_i. The points on the graph are averages of 4 separate readings.

and an adjacent displacement occurred. However, there is no evidence for mechanisms involving pseudorotation in phosphoryl and nucleotidyl transferases. Furthermore, in all the cases where there is compelling evidence for a phosphoenzyme intermediate, either from kinetic approaches or from isolation, overall retention has been observed.

Thus the simplest interpretation of the stereochemical results in Table 3.1 is that individual enzyme-catalysed displacement reactions at phosphorous proceed by an associative in-line mechanism presumably involving a pentacoordinated transition state (or intermediate) with trigonal bipyramidal geometry and the in-coming and leaving groups in the apical positions. However, it is impossible to completely rule out a dissociative pathway that could still give inversion of configuration in which the initially formed metaphosphate is either tightly bound by the enzyme and prevented from tumbling in the active site or trapped by the second substrate before rotation can occur. To date, there is still some debate as to the whether the transition states in enzyme catalysed phosphoryl transfer reactions are predominantly associative or dissociative in character (eg. see Herschlag and Jencks (1987); Jones *et al.* (1991); Westheimer (1987)).

In the work described in this chapter, it was planned to investigate the feasibility of the stereochemical analysis of the gyrase ATPase by characterising the interaction of $ATP_{\gamma}S$ with the enzyme.

3.2. RESULTS

3.2.1. Positional isotope exchange (PIX) experiments with (β,γ-^{18}O) ATP

ATP specifically labelled with ^{18}O in the β,γ-bridge position was a gift of Paul Cullis (Department of Chemistry, this University). Control experiments established that this sample behaved identically to authentic ATP in gyrase supercoiling assays and ATPase assays (data not shown). ^{31}P-NMR was used to confirm that the ^{18}O isotope was present in the β,γ-bridge position. This analysis was based on the fact that ^{18}O gives rise to a small upfield shift in the ^{31}P signal of the phosphorous to which it is bonded and that the magnitude of this shift increases with increasing bond order (Cohn and Hu, 1978). The spectrum was consistent with the sample containing approximately 95% (β,γ-^{18}O) ATP, approximately 3% unlabelled ATP (which was identified by adding authentic ATP and rerecording the NMR), and approximately 2% (β-^{18}O) ATP (^{18}O in the non-bridge position of the β-phosphate).

It was planned to utilise the β,γ-^{18}O-ATP material to investigate whether scrambling of the label could be detected in the gyrase ATPase reaction as described in the introduction to this chapter. Thus gyrase was to be incubated with the labelled ATP and hydrolysis allowed to progress to approximately 50% before stopping the reaction and isolating the remaining ATP for analysis of the position of the ^{18}O label. In order to find out the length of incubation time required in the PIX experiments for extensive ATP hydrolysis (ca. 60%) to occur, gyrase was incubated with unlabelled ATP and DNA in the standard reaction buffer (Section 2.26.1) and aliquots were removed at intervals and assayed for P_i formation by the malachite green procedure (Section 2.26.1). The results of this analysis are shown in Fig 3.3. It can be seen that initially the rate of P_i formation was nearly linear but slowed considerably with time. This probably reflected the depletion of ATP and inhibition by the resulting ADP. The possibility that the decrease in the rate of the ATPase with time was due to denaturation of the gyrase was eliminated by the addition of

fresh enzyme after 11.5 hours which did not give rise to significant further Pi formation after an additional 120 min.

Three different PIX reactions were performed. All the reactions contained the standard ATPase reaction mixture with gyrase at 75nM, (β,γ-^{18}O) ATP at 1.4mM, and DNA at 10μg/ml in a total volume of 8ml. In two of the reactions the DNA cofactor employed was relaxed pBR322 while in the third reaction linear 172 bp DNA was present. Ap_5A (0.1mM) was included in the reaction with linear DNA and one of the reactions with relaxed DNA in order to inhibit any adenylate kinase contamination (Lienhard and Secemski, 1973) which could otherwise give rise to scrambling of the ^{18}O label. In the other reaction with relaxed DNA Ap_5A was not added in order to determine whether adenylate kinase was present in the gyrase preparation. (Control supercoiling and ATPase experiments confirmed that Ap_5A, at a concentration of up to 1mM, had no effect on the activity of gyrase). The PIX reactions were incubated at 25°C and followed by periodically removing small aliquots and analysing the relative amounts of ATP and ADP by TLC on PEI-cellulose plates. Initially the formation of ADP appeared to be fairly rapid but became much slower with time as expected from Fig. 3.3. After 11 hours approximately 50-60% ATP hydrolysis appeared to have occurred in each of the 3 reactions and, after 12 hours, the reactions were stopped by the addition of 100mM EDTA and the nucleotides were extracted with an equal volume of $CHCl_3$/*iso*amyl alcohol. The aqueous solutions were then applied to columns (25 cm X 1 cm) of DEAE-Sephadex and eluted with 1L of TEAB (200-800mM gradient) to separate the ATP and ADP. Analysis of the eluents by A_{260} indicated the presence of 40% ATP and 60% ADP suggesting an extent of ATP hydrolysis of 60% in all 3 reactions which is consistent with Fig 3.3. The reisolated ATP in each of the 3 reactions (approximately 4 μmoles) was then subjected to analysis by ^{31}P-NMR in order to determine the extent to which the ^{18}O label had scrambled out of the β,γ-bridge position. For the NMR's, the ATP was dissolved in 100mM CAPS buffer (3-cyclohexylamino-1-propanesulfonic acid), 10mM

EDTA, and 50% D_2O. Spectra were recorded at 121.5MHz and 202.5MHz on Bruker AM300 and AM500 machines respectively.

No scrambling of the ^{18}O label out of the β,γ-bridge position was detected in any of the reactions in the presence of linear or closed-circular DNA and in the presence or absence of Ap_5A. Given the sensitivity of the NMR method, it was estimated that a maximum of approximately 2% ^{18}O scrambling could have gone undetected. Calculation of a maximum rate for the ^{18}O scrambling undetected in these experiments is complicated by the fact that the ATP concentration was constantly changing during the reaction. Taking the maximum scrambling of the ^{18}O label to be 2% in 12 hours at an ATP concentration of 0.56mM (the concentration after 12 hours) a maximum net rate of scrambling of 2.59 X 10^{-10}M/s can be calculated. Dividing by the gyrase concentration (75nM), gives the maximum specific rate of scrambling which is 3.46 X 10^{-3}/s. Taking the value of k_{-2}/k_3 to be approximately 0.4 in the absence of an ATP regenerating system (D. Hackney, A. Maxwell, M. Gellert, unpublished manuscript) and allowing for the fact that the probability of bridge to non-bridge ^{18}O scrambling during enzyme bound resynthesis of ATP (step k_{-2} in Eqn. 3.1) is 2/3, approximately 0.27 of the E.ATP would contain ^{18}O scrambled to the β-phosphate non-bridge positions. The maximum rate of k_{-1} in Eqn 3.1 is therefore given by 3.46 X 10^{-3} X 1/0.27 = 0.013/s divided by the fraction of the total enzyme present as E.ATP.

3.2.2. Gyrase-catalysed hydrolysis of $ATP_\gamma S$

Stereochemical analysis of the gyrase ATPase reaction would require isotopically chiral $ATP_\gamma S$ (as described in the introduction to this chapter) and would necessitate that gyrase is capable of hydrolysing $ATP_\gamma S$. In order to determine the feasibility of such a stereochemical analysis, the ability of gyrase to hydrolyse $ATP_\gamma S$ was investigated. Commercial $ATP_\gamma S$ was found to contain significant levels of ADP by reverse phase HPLC analysis and the nucleotide was therefore purified by chromatography on a DEAE-

Sephadex column eluting with TEAB. The purified material gave a single peak on HPLC analysis.

Hydrolysis was assayed by the malachite green procedure (Section 2.26.1). Although this method detects inorganic phosphate and hydrolysis of $ATP_{\gamma}S$ produces inorganic thiophosphate, it was reasoned that at the acidic pH of the assay the thiophosphate would be immediately desulphurised to form phosphate. Gyrase (75nM) was incubated with $ATP_{\gamma}S$ (1mM) and DNA (linear 172 bp fragment; 90nM) in standard ATPase reaction mixture. At intervals, 30µl were removed and the reaction was stopped by addition of EDTA (100mM) and assayed for P_i formation. No P_i was found even after 11.5 hours. Given the sensitivity of the assay, 1% hydrolysis (10µM) of $ATP_{\gamma}S$ should have been detected. Therefore, the failure to detect any hydrolysis was consistent with a maximum rate of hydrolysis of $ATP_{\gamma}S$ catalysed by gyrase of 3×10^{-3}/s. Thus the rate of hydrolysis was over 300-fold slower than ATP.

Hydrolysis of $ATP_{\gamma}S$ was also investigated by the use of ^{35}S-labelled $ATP_{\gamma}S$. In these experiments, gyrase (75nM) was incubated with $ATP_{\gamma}{}^{35}S$ (1mM; cpm ~ 100,000) and DNA (linear pBR322; 10µg/ml) in the usual ATPase reaction mixture. After various times, the products were separated by TLC on PEI-cellulose plates and the relative amounts of $P^{35}S_i$ and $ATP_{\gamma}{}^{35}S$ were quantitated by scintillation counting (Section 2.26.4). Even after 12 hour incubations at 37°C no $P^{35}S_i$ formation was detected. It was estimated that the sensitivity of the assay was approximately 5% $ATP_{\gamma}S$ hydrolysed. Thus failure to detect any hydrolysis was consistent with the malachite green experiments. The sample of $ATP_{\gamma}{}^{35}S$ used contained significant levels of PS_i (as detected from scintillation counting of the TLC separated sample on its own). This probably decreased the sensitivity of the assay to the formation of further PS_i and it may have been possible to increase the sensitivity of the assay by purifying the $ATP_{\gamma}{}^{35}S$ sample before use.

The inhibition of the gyrase ATPase reaction by $ATP_{\gamma}S$ was briefly investigated by the malachite green procedure. Gyrase (75nM) was incubated with ATP at either 0.3mM or 1mM together with various concentrations of $ATP_{\gamma}S$ in standard ATPase reactions. After 210 min. the reactions were analysed for P_i in the usual way. It was found that the concentrations of $ATP_{\gamma}S$ required to inhibit the P_i formation by 50% were approximately 0.03mM (for ATP concentration of 0.3mM) and 0.1mM (for ATP concentration of 1mM). A full kinetic analysis of $ATP_{\gamma}S$ inhibition should be possible with the PK/LDH assay since $ATP_{\gamma}S$ is such a poor substrate. Although this was not investigated, it would be interesting to see whether $ATP_{\gamma}S$ inhibition gave rise to sigmoidal rate plots in the same way as ADP (Maxwell *et al.*, 1986) and free ATP (uncomplexed to a divalent metal ion; Section 5.2.4.2 and Figs. 5.13 and 5.14).

3.2.3. $ATP_{\gamma}S$ as a substrate for gyrase-catalysed supercoiling

In view of the failure to detect hydrolysis of $ATP_{\gamma}S$, it was of interest to discover whether this nucleotide supported DNA supercoiling with gyrase. It has been shown that ADPNP, an ATP analogue that is not hydrolysed by gyrase, can support stoichiometric supercoiling (Sugino *et al.*, 1978). Thus catalytic supercoiling with $ATP_{\gamma}S$ would imply that this nucleotide is hydrolysed by gyrase whereas stoichiometric supercoiling would be consistent with $ATP_{\gamma}S$ not being hydrolysed.

A brief investigation into the inhibition of ATP-dependent supercoiling by $ATP_{\gamma}S$ is shown in Fig. 3.4. This reveals that at the ATP concentration of the experiment (0.3mM), the concentration of $ATP_{\gamma}S$ to cause approximately 50% inhibition of supercoiling was between 0.01mM and 0.03mM (i.e. approximately 10-fold lower than the ATP concentration). This finding is broadly similar to the inhibition of the ATPase by $ATP_{\gamma}S$.

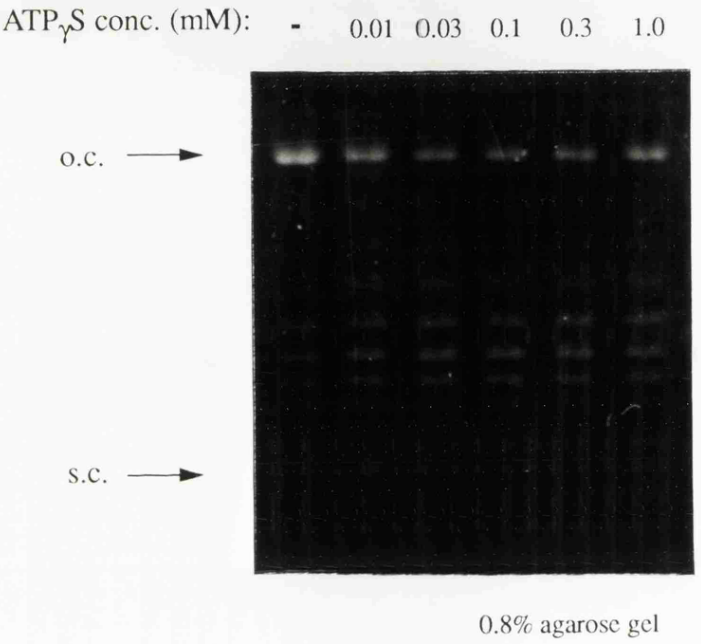

Figure 3.4. Inhibition of ATP-dependent supercoiling by ATPγS. The ATP concentration was 0.1mM and the gyrase concentration was 25nM in 30µl reaction volumes.

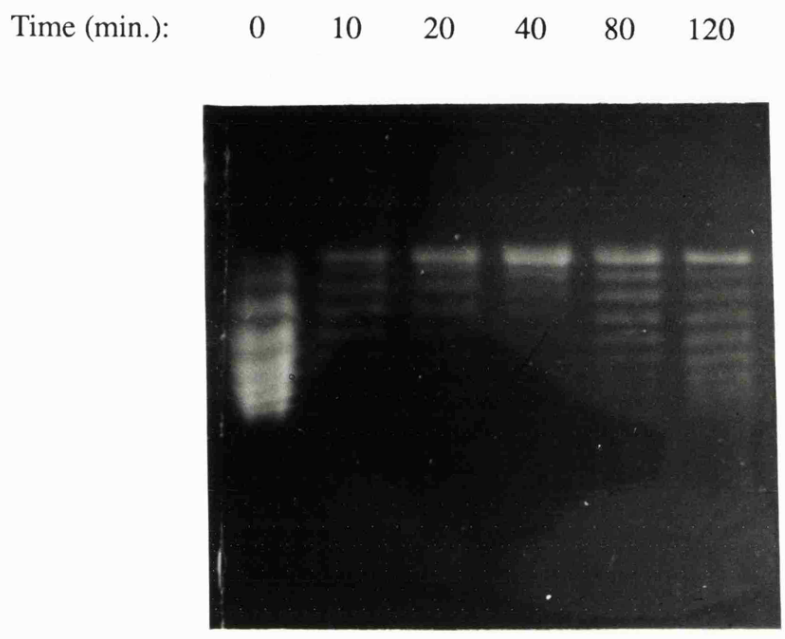

Figure 3.5. Supercoiling supported by $ATP_{\gamma}S$. The reaction (total volume 150µl) contained gyrase (25nM), $ATP_{\gamma}S$ (1mM) in the usual supercoiling reaction mixture. At the intervals shown, 30µl were removed and the reaction was stopped in the usual way.

Fig. 3.5 shows an experiment where supercoiling with $ATP_{\gamma}S$ was monitored over a long time course. After 120 min. a ΔLk of approximately -10 was seen (as confirmed by a chloroquine gel (not shown)). Furthermore there was no evidence that the supercoiling reaction had reached completion. In this experiment the gyrase concentration was 25nM and the DNA concentration was 3.4nM. Therefore, the concentration of superhelical turns introduced was 34nM. Since gyrase changes the linking number of DNA in steps of two, a stoichiometric supercoiling mechanism could account for a concentration of superhelical turns twice that of the gyrase concentration (50nM in this case). Thus initially it would appear that this experiment does not rule out a stoichiometric mechanism for $ATP_{\gamma}S$ supported supercoiling. However, it was shown in the Appendix to this thesis that the gyrase preparation contained considerable amounts of enzyme that was inactive in the supercoiling reaction and incapable of binding to DNA (due to inactivity of a proportion of the B subunit). An upper limit to the active component of the preparation was 20% of the total protein concentration. Taking this value for the proportion of active gyrase in the supercoiling experiment with $ATP_{\gamma}S$ in Fig. 3.5, a stoichiometric mechanism could give a maximum concentration of superhelical turns of 10nM. Since the actual level of supercoiling after 120min. is over 3 times this value it would appear that the reaction is catalytic. The minimum level of hydrolysis of $ATP_{\gamma}S$ required to support the observed supercoiling can be calculated to be 9.44×10^{-4}/s per active gyrase tetramer. This is consistent with the maximum level of hydrolysis estimated from Section 3.2.2.

3.3. DISCUSSION

The lack of a detectable PIX with (β,γ-^{18}O) ATP is consistent with the off-rate for ATP (k_{-1} in Eqn. 3.1) being slow with respect to k_2. This is in agreement with the ^{18}O water $\rightleftharpoons$ ATP exchange studies on gyrase (D. Hackney, A. Maxwell, M. Gellert, unpublished manuscript). The (β,γ-^{18}O) ATP experiments are mechanistically complementary to the ^{18}O water experiments since they rely on different assumptions about the rotational freedom of the bound products complex. In order for water-derived oxygen to be incorporated into ATP after its resynthesis on the enzyme from bound ADP and P_i, the P_i must be free to tumble in the enzyme active site and two accompanying proton transfers must take place. In many enzymes these criteria seem to be met (Dale and Hackney, 1987; Hackney, 1980; Sines and Hackney, 1986; Sleep and Hackney, 1980). The observation of an intermediate phosphate $\rightleftharpoons$ water exchange by Hackney *et al.* for gyrase suggests that, here too, the above criteria are satisfied. In contrast to phosphate $\rightleftharpoons$ water exchange, scrambling of the β,γ-bridge-^{18}O during ATP resynthesis requires that the β-phosphoryl group of bound ADP is free to rotate. Examples of this type of PIX are glutamine synthetase (Midelfort and Rose, 1976), carbamoyl phosphate synthetase (Meek *et al.*, 1987; Raushel and Villafranca, 1980; Rubio *et al.*, 1981; Wimmer *et al.*, 1979) and CTP synthetase (von de Saal *et al.*, 1985). Examples where this type of PIX is not evidenced are biotin carboxylase (Ogita and Knowles, 1988; Tipton and Cleland, 1988), myosin (Dale and Hackney, 1987), and N^{10}-formyltetrahydrofolate synthetase (Mejillano *et al.*, 1989).

The lack of PIX in gyrase may be due to one of two factors; either the off-rate of ATP is slow or the β-phosphoryl group of the enzyme-bound ADP is not free to rotate. While this rotation is favoured on thermodynamic grounds (Midelfort and Rose, 1976), constraints imposed by the enzyme's active site or by complexation with the divalent metal may disrupt the torsional symmetry of the phosphoryl group (Dale and Hackney, 1987; Herschlag and Jencks, 1987; Tipton and Cleland, 1988). Despite this ambiguity,

the lack of a PIX for the gyrase ATPase is consistent with the very low rate of ^{18}O water $\rightleftharpoons$ ATP exchange measured by Hackney *et al.* Taken together these results strongly suggest that the ATP off-rate is slow and that binding of ATP to gyrase is largely irreversible. The most likely explanation of this is that nucleotide binding is a two step process with a rapid and reversible initial step followed by a slow, essentially irreversible, step involving a protein conformational change.

Studies of the electric dichroism of gyrase-DNA complexes have also suggested the existence of a nucleotide-induced conformational change of the enzyme (Rau *et al.*, 1987). Furthermore, it has been shown that the off-rate for the non-hydrolysable ATP analogue, ADPNP, is very slow with gyrase (Tamura *et al.*, 1992) and with the N-terminal GyrB fragment (43kDa protein) (J. A. Ali *et al.*, manuscript in preparation). The crystal stucture of the 43kDa protein also suggests that this fragment dimerises on binding ATP (Wigley *et al.*, 1991) which is supported by gel filtration studies which show that the 43kDa protein is a monomer in the absence of nucleotide and a dimer in the presence of ADPNP (J. A. Ali, personal communication).

The kinetic scheme in Eqn 3.1 can therefore be modified to reflect the additional binding step of ATP as follows:

$$\mathrm{ATP + E} \underset{k_{-1}}{\overset{k_1}{\rightleftharpoons}} \mathrm{E.ATP} \underset{k_{-2}}{\overset{k_2}{\rightleftharpoons}} \mathrm{E^*.ATP} \underset{k_{-3}}{\overset{k_3}{\overset{H_2O}{\rightleftharpoons}}} \mathrm{E.ADP.P_i} \underset{k_{-4}}{\overset{k_4}{\rightleftharpoons}} \mathrm{E + ADP + P_i}$$

(eqn. 3.2)

E^* = conformational change of enzyme.

Eqn. 3.2 does not take into account the fact that two ATP's are thought to be bound prior to hydrolysis and that this hydrolysis is believed to be a cooperative process (see Section

4.3 and references therein). Incorporating this information into the ATPase model in Eqn. 3.2 allows a more complete scheme to be proposed as shown below.

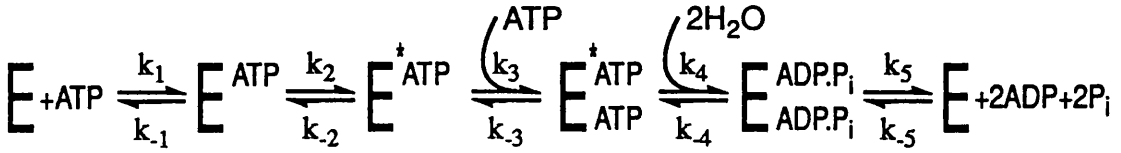

(eqn. 3.3)

The enzyme conformational change may occur either on binding of one ATP as shown in the scheme above or on binding of two ATP's. However, the former hypothesis is strongly favoured by binding experiments with ADPNP (Tamura *et al.*, 1992).

The sensitivity of the PIX analysis in this study was lower than the analogous medium ATP $\rightleftharpoons$ water exchange because ^{31}P-NMR was used as opposed to mass spectroscopy. While mass spectroscopy is intrinsically more sensitive it cannot readily be applied to measuring scrambling of ^{18}O between the β,γ-bridge and β-non-bridge positions in ATP. This is because the mass spectroscopy analysis requires the specific degradation of the ATP at the γ-phosphate to give P_i and, unfortunately, enzymatic cleavage of ATP at the γ-phosphate occurs with the β,γ-bridge oxygen being retained with ADP and information regarding scrambling is lost since the bridging and non-bridging oxygens become equivalent. An alternative enzymatic degradation scheme involving 5-phospho-D-ribosyl 1-pyrophosphate synthetase has been developed (Dale and Hackney, 1987) which results in the formation of P_i containing the β,γ-bridge oxygen of ATP. This procedure could be used in future PIX experiments on gyrase in order to quantitate the slow ATP off-rate. It may also be possible to observe the ^{18}O bridge to non-bridge scrambling directly, without any degradation or derivatisation steps, by negative ion fast atom bombardment mass spectroscopy on the reisolated ATP (Connolly *et al.*, 1984) although experiments by

Hilscher *et al.* (1985) suggest that a chemical or enzymatic degredation scheme is required.

No hydrolysis of $ATP_{\gamma}S$ by gyrase was detected which gave a maximum limit to the turnover number of this nucleotide of 3 X 10^{-3}/s. However, $ATP_{\gamma}S$ did appear to promote catalytic supercoiling which gave a presumed minimum turnover number for the hydrolysis of approximately 1 X 10^{-3}/s. Thus the rate of hydrolysis of $ATP_{\gamma}S$ is about 10^{-3}/s. Although no rigorous kinetic analysis of this slow rate of hydrolysis was possible, it is likely that the rates above approximate to the k_{cat} value for $ATP_{\gamma}S$ hydrolysis since inhibition studies revealed that the nucleotide caused significant inhibition of the ATPase and ATP-dependent supercoiling reactions at concentrations 10-fold lower than the ATP concentration. Thus the rate of $ATP_{\gamma}S$ hydrolysis appears to be approximately 300 to 1000-fold slower than ATP hydrolysis. The slower rate of thiophosphoryl transfer compared to phosphoryl transfer is seen in many enzymes and has been cited as evidence for an associative mechanism since thiophosphates react more rapidly *via* a dissociative reaction than their oxygen counterparts (Breslow and Katz, 1968). However, other factors may be dominant in controlling the rate of the $ATP_{\gamma}S$ reaction such as steric effects, changes in pK_a, or metal ion coordination.

The results with $ATP_{\gamma}S$ suggest that it should be possible to use this ATP analogue in an isotopically chiral form to investigate the stereochemical pathway of the gyrase ATPase. The stereochemical analysis by the methods of Webb and Trentham (1980a) or Arnold and Lowe (1986) require that at least 5 μmoles of $ATP_{\gamma}S$ be turned over. Taking the minimum turnover number for $ATP_{\gamma}S$ hydrolysis by gyrase of 1 X 10^{-3}/s, a 12 hour incubation would therefore require 116 nmoles (43 mg) of gyrase. This large amount of enzyme would require a fairly large reaction volume and consequently, on economic grounds, it would be preferable to hydrolyse (γ-^{17}O,^{18}O, S) ATP in ^{16}O-water to produce isotopically chiral PS_i (Webb and Trentham, 1981) as opposed to hydrolysing

(γ-^{16}O, ^{18}O, S) ATP in ^{17}O-water. At the time of the experiments reported here the substantial quantity of enzyme required was not available. However, large fermenter preparations of the gyrase subunits have recently been performed (J. Ali, personal communication) and the stereochemical analysis of the gyrase ATPase may now be feasible. Alternatively, it may be possible to use the 43kDa protein in stereochemical experiments since large quantities of this protein are more easily prepared than the intact gyrase proteins. However, the 43kDa protein has a considerably lower turnover number for ATP than gyrase (approximately 100-fold lower; see Section 5.2.4) and, if this difference was reflected in $ATP_{\gamma}S$, the advantage from the ease of production of the 43kDa protein would be outweighed by the need for more of the protein in $ATP_{\gamma}S$ experiments.

Given that the on-enzyme ATP hydrolysis step is reversible (as discussed earlier) it will be important in a future stereochemical investigation to establish that no such reversal occurs with $ATP_{\gamma}S$ since this could lead to racemisation and misleading results. The fact that $ATP_{\gamma}S$ hydrolysis is very slow suggests that the products (ADP and PS_i) will probably dissociate from the enzyme before any resynthesis of $ATP_{\gamma}S$ can occur. This has been found to be the case in other enzyme systems and forms the basis of the chiral thiophosphate stereochemical approach (Webb, 1982).

3.4. SUMMARY

ATP uniquely labelled with ^{18}O in the β,γ-bridge position has been used to investigate whether β,γ-bridge to β-non-bridge scrambling of the label occurs during the gyrase ATPase reaction. No such scrambling was detected by ^{31}P-NMR which, together with ^{18}O water experiments by Hackney *et al* (unpublished manuscript), can be interpreted in terms of the ATP off-rate being very slow. It is proposed that ATP binding to gyrase is a two step process with an initial reversible binding step being followed by an enzyme conformational change.

In experiments towards the stereochemical analysis of the gyrase ATPase, the hydrolysis of $ATP_\gamma S$ has been examined. No hydrolysis of this nucleotide was detected even after 12 hours which was consistent with a rate of $ATP_\gamma S$ turnover by gyrase of less than 3 X 10^{-3}/s. However, $ATP_\gamma S$ appeared to promote catalytic supercoiling which required a minimum rate of $ATP_\gamma S$ turnover of 1 X 10^{-3}/s. Thus the turnover of $ATP_\gamma S$ was between 300 to 1000-fold slower than ATP. These results suggest that stereochemical analysis of the gyrase ATPase using isotopically chiral $ATP_\gamma S$ is feasible but would require large quantities (approximately 40 mg) of enzyme.

Chapter 4

Energy Coupling and Nucleotide Stereospecificity in DNA Gyrase

4.1. INTRODUCTION

All known ATPases, GTPases, and kinases interact with the nucleotide complexed to a divalent metal ion, usually Mg^{2+} or Ca^{2+}, which is important in catalysis. Theoretically a 1:1 Mg-ATP complex can exist in solution as an equilibrium of 17 different stereoisomers (Huang and Tsai, 1982) only one of which will probably be the optimum substrate for a specific enzyme. The potential role of the metal ion may be gauged from the type of complex handled by the enzyme. For example, metal coordination to γ-phosphoryl oxygens, may serve to neutralise charge and facilitate attack of the nucleophile in an associative reaction. Also, for hydrolysis reactions, the metal may actually deliver the reacting water molecule from one of its coordination sites to the phosphate monoester in an intramolecular reaction. Complexation to the α,β-phosphoryl groups would tend to stabilise ADP as a leaving group, which would promote either associative or dissociative pathways.

Recent work on the GTP binding Ha-Ras p21 protein from the *ras* oncogene family has suggested a role for the metal ion in mediating a conformational change (Pai *et al.*, 1990; Schlichting *et al.*, 1990). The p21 protein is thought to be involved in a growth promoting signal transduction process and appears to exist in an active state when bound to GTP which can interact with an effector protein, and an inactive state when bound to GDP. Time resolved X-ray crystallographic studies, using caged GTP photolysed in the crystal, have identified important differences in the coordination of the bound Mg^{2+} ion on GTP hydrolysis which may trigger the required protein conformational change (Schlichting *et al.*, 1990). The proposed mechanism of gyrase (Fig. 1.7) requires at least one conformational change associated with hydrolysis of ATP and thus the Mg^{2+} ion complexed to the nucleotide may be important in this process.

Two approaches using ATP analogues have been used to elucidate the active metal-nucleotide complex in various enzymes. Briefly these approaches are based on the use of

substitution-inert complexes such as Cr^{III} and Co^{III} complexes of ATP and ADP (Cornelius and Cleland, 1978; Dunaway-Mariano and Cleland, 1980a), and the use of nucleoside phosphorothioate metal complexes (Jaffe and Cohn, 1978b). In this chapter the latter approach has been employed and the specificity of gyrase towards phosphorothioate analogues of ATP, with the sulphur atom in non-bridging positions of the polyphosphate chain, has been characterised. This has enabled predictions of the active Mg-ATP complex to be made.

The coupling of the hydrolysis of ATP to the introduction of negative superhelical stress into DNA by gyrase represents one of the simpler examples of biological energy transduction. Therefore gyrase is a good model for the study of energy coupling. The phosphorothioate ATP analogues enable interactions of gyrase with ATP to be probed. In addition it is possible to investigate the effects of each analogue on both the ATP hydrolysis and DNA supercoiling reactions of gyrase and thus explore the coupling of the two reactions. This approach has yielded information hitherto unavailable from the use of the natural substrate, ATP.

4.2. RESULTS

4.2.1a. Synthesis and characterisation of the Rp and Sp diastereoisomers of $ATP_{\beta}S$

The synthesis of $ADP_{\beta}S$ was based on that of Goody and Eckstein (1971) and involved the reaction of a protected thiophosphate with an activated AMP derivative. The synthesis of the protected thiophosphate derivative is shown in Fig. 4.1. below.

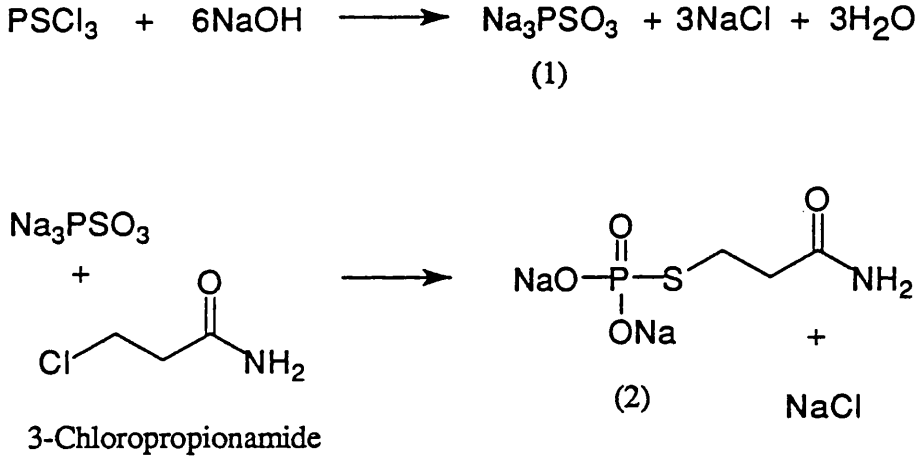

(1) = Trisodium thiophosphate
(2) = S-2-carbamoylethyl thiophosphate

Figure 4.1. The synthesis of S-2-carbamoylethyl thiophosphate

Initial attempts to prepare the trisodium salt of thiophosphate (1) using 6 equivalents of NaOH to 1 equivalent of thiophosphoryl chloride (as the stoichiometric equation would suggest) were unsuccessful, resulting in complete desulphurisation and formation of inorganic phosphate. However, when 8 equivalents of NaOH were used, the reaction proceeded smoothly and in high yield. The S-2-carbamoylethyl derivative (2) was obtained by the reaction of the thiophosphate with 3-chloropropionamide as shown above.

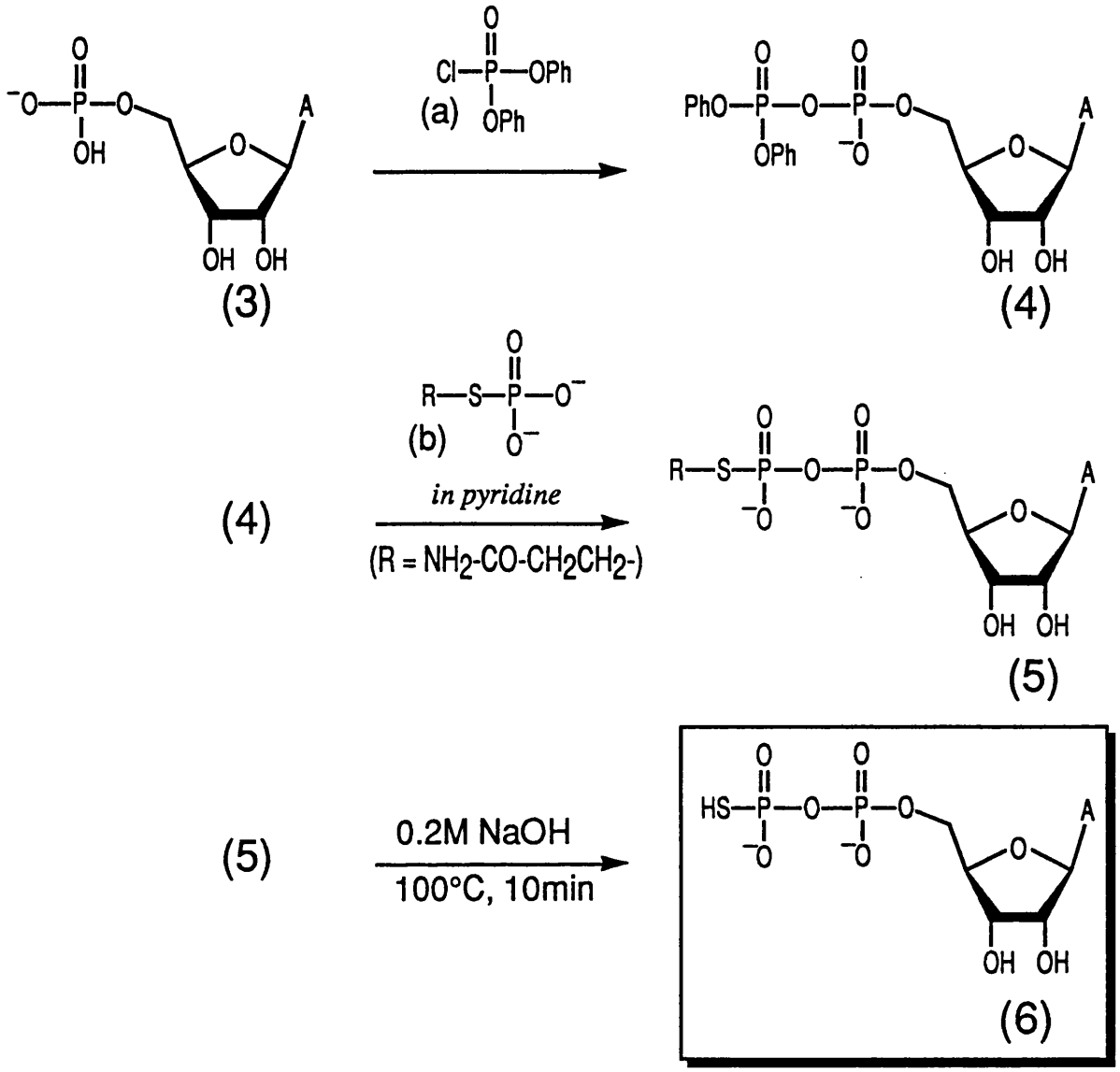

(3) = Adenosine 5'-monophosphate
(4) = P^1-diphenyl P^2-adenosine 5'-pyrophosphate
(5) = P^1-S-2-carbamoylethyl P^2-adenosine 5'-pyrophosphate
(6) = Adenosine 5'-O-(2-thiodiphosphate); $ADP\beta S$

(a) = Diphenyl phosphorochloridate
(b) = S-2-carbamoylethyl thiophosphate

Figure 4.2. The Synthesis of Adenosine 5'-O-(2-thiodiphosphate), $ADP\beta S$

After conversion to its tri-*n*-butylammonium salt, the S-2-carbamoylethyl thiophosphate was reacted with the activated AMP derivative [(4); Fig. 4.2] in a Michelson-type coupling procedure (Michelson, 1964). In this reaction pyridine was employed as both a solvent and nucleophilic catalyst with the probable transient formation of a pyridinium phosphoramidate species (7) which reacted with the thiophosphate derivative to give the protected $ADP_{\beta}S$ species (5).

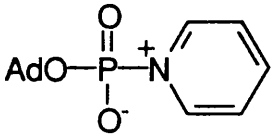

(7)

After removal of the protecting group in alkaline conditions and purification by anion-exchange chromatogaphy, pure $ADP_{\beta}S$ (6) was obtained in 19% yield, which, while rather low (lit. yield (Goody and Eckstein, 1971) was 35%), represented plenty of material for biological experiments.

Table 4.1. Stereospecificity of some of the kinases from steady-state experiments[a]

Enzyme	$ATP_{\alpha}S(Sp)$	$ATP_{\alpha}S(Rp)$	$ATP_{\beta}S(Sp)$	$ATP_{\beta}S(Rp)$
Pyruvate kinase	+	-	+	-
Hexokinase	+	-	-	+
Acetate kinase	+	-	+	-
Myosin	+	+	+	-
Arginine kinase	-	+	-	+
Creatine kinase	-	+	-	+
Adenylate kinase	+	-	+	-
Phosphoglycerate kinase	+	-	+	-

[a]The stereospecificities are not absolute; rigorous analysis requires comparisons of V_{max}/K_M for each epimer but, since such information is incomplete, a qualitative summary is shown in the table.

Since enzymes are themselves chiral they can exhibit stereospecificity at prochiral centres such as $ADP_{\beta}S$. Many kinases have been shown to be selective for the different epimers of $ATP_{\alpha}S$ and $ATP_{\beta}S$ and some of these are listed in Table 4.1 above. In this work the Rp and Sp epimers of $ATP_{\beta}S$ were prepared from $ADP_{\beta}S$ enzymatically as shown in Fig. 4.3. Pyruvate kinase was used to give predominantly the Sp isomer while acetate kinase was used to furnish the Rp isomer. The reactions were incubated at 25°C and followed by TLC. After 4 hours small aliquots were taken for HPLC analysis while the reaction mixtures were loaded directly onto ion-exchange columns for purification. Fig. 4.4 shows some of the results of the HPLC analysis. Under the conditions used, both epimers of $ATP_{\beta}S$ were resolved thus allowing direct visualisation of the stereospecificities of the reactions. Fig. 4.4(a) shows that in the pyruvate kinase reaction significant amounts of the minor Rp epimer were present while in the acetate kinase reaction [Fig. 4.4(b)] little contaminating Sp epimer was evident.

After ion-exchange chromatography the $ATP_{\beta}S$ samples were freed of their contaminating minor isomers by degradation with hexokinase or myosin respectively as shown in Fig. 4.3. These reactions were followed by HPLC [Fig. 4.4. (d)-(g)]. After 30 min. incubation with hexokinase, the Rp epimer contaminant in the $ATP_{\beta}S$(Sp) sample had been completely degraded [Fig. 4.4(e)] and, similarly, the small amount of Sp epimer in the $ATP_{\beta}S$(Rp) sample had been degraded by myosin [Fig.4.4(g)]. The reactions were continued for 90 min. and then applied to DEAE-Sephadex columns for purification to yield pure Rp and Sp epimers of $ATP_{\beta}S$. The diastereomeric purity was estimated to be > 99.5% and compounds gave the expected ^{31}P-NMR spectra (Fig. 4.5).

4.2.1b. Synthesis and characterisation of the Rp and Sp epimers of $ATP_{\alpha}S$.

$ATP_{\alpha}S$ was synthesised as a racemic mixture by the method of Ludwig and Eckstein (1989) as described in Section 2.2.6. and illustrated in Fig. 4.6. 2',3'-protected

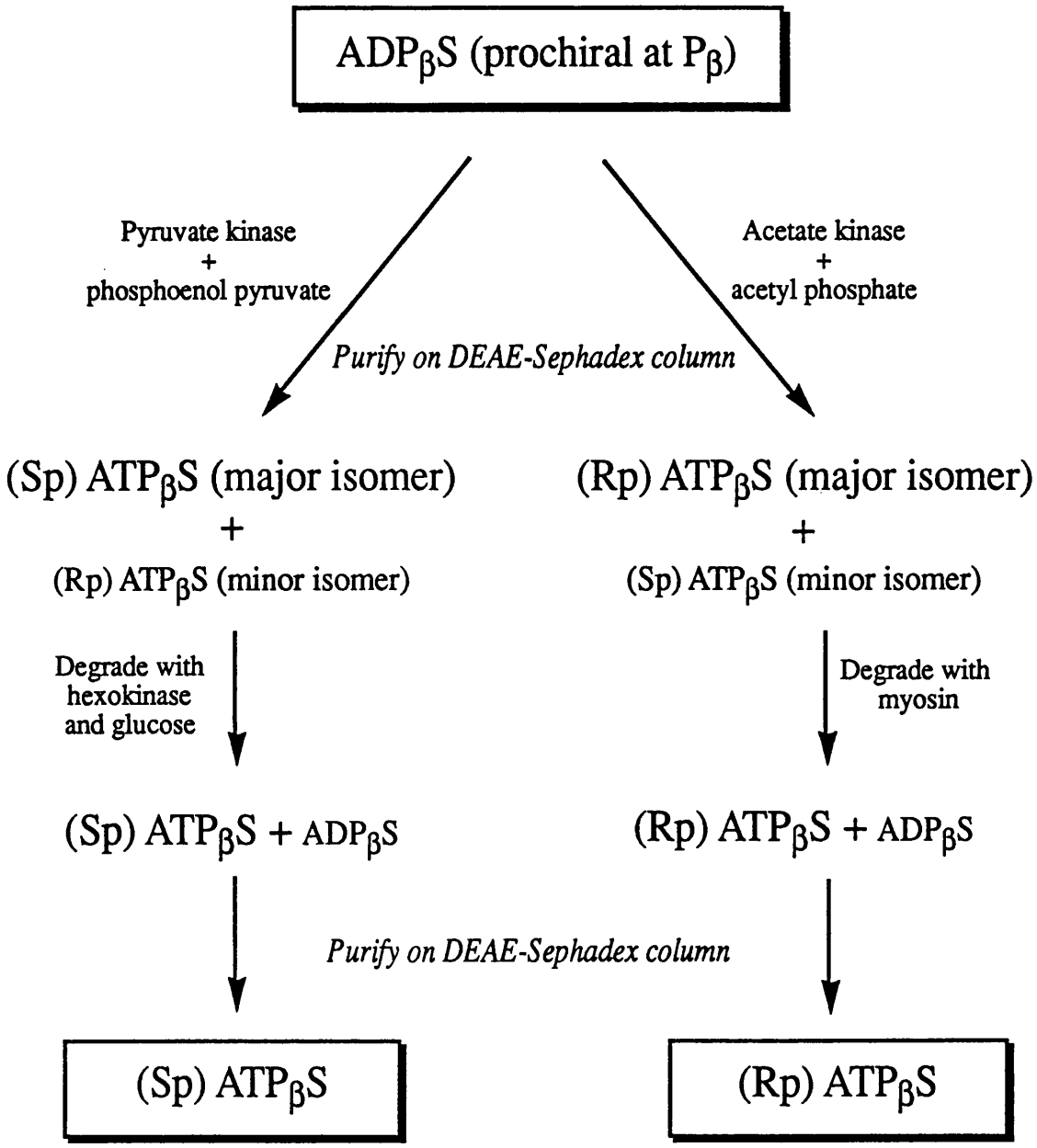

Figure 4.3. Stereospecific Synthesis of Sp & Rp ATPβS

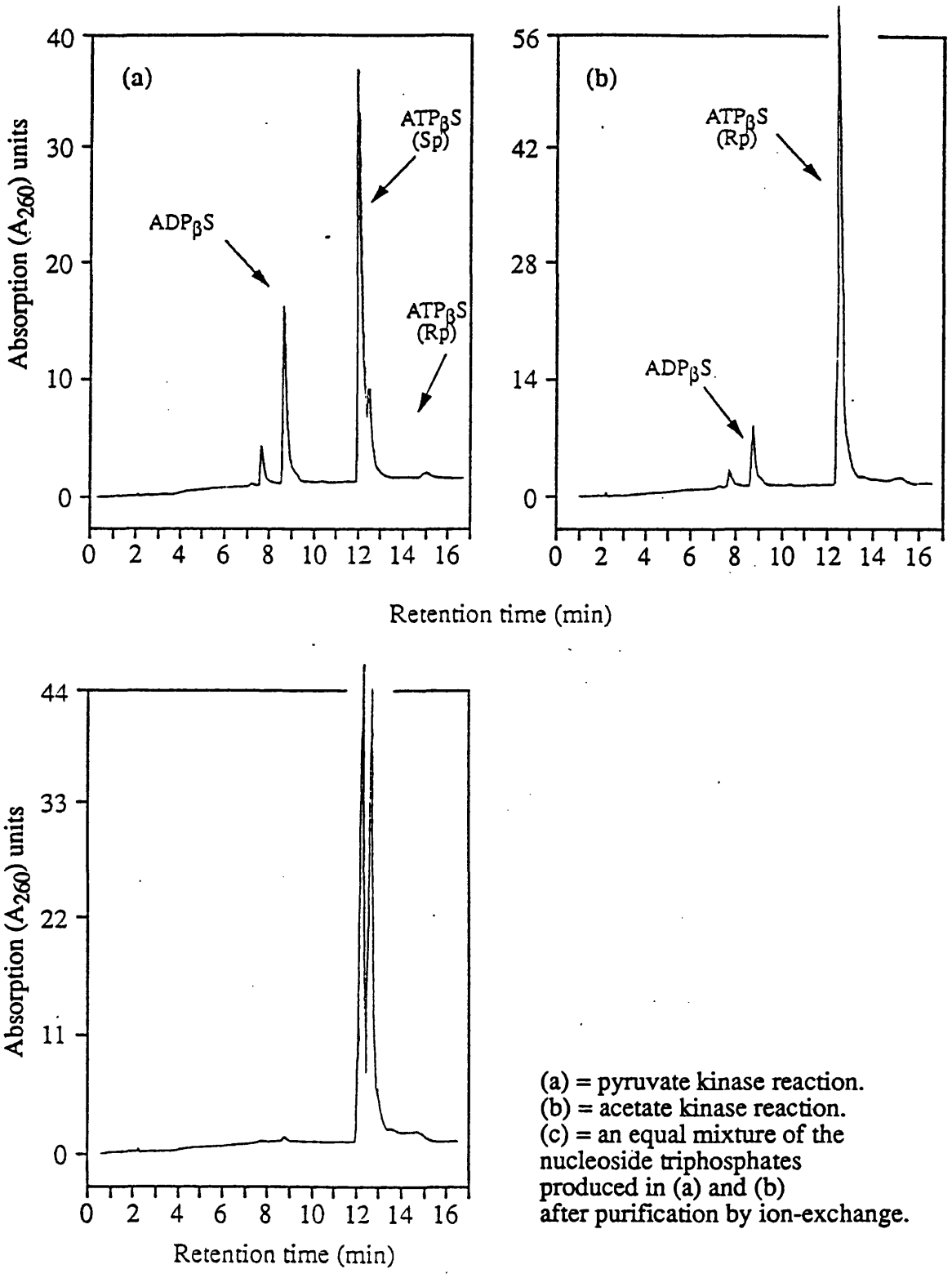

Figure 4.4. (a)-(c). HPLC analyses of the pyruvate kinase and acetate kinase reactions with ADPβS. Samples were analysed on an analytical reverse-phase column, eluting with 150mM TEAB with 20mM $MgCl_2$ and a 0-4.5% linear gradient of acetonitrile in 15min at a flow rate of 1.5ml/min.

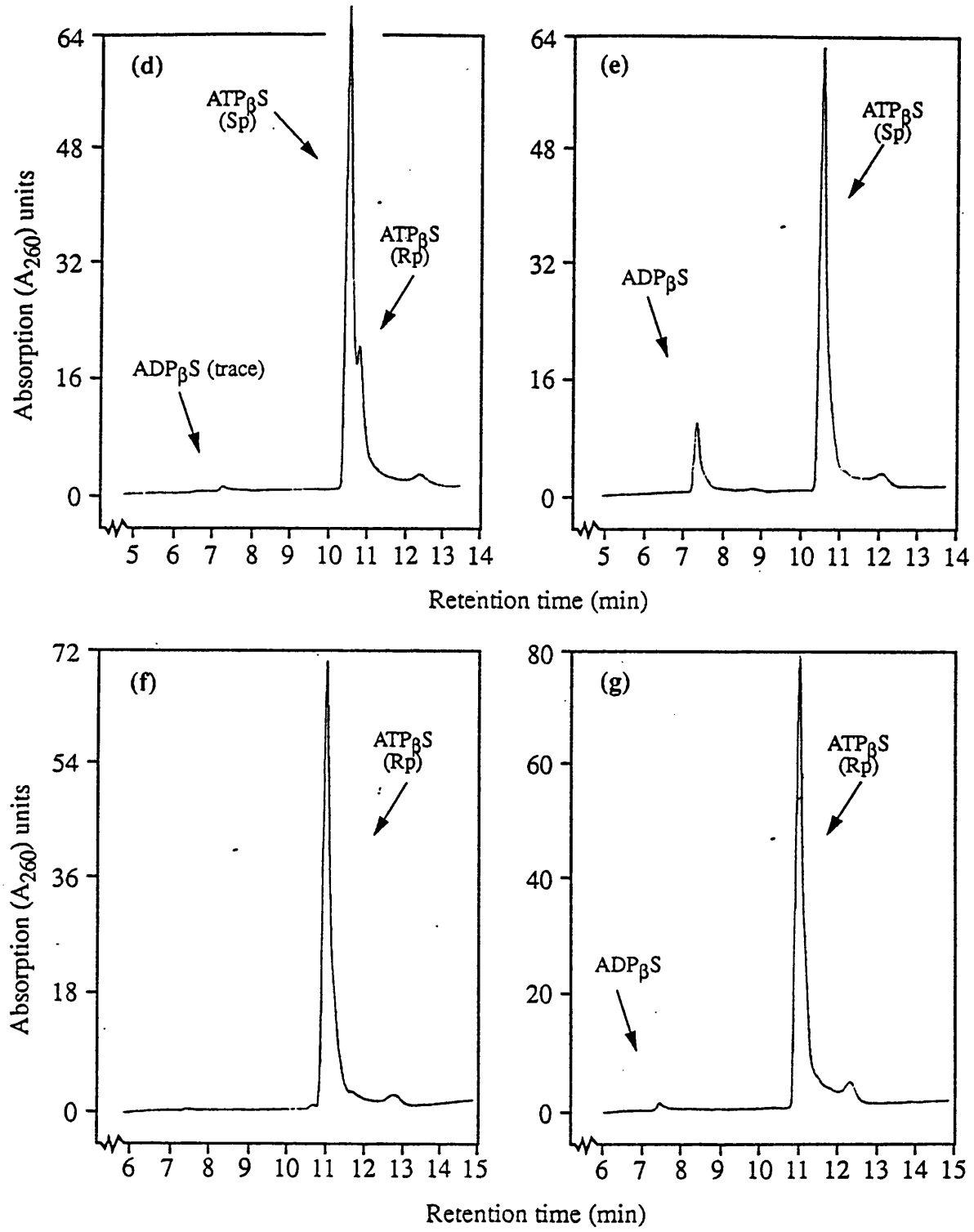

Figure 4.4. (d)-(g). HPLC analysis of the stereospecific degradation of ATPβS with hexokinase and myosin. Conditions were the same as in (a)-(c) except that the flow rate was 2ml/min as opposed to 1.5ml/min.
(d) = the nucleoside triphosphate product of (a) after purification by ion-exchange.
(e) = the reaction of (d) with hexokinase after 30min.
(f) = the nucleoside triphosphate product of (b) after purification by ion-exchange.
(g) = the reaction of (f) with myosin after 30min.

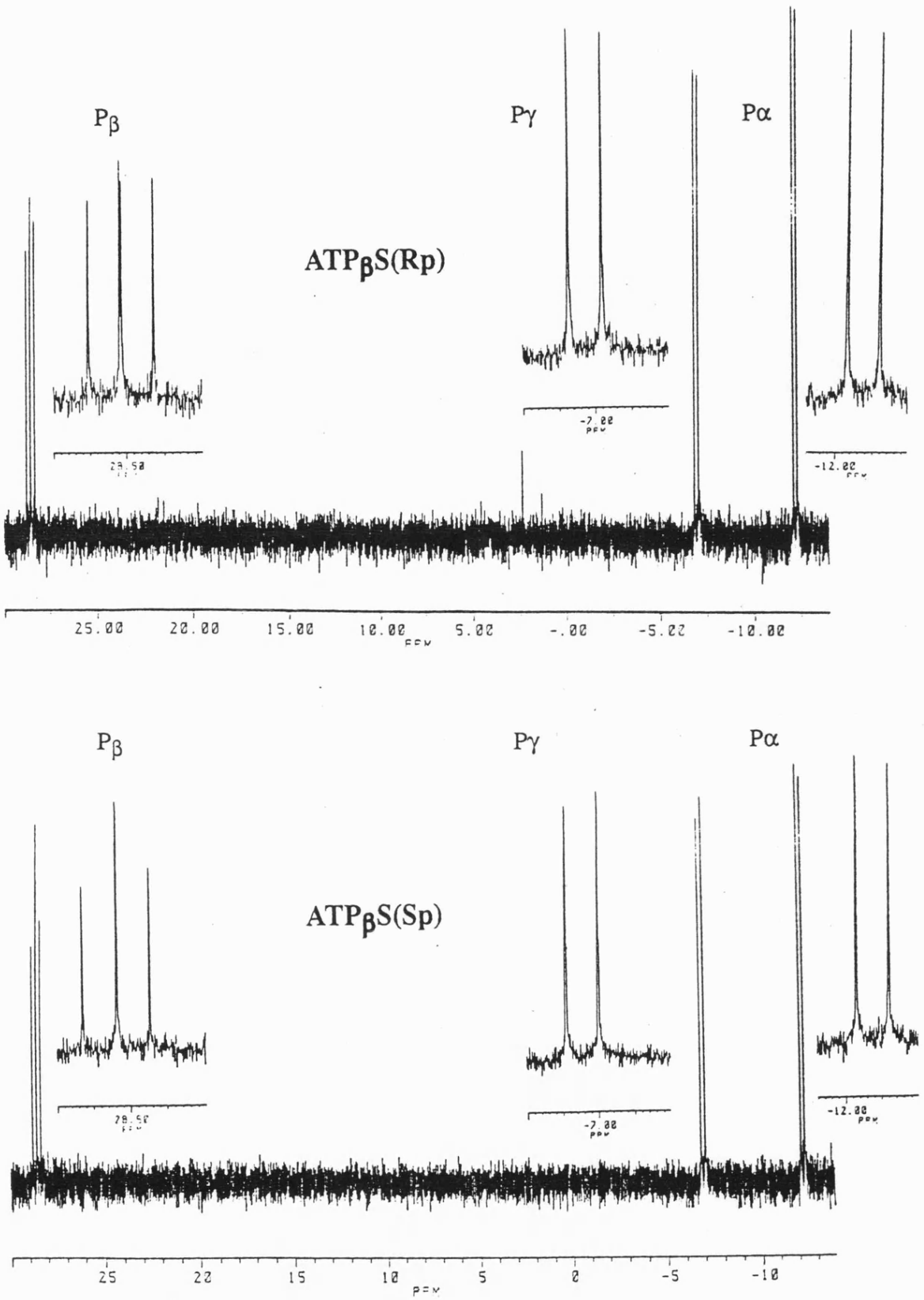

Figure 4.5. ^{31}P-NMR (121.5MHz) proton decoupled spectra of the Rp and Sp epimers of ATPβS. Samples consisted of 11.9mM nucleotide dissolved in Tris.HCl (pH 8.8; 200mM), 10% D_2O, 10mM EDTA; total volume 0.5ml.

ATPβS(Sp): ^{31}P-NMR δ(121.5 MHz, D_2O) -12.20 (d, J = 27Hz; P_α), +28.59 (overlapping dd; P_β), -6.89 (d, J = 28Hz; P_γ).
ATPβS(Rp): ^{31}P-NMR δ(121.5 MHz, D_2O) -12.19 (d, J = 26Hz; P_α), +28.54 (overlapping dd; P_β), -6.93 (d, J = 28Hz; P_γ).

adenosine (8) was phosphitylated with 2-chloro-4*H*-1,3,2-benzodioxaphosphorin-4-one (salicyl phosphorochloridite) to give the intermediate (9) which was converted to the mixed phosphate-phosphite species (10) in two consecutive displacement reactions with pyrophosphate. Oxidation with a suspension of sulphur followed by deprotection of the ribose hydroxyls gave $ATP_{\alpha}S$ (12) in 69% yield (lit. yield = 60-75%; (Ludwig and Eckstein, 1989)).

The epimers of $ATP_{\alpha}S$ are much more easily separated by reverse phase HPLC than those of $ATP_{\beta}S$ even without the addition of divalent metal ions (Marquetant and Goody, 1983). Therefore preparative HPLC was used to obtain the pure Rp and Sp epimers of $ATP_{\alpha}S$. A typical separation is shown in Fig. 4.7. Up to 5μmoles of nucleotide could be applied to the column without significant loss of resolution. After passage through the column, peak fractions were pooled and small aliquots were taken, diluted, and reapplied to the column to ascertain their purity. In all cases a single peak was observed with no trace of the other isomer. Samples were then freed of triethylammonium bicarbonate and stored frozen as concentrated aqueous solutions. Further HPLC analysis of these concentrated samples on an analytical column gave a diastereomeric purity of > 99.8%. In addition, the epimers were distinguished by their different α–phosphoryl chemical shifts in ^{31}P-NMR (Fig.4.8).

One problem that was encountered is worth highlighting as a potential pitfall. The triethylamine used for HPLC was usually purified by distillation over potassium hydroxide (Section 2.1). Initial experiments, however, used triethylamine distilled from phthalic anhydride (13). Chromatograms obtained showed a single broad peak where the peaks for the $ATP_{\alpha}S$ epimers were expected. At first this was ascribed to a lack of resolution of the column but when runs were performed with triethylamine distilled from potassium hydroxide two well resolved peaks were obtained. It is thought that either some phthalic anhydride, a ring-opened derivative of phthalic anhydride, or an impurity

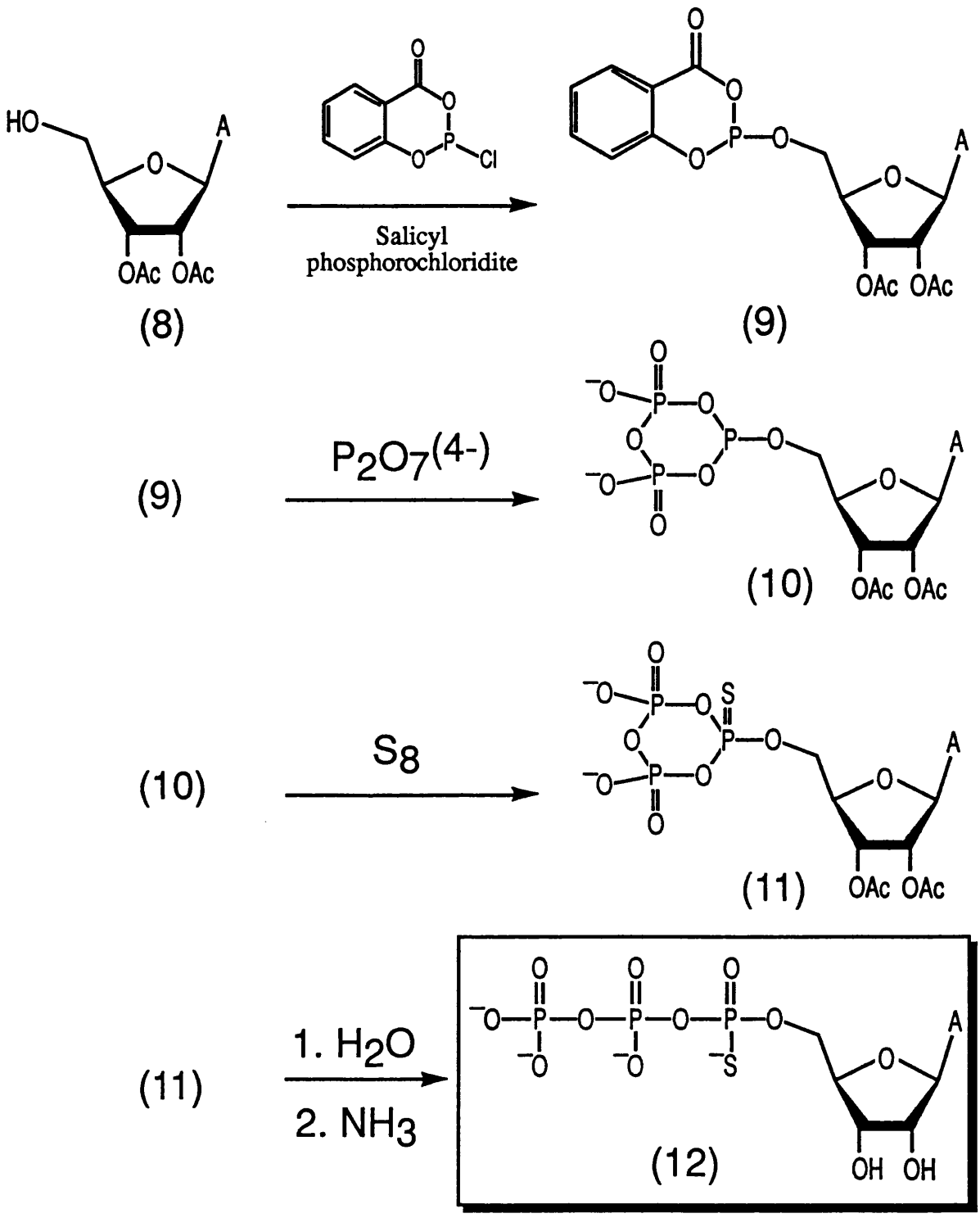

(8) = 2',3'-Di-O-acetyladenosine
(9) = 2-(2',3'-Di-O-acetyladenosyl)-4*H*-1,3,2-benzodioxaphosphorin-4-one
(10) = P^1-(2',3'-Di-O-acetyladenosyl)-P^2,P^3-dioxo-cyclotriphosphite
(11) = 2',3'-Di-O-acetyladenosine 5'-thiocyclotriphosphate
(12) = Adenosine 5'-O-(1-thiotriphosphate); racemic mixture

Figure 4.6. The Synthesis of Adenosine 5'-O-(1-thiotriphosphate), $ATP_{\alpha}S$

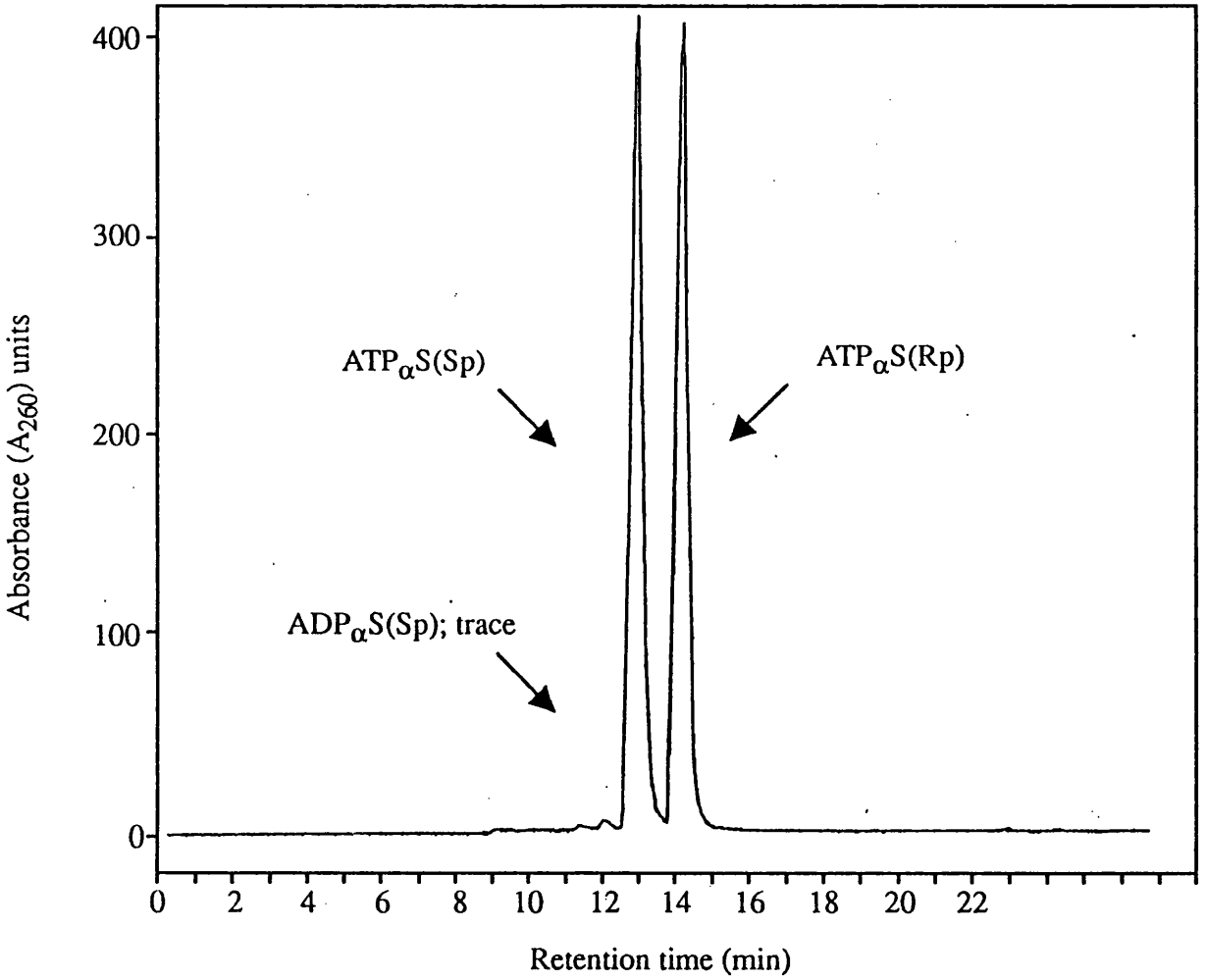

Figure 4.7. Typical separation of $ATP_{\alpha}S$ (racemic mixture) on a semipreparative reverse phase HPLC column. The column was eluted with 150mM TEAB and a 0-20% linear gradient of acetonitrile in 30min at a flow rate of 4ml/min.

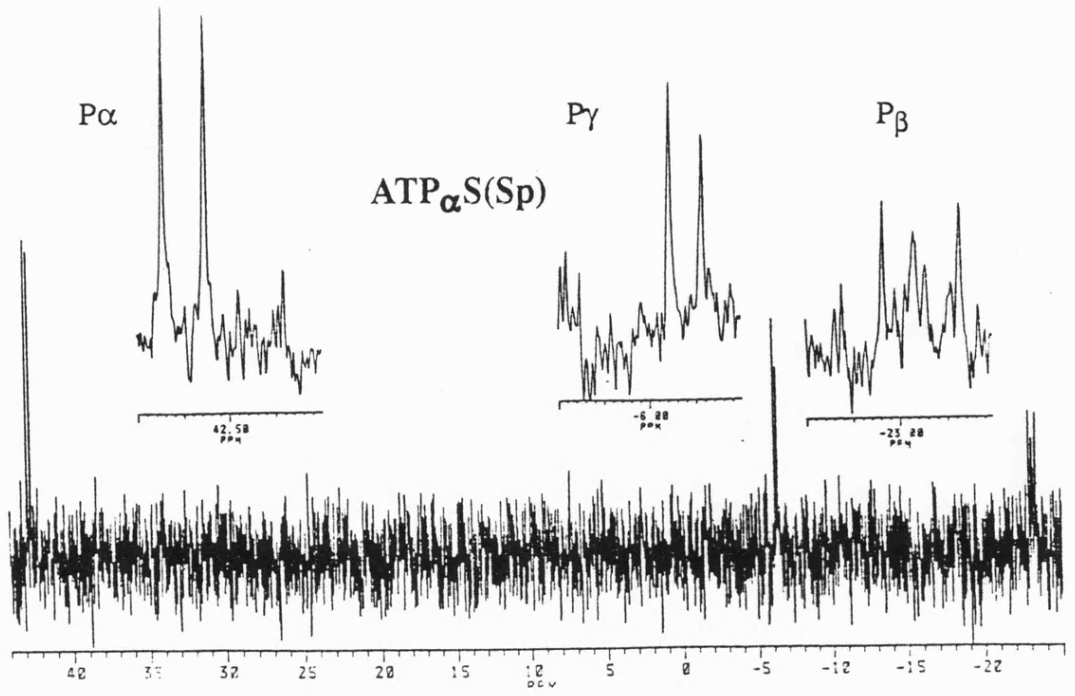

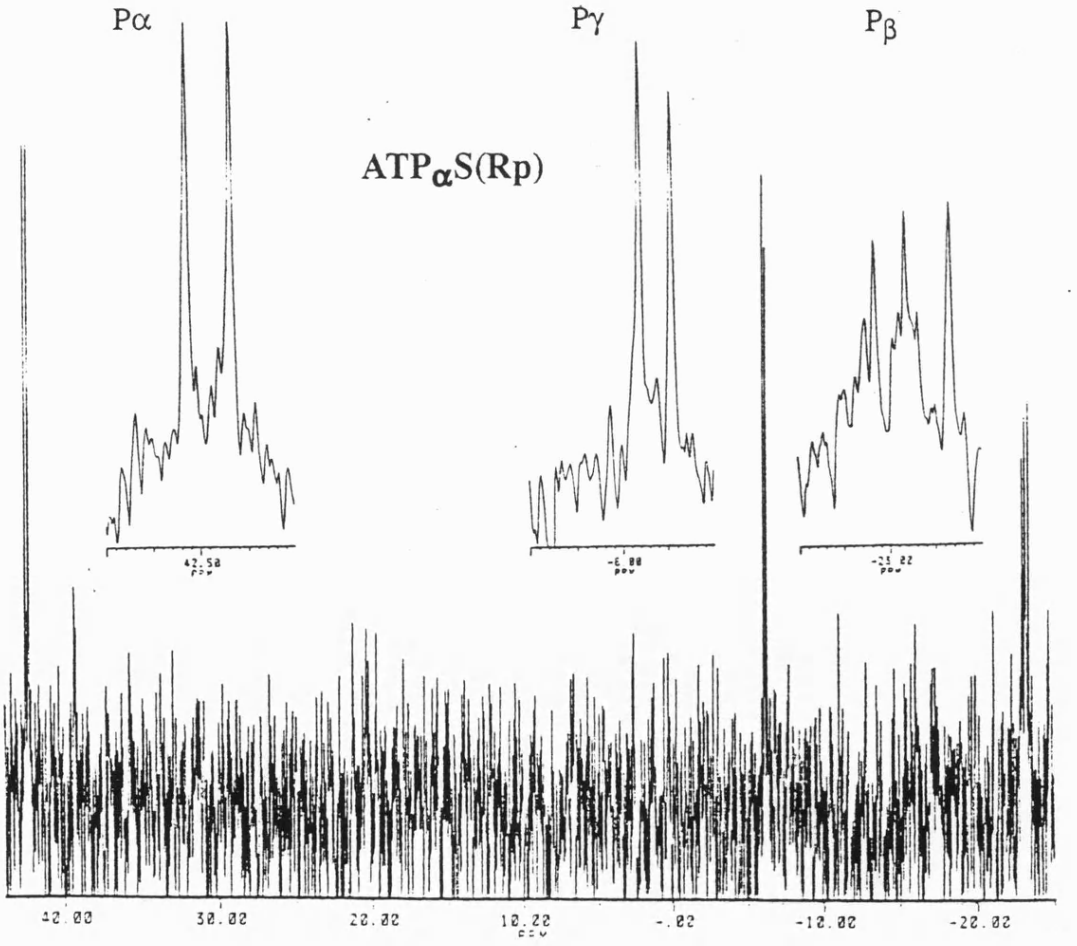

Figure 4.8. ^{31}P-NMR (121.5MHz) proton decoupled spectra of the Rp and Sp epimers of $ATP_{\alpha}S$. Samples consisted of 2mM nucleotide dissolved in 100mM CAPS buffer (pH 9.6), 10% D_2O, 10mM EDTA; total volume 0.5ml.

$ATP_{\alpha}S$(Sp): ^{31}P-NMR δ(121.5 MHz, D_2O) +42.75 (d, J = 28Hz; P_{α}), -23.11 (overlapping dd; P_{β}), -6.20 (d, J = 20Hz; P_{γ}).

$ATP_{\alpha}S$(Rp): ^{31}P-NMR δ(121.5 MHz, D_2O) +42.44 (d, J = 28Hz; P_{α}), -23.13 (overlapping dd; P_{β}), -6.19 (d, J = 20Hz; P_{γ}).

associated with it, distilled across with the triethylamine and was concentrated on the column, eluting over the same range as the nucleotide and masking its presence.

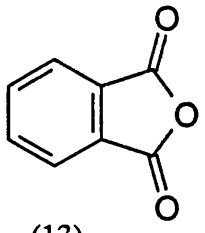

(13)

4.2.2. Synthesis of 2'(3')-O-(N-methyl)anthraniloyl adenosine 5' triphosphate (mantATP) and a preliminary investigation of its properties as a substrate for DNA gyrase.

MantATP (14) was synthesised according to Hiratsuka (1983) (Section 2.2.8). Initially the reaction mixture was purified by chromatography on Sephadex LH20 resin (which separates compounds according to their hydrophobicities), eluting with water. Separation of ATP and mantATP was judged from TLC analysis to be incomplete by this procedure and further purification was effected by anion-exchange chromatography on Sephadex A25 resin. This gave a good separation and pure mantATP was isolated. It was important that no ATP contamination was present since this could have given a misleading result in gyrase supercoiling assays

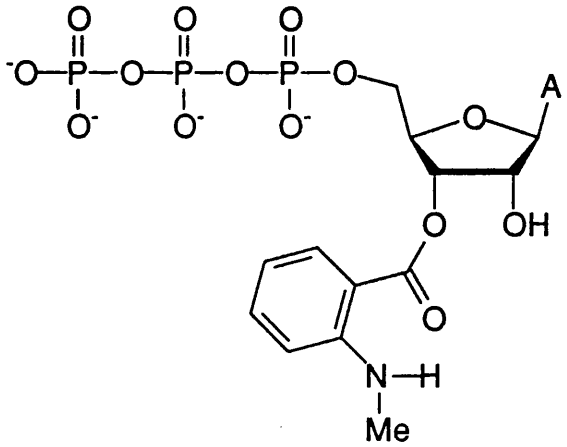

(14)

The ability of mantATP to substitute for ATP in the gyrase supercoiling reaction was briefly investigated. Fig. 4.9 shows that the ATP analogue did support supercoiling to a low level compared to ATP. The ladder of topoisomers produced suggests that gyrase operated in a distributive fashion with mantATP, dissociating from the DNA after each round of supercoiling. In contrast, with ATP as a substrate, gyrase operates processively, remaining bound to the DNA during multiple rounds of supercoiling. In view of the apparent distributive mechanism with mantATP it is difficult to compare its effectiveness as a substrate to that of ATP. An approximate estimate would be that mantATP is between 10- and 50-fold less effective than ATP, based on the concentration of enzyme required to give equivalent levels of supercoiling. The gyrase-catalysed hydrolysis of mantATP was investigated by the malachite green phosphate assay. Single 5 hour time points revealed that mantATP was hydrolysed approximately 10-fold slower than ATP (see Table 4.4).

These preliminary results suggest that mantATP is a reasonable substrate for gyrase. Since the mant group is fluorescent it may be possible to investigate the occurrence of any conformational changes during the gyrase ATPase with this analogue and its non-hydrolysable counterpart, 2'(3')-O-(N-methyl)anthraniloyladenosine 5'-(β,γ-imido)triphosphate, (mantp(NH)ppA). This approach has proved useful in studies of GTP hydrolysis by $p21^{NRAS}$ (Neal *et al.*, 1990) and is currently being pursued with gyrase (A. P. Jackson, personal communication).

4.2.3. $ATP_{\alpha}S$ (Rp) and (Sp) as substrates for the gyrase catalysed supercoiling reaction.

Supercoiling assays where ATP was replaced by the epimers of $ATP_{\alpha}S$ are shown in Fig. 4.10. The nucleotide concentration was kept constant at 1mM while the enzyme concentration was varied. In this way the concentration of enzyme required to convert approximately 50% of the relaxed plasmid pBR322 to the supercoiled form in 1 hour at

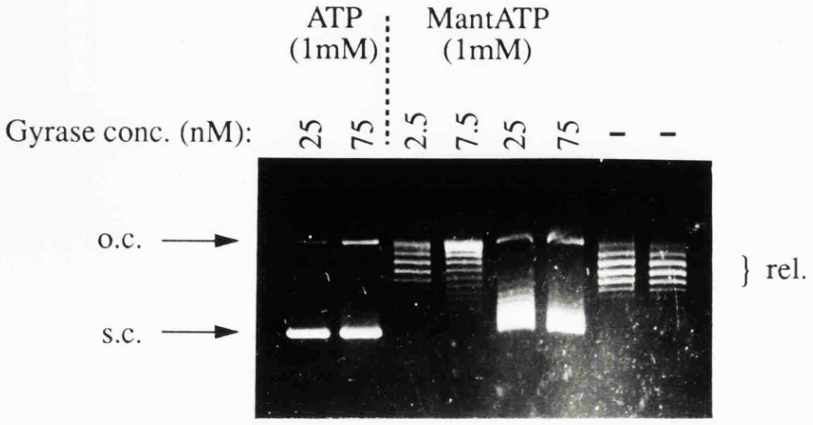

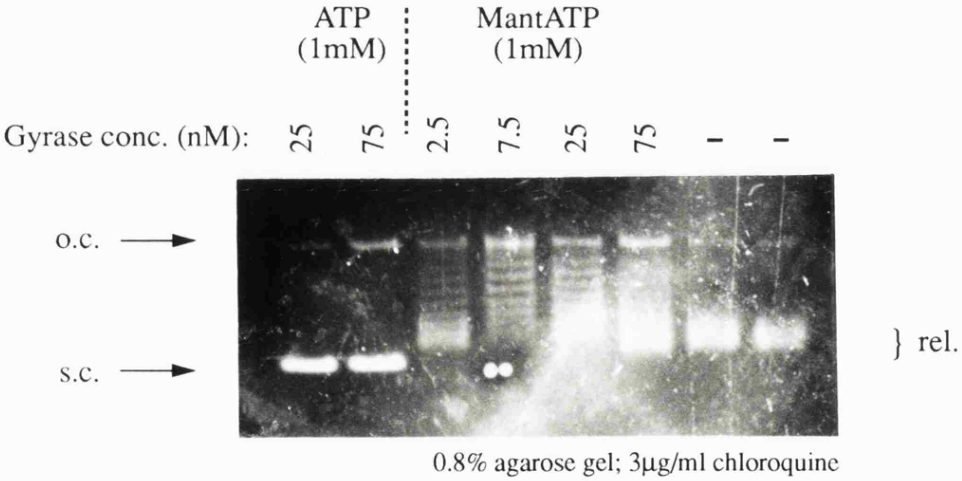

Figure 4.9. Supercoiling assay of mantATP

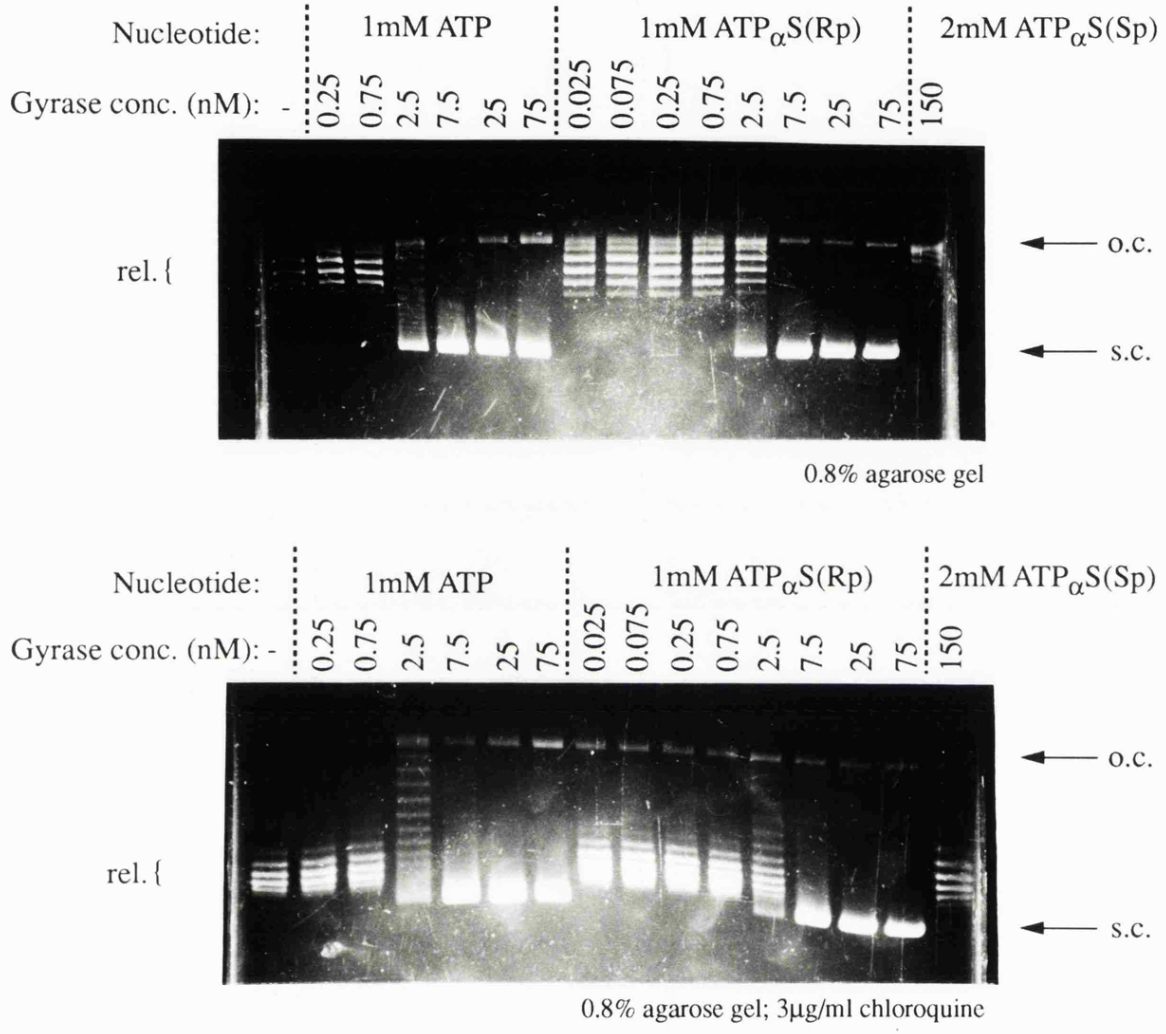

Figure 4.10. Comparison of ATP- and ATP$_\alpha$S-supported supercoiling at different enzyme concentrations

25°C was compared for each nucleotide. The results showed a striking preference for the Rp epimer over the Sp epimer of $ATP_{\alpha}S$ as shown in the table below.

Table 4.2. Comparison of the epimers of $ATP_{\alpha}S$ *versus* ATP as substrates for gyrase.

Nucleotide (1mM)	Gyrase conc. for 50% supercoiling (nM)	Relative effectiveness as substrate
ATP	1.5	1
$ATP_{\alpha}S$ (Rp)	1.5	1
$ATP_{\alpha}S$ (Sp)	»150	«0.01

$ATP_{\alpha}S$ (Rp)-supported supercoiling was indistinguishable from that of ATP at 1mM, while no activity with the Sp epimer of $ATP_{\alpha}S$ was evident at this concentration; at 2mM $ATP_{\alpha}S$ (Sp), as shown in Fig. 4.10, a very low level of supercoiling was apparent with a change in Lk of approximately -2 at the highest gyrase concentration of 150nM.

The $ATP_{\alpha}S$ (Rp)-supported reaction was investigated further by varying the nucleotide concentration at a constant enzyme concentration. Fig. 4.11 shows such an experiment. It was found that the sulphur analogue of ATP supported equivalent supercoiling at a 10-fold lower concentration than ATP as evidenced in Fig. 4.11 where tracks 3 and 7, and 4 and 8 are roughly comparable. Thus, at low concentrations, $ATP_{\alpha}S$ (Rp) appeared to be a better substrate than ATP.

Fig. 4.12 shows a comparison of the rate of supercoiling supported by $ATP_{\alpha}S$ (Rp) and ATP. The graph in Fig. 4.12(a) was obtained by laser densitometer scanning of gels such as those shown in Fig. 4.12(b) to determine the % intensity of the DNA in the supercoiled band. It can be seen that the progress of the supercoiling reaction is very similar for ATP at 1mM and $ATP_{\alpha}S$ (Rp) at 0.1mM and 1mM. With ATP at 0.1mM and $ATP_{\alpha}S$ (Rp) at 0.01mM the supercoiling rate is again very similar but greatly reduced

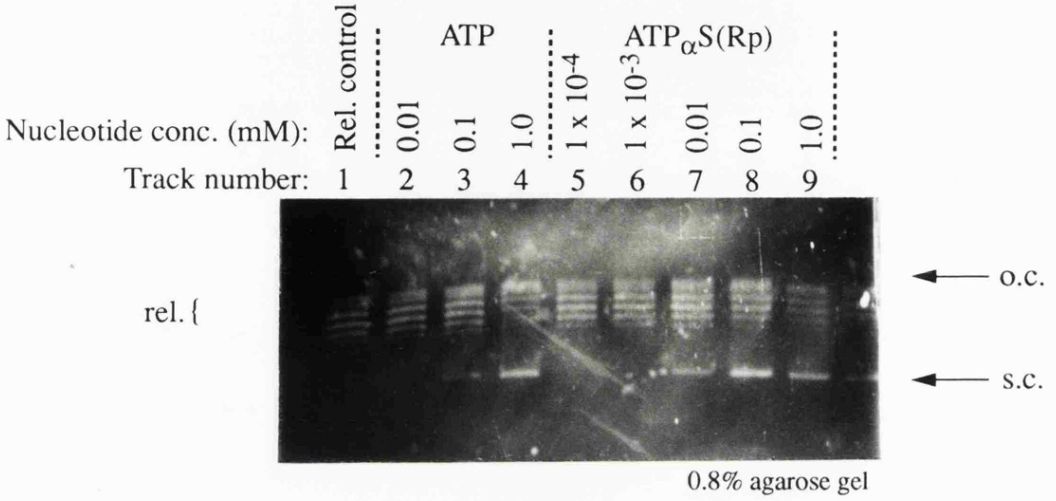

Figure 4.11. Comparison of ATP- and ATP$_\alpha$S-supported supercoiling at different concentrations

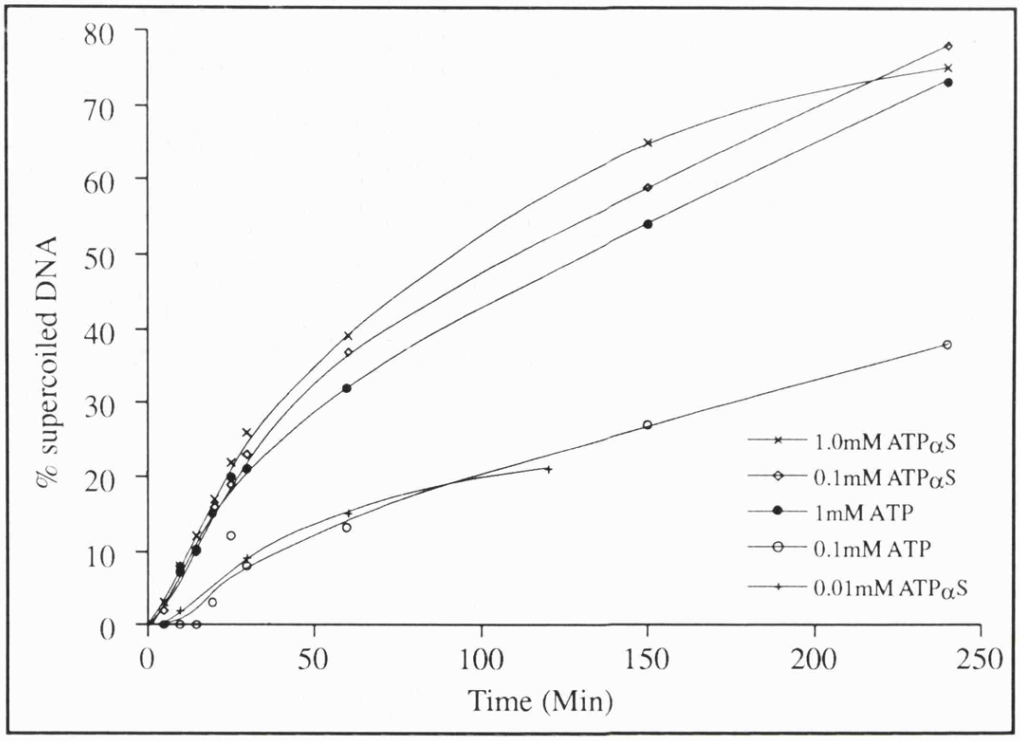

Figure 4.12(a). Comparison of time course of supercoiling supported by ATP and $ATP_{\alpha}S(Rp)$ at various concentrations.

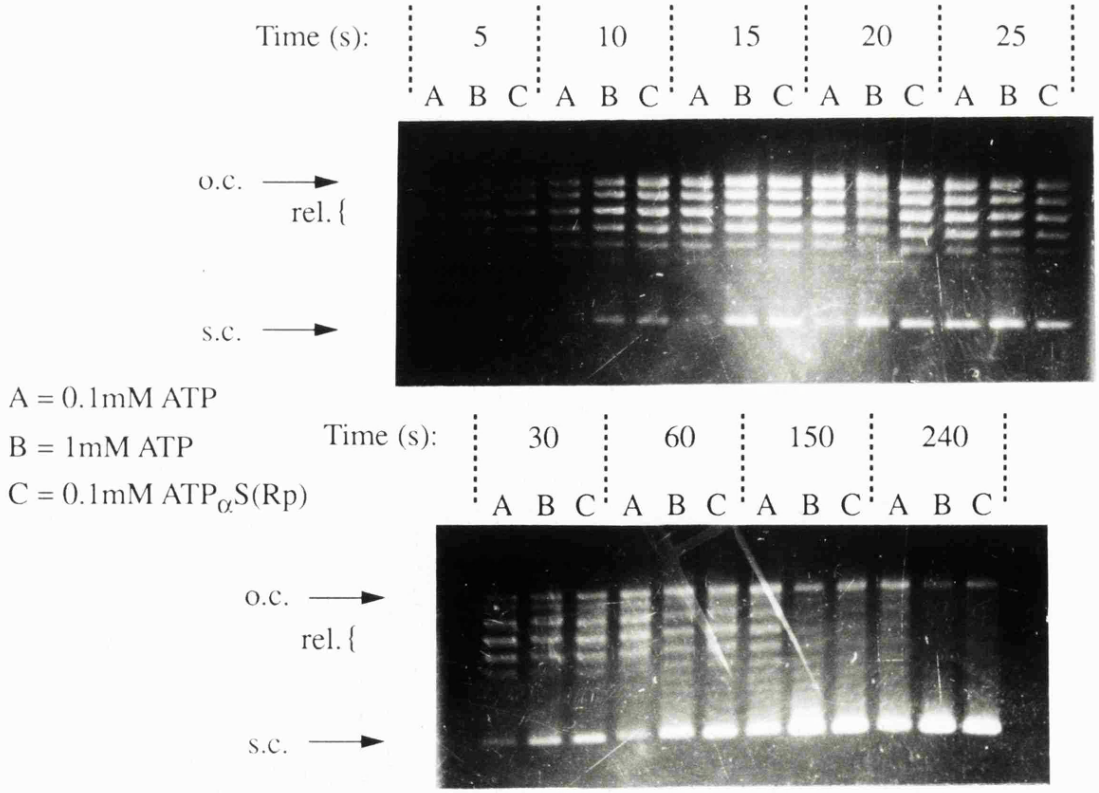

Figure 4.12(b). Time course of supercoiling supported by ATP (at 0.1mM & 1mM) and $ATP_{\alpha}S(Rp)$ (at 0.1 mM); gyrase conc. = 2nM.

from reactions at the higher nucleotide concentrations. A comparison of the apparent rate of supercoiling for ATP and the analogue at 0.1mM reveals that $ATP_{\alpha}S$ (Rp)-supported supercoiling is roughly 4-5 times faster than that with ATP. The apparent rates shown in the graph are not linear but curve off with increasing time. This probably reflects the fact that the supercoiled band on an agarose gel consists of many topoisomers with specific linking differences of roughly -0.04 or more. Thus the experiment described here only monitors the formation of moderately supercoiled topoisomers and cannot follow further supercoiling.

As shown above, the Sp epimer of $ATP_{\alpha}S$ supported very limited supercoiling even at high concentration. ADPNP has been shown not to be hydrolysed by gyrase (Tamura *et al.*, 1992) and to promote stoichiometric supercoiling (Sugino *et al.*, 1978). A brief investigation into whether $ATP_{\alpha}S$(Sp) supported catalytic or stoichiometric supercoiling was inconclusive. For stoichiometric supercoiling ΔLk should reach a maximum after sufficient time which is proportional to the gyrase concentration. This was not observed for $ATP_{\alpha}S$(Sp) and instead a slow but steady increase in ΔLk was seen up to about -8 in 12 hours at 150nM gyrase (data not shown). Since this level of supercoiling is below the level expected from stoichiometric supercoiling (even allowing for a proportion of inactive GyrB; see Appendix I), it does not unequivocally indicate enzyme turnover. However, the observation of slow but apparently catalytic hydrolysis of $ATP_{\alpha}S$(Sp) (see section 4.2.9; Fig. 4.27) strongly suggests that the supercoiling reaction is also catalytic but very slow.

In order to explore the binding of this analogue to the enzyme its properties as an inhibitor of the ATP-dependent supercoiling reaction were investigated. Fig. 4.13. shows an experiment where the concentration of $ATP_{\alpha}S$(Sp) was varied at a constant ATP concentration of 0.03mM. Approximately 50% inhibition occurred at a concentration of 1.0mM $ATP_{\alpha}S$(Sp), roughly 35-fold higher than the ATP concentration.

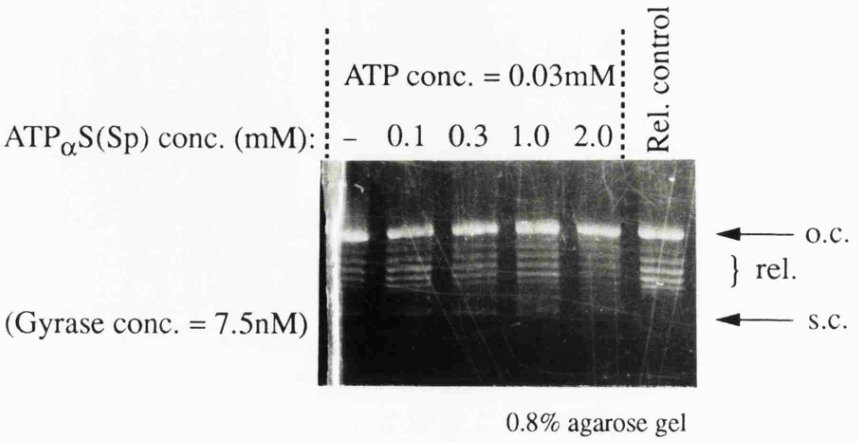

Figure 4.13. Inhibition of ATP-dependent supercoiling by ATP$_\alpha$S(Sp).

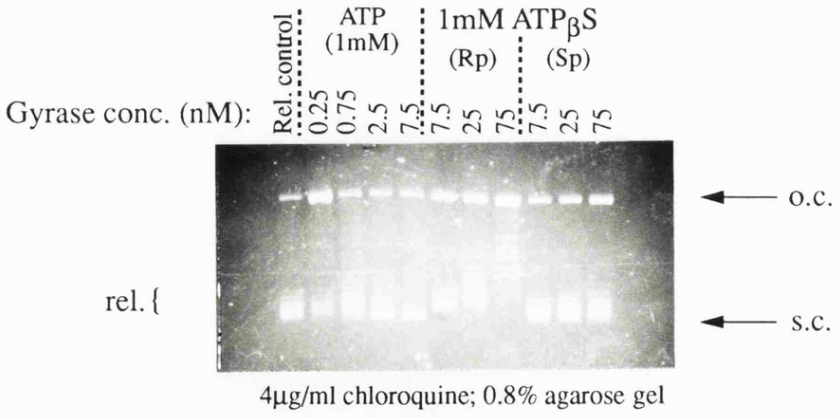

Figure 4.14. ATP- and ATP$_\beta$S-supported supercoiling at various gyrase concentrations

4.2.4. $ATP_{\beta}S$ (Rp) and (Sp) as substrates for the gyrase catalysed supercoiling reaction.

Gyrase exhibited a preference for the Rp epimer of $ATP_{\beta}S$ over the Sp epimer. In a 1-hour supercoiling assay no activity was observed for $ATP_{\beta}S$(Sp) while a slow introduction of superhelical turns was noted with $ATP_{\beta}S$(Rp) as shown in Fig. 4.14. It can be seen that at high enzyme concentration (75nM) a ΔLk of about -6 was produced with the Rp epimer. The figure also shows a comparison of the effectiveness of $ATP_{\beta}S$ and ATP. For $ATP_{\beta}S$(Rp) a gyrase concentration of 75nM gave less supercoiling than a gyrase concentration of 0.75nM with ATP. Thus the effectiveness of $ATP_{\beta}S$(Rp) was < 0.01 compared to ATP under these conditions.

The low level of supercoiling with $ATP_{\beta}S$ was further investigated by monitoring the progress of the supercoiling reaction over a long time course. Fig. 4.15. shows such an experiment for $ATP_{\beta}S$(Rp). After 8 hours incubation, a ΔLk of approximately -8 was seen which corresponds to 4 rounds of supercoiling. The gyrase concentration was 25nM and the DNA concentration was 3.4nM in this experiment and so the proportion of enzyme to DNA was roughly 7:1. Therefore it would seem that the low level of supercoiling observed could be ascribed to a stoichiometric mechanism. However three pieces of evidence strongly argue against this. Firstly, the proportion of active gyrase is considerably less than the total protein concentration (see Appendix I). Secondly, there is no evidence of the reaction reaching a plateau in the level of supercoiling. Thirdly, $ATP_{\beta}S$(Rp) is hydrolysed by gyrase (see section 4.2.6 and 4.2.8). Thus it would appear that $ATP_{\beta}S$(Rp) promotes a slow but catalytic supercoiling reaction.

The time course of supercoiling with the Sp epimer of $ATP_{\beta}S$ is shown in Fig. 4.16. Here the DNA concentration was 3.4nM. No negative supercoiling was seen and instead the DNA became slowly positively supercoiled which was confirmed on chloroquine gels (not shown). The same positive supercoiling was seen with or without $ATP_{\beta}S$(Sp)

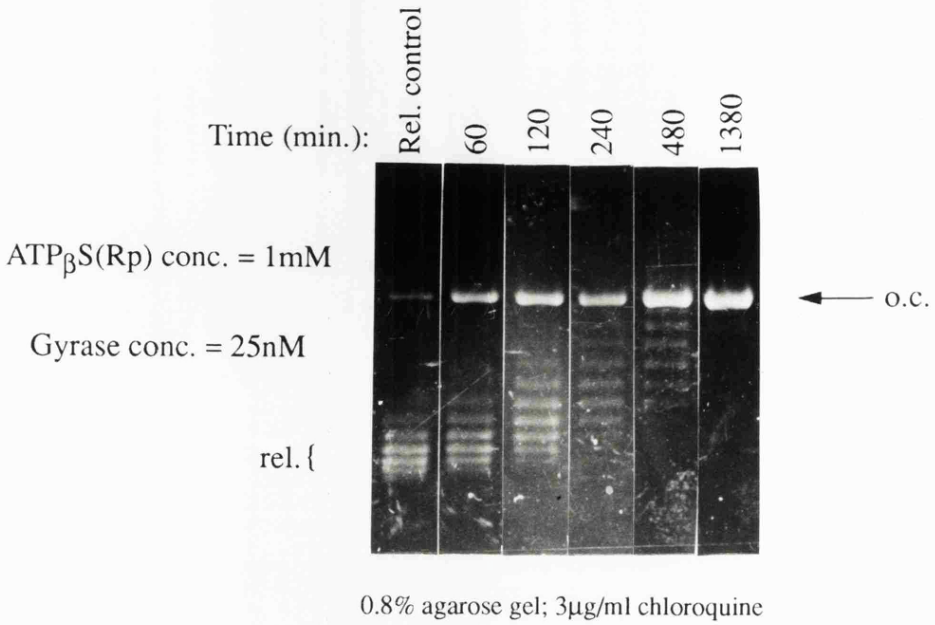

Figure 4.15. Time course of supercoiling with $ATP_{\beta}S(Rp)$

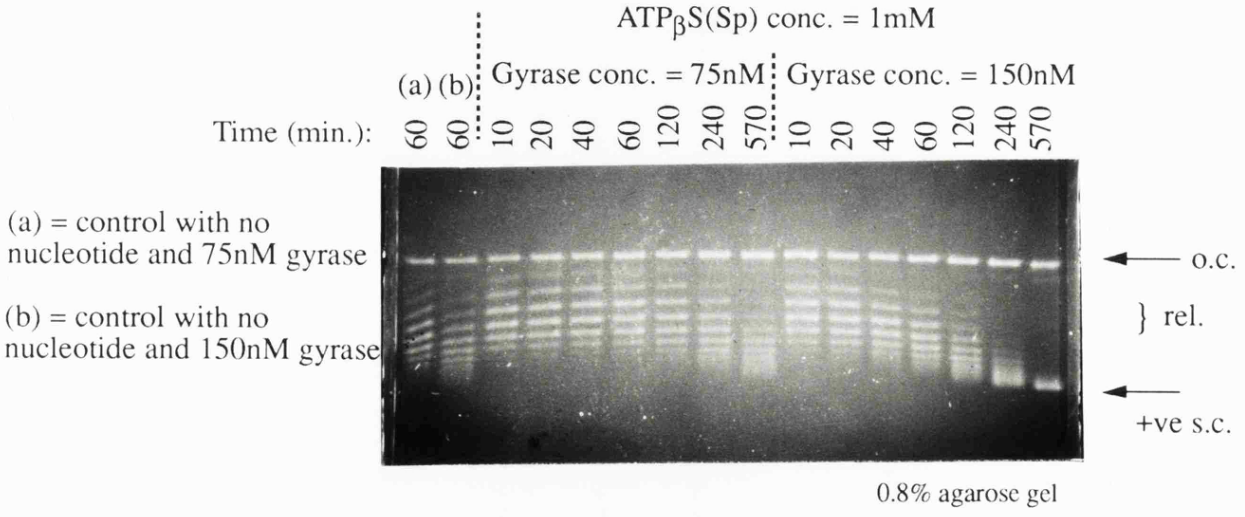

Figure 4.16. Time course of supercoiling with $ATP_{\beta}S(Sp)$

present (as shown by control (b) in the figure and other experiments not shown) and was thus not due to the interaction of the nucleotide with the enzyme. A more rapid and extensive introduction of positive supercoils into the DNA occurred with the higher enzyme concentration (150nM) although even here the reaction did not appear to have reached completion after 9.5 hours. After this time a ΔLk of between +6 to +10 appeared to have occurred in the reaction at 150nM gyrase while at the lower gyrase concentration the ΔLk was approximately +4. Thus the positive supercoiling appeared to be a general property of gyrase (in the absence of active nucleotide) at high enzyme to DNA ratios. A mechanism for this interesting reaction is proposed in Fig. 4.17. which is based on the model for the negative supercoiling reaction shown in Fig. 1.7. In the figure three gyrase tetramers are shown bound to the DNA. Since each copy of gyrase is thought to bind to DNA with a positive wrap (Liu and Wang, 1978b), the resulting torsional stress elsewhere in the DNA is relieved by three negative writhes. This apparently negatively supercoiled DNA can be relaxed by one of the bound gyrases (shown in the figure as essentially a reverse of the negative supercoiling reaction of Fig. 1.7). After removal of bound protein the result is positively supercoiled DNA. The key feature of this proposal is that the positive supercoiling is a passive process driven by the binding energy of the DNA-protein interaction. Thus the maximum number of positive supercoils introduced should be limited by the stoichiometry of gyrase to DNA. In the experiment illustrated in Fig. 4.16. up to 4 supercoils are produced with a gyrase concentration of 75nM and a gyrase to DNA ratio of 22. Assuming that 9% of the GyrB is active (see Appendix I) then the effective concentration of gyrase tetramers in the reaction was 6.8nM and the active gyrase to DNA ratio was roughly 2:1. Thus the positive supercoiling may have approached its limit after 9.5 hours. It would be interesting to probe the stoichiometry of this phenomenon further with longer time points.

In view of the data discussed above that showed that $ATP_{\beta}S(Sp)$ exerted no detectable effect on gyrase-catalysed supercoiling the question arose as to whether this nucleotide

Figure 4.17. A proposed mechanism for positive supercoiling at high gyrase to DNA ratios. The figure is based on the scheme for negative supercoiling shown in Fig. 1.7 and relaxation is depicted as essentially a reverse of the supercoiling reaction. In pBR322 as many as 20 copies of gyrase may be bound at high protein to DNA ratios; in the figure 3 gyrase molecules are shown bound to initially relaxed cccDNA. The DNA is wrapped in a positive superhelical sense around the protein (Liu and Wang, 1978) which induces 3 negative writhes elsewhere in the DNA to relieve torsional stress as shown in the structure in the top right of the figure. It is proposed that gyrase is able to relax the apparently negatively supercoiled DNA as shown for one of the bound gyrases in the structure in the bottom right of the figure. The relaxation reaction is shown in progress with DNA translocation half-complete. (In the figure this DNA translocation is shown coming out of the page towards the reader as indicated by the arrow). The DNA is translocated through the protein and then through a transient double-stranded gap in the wrapped DNA. After resealing of the DNA this process results in an increase in the linking number of 2; positively supercoiled DNA is obtained after removal of the bound protein.

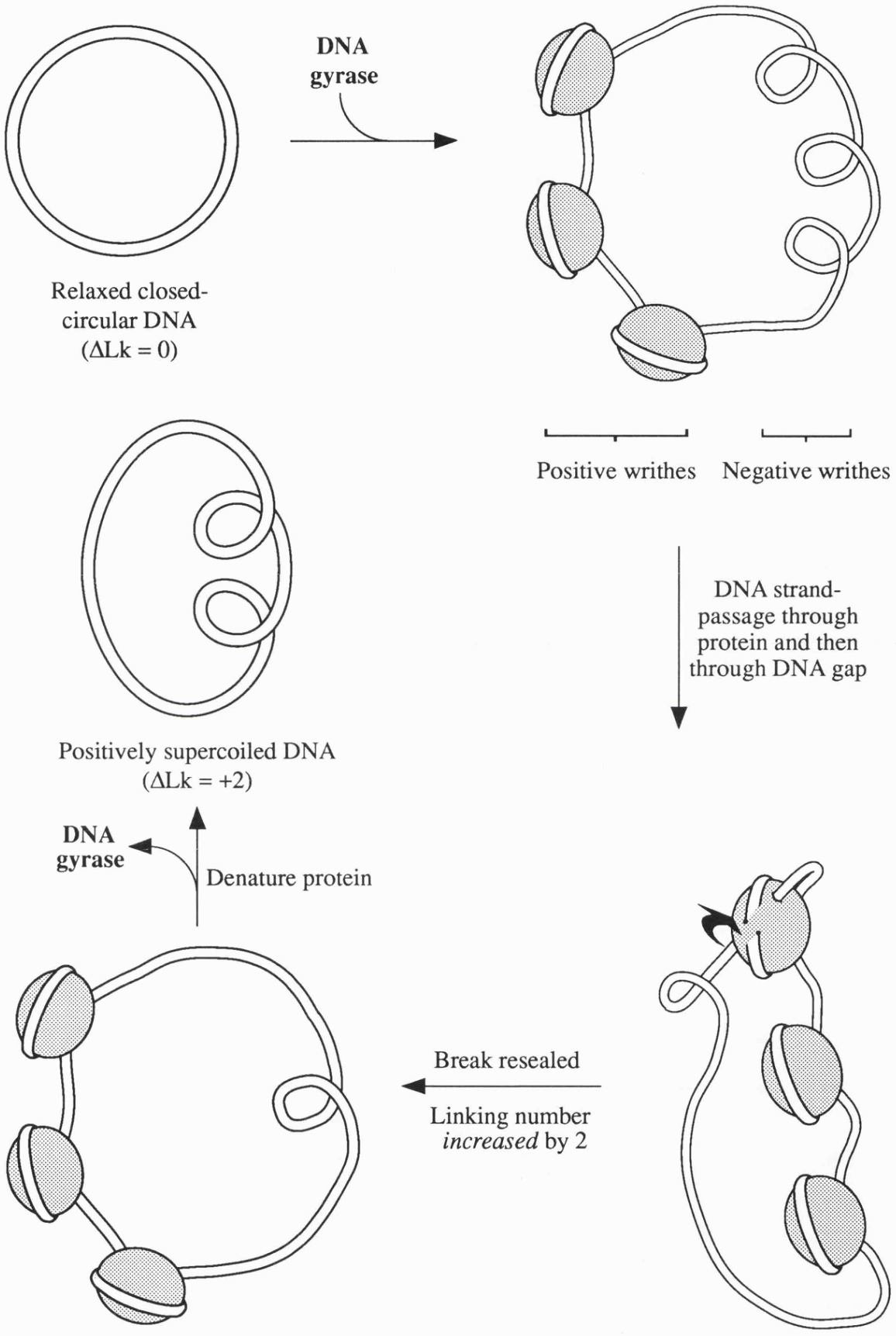
DNA
gyrase
Relaxed closed-
circular DNA
(ΔLk = 0)
Positive writhes
Negative writhes
DNA strand-
passage through
protein and then
through DNA gap
Positively supercoiled DNA
(ΔLk = +2)
DNA
gyrase
Denature protein
Break resealed
Linking number
increased by 2

bound to gyrase at all. This was addressed by investigating the ability of both epimers of $ATP_{\beta}S$(Sp) to inhibit ATP-dependent supercoiling (Fig. 4.18).

Table 4.3. Inhibition of ATP-dependent supercoiling by $ATP_{\beta}S$

Nucleotide	Conc. giving 50% inhibition of supercoiling (with ATP at 0.3mM)
$ATP_{\beta}S$(Rp)	0.3mM
$ATP_{\beta}S$(Sp)	~0.6mM

The results showed that under these conditions both epimers of $ATP_{\beta}S$ were moderate inhibitors and suggested that $ATP_{\beta}S$(Rp) was bound by gyrase approximately as tightly as ATP while $ATP_{\beta}S$(Sp) was bound roughly 2-fold weaker than ATP.

4.2.5. Hydrolysis of $ATP_{\alpha}S$ and $ATP_{\beta}S$ by gyrase.

Preliminary information on nucleotide hydrolysis was obtained from the malachite green assay (a single time point colorimetric assay measuring the release of phosphate; see section 2.26.1). However, for a more detailed analysis of nucleotide hydrolysis a continuous assay was desirable. The well known pyruvate/lactate dehydrogenase coupled ATPase assay (eg. Trentham *et al.*, 1976) has been used successfully with gyrase (Tamura and Gellert, 1990). This system regenerates ATP hydrolysed by the enzyme under study using pyruvate kinase and PEP (Fig. 4.19.). This feature, which is often desirable in ATPase measurements, imposes limitations on the application of the assay to the hydrolysis of $ATP_{\alpha}S$ and $ATP_{\beta}S$. With $ATP_{\beta}S$, both the Rp and Sp epimers are hydrolysed to prochiral $ADP_{\beta}S$. Since the stereospecificity of pyruvate kinase is not absolute, both the Rp and Sp epimers of $ATP_{\beta}S$ will be regenerated resulting in the contamination of epimerically pure starting material and drastically altering the kinetics in an unpredictable fashion. With $ATP_{\alpha}S$, hydrolysis yields $ADP_{\alpha}S$ which

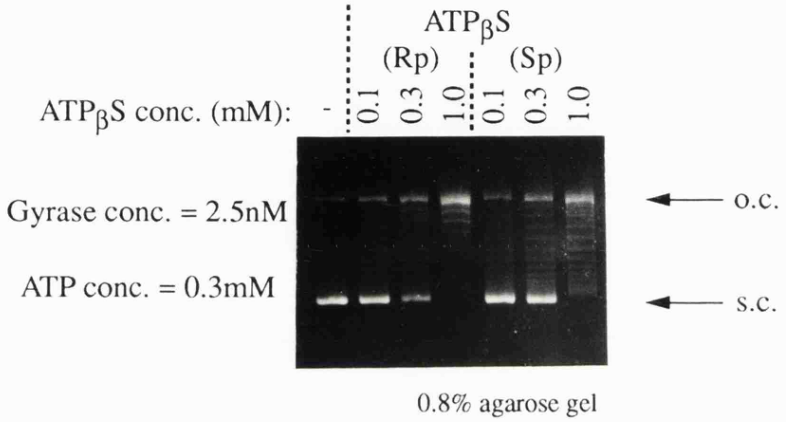

Figure 4.18. Inhibition of ATP-dependent supercoiling by (Rp) and (Sp) $ATP_{\beta}S$

still retains its chirality and therefore, in principal, the coupled assay should be suitable. However, the sulphur analogues of ATP are much worse substrates for pyruvate kinase, and so large amounts of this enzyme would be required in the assay in order that it was not rate limiting. Such large concentrations of coupling enzyme may give problems from solubility or the presence of minor contaminants.

Fortunately a coupled assay measuring phosphate release (Fig. 4.20) has recently been developed (Banik and Roy, 1990) and this was successfully used to investigate the hydrolysis by gyrase of $ATP_{\alpha}S$ and $ATP_{\beta}S$ compared to ATP.

4.2.6. Hydrolysis of nucleotides as measured by the malachite green assay.

The results for MantATP and $ATP_{\beta}S$ hydrolysis compared to ATP are shown in Table 4.4 below. For a discussion of the mantATP result see section 4.2.2 above.

Table 4.4. Comparison of the hydrolysis of various nucleotides with ATP.

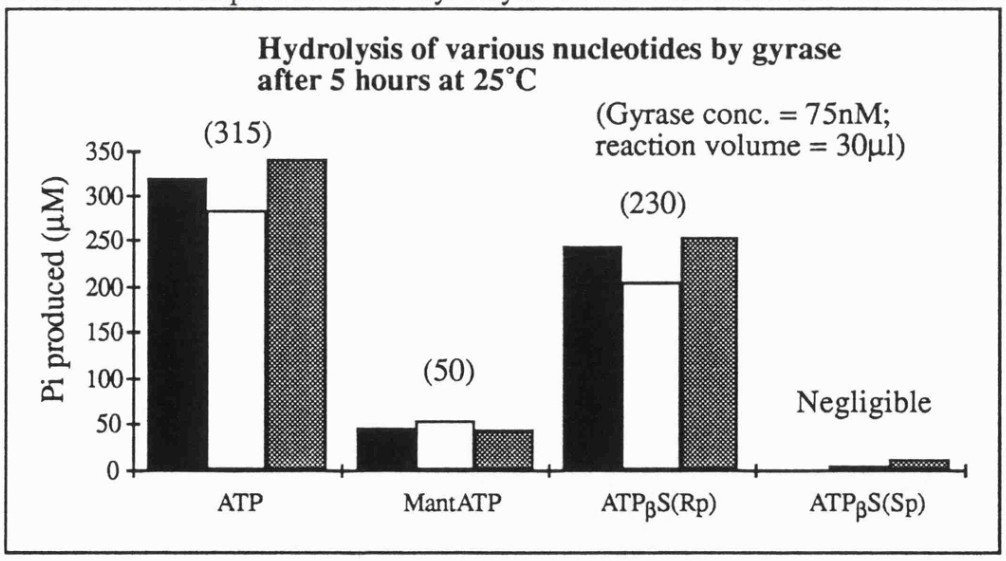

In the table three sets of data are shown with an average value given above the columns. Reactions were incubated at 25°C for 5 hours and in all cases the initial nucleotide

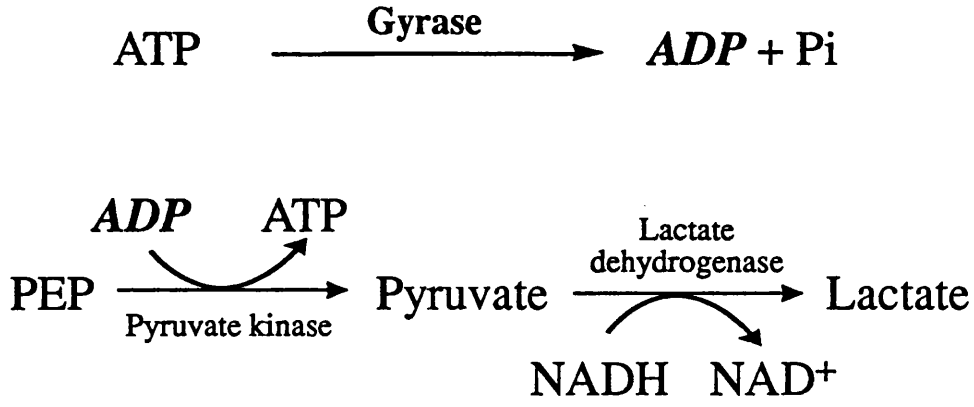

Figure 4.19. Pyruvate kinase/lactate dehydrogenase coupled ATPase assay.

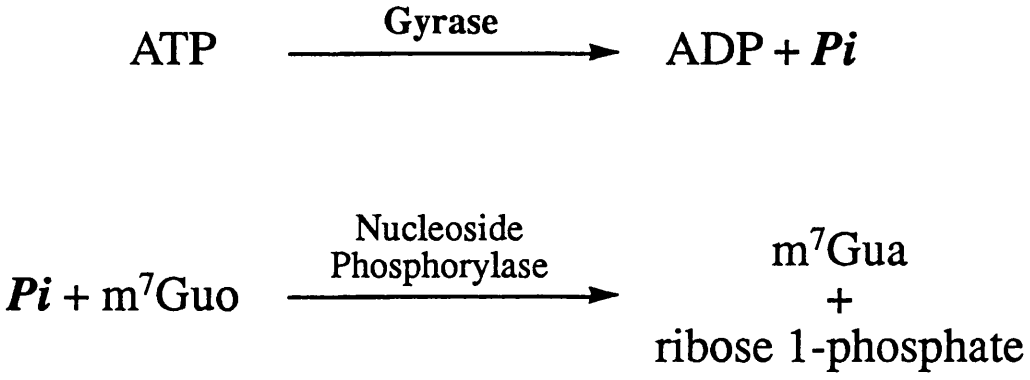

Figure 4.20. Fluorimetric coupled assay used to monitor the hydrolysis of ATP and its analogues

concentration was 1mM. For ATP, a concentration of 315 μM phosphate (in a 30μl reaction volume) was produced which gives an apparent turnover number for gyrase of 0.23/s averaged over the time period of 5 hours. This is considerably lower than published values which are closer to 1/s (Maxwell and Gellert, 1984) obtained from initial rate measurements and may be due to ADP inhibition; ADP has been reported to be a competitive inhibitor with a K_i of 70μM (Sugino and Cozzarelli, 1980) although the significance of K_M and K_i values for gyrase is uncertain (Maxwell *et al.*, 1986; see also Section 4.3 in this chapter).

Less than 10μM P_i was detected for the $ATP_\beta S$(Sp) reaction which was at the limit of the sensitivity of the assay. This gives a maximum turnover for $ATP_\beta S$(Sp) of 0.44/min averaged over the 5 hour period. In contrast, the Rp epimer was well hydrolysed with approximately 230μM P_i formed in 5 hours giving an apparent turnover of 0.17/s. This value probably overestimates the level of enzymatic hydrolysis of $ATP_\beta S$ because the $ADP_\beta S$ formed is unstable at the acidic pH of the assay and probably undergoes chemical hydrolysis to liberate AMP and thiophosphate which desulphurises to give phosphate. Thus two moles of phosphate are liberated when one mole of $ATP_\beta S$ is hydrolysed enzymatically. Correcting for this effect gives a value for $ATP_\beta S$ hydrolysis which is 37% of the value for ATP.

4.2.7. Characterisation of the continuous fluorimetric phosphate assay to measure the gyrase ATPase.

Control experiments indicated that the coupling system was active in gyrase supercoiling buffer giving a linear decrease in fluorescence with increasing phosphate concentrations up to about 20μM (Fig. 4.21). In this graph the phosphate concentration is plotted against $(F_0\text{-}F/F_0)$ where F is the fluorescence after addition of phosphate and F_0 is the initial fluorescence. Not surprisingly, it was found to be necessary to omit BSA from the reaction as this gave a large fluorescence quenching effect. Control supercoiling and

PK/LDH ATPase experiments with gyrase in the absence of BSA gave identical results to when it was present.

The emission wavelength was optimised from a difference spectrum of m^7Guo (Fig. 4.22). This was obtained by subtracting the emission profile of m^7Gua from the profile of m^7Guo. A peak at 395nm was obtained and this wavelength was used in further experiments.

Fig. 4.23 shows a typical trace following ATP hydrolysis by gyrase over 1000s and demonstrates that the decrease in fluorescence was linear over this time. The effect of withholding various components of the assay was tested to ensure that the rates observed were not a result of any contaminants. As expected, omission of ATP, gyrase, or nucleoside phosphorylase resulted in no reaction. Control experiments to check that the coupling enzyme was not rate limiting were also performed by establishing a rate with gyrase and then adding further nucleoside phosphorylase. Even at a 10-fold lower concentration of nucleoside phosphorylase (0.13units/ml) than that used in the standard assay (1.3units/ml) it was found not to be rate limiting.

The gyrase concentration-dependence of the initial rate of ATP hydrolysis is shown in Fig. 4.24. The data indicated that the rate was proportional to the enzyme concentration over the range tested (0-150nM).

4.2.8. A steady-state analysis of the hydrolysis of ATP, $ATP_{\alpha}S$, and $ATP_{\beta}S$.

The steady-state kinetics for ATP hydrolysis investigated by both the PK/LDH assay and the fluorimetric phosphate assay are shown in Fig 4.25. A hyperbolic curve of the form of the Michaelis-Menten equation was fitted to the data and a least-squares non-linear regression program was used to obtain values for V_{max} and K_M. In this analysis the

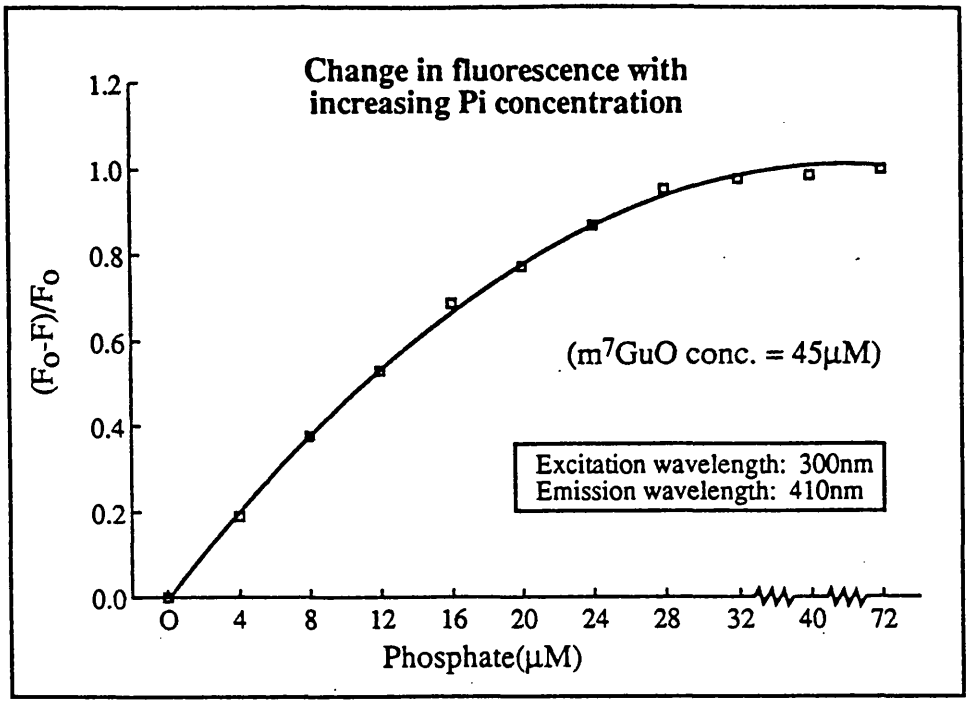

Figure 4.21. Calibration of the nucleoside phosphorylase phosphate assay in gyrase supercoiling buffer. (Each point on the graph is an average of two readings).

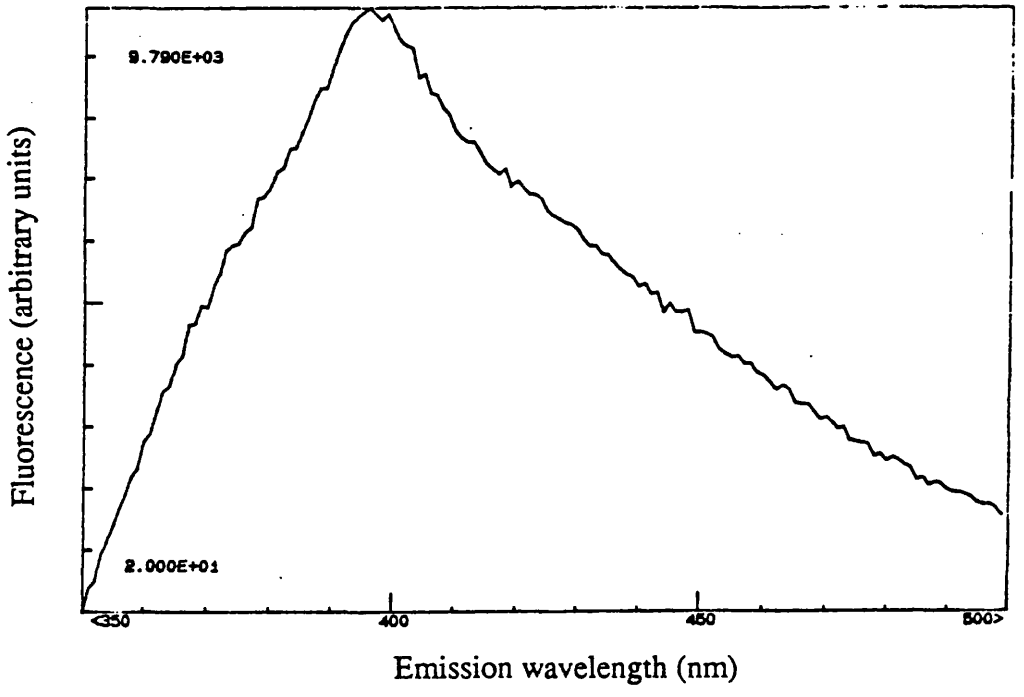

Figure 4.22. An excitation-emission difference spectrum at various emission wavelengths for m^7Guo in assay buffer conditions.

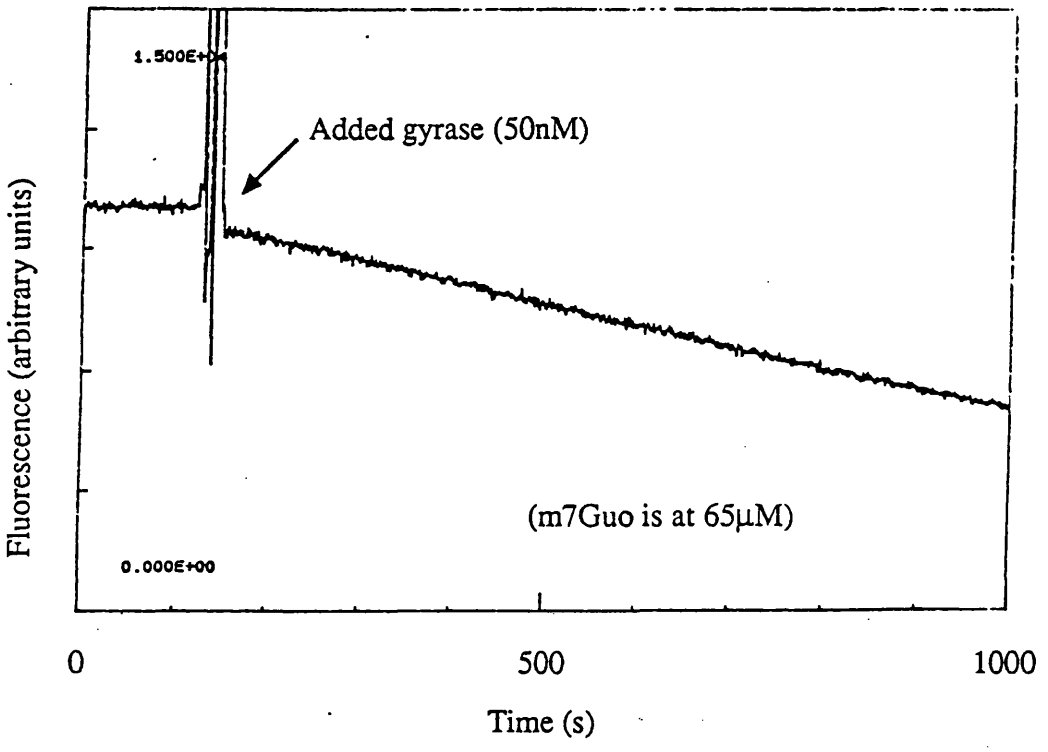

Figure 4.23. A typical fluorimeter trace showing the rate obtained with 1mM ATP and 50nM gyrase.

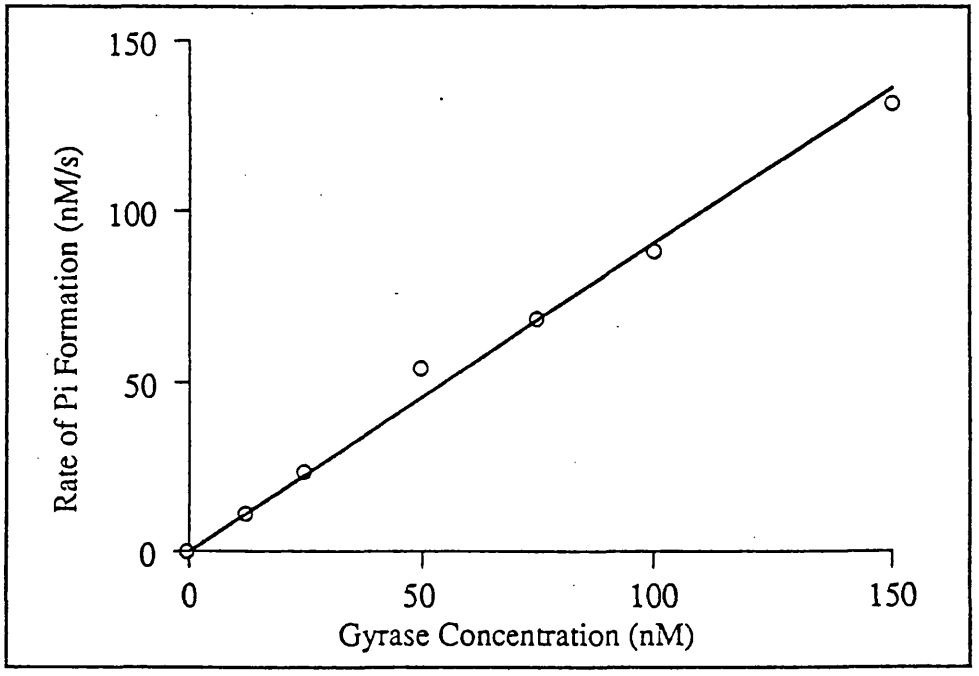

Figure 4.24. The dependence of the ATPase rate on gyrase concentration

presence of two ATP sites and the probable cooperativity between the two sites was not considered (see Section 4.3). It can be seen that there was a reasonable comparison between the two assays giving similar values for K_M^{app} and k_{cat}^{app} which compared favourably with those reported in the literature. Fig. 4.26. shows the initial rate of hydrolysis plotted against nucleotide concentration for $ATP_\alpha S(Rp)$ and $ATP_\beta S(Rp)$; no hydrolysis was detected for the Sp epimers which explained their inability to substitute for ATP in the supercoiling reaction (Sections 4.2.3 and 4.2.4).

$ATP_\alpha S(Rp)$ was well hydrolysed by gyrase and gave a similar k_{cat}^{app} to ATP of roughly 1.1/s while the K_M^{app} was almost 12-fold lower than that of ATP. These kinetic properties of $ATP_\alpha S(Rp)$ are reflected in its effectiveness as a substrate for supercoiling where $ATP_\alpha S(Rp)$ had an equivalent activity to ATP at a concentration roughly 10-fold lower (section 4.2.3; Fig 4.11). Furthermore, at high concentrations (1mM) of ATP and $ATP_\alpha S(Rp)$, well above their respective apparent K_M's, their effectiveness in the supercoiling reaction was roughly equivalent (Fig. 4.10) which corresponds to the similar rates of hydrolysis at 1mM nucleotide in Figs. 4.25 and 4.26. An additional correlation between hydrolysis and supercoiling with these nucleotides is available from a comparison of the rates of supercoiling at different nucleotide concentrations (Fig. 4.12) and the rates of hydrolysis in Figs. 4.25.and 4.26; for example, in the supercoiling experiments, the rate with 0.1mM $ATP_\alpha S(Rp)$ is between 4 to 5 -fold faster than with 0.1 mM ATP while $ATP_\alpha S(Rp)$ is hydrolysed roughly 4-fold faster than ATP. Thus, in this respect, the hydrolysis of this analogue appears to be well coupled to the supercoiling reaction.

$ATP_\beta S(Rp)$ is also a good substrate for hydrolysis with a similar K_M^{app} to ATP and a k_{cat} approximately 2-fold lower than that of ATP. This confirms the preliminary data from the malachite green assay (Section 4.2.6; Table 4.4). Section 4.2.4 showed that this analogue was a poor substrate for supercoiling supporting only a very slow reaction.

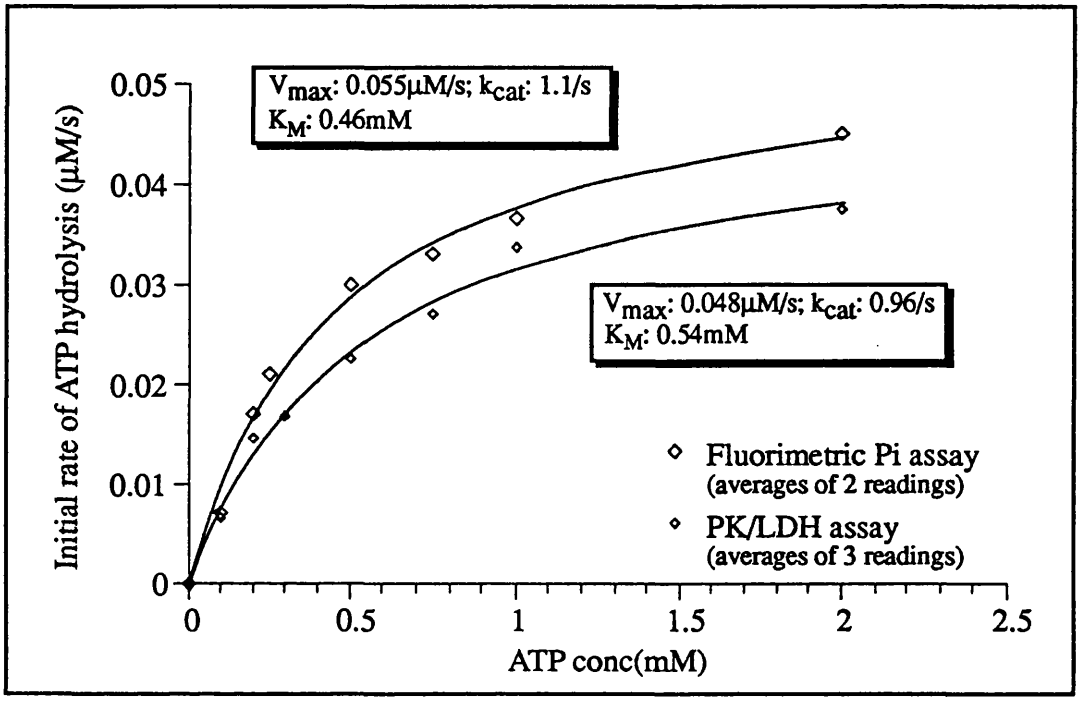

Figure 4.25. Comparison of the steady state kinetics as measured by the PK/LDH assay and the fluorimetric phosphate assay.

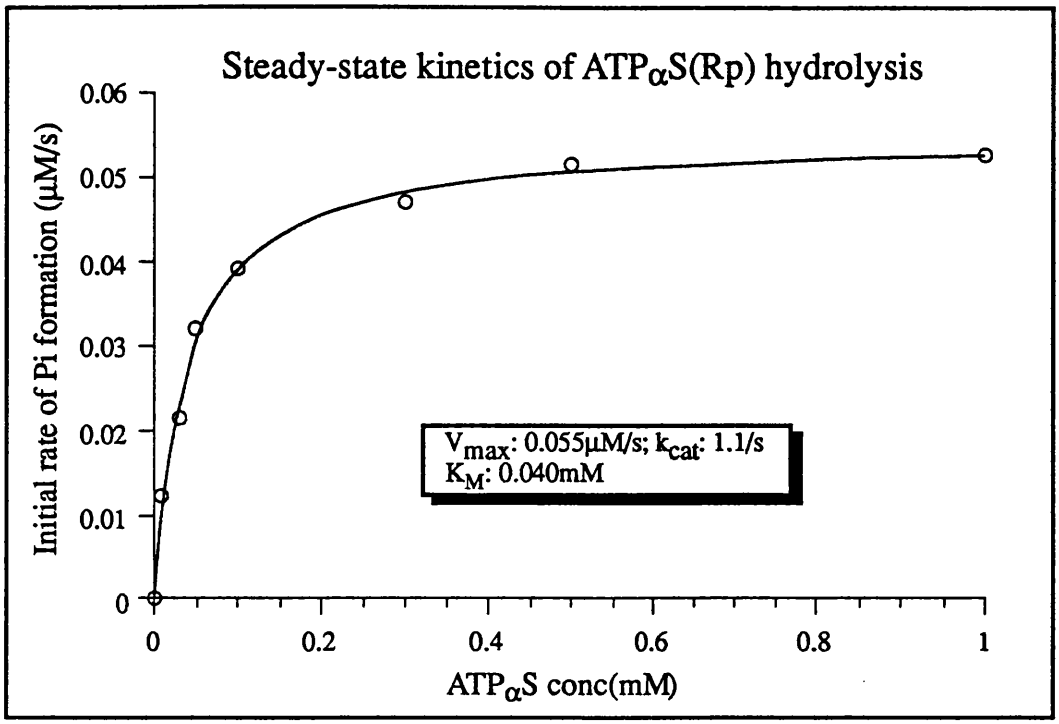

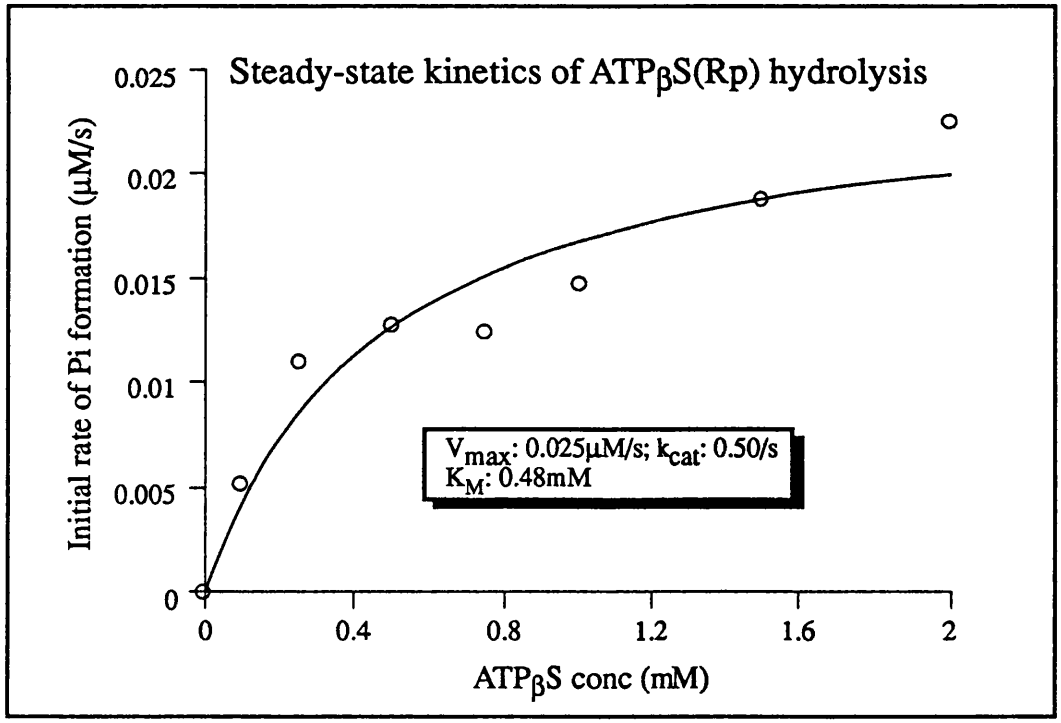

Figure 4.26. Steady-state analysis of $ATP_{\alpha}S(Rp)$ and $ATP_{\beta}S(Rp)$ hydrolysis. (The points on the graph are averages for two readings). Assay volumes were 150μl.

Thus the hydrolysis of $ATP_{\beta}S$(Rp) by gyrase appears to be uncoupled from DNA supercoiling.

4.2.9. Stereoselectivity of gyrase with $ATP_{\alpha}S$ confirmed by HPLC.

The hydrolysis of a racemic mixture of $ATP_{\alpha}S$ was analysed over a long time course by reverse phase HPLC (Fig. 4.27). Reactions comprised 150nM gyrase and 1mM nucleotide in a total volume of 30µl. It can be seen that after 112 min. almost all of the Rp epimer of $ATP_{\alpha}S$ was hydrolysed to the corresponding epimer of $ADP_{\alpha}S$ with virtually no hydrolysis of $ATP_{\alpha}S$(Sp). This gives an average turnover rate over this period of about 0.5/s. After 400 min.and 1320 min. low levels of hydrolysis of $ATP_{\alpha}S$(Sp) were detected up to about 15%. This corresponds to about 75µM $ATP_{\alpha}S$(Sp) hydrolysed and an average turnover rate of 0.38/min. or 6.3×10^{-3}/s which is just below the threshold detectable by the malachite green assay (Section 4.2.6).

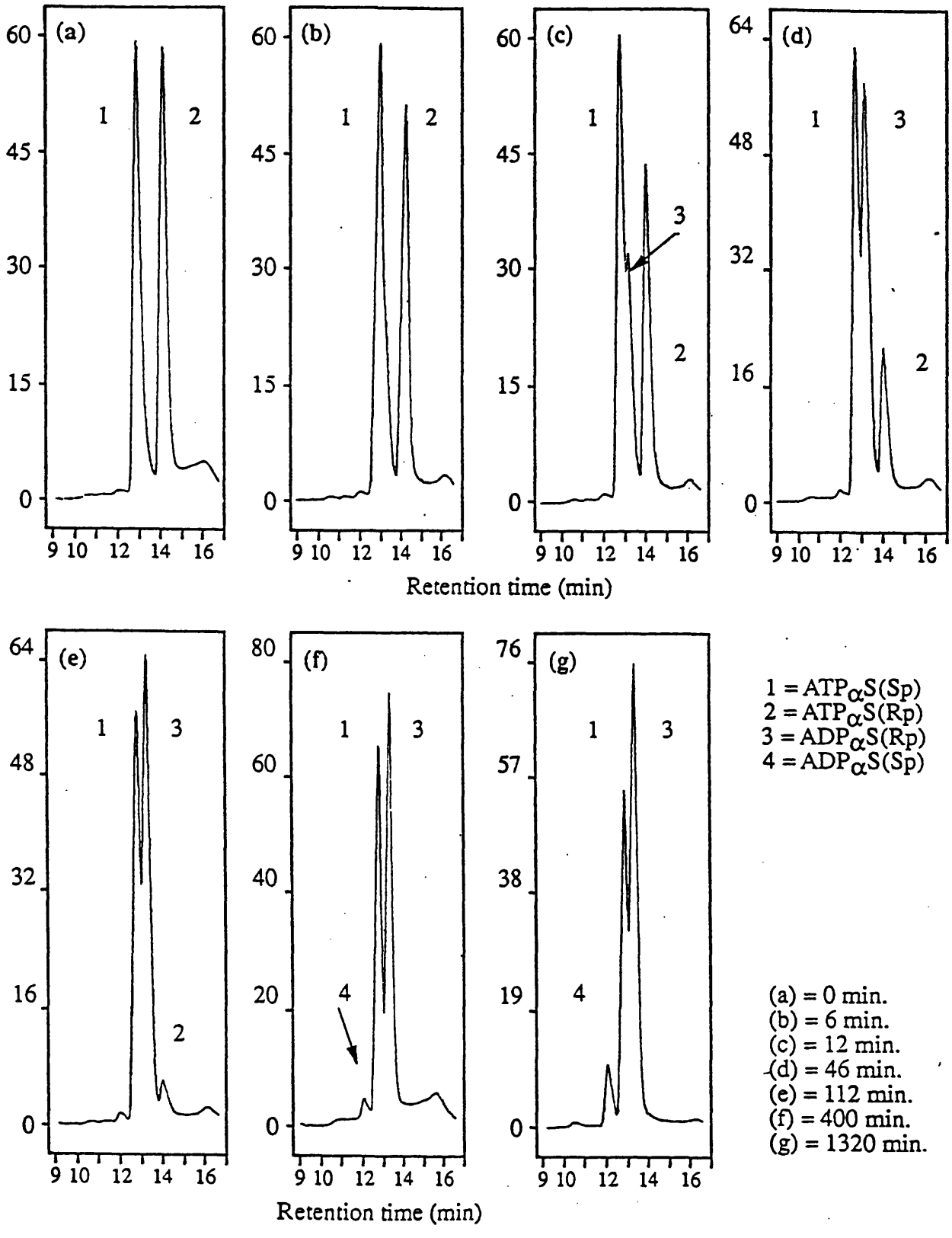

Figure 4.27. HPLC time course of the hydrolysis of a racemic mixture of $ATP_{\alpha}S$ by gyrase. Samples were analysed on an analytical reverse-phase column using the same conditions as stated in Fig. 4.7 except that the flow rate was 1.5ml/min.

4.3. DISCUSSION

Gyrase exhibited marked specificity for the Rp epimer of both $ATP_{\alpha}S$ and $ATP_{\beta}S$ with Mg^{2+} as the activating metal ion. The simplest interpretation of this result has the Mg^{2+} ion coordinated to the α– and β-phosphoryl groups. Since Mg^{2+} exhibits a strong preference for coordination to oxygen over sulphur, the active Mg-complexes of $ATP_{\alpha}S$ and $ATP_{\beta}S$ probably involve oxygen coordination and exposed sulphur as shown in Fig. 4.28. Assuming this to be the case, the specificity of gyrase towards the Rp epimers of $ATP_{\alpha}S$ and $ATP_{\beta}S$ defines the geometry of the active metal complex as in Fig. 4.28 where the Mg^{2+} ion is complexed to the *pro*-S oxygens of the α and β phosphates in ATP. In this figure the possibility of an additional coordination to the metal from the γ-phosphate is ignored for simplicity; the involvement of the γ-phosphate does not contribute to the chirality of the complex since P_{γ} *pro-pro*-chiral.

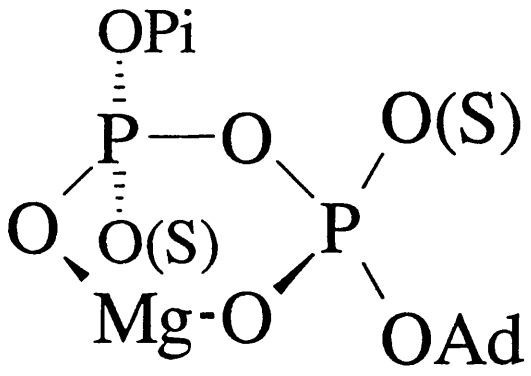

Figure 4.28. The proposed active metal complexes for $ATP_{\alpha}S$(Rp) and $ATP_{\beta}S$(Rp), focussing on the α,β-chelate, showing the positions of S substitution and the geometry of the metal complex with the metal coordinated to the *pro*-S oxygens of P_{α} and P_{β}.

There are examples in the literature of enzymes, such as hexokinase, which are believed to handle a β,γ-bidentate metal-ATP complex (Cornelius and Cleland, 1978; Dunaway-Mariano and Cleland, 1980a; Jaffe and Cohn, 1979) and yet show selectivity for one of the two epimers of $ATP_{\alpha}S$ (Jaffe and Cohn, 1979). Thus stereospecificity at a

thiophosphoryl centre does not unambiguously indicate metal ion coordination and the reversal of stereospecificity in the presence of hard and soft activating metal ions is often used to confirm the nature of the active metal-nucleotide complex (Cohn, 1982; Eckstein, 1985; Frey, 1989). However, with gyrase, the fact that the sensitivity to the stereochemistry of sulphur substitution in both the α and β sites is so pronounced strongly suggests coordination to the metal. Assuming that constraints within the enzyme's binding site do not overcome the preference for Mg^{2+} to coordinate oxygen over sulphur, the predicted geometry of the Mg-ATP complex in Fig. 4.28 is reasonable; it is highly unlikely that forced coordination of Mg^{2+} to sulphur is responsible for the observed stereochemical preference since both $ATP_{\alpha}S(Rp)$ and $ATP_{\beta}S(Rp)$ are such good substrates compared to ATP.

Thus the stereospecificity observed for the α and β phosphorothioate ATP analogues strongly predicts that the active Mg-ATP complex involves α,β-chelation to the *pro*-S oxygens. The phosphorothioates do not address the question of the participation of the γ-phosphate in coordination to the metal. On the basis of mechanistic considerations, coordination to P_{γ} is attractive. Current evidence on the mechanisms of phosphoryl transfer enzymes is consistent with an in-line associative reaction (Cullis, 1988; Knowles, 1980) which would be favoured by metal coordination to P_{γ} since this would tend to reduce negative charge enhancing the electrophilicity of P_{γ}. In addition, evidence from X-ray crystallography (Wigley *et al.*, 1991) suggests that, in gyrase, P_{γ} is coordinated to the metal. The corresponding tridentate complex is shown in Fig. 4.29 which includes γ-phosphate coordination to the metal. Thus the overall complex has Λ-exo screw sense geometry (where Λ refers to the geometry of the β,γ-chelate ring and exo refers to the fact that adenosine and the γ-phosphate are on opposite sides of the α,β-chelate ring). Interestingly, this is the same configuration as that found for the metal-ATP complex in creatine kinase (Burgers and Eckstein, 1980; Leyh *et al.*, 1985; Leyh *et al.*, 1982).

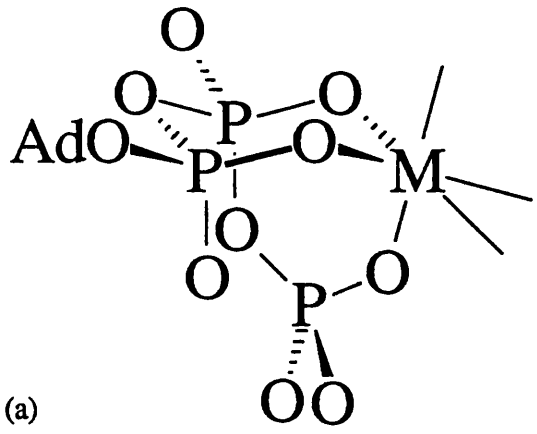

(a)

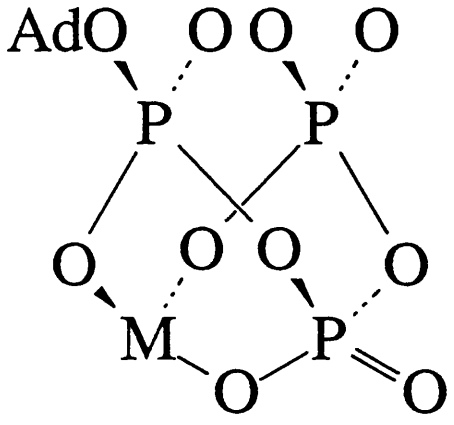

(b)

Figure 4.29. A proposed structure for the active Mg-complex of ATP with gyrase based on the stereospecificity with $ATP_{\alpha}S$ and $ATP_{\beta}S$. Part (a) gives a structure for the Mg-ATP complex where the metal is bound to the *pro*-S oxygens of the α- and β-phosphoryl groups. The tridentate complex is designated Λ-exo according to the nomenclature of Cornelius and Cleland (1978). The metal is shown at the centre of an octahedral complex with the ligands other than the phosphates not specified and the β,γ-chelate ring is shown in a boat-like configuration while the α,β-chelate ring is shown in a chair-like configuration based on simple model building. The same structure is shown in part (b) but drawn according to the convention of Cornelius and Cleland (1978).

Recently an N-terminal fragment of the GyrB protein has been cloned and crystallised (Jackson *et al.*, 1991) and the structure has been solved to 2.5Å resolution (Wigley *et al.*, 1991). This fragment contains the site of ATP hydrolysis and was crystallised in the presence of the non-hydrolysable ATP analogue, ADPNP. Electron density corresponding to the Mg^{2+} ion revealed its coordination to the nucleotide analogue and the protein. Each of the three phosphates appears to be a ligand, with two water molecules and the amide side chain of Asn 46 making up the other three ligands. Interestingly, the coordination geometry of the complex can be seen to correspond to the complexation of the *pro*-S oxygens of P_α and P_β. Importantly, this agrees with the prediction from the phosphorothioate ATP analogues.

Taken on its own, the crystallographic data is subject to certain qualifications as a model for the interaction of ATP and gyrase. Firstly, the protein is only a truncated form of the B subunit and may differ in its ATP binding microstructure. Secondly, ADPNP may be bound differently to ATP. Thirdly, crystal packing forces may distort the configuration of the nucleotide-metal complex or the conformation of the protein. The close agreement between the predictions from the phosphorothioate ATP analogues and the crystal structure thus provides valuable evidence in support of the N-terminal fragment as a relevant model for the ATP-site of intact gyrase.

A closer look at the crystal structure has provided a possible explanation for the observed stereochemical preference by gyrase. Fig. 4.30 shows a cartoon of the Mg-ATP complex in the active site based on 3-dimensional computer graphics. Residues contacting the metal ion or forming hydrogen bonds with non-bridging oxygens of ATP have been included. Focussing on P_α, the unliganded *pro*-R oxygen only interacts with a single water molecule via a hydrogen bond. In contrast, the *pro*-S oxygen is involved in multiple interactions; in addition to metal ion coordination it forms hydrogen bonds with the amide side chain of Asn46 and with one of the waters in the coordination sphere of

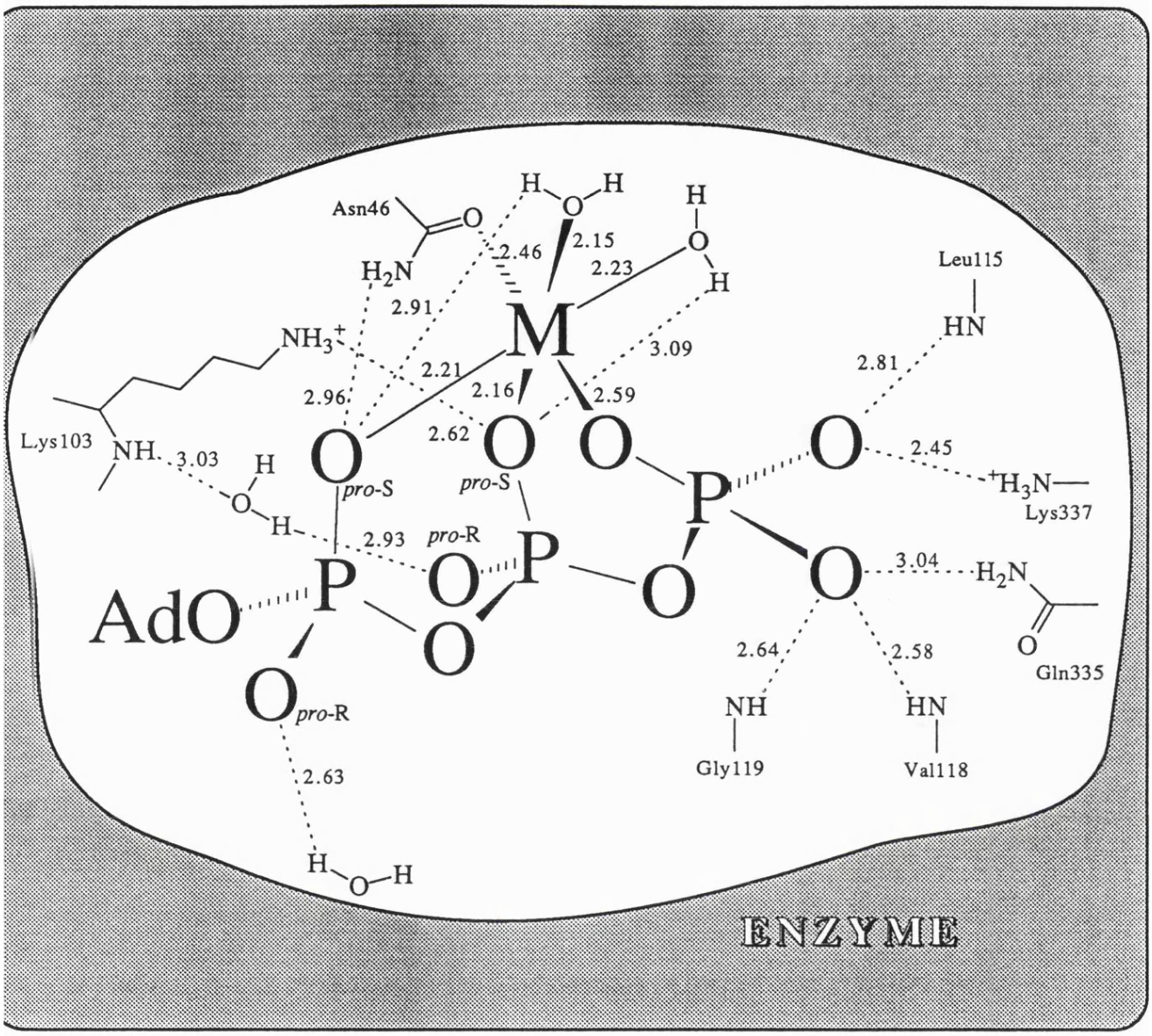

Figure 4.30. Metal-ATP complex in the active site as seen in the crystal structure of the N-terminal fragment of gyr B. The protein residues interacting with the metal ion or the non-bridging oxygens of the triphosphate chain are shown. The dashed lines correspond to hydrogen bonding interactions or salt-bridges (distance between donor and acceptor atom < 3.2Å; the distances are given next to the lines in Å). Note that the contiguous 6-membered chelate rings of the tridentate complex probably possess strain that may be relieved somewhat in the transition state (where the scissile bond is stretched) and in the products.

the metal. Moreover the environment around the *pro*-S oxygen is generally more crowded than in the vicinity of the *pro*-R oxygen (not shown in the figure). Complexation of the *pro*-R oxygen instead of the *pro*-S oxygen by the metal would move the *pro*-S oxygen further round to this crowded region of the active site and would probably involve many repulsive interactions in addition to the loss of the hydrogen bond between the water and the unliganded *pro*-R oxygen. This may explain why metal coordination to the *pro*-S oxygen appears to be favoured. At P_β, a similar argument can be made. Once more the *pro*-R oxygen only interacts with one water molecule while the *pro*-S oxygen is involved in metal coordination, as well as forming a salt-bridge with the ε-amino group of lys103 and a hydrogen bond with one of the waters in the coordination sphere of the metal.

The above considerations may also partly explain why the Rp epimer of $ATP_\alpha S$ is hydrolysed with lower K_M^{app} than ATP. In the crystal structure the bound ADPNP molecule appears to be almost completely engulfed by the protein in a site which is not accessible to solvent. As discussed above, in the metal-ATP complex, the *pro*-R oxygen appears to occupy a comparatively poor solvating site with just one hydrogen bond to water. The substitution of this *pro*-R oxygen by sulphur [as in $ATP_\alpha S$(Rp)] would thus place the sulphur atom into this poor solvating environment. Since sulphur is larger and more polarisable than oxygen and therefore accommodates lower charge densities, thiophosphates would be expected to be less hydrophilic than phosphates (Hine, 1975). (The effect on hydrophilicities of oxygen substitution by sulphur in alcohols and thiols has been measured (Hine and Mookerjee, 1975; Wolfenden *et al.*, 1979) and supports this expectation). Given these likely differences in hydrophilicities between the P=O and P=S groups, intuitively one would anticipate the thiophosphate to be bound more tightly by gyrase as appears to be the case with $ATP_\alpha S$(Rp). The favoured desolvation of thiophosphates over phosphates may also contribute to the binding of $ATP_\beta S$(Rp) although here the K_M^{app} is approximately equal to that of ATP. The importance of

desolvation in ligand-protein interactions has recently been demonstrated in the zinc protease, thermolysin, with a series of transition-state peptide analogues (Merz and Kollman, 1989; Morgan *et al.*, 1991).

Another factor that may be important in the binding of $ATP_{\alpha}S(Rp)$ involves the way in which Mg^{2+} is bound to the nucleotide in solution. The substitution of $ATP_{\alpha}S(Rp)$ for ATP does not change the number of complexes in the case of β,γ-chelation but reduces from four to two the number available for α,β- or α,β,γ-chelates. This leads to an increase in concentration of these two complexes over the total nucleotide concentration and may account for the lower apparent K_M for $ATP_{\alpha}S(Rp)$ over ATP. A similar argument to this was used to explain the higher apparent second-order rate constant for $ATP_{\alpha}S(Sp)$ than ATP in myosin (Goody and Hofmann, 1980). A corollary to this, however, is the report by Pecoraro and Cleland (1984) that the proportion of tridentate coordination in solution for Mg-ATP is 50-60% while for Mg-$ATP_{\alpha}S$ it is about 27%.

It is important, when considering the gyrase ATPase, to treat kinetic constants such as K_M with caution since the kinetics are thought to deviate from the simple Michaelis-Menten scheme. Therefore, in the measurements of nucleotide hydrolysis, the kinetic constants obtained are quoted as apparent values. This reflects the fact that there are two ATP binding sites per gyrase tetramer, one associated with each B subunit (Tamura and Gellert, 1990; Wigley *et al.*, 1991) and cooperativity between the sites is likely. Briefly the evidence for such cooperativity is as follows. Firstly, it has been estimated that approximately two molecules of ATP are hydrolysed per round of supercoiling (Sugino and Cozzarelli, 1980). Secondly, experiments on ATPase inhibition by ADP have shown deviations from Michaelis-Menten type kinetics giving curved Eadie-Hofstee plots. Computer-assisted modelling of these results predicted that two ATP molecules were bound prior to hydrolysis (Maxwell *et al.*, 1986). Thirdly, thermodynamic considerations suggest that the final two superhelical turns to generate the maximum

specific linking difference achievable by gyrase (-0.11; Bates and Maxwell, 1989) requires a free energy input of roughly 114 kJ/mol (Horowitz and Wang, 1984) while the energy associated with the hydrolysis of two ATP molecules has been calculated to be approximately 120 kJ/mol (Simmons and Hill, 1976). Thus one round of supercoiling at high specific linking differences may require the concerted hydrolysis of two ATP molecules (see also Chapter 6). Fourthly, the crystal structure of the N-terminal fragment of GyrB indicates a dimer in which Tyr 5 on an N-terminal arm from one subunit interacts with the 2' hydroxyl of the ribose ring of ADPNP bound at the other subunit and *vice versa*. This direct interaction of the two subunits may be important in mediating positive cooperativity in ATP hydrolysis in the full gyrase structure. Fifthly, recent experiments on the kinetics of interaction between gyrase and ADPNP in the presence and absence of ATP have provided evidence for cooperativity between the nucleotide binding sites (Tamura *et al.*, 1992).

The ADPNP binding experiments (Tamura *et al.*, 1992) have suggested that binding of one ADPNP molecule to gyrase is followed by a slow protein conformational change which then facilitates the fast binding of a second ADPNP molecule. The same two-step binding of ATP was also proposed. Since the second ATP molecule binds fast relative to the conformational change the overall ATPase reaction would still appear to follow Michaelis-Menten kinetics although with an inhibitor such as ADP deviations from this paradigm could become manifest. Thus in the kinetics of the phosphorothioate ATP analogues some caution in interpreting the significance of K_M^{app} values is advisable (see also Section 5.3).

The results for the hydrolysis and supercoiling experiments with ATP, $ATP_{\alpha}S$, and $ATP_{\beta}S$ are summarised in Table 4.5 below. For comparisons of nucleotide hydrolysis, the kinetic parameters obtained from the fluorimetric phosphate assay are used. This did not detect any hydrolysis of the Sp epimers of the ATP analogues which is indicated in

the table by dashes. A simplified summary of the supercoiling experiments is given to emphasise the correlation between hydrolysis and supercoiling.

Table 4.5. Comparison of hydrolysis and supercoiling for ATP, $ATP_{\alpha}S$ and $ATP_{\beta}S$.

Nucleotide	Hydrolysis		Supercoiling
	K_M^{app} (mM)	k_{cat} (s^{-1})	
ATP	0.46	1.1	Fast
$ATP_{\alpha}S$(Rp)	0.040	1.1	Fast
$ATP_{\alpha}S$(Sp)	-	-	Very slow
$ATP_{\beta}S$(Rp)	0.48	0.5	Very slow
$ATP_{\beta}S$(Sp)	-	-	None

The difference in the hydrolysis of the two epimers of $ATP_{\alpha}S$ was dramatic. No reaction was detected for the Sp epimer while the Rp epimer was found to be a better substrate at low concentrations than ATP. When the hydrolysis of $ATP_{\alpha}S$(Sp) was followed over a long time course by HPLC a slow hydrolysis was detected giving an average turnover rate at least 80-fold lower than that for the Rp epimer. Inhibition of ATP-dependent supercoiling by 50% required an excess of $ATP_{\alpha}S$(Sp) over ATP of approximately 35 under the conditions of the experiment (Section 4.2.3). This suggests that the slow reaction with this analogue may, in part, be due to weak binding to the enzyme.

With $ATP_{\alpha}S$(Rp) the supercoiling results reflected the hydrolysis kinetics; at low concentrations (such as 0.1mM) the analogue was a better substrate than ATP in the supercoiling reaction while at higher concentrations, such as 1mM, the two nucleotides were both equally effective. This is consistent with the hydrolysis data which suggests a much lower K_M^{app} for $ATP_{\alpha}S$(Rp) compared with ATP. Thus at 0.1mM nucleotide, $ATP_{\alpha}S$(Rp) is hydrolysed roughly 4-fold faster than ATP while at 1mM both nucleotides are close to saturation. The correlation of the hydrolysis and supercoiling reactions with

$ATP_{\alpha}S(Rp)$ was further underlined by an experiment following the rate of supercoiling with this analogue and ATP which showed that at 0.1mM the rate of $ATP_{\alpha}S(Rp)$-supported supercoiling was between 4-5-fold greater than with ATP as would be expected from the corresponding rates of hydrolysis. Thus in this respect the hydrolysis of $ATP_{\alpha}S(Rp)$ appears well coupled to supercoiling.

$ATP_{\beta}S$ was a relatively good substrate for hydrolysis as shown in Table 4.5; a value for K_M^{app} similar to that for ATP was obtained and the k_{cat}^{app} was found to be reduced by a factor of two compared with ATP. However, this analogue was found to be a very poor substrate for supercoiling. Thus the hydrolysis of $ATP_{\beta}S(Rp)$ by gyrase appears to be to uncoupled from the supercoiling reaction. This is the first report of such a specific uncoupling, and its mechanistic basis is intriguing. One possible explanation draws on the crystal structure of the N-terminal fragment of the gyrase B protein referred to above. As already pointed out the protein crystallises as a dimer. Each monomer consists of two domains and the ATP binding site is located on the N-terminal domain (domain 1). At the linkage between these domains, there are two consecutive glycine residues which have been suggested to form a flexible hinge between the domains. Interestingly the side chains of Gln 335 and Lys 337 from domain 2 interact with the γ-phosphate of ADPNP in domain 1. These interactions may be important in a conformational change, involving the movement of domain 2 with respect to domain 1, on nucleotide hydrolysis. The interaction of these two residues with $ATP_{\beta}S(Rp)$ may be impaired as a consequence of a different orientation of the γ-phosphate which still allows reasonable proximity to the catalytic apparatus. Thus hydrolysis could occur largely without the usual associated conformational change. An alternative explanation centres on the bound metal ion. On hydrolysis the loss of P_{γ} coordination may promote a movement of the Mg^{2+} ion and a rearrangement of the configuration of the complex which could be transmitted to other parts of the protein as a conformational change. If the presence of sulphur restricts the movement of the metal ion it would be possible for hydrolysis to occur uncoupled to

DNA supercoiling. While these hypotheses are speculative, the availability of a substrate whose hydrolysis is uncoupled from DNA supercoiling should give further insights into the mechanism of energy coupling in gyrase.

Neither supercoiling or statistically significant hydrolysis was detected for $ATP_{\beta}S(Sp)$. This analogue was found to bind to gyrase, giving 50% inhibition of supercoiling at a concentration roughly 2-fold higher than the ATP concentration. It is possible that a low level of hydrolysis was undetected and that this hydrolysis was poorly coupled to supercoiling as in the Rp epimer. The lack of supercoiling with $ATP_{\beta}S(Sp)$ led to the discovery of the general property of limited positive supercoiling by gyrase in the absence of nucleotide (or effective nucleotide). This phenomenon has not been noted previously for intact gyrase probably because the reaction is so slow. However, a complex of GyrA and a 50 kDa C-terminal fragment of GyrB has been reported to support limited positive supercoiling by a mechanism analogous to that proposed here for intact gyrase (Brown *et al.*, 1979). Thus it is possible that the positive supercoiling with gyrase was due to limited proteolysis of the B protein during the reaction to generate the 50 kDa fragment. While not significant *in vivo* where the ATP concentration is relatively high, the observation of limited positive supercoiling by gyrase lends further support to the hypothesis that DNA is wrapped around gyrase in a positive superhelical sense and complements previous experiments where gyrase was bound to nicked-circular DNA which was then sealed with DNA ligase and isolated in a positively supercoiled form (Liu and Wang, 1978b; Reece and Maxwell, 1991a).

4.4. SUMMARY

Various aspects of the interaction of gyrase with the diastereoisomers of $ATP_{\alpha}S$ and $ATP_{\beta}S$ have been explored which has yielded information on the type of Mg-ATP complex handled by the enzyme, and the relationship between the hydrolysis of the ATP analogues and their ability to support DNA supercoiling.

The strong preference of gyrase for the Rp epimers of $ATP_{\alpha}S$ and $ATP_{\beta}S$ presented in this study together with the known preference of Mg^{2+} to coordinate to oxygen over sulphur predicts that the Mg^{2+} ion is coordinated to the *pro*-S oxygens of the α– and β-phosphates of ATP during the rate-limiting step of the gyrase ATPase (Fig. 4.29). This is consistent with the recently solved crystal structure of an N-terminal fragment of the gyrase B protein containing the ATP binding site which suggests that the γ-phosphate is also involved in the Mg-ATP complex (Fig. 4.30). Thus an α,β,γ-tridentate Mg-ATP complex having Λ-exo geometry [nomenclature according to Cornelius and Cleland (1978)] is proposed. In this complex the metal ion may have a dual role, assisting nucleophilic attack of water at P_{γ} in an in-line associative reaction, and enhancing the properties of ADP as a leaving group. Furthermore, strain in the 2 contiguous 6-membered chelate rings may destabilise the substrate-complex and contribute to catalysis.

The hydrolysis of the ATP analogues by gyrase was compared to their ability to support DNA supercoiling. For the preferred epimer (Rp) of $ATP_{\alpha}S$, its effectiveness as a substrate in the supercoiling reaction mirrored its effectiveness in the hydrolysis reaction; the maximum rates of the ATP and $ATP_{\alpha}S$(Rp) reactions appeared to be very similar while the sulphur analogue was a better substrate than ATP at low nucleotide concentrations giving an approximately 10-fold lower apparent binding constant. Thus hydrolysis was apparently well-coupled to supercoiling. When the sulphur substitution was at P_{β}, the preferred epimer was $ATP_{\beta}S$(Rp). This was a good substrate for hydrolysis with comparable kinetics to ATP but was a poor substrate for DNA

supercoiling. Thus the energy coupling between the reactions is impaired. Two hypotheses to explain this effect are presented and it is hoped that future work will shed more light on the mechanism of energy coupling in gyrase.

Chapter 5

Metal Ion Studies and Crystallography Trials on DNA Gyrase

5.1. INTRODUCTION

In many studies on the metal-nucleotide complexes involved in phosphoryl transfer enzymes, the structure and configuration of the active metal-nucleotide complex has been deduced by comparing the diastereoisomers of phosphorothioate ATP (or GTP) analogues as substrates in the presence of different metal ions.

The method is based on that fact that, at the thiophosphoryl centres, metal ions can coordinate to either an oxygen or a sulphur atom. It has been shown by NMR (Jaffe and Cohn, 1978a) that Mg^{2+} prefers to chelate *via* oxygen and Cd^{2+} shows a preference for sulphur in complexes with phosphorothioate nucleotide analogues as would be expected from the consideration that Mg^{2+} is a hard Lewis acid and Cd^{2+} is a soft Lewis acid while oxygen and sulphur are hard and soft Lewis bases respectively (Cotton and Wilkinson, 1972; Pearson, 1966). These effects were placed on a quantitative footing by Pecoraro *et al.* (1984) who used stability constants of Mg^{2+} and Cd^{2+} complexes of phosphorothioate analogues of ATP and ADP to calculate the preference for oxygen and sulphur coordination.

A consequence of the metal ion coordination preferences, is that the *Sp epimer* of $ATP_{\alpha}S$ (or $ATP_{\beta}S$) when complexed to Mg^{2+}, has the same screw sense (as defined by Cornelius and Cleland, 1978) as the Cd^{2+} complex of the *Rp epimer* (i.e. they have the same relative configuration in terms of the metal chelate). By the same reasoning, the Mg^{2+} chelate of the *Rp epimer* of $ATP_{\alpha}S$ (or $ATP_{\beta}S$) and the Cd^{2+} chelate of the *Sp epimer* of $ATP_{\alpha}S$ (or $ATP_{\beta}S$) will have the opposite screw sense to that formed above.

In experiments with hexokinase, it was found that $ATP_{\beta}S$(Rp) was the better substrate with Mg^{2+} while $ATP_{\beta}S$(Sp) was favoured with Cd^{2+} (Jaffe and Cohn, 1978b; Jaffe and Cohn, 1979). This reversal of stereoselectivity was taken as evidence for the coordination of the metal to the β-phosphate of ATP in the enzyme reaction. In identical

experiments with $ATP_{\alpha}S$ no reversal of stereoselectivity was observed and it was concluded that, in the hexokinase-Mg-ATP complex, the metal probably is not coordinated to the α-phosphate.

This approach has been applied to many phosphoryl transferases and adenylyl transferases and has been extensively reviewed (Cohn, 1982; Eckstein, 1980; Eckstein, 1985; Frey, 1989). Generally, reversal of stereoselectivity has been taken as unequivocal evidence for the involvement of the particular phosphate group in metal coordination. When reversal of stereoselectivity is only seen with $ATP_{\beta}S$ (as was the case with hexokinase above), a β,γ-bidentate metal chelate has been proposed, the involvement of the γ-phosphate being likely due to the greater thermodynamic stability of the 6-membered β,γ-chelate ring over a β-monodentate complex (Huang and Tsai, 1982).

In cases where no reversal of stereoselectivity is seen the interpretation is ambiguous. One possibility is that the metal ion does not coordinate to this phosphoryl centre. However, another possibility is that constraints imposed by the enzyme active site stabilise an otherwise unfavourable metal-ligand interaction (such as Mg-S or Cd-O coordination). One such case is RNA polymerase (Armstrong *et al.*, 1979), where Mg-S coordination was proposed to be stabilised by an interaction of the non-coordinated oxygen with the enzyme.

The results obtained in Chapter 4 with the diastereoisomers of $ATP_{\alpha}S$ and $ATP_{\beta}S$ in the presence of Mg^{2+} suggest that the likely configuration of the active Mg-ATP complex handled by the enzyme is tridentate with the *pro*-S oxygens of both the α– and β-phosphates coordinated to the metal. It was therefore of interest to test this conclusion, and it was decided to investigate whether reversal of stereoselectivity could be demonstrated in the presence of different metal ions. In addition the metal ion dependence of the reactions of gyrase was to be characterised.

5.2. RESULTS

5.2.1. Investigation of the effects of different metal ions on the relaxation and supercoiling reactions of gyrase.

The following divalent metal ions (all as their chloride salts) were studied: Mg^{2+}, Ca^{2+}, Mn^{2+}, Co^{2+}, Ni^{2+}, Zn^{2+}, Cd^{2+}. In supercoiling experiments it was noticed that a dark red precipitate was formed on the addition of $CoCl_2$ and $NiCl_2$. This was found to be caused by DTT in the reaction mixture (which was present at 5mM; Section 2.27) from experiments where the components were systematically varied. A possibility is that a DTT-metal complex was formed with these metals and two possible structures are illustrated in Fig. 5.1, where the complex is assumed to be octahedral; other structures with different geometries may also be possible. Colourless complexes with the other soft Lewis acid metal ions such as Zn^{2+} and Cd^{2+} may also have been formed but not detected. In view of this unwanted side-reaction, DTT was omitted from reaction mixtures and gyrase, previously dialysed into enzyme buffer minus DTT, was used in subsequent experiments with different metal ions. Control experiments showed that the supercoiling activity of the enzyme was unaffected by these modifications.

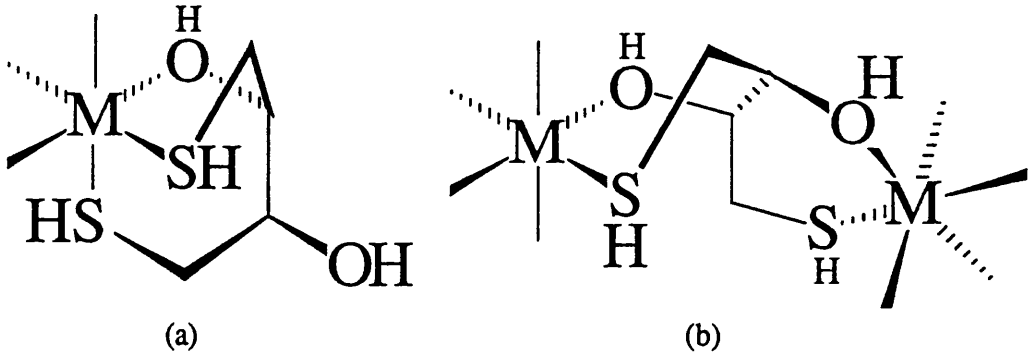

Figure 5.1. Two possible types of metal complexes formed with DTT. For clarity, the diagram shows just one DTT molecule bound to the metal ion. Part (a) shows DTT binding as a tridentate ligand. Part (b) shows DTT bridging between two metal ions; this type of coordination could give rise to a lattice of DTT molecules and metal ions. Mixed complexes with both types of binding could also be envisaged with water molecules satisfying any free coordination sites.

Fig. 5.2 shows an analysis of supercoiling with different metals and ATP, $ATP_{\alpha}S(Rp)$ and $ATP_{\alpha}S(Sp)$. With Mg^{2+}, gyrase was shown to be active with ATP and $ATP_{\alpha}S(Rp)$ while a very low level of supercoiling with $ATP_{\alpha}S(Sp)$ was evident as expected from Chapter 4. In the reactions with Ca^{2+} and Mn^{2+}, again supercoiling was shown for ATP and $ATP_{\alpha}S(Rp)$ while no supercoiling was detected for the Sp epimer. For the remaining metal ions tested (Co^{2+}, Ni^{2+}, Zn^{2+} (not shown in Fig. 5.2), and Cd^{2+}), no supercoiling activity was detected.

The lack of activity with the different metal ions was investigated further. Fig. 5.3 shows an analysis of the nucleotide-independent gyrase-catalysed relaxation of negatively supercoiled DNA in the presence of the various divalent metal ions. Complete relaxation was seen with Mg^{2+} as shown in the figure, while partial relaxation occurred with Ca^{2+} under the experimental conditions. Considerable linearisation of the DNA took place with Mn^{2+} which may have masked any relaxation activity. Interestingly, no linearisation was evident in the supercoiling experiments with this metal ion. This may be due to the presence of spermidine in the supercoiling experiments which was absent in the relaxation protocol or to a difference in the mechanism of relaxation and supercoiling. No relaxation was seen with Co^{2+}, Ni^{2+}, Zn^{2+}, and Cd^{2+} which parallelled the supercoiling results. In the Cd^{2+} reaction less DNA appeared to reach the gel as shown by the weaker bands in Fig 5.3. This effect, which was sometimes seen in supercoiling experiments as well, did not appear to be dependent on the presence of gyrase and cannot be explained at present.

The concentration of metal ions required for the relaxation reaction was investigated as shown in Fig. 5.4. No relaxation was seen with Cd^{2+} throughout the concentration range studied. This eliminated the possibility that low levels of Cd^{2+} could support a reaction which was inhibited at higher Cd^{2+} concentrations. With Mg^{2+}, full relaxation in 1 hour required 4mM metal while lower levels of relaxation were seen at 2mM and 1mM concentrations; the low level of relaxation with 1mM Mg^{2+} was only detected on a

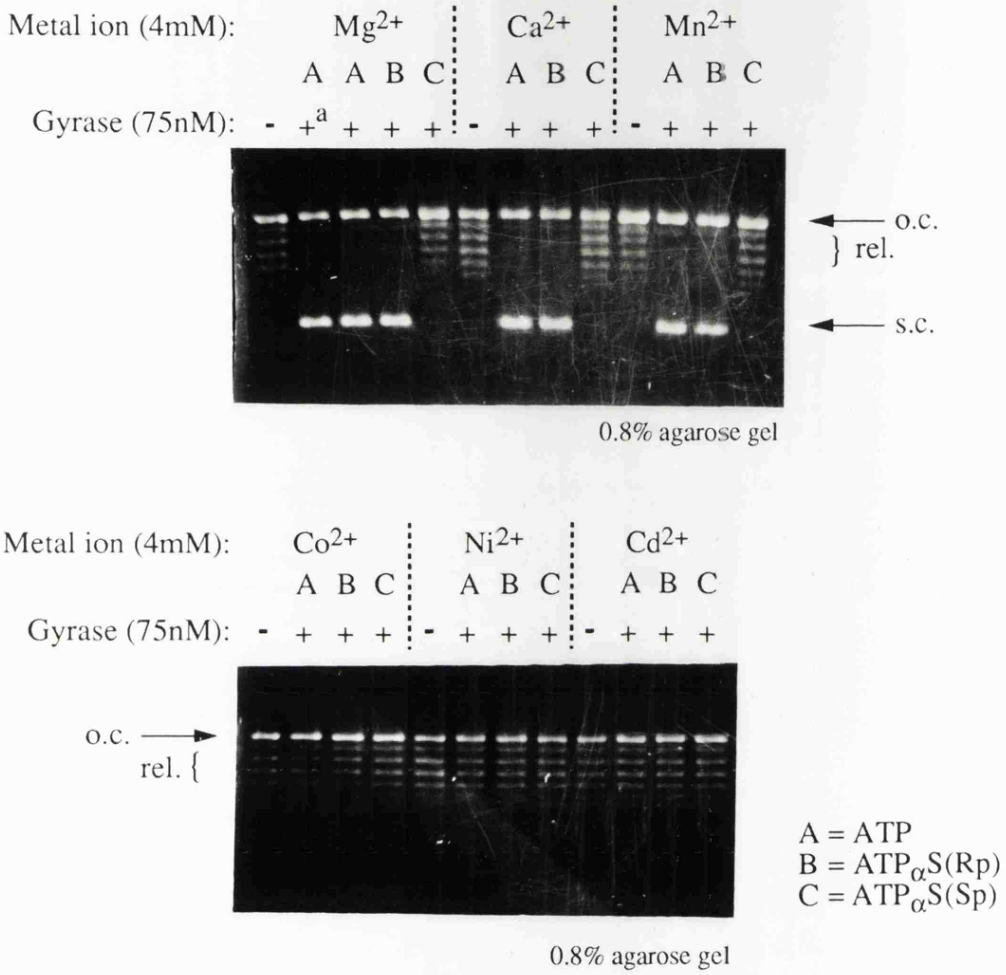

[a]Control with gyrase not dialysed into EB-DTT.

Figure 5.2. Supercoiling with ATP, and the two epimers of $ATP_{\alpha}S$ in the presence of different divalent metal ions. The nucleotide concentration was 1mM and the metal ion concentration was 4mM. The reactions were incubated at 25°C for 1 hour.

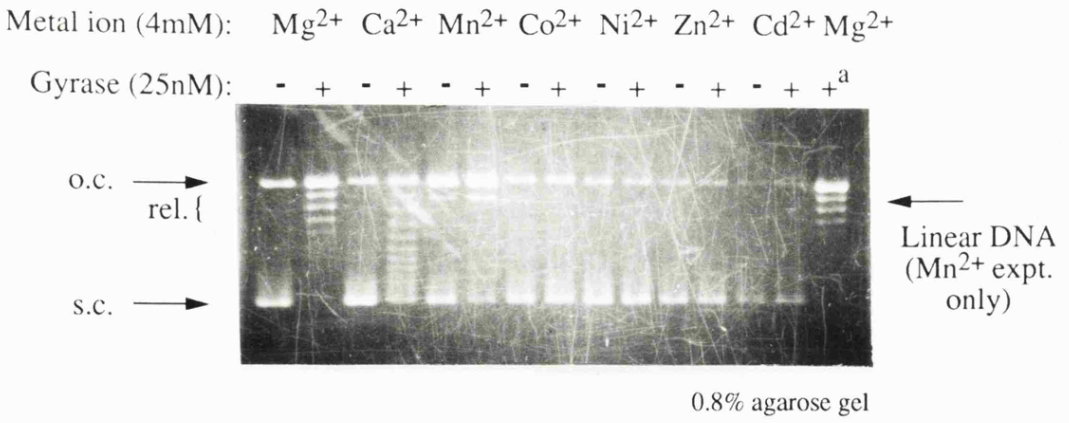

[a]Control with gyrase not dialysed into EB-DTT.

Figure 5.3. Relaxation of negatively supercoiled DNA with different metal ions.

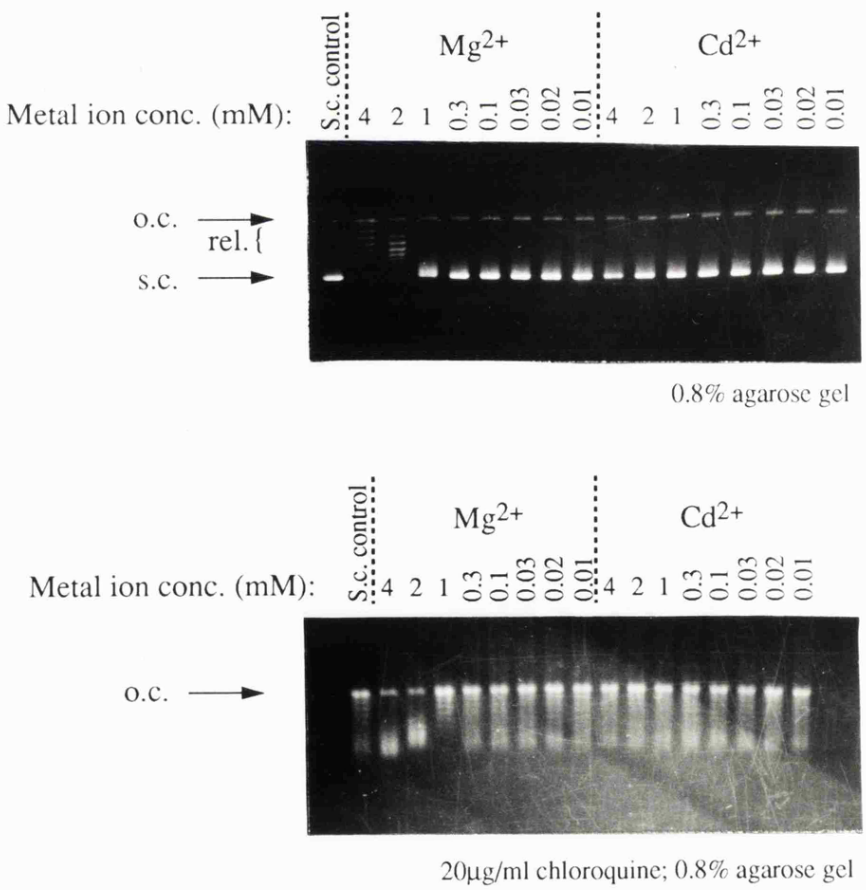

Figure 5.4. Investigation of the effect of the concentration of metal ions on relaxation.

chloroquine gel as shown in Fig. 5.4. At concentrations less than 1mM Mg^{2+} no relaxation was seen.

Formation of a gyrase-DNA complex has been shown to require Mg^{2+} (Higgins and Cozzarelli, 1982; Maxwell and Gellert, 1984; Rau *et al.*, 1987) as demonstrated by filter binding and gel retardation assays (eg. see Appendix I). Thus the metal ion dependence of the relaxation reaction may simply be a consequence of the metal ion requirement of the DNA-protein interaction. Alternatively, it is possible that the relaxation reaction has a specific requirement for Mg^{2+} as discussed further in Section 5.3. The important point here is that metal ions have at least two separate roles in the supercoiling reaction, namely the interaction of gyrase with DNA and the interaction of gyrase with ATP.

5.2.2. Probing the specificity of gyrase towards different metal-nucleotide complexes by supercoiling assays.

The lack of relaxation and supercoiling activity with soft Lewis acids such as Zn and Cd appeared initially to rule out the possibility of investigating any reversal of stereospecificity with the nucleoside phosphorothioates. However, gyrase-DNA complexes have been shown previously to be stable when dialysed from a high Mg^{2+} concentration buffer (required to form the complex) into a low Mg^{2+} concentration buffer (Rau *et al.*, 1987). This suggested the possibility of preparing a gyrase-DNA complex in the net absence of external Mg^{2+} by preforming the complex in the usual way and then removing excess Mg^{2+} by gel filtration on spin-columns (see Section 2.25). Such a procedure potentially offered a way of studying the metal ion requirement of the gyrase-ATP interaction in isolation from the gyrase-DNA interaction and thus suggested an approach to reversal studies.

The method involved incubating gyrase and DNA together in standard supercoiling buffer without nucleotide for 60 min. The DNA-protein complex was then applied to a 1ml

column of Sephadex G50 equilibrated in supercoiling buffer minus $MgCl_2$ and DTT. After centrifugation, the eluents, containing the gyrase-DNA complexes, were added to supercoiling assays containing the various nucleotides and metal ions under study. Fig. 5.5 shows such a spin-column experiment to investigate the metal ion specificity of gyrase with ATP. Essential to the design of the spin-column experiments was the assumption that the excess Mg^{2+} would be retained by the gel filtration matrix and this was addressed by the controls shown in the first 6 lanes of the gels in Fig. 5.5; the first 3 lanes are controls where the gyrase-DNA complex reaction mixture was not applied to spin-columns but was added directly to the nucleotide buffer containing various concentrations of ATP, as indicated in the figure, and no additional metal ions. As expected these controls supported supercoiling since the Mg^{2+} concentration was 4mM in each. The next 3 lanes are controls where the spin-column eluate was added to nucleotide buffer containing various concentrations of ATP as specified and no metal ions. The use of 3 different ATP concentrations in these controls minimised the possibility of inhibition of free ATP (see Section 5.2.4.2 and Figs. 5.13 and 5.14) obscuring any activity as a result of contaminating Mg^{2+}. Taking into account the effect of free ATP inhibition, the complete lack of supercoiling in these controls was consistent with less than 0.04mM free Mg^{2+} ions leaking through the spin-columns. This can be justified as follows. Concentrating on the 0.01mM ATP controls (since these are least likely to suffer from free ATP inhibition), it can be seen that the sample with no spin and 4mM Mg^{2+} gave a low level of supercoiling (most clearly detected on the chloroquine gel). Considering the stability constant for $MgATP^{2-}$ (Pecoraro *et al*, 1984), a solution containing 0.04mM Mg^{2+} and 0.01mM ATP can be estimated to contain approximately 63% of the total nucleotide in the complexed form. Reference to the inhibition of the 43 kDa fragment ATPase by free ATP in Fig. 5.13 and assuming that the supercoiling reaction of gyrase may be similarly affected by free ATP would suggest that a reasonable rate of reaction could be expected under these conditions.

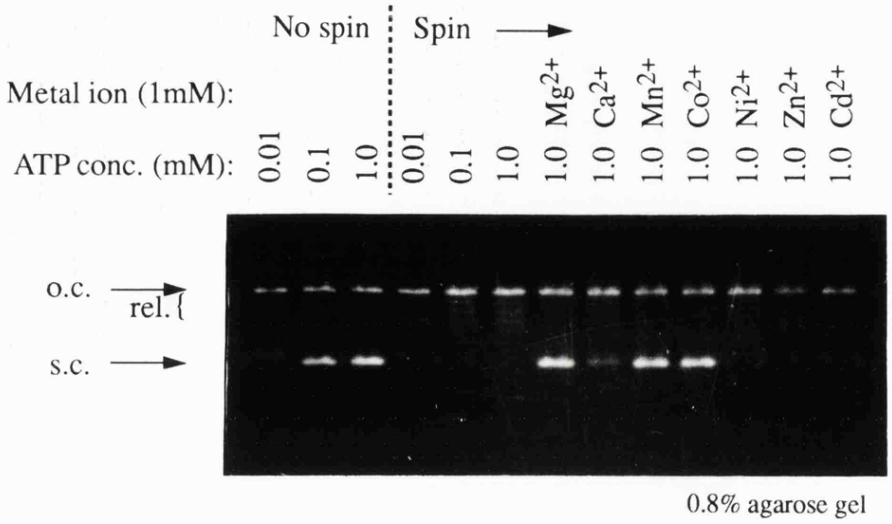

0.8% agarose gel

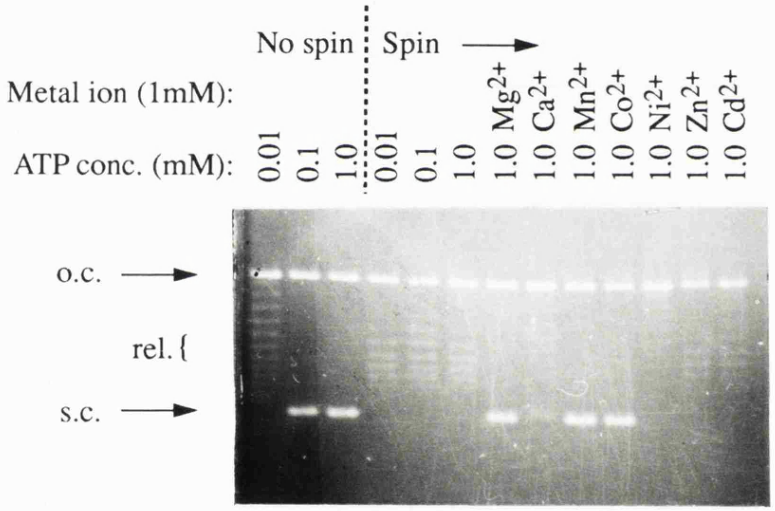

1.5μg/ml chloroquine; 0.8% agarose gel

Figure 5.5. Investigation of the metal ion specificity in the supercoiling reaction using a gyrase-DNA complex isolated via spin-columns. The gyrase-DNA complex reaction comprised: gyrase (100nM); relaxed pBR322 (10μg/ml); supercoiling buffer minus DTT (total volume 1400μl). This was incubated for 60min. at 25°C. Spin columns were made up in 1ml syringes packed with Sephadex G50 and thoroughly equilibrated with supercoiling buffer minus $MgCl_2$ and DTT. The gyrase-DNA complex solution was applied in 100μl aliquots to the columns which were spun at 1500rpm for 2 min. The eluent (100μl) containing the gyrase-DNA complexes was added to nucleotide buffer (100μl) comprising supercoiling buffer minus DTT with ATP and various metal ions to give the total concentrations as specified.

It can be seen that Mg^{2+}, Ca^{2+}, Mn^{2+}, and Co^{2+} all supported supercoiling. In addition low levels of supercoiling were seen with Ni^{2+}. The activity with Co^{2+} and Ni^{2+} was interesting since these metals did not support supercoiling in the simple assay of Fig.5.2. With Zn^{2+} and Cd^{2+} no supercoiling was detected. Thus this experiment suggested that gyrase can accept Co^{II} and Ni^{II} ATP complexes as well as those of Mg^{II}, Ca^{II}, and Mn^{II}. It should be pointed out that the metal ion concentration in these reactions was the same as the ATP concentration at 1mM. Using the stability constants for MgATP and CdATP published by Pecoraro *et al.* (1984) it can be calculated that for Mg, 88% is in the complexed form while for Cd this value is 81%. Although stability constants for the other metal-ATP complexes are not available it is believed that they would give similar values to Mg and Cd.

A potential problem with the spin-column experiments is the possibility that Mg^{2+} ions involved in the gyrase-DNA complex may exchange with the metal-nucleotide complex resulting in Mg-ATP being formed. While this possibility was not addressed by the controls described above, it is unlikely that it could have contributed to a great extent in view of the amounts of gyrase and DNA present in the reactions; assuming that the DNA was bound to Mg^{2+} with a stoichiometry of one Mg^{2+} ion per phosphate of DNA (which is probably an overestimate), the maximum level of Mg^{2+} ions carried through the column would be 0.03mM (the DNA (4361 bp) concentration in the reactions was 3.4nM giving a concentration of the backbone phosphates of 0.03mM).

The metal ion dependence of the supercoiling reaction with the diastereoisomers of $ATP_{\alpha}S$ was investigated by the spin-column methodology. Fig. 5.6 (a) and (b) shows the results of such an experiment. The first 4 tracks in part (a) are controls to test for leakage of Mg^{2+} through the columns. In the first two lanes, the gyrase-DNA complex was not spun through a column but was added directly to nucleotide buffer containing 1mM ATP or $ATP_{\alpha}S$(Rp). The next two lanes are corresponding experiments where the

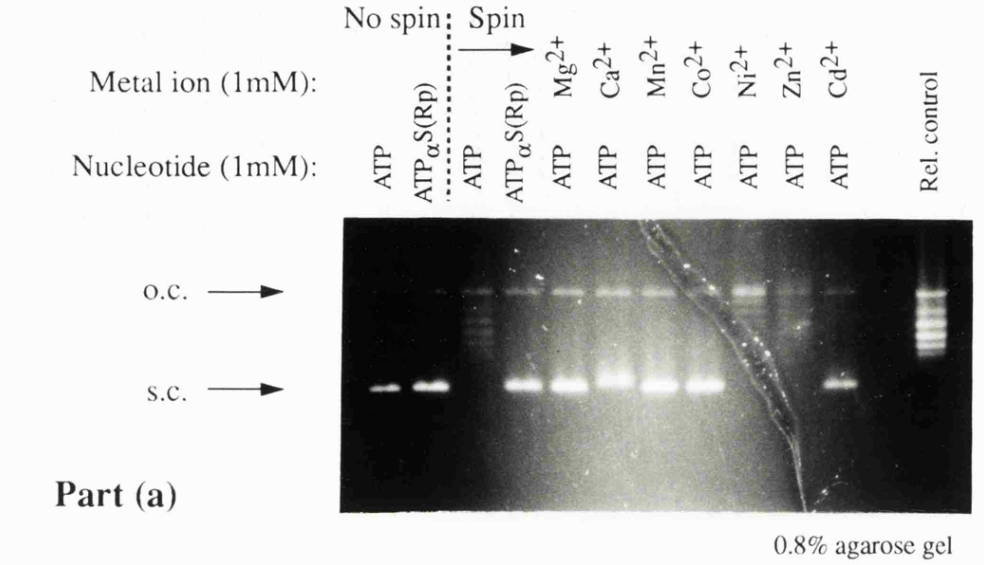

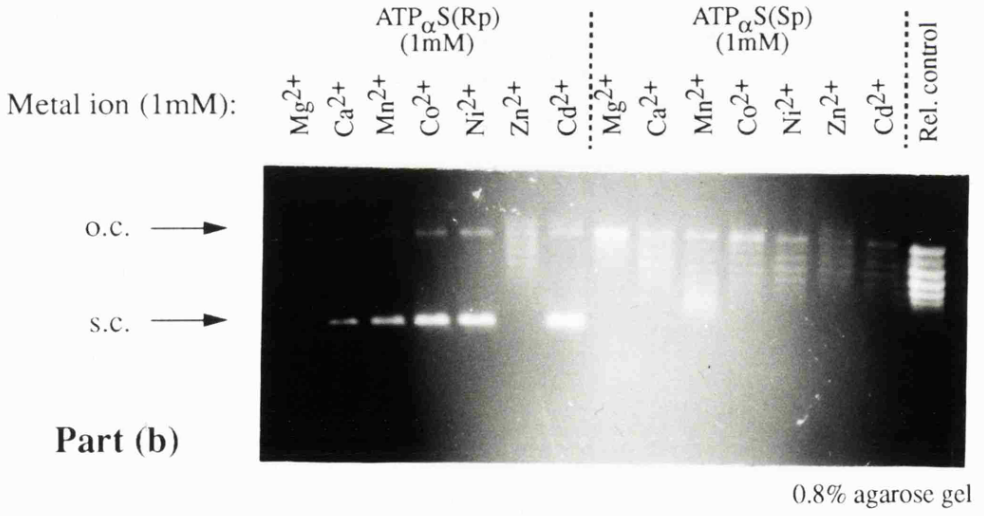

Figure 5.6. The metal ion dependence of the supercoiling reaction with ATP and the diastereoisomers of $ATP_{\alpha}S$ investigated by the spin-column approach. Conditions were essentially the same as described in Fig. 5.5. Part (a) shows various controls and the results with various metal ATP solutions. Part (b) shows the results with $ATP_{\alpha}S$ and various metal ions. See text for further explanation.

gyrase-DNA complexes were spun through columns before being added to the nucleotide buffer containing ATP or $ATP_{\alpha}S(Rp)$. The sulphur analogue was included as a control because it has a lower K_M^{app} than ATP (Chapter 4) and was therefore expected to detect lower levels of contaminating Mg^{2+}. Indeed the control with $ATP_{\alpha}S(Rp)$ and gyrase-DNA complex spun through the column did give considerable supercoiling indicating that in this experiment at least 0.01mM Mg^{2+} ions were leaking through the column. As in Fig. 5.5, ATP in the presence of Mg^{2+}, Ca^{2+}, Mn^{2+}, and Co^{2+} all gave considerable supercoiling. In addition, supercoiling was seen with Cd^{2+} which was not the case in Fig. 5.5. The detection of contaminating Mg^{2+} ions in this experiment, however, creates a problem in interpreting these results since the supercoiling observed may be attributable to this contamination. Although no supercoiling was seen in the control with ATP and the gyrase-DNA complex spun through a column, this may have been because of inhibition of free ATP over any contaminating Mg^{2+}-ATP complex present (see Section 5.2.4.2 and Figs. 5.13 and 5.14). This could account for the apparent activity of CdATP which may have been caused by Mg^{2+} ions present; Cd^{2+} could have merely served to complex free ATP and reduce its inhibition. While this argument could be used for all of the apparently active metals with ATP in this experiment, previous experiments (Figs. 5.2 and 5.5) would strongly suggest that the activity seen with Ca-ATP, Mn-ATP, and Co-ATP are real effects. The results for $ATP_{\alpha}S$ in part (b) of Fig. 5.6. must again be treated with caution. For $ATP_{\alpha}S(Rp)$, the supercoiling with all of the metal ions could simply be due to contaminating Mg^{2+} since the control showed supercoiling. The lack of supercoiling with Zn^{2+} shows that this metal inhibits the supercoiling reaction. The results with $ATP_{\alpha}S(Sp)$ are interesting. As expected from Chapter 4, very little supercoiling was seen with Mg^{2+}. However, with Mn^{2+} and Co^{2+} a greater level of supercoiling was observed which was confirmed on a chloroquine gel (not shown). No supercoiling was detected with Ni^{2+}, Zn^{2+}, and Cd^{2+}.

5.2.3. The metal ion specificity of quinolone-induced DNA cleavage by gyrase.

As discussed in Section 1.2.3, gyrase induces double-stranded DNA-cleavage in the presence of quinolones (originally nalidixic acid) and, more recently, fluoroquinolones [such as ciprofloxacin (CFX)] following protein denaturation with SDS (Gellert *et al.*, 1977; Sugino *et al.*, 1977). This cleavage reaction probably represents part of the supercoiling reaction. Quinolone-induced DNA cleavage has been reported to require Mg^{2+} (Sugino *et al.*, 1977) and thus it was of interest whether other metal ions would support the reaction. Control experiments established that no DNA cleavage was detected in the absence of divalent metal ions (data not shown). Fig. 5.7 shows the results of a cleavage assay with various metal ions; it can be seen that all the metals supported cleavage to some extent. The order of effectiveness in supporting cleavage was $Mg^{2+} \approx Mn^{2+} \approx Co^{2+} \approx Cd^{2+} > Ni^{2+} > Ca^{2+} > Zn^{2+}$. It should be noted that some cleavage was shown by Mn^{2+} without CFX (Fig. 5.2) and this may have contributed to the cleavage shown here. The cleavage pattern (Sugino *et al.*, 1978) produced from gyrase action at preferred cleavage sites in linear pBR322 was also examined with the different metal ions as in Fig. 5.8. Here the order of effectiveness in supporting cleavage appeared to be $Mn^{2+} \approx Co^{2+} > Mg^{2+} > Ca^{2+} > Cd^{2+} > Ni^{2+} \approx Zn^{2+}$. Mg^{2+} and Ca^{2+} appeared to give similar cleavage patterns while the other metals appeared to give slightly different cleavage site preferences. The area on the gel where this difference is most apparent is indicated in Fig. 5.8.

The above results show that all the metal ions tested support some quinolone-induced DNA cleavage. This suggests that the cleavage reaction has a greater tolerance for metal ions than the relaxation and supercoiling reactions. Formation of a gyrase-DNA complex has also been shown to require Mg^{2+} (Higgins and Cozzarelli, 1982; Maxwell and Gellert, 1984; Rau *et al.*, 1987) as demonstrated by filter binding and gel retardation assays. Gyrase-catalysed DNA supercoiling, relaxation and cleavage all require

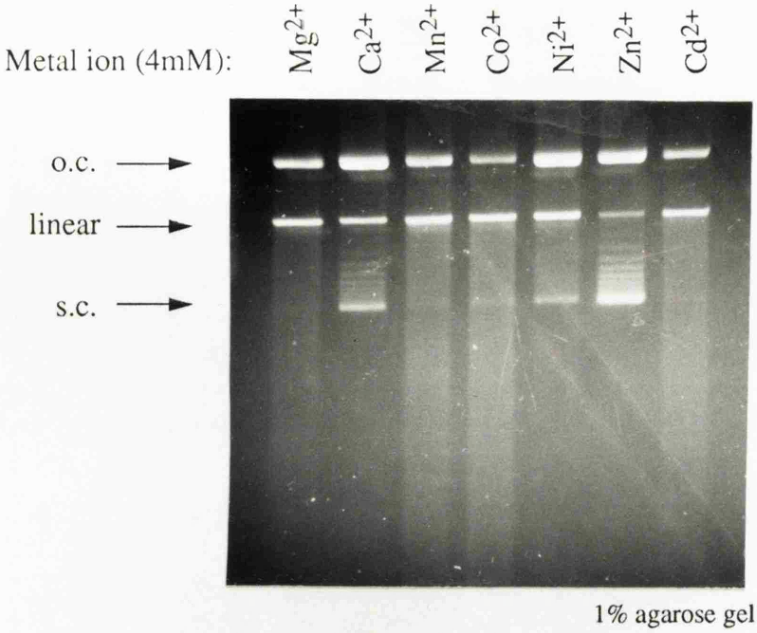

Figure 5.7. Quinolone-induced cleavage with different metal ions. Reactions (30µl) comprised: gyrase (75nM); various metal ions (4mM); native supercoiled pBR322 (10µg/ml); CFX (3.3µg/ml) in supercoiling buffer - DTT. After incubation at 25°C for 60 min. 7µl of proteinase K (1.9mg/ml final conc.) was added followed by a further incubation at 37°C for 30 min. The DNA was extracted with phenol/$CHCl_3$ and displayed by electrophoresis.

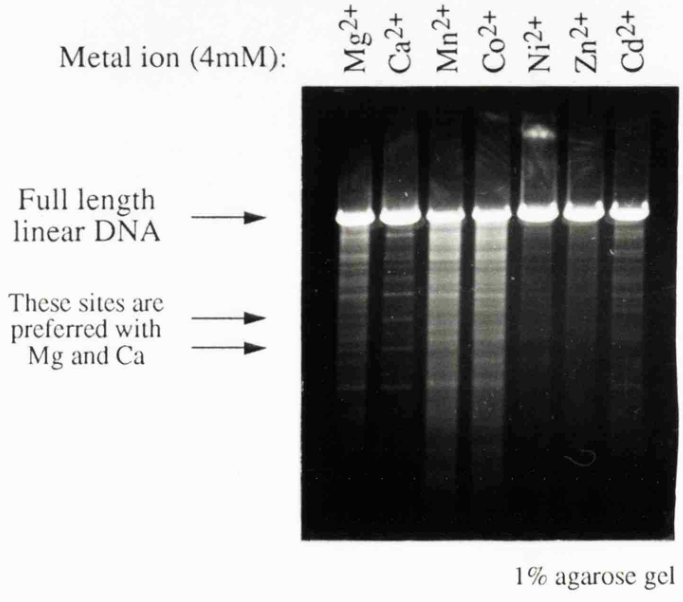

Figure 5.8. Gyrase cleavage profile with different metal ions. The reactions (30µl) comprised: linear pBR322 (66µg/ml); gyrase (150nM); various metal ions (4mM) in supercoiling buffer - DTT. After 60 min. at 25°C, CFX (3.2µg/ml final conc.) was added and the reactions were incubated for a further 10 min. SDS and proteinase K were added as described in Fig. 5.7 and the DNA was displayed by electrophoresis.

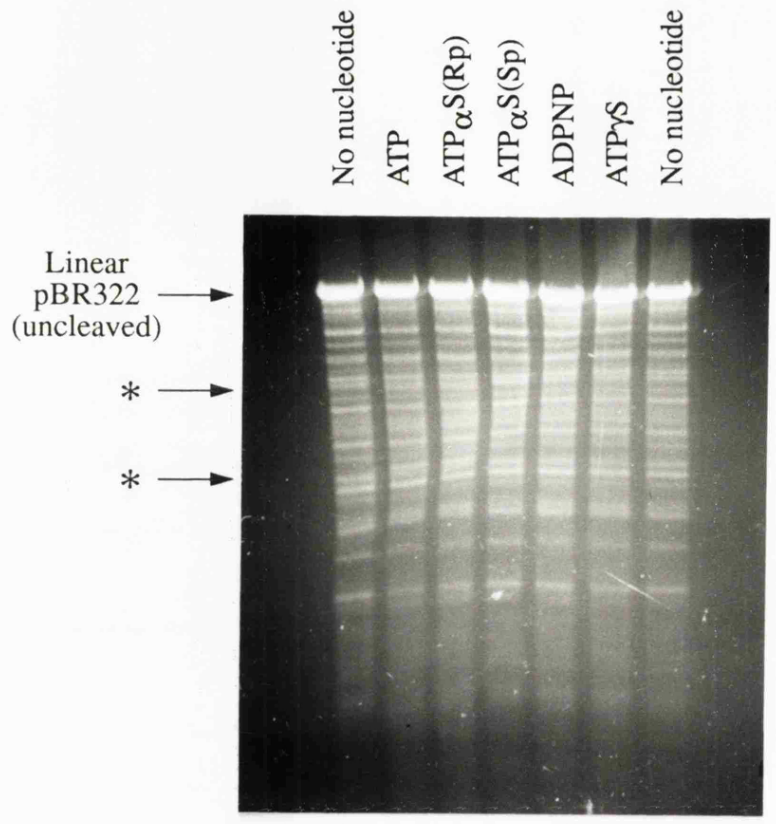

*Areas where the different patterns with ATP and ATP$_\alpha$S(Rp) are most pronounced

Figure 5.9. Gyrase cleavage profile with different nucleotides. The reactions (30µl) comprised: linear pBR322 (66µg/ml), gyrase (150nM), CFX (3.0µg/ml), various nucleotides (1mM) in supercoiling buffer. The reactions were incubated for 60 min. at 25°C and SDS and proteinase K were then added as described in Fig. 5.7. The DNA was displayed by electrophoresis.

interaction of the protein with DNA. In addition the relaxation and supercoiling reactions are thought to involve wrapping of the DNA around the protein in a positively superhelical sense (Liu and Wang, 1978b) whereas this wrapping is presumably not a prerequisite for DNA cleavage. A hypothesis which is consistent with the observed metal ion specificity of the cleavage, relaxation and supercoiling reactions is that all the metals tested can support a 'loose' gyrase-DNA complex competent for the cleavage reaction but the formation of the wrapped DNA complex required for relaxation and supercoiling may be less tolerant towards different metal ions with only Mg^{2+}, Ca^{2+}, and Mn^{2+} being accepted. In support of this hypothesis is the observation, from Fig 5.8, that metals not competent for the supercoiling or relaxation reaction, such as Cd^{2+} and Co^{2+}, seem to give a different cleavage pattern to Mg^{2+}. This is only one possible explanation of the results and other hypotheses involving a more direct participation of the Mg^{2+} ion in relaxation and supercoiling, such as the stabilisation of an intermediate in DNA translocation, cannot be excluded.

The cleavage pattern produced from cleavage of linear pBR322 was also investigated in the presence of various nucleotides as shown in Fig. 5.9. It can be seen that under the conditions of the experiment the reactions with no nucleotide, $ATP_{\alpha}S$(Sp), ADPNP, and $ATP_{\gamma}S$ all gave the same cleavage profiles. Interestingly the reactions with ATP and $ATP_{\alpha}S$(Rp) gave patterns that showed small but reproducible differences to the patterns with the other nucleotides. Thus the nucleotides which were catalytically competent and good substrates appeared to shift the cleavage site preference in pBR322. It has previously been reported that ADPNP shifts the cleavage site preference of gyrase in ColE1 DNA (Sugino *et al.*, 1978) but under the conditions of this experiment no such effect was seen in pBR322.

5.2.4. Nucleotide stereospecificity in the N-terminal fragment of GyrB (43kDa protein).

In view of the difficulty in using supercoiling as a criterion to probe the specificity of gyrase for different metal-phosphorothioate ATP complexes, it was decided to focus directly on the gyrase ATPase. The 43kDa fragment of the B protein was chosen as a simple model since this protein, unlike the intact gyrase tetramer (Maxwell and Gellert, 1984; Sugino and Cozzarelli, 1980), does not require DNA for full ATPase activity (data not shown).

The protein was prepared as described in Section 2.24 based on the method used by Jackson *et al* (1991). After purification by Heparin-Sepharose and FPLC Mono Q (or High Load equivalent) ion-exchange chromatography, the protein was obtained in a >99% pure form as judged by SDS-PAGE.

5.2.4.1. Steady-state analysis of the hydrolysis of ATP, $ATP_{\alpha}S$, and $ATP_{\beta}S$ by the 43kDa protein with Mg^{2+} as the activating metal ion.

Fig. 5.10 shows that the ATPase of the 43kDa fragment (as measured by the continuous fluorescent phosphate assay; Section 4.27) exhibited a greater than first order dependence upon protein concentration which agrees with the observations of Ali *et al.* (1992). In all further ATPase experiments with the 43kDa fragment, the protein concentration used was 15μM. Fig. 5.11 shows the steady-state kinetics of ATP hydrolysis by the 43kDa fragment at this protein concentration. The reaction was seen to follow saturation kinetics giving values for K_M^{app} of 0.99mM and k_{cat}^{app} of 0.014/s. It is important to note that the kinetics of the 43kDa protein has recently been shown to deviate from a simple Michaelis-Menten model and that these kinetic constants are only apparent values. Their significance is discussed further in Section 5.3.

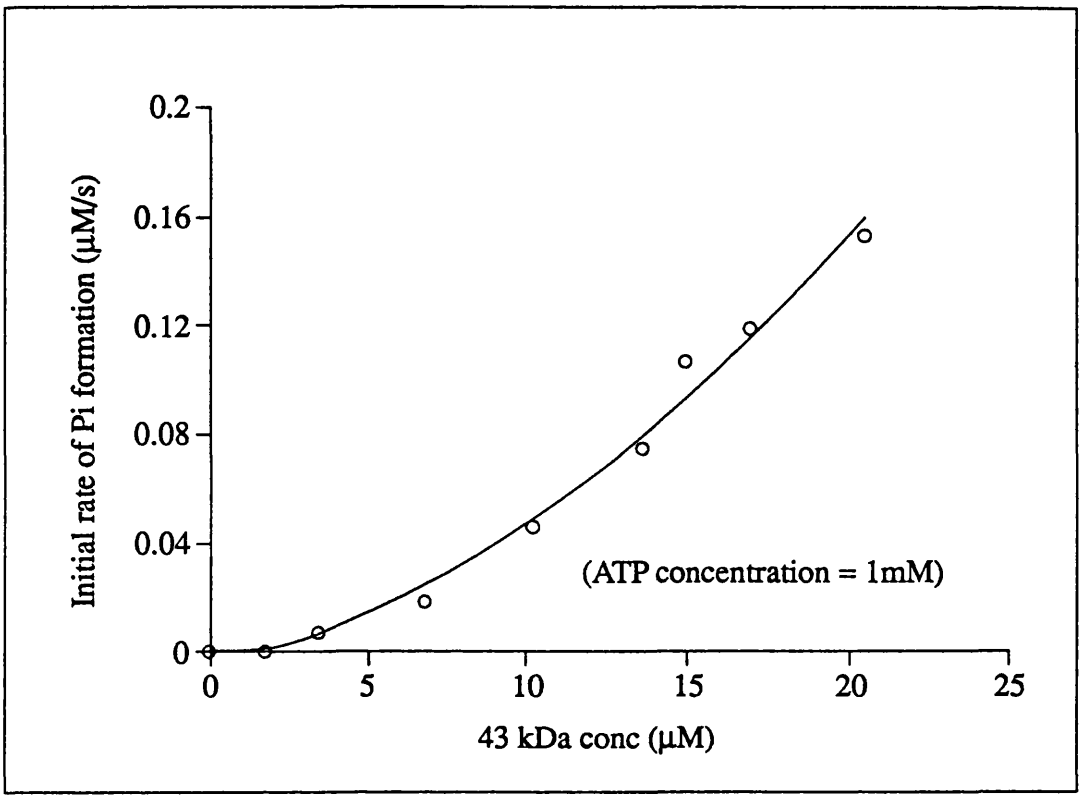

Figure 5.10. The protein concentration dependence of the 43kDa protein ATPase. (The points on the graph are averages of two readings).

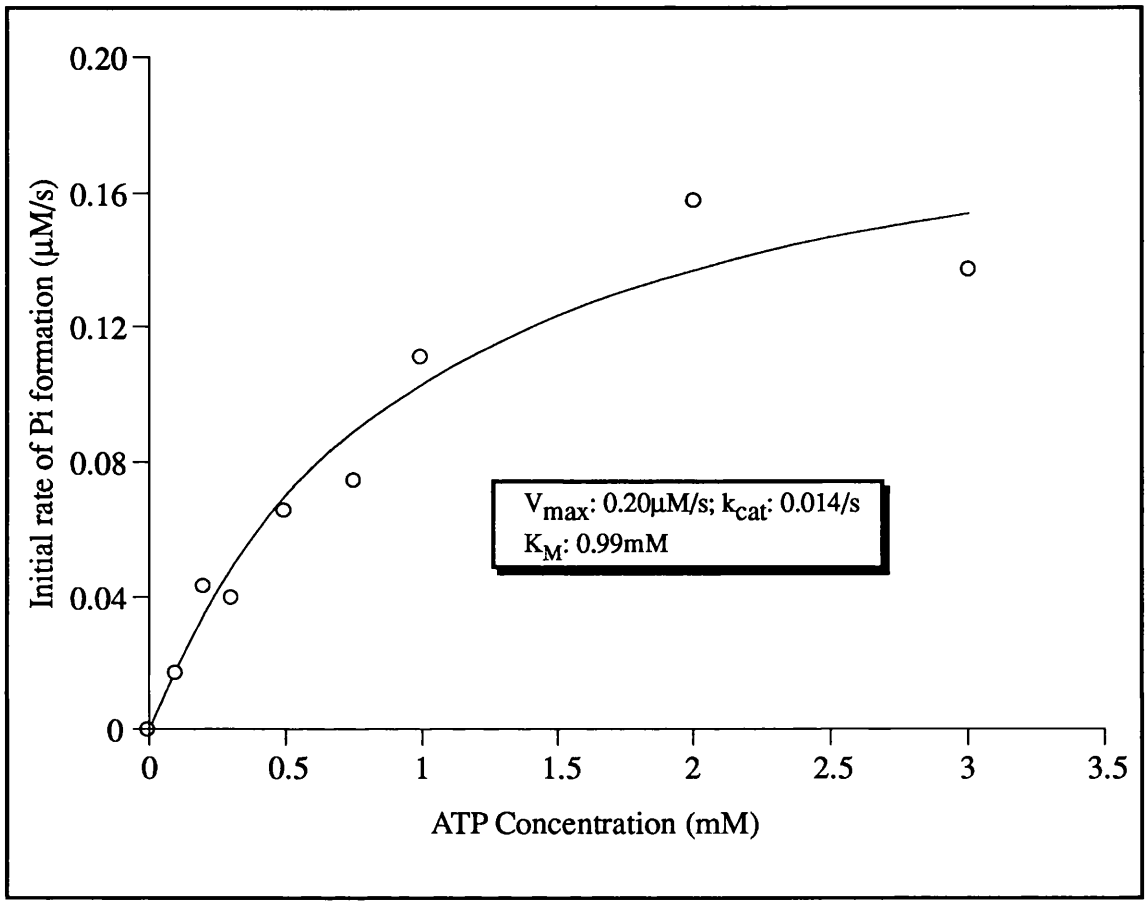

Figure 5.11. Steady-state kinetics of ATP hydrolysis by the 43kDa fragment. (The points on the graph are averages of two readings). The protein concentration was 15μM in a total assay volume of 100μl. The Mg^{2+} concentration was 4mM above the nucleotide concentration. Note that in all of the steady-state kinetic analyses of the 43kDa protein the enzyme was at a concentration of 15mM and only the initial phase of the reaction was followed corresponding to about two turnovers of the enzyme. Thus the reaction may only just have attained the steady-state.

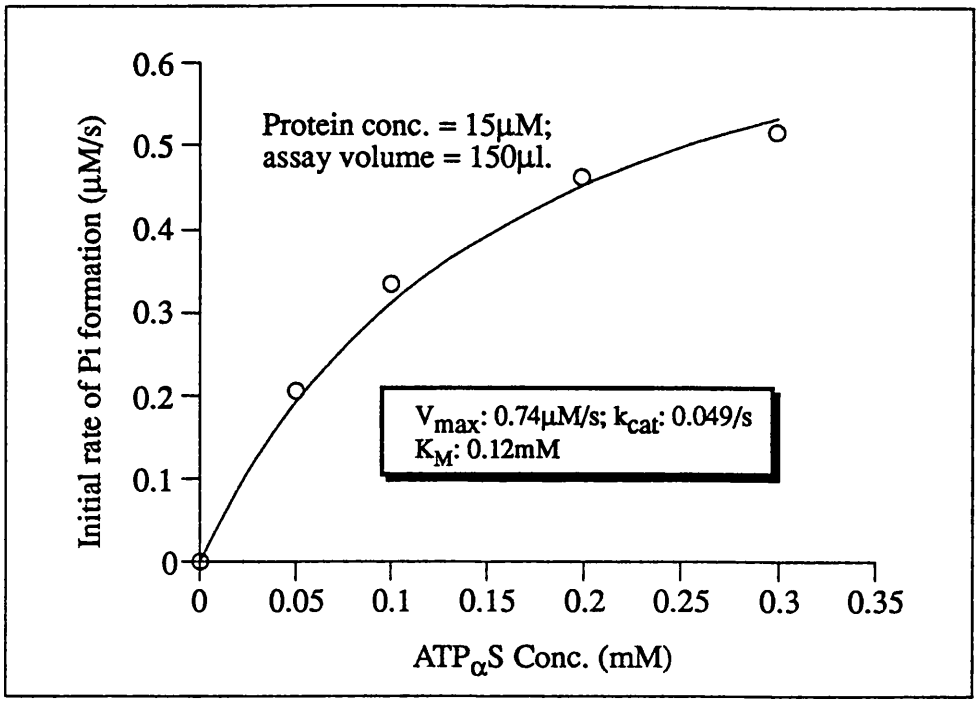

Figure 5.12(a). Steady-state hydrolysis of $ATP_\alpha S$(Rp). (The points on the graph were averages of two readings).

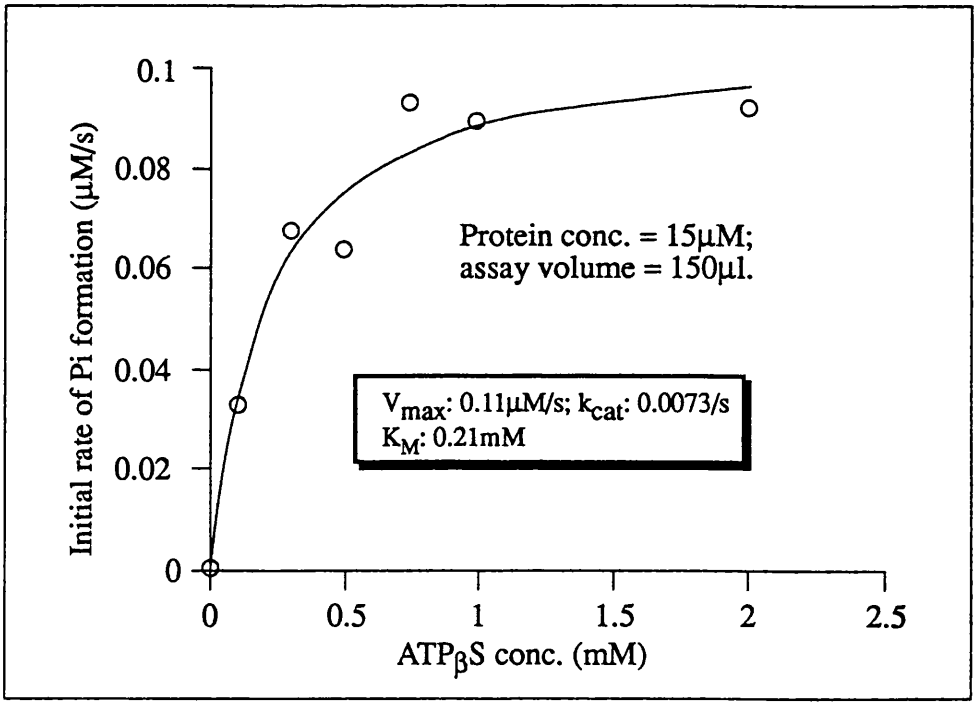

Figure 5.12(b). Steady-state hydrolysis of $ATP_\beta S$(Rp). (The points on the graph were averages of two readings).

Table 5.1. Steady-state kinetics of nucleotide hydrolysis by the 43kDa protein[a] with Mg^{2+} as the activating metal ion.

Nucleotide	K_M^{app} (mM)	k_{cat}^{app} (s^{-1})
ATP	0.99	0.014
$ATP_\alpha S$(Rp)	0.12	0.049
$ATP_\alpha S$(Sp)	-	-
$ATP_\beta S$(Rp)	0.21	0.0073
$ATP_\beta S$(Sp)	-	-

[a]Protein concentration was 15μM

Figs. 5.12(a) and 5.12(b) show the steady-state kinetics for the active isomers of the phosphorothioate ATP analogues, $ATP_\alpha S$ and $ATP_\beta S$ respectively. In each case, only the Rp epimers gave measurable rates of hydrolysis which was the same stereospecificity as seen with intact gyrase (Chapter 4).

The kinetic constants derived for the 43kDa protein, shown in Table 5.1, differ significantly from the values for intact gyrase discussed in Chapter 4 (see Section 4.2.8 and 4.3). The most dramatic difference is shown with $ATP_\alpha S$ (Rp). With intact gyrase this analogue had a similar k_{cat}^{app} to ATP while its K_M^{app} was approximately 10-fold lower than that for ATP. Thus with intact gyrase the difference in the kinetics of $ATP_\alpha S$(Rp) compared to ATP was manifested in a 10-fold lower K_M^{app}. In contrast, with the 43kDa protein, $ATP_\alpha S$ has a 3.5-fold greater k_{cat}^{app} than ATP and a K_M^{app} approximately 8-fold lower than ATP. Thus with this GyrB fragment, the difference in the kinetics of $ATP_\alpha S$(Rp) compared to ATP is manifested in both a lower K_M^{app} and a higher k_{cat}. There are also differences in the hydrolysis of $ATP_\beta S$(Rp) as compared to ATP for the two proteins. With intact gyrase $ATP_\beta S$(Rp) gave a similar K_M^{app} to ATP and a k_{cat}^{app} approximately half of the value for ATP. For the 43kDa protein, $ATP_\beta S$(Rp) had a k_{cat}^{app} again approximately half of the ATP value but the K_M^{app} was

nearly 5-fold lower than ATP. The significance of these differences between intact gyrase and the 43kDa fragment is discussed later in Section 5.3.

5.2.4.2. The metal ion dependence of the hydrolysis of ATP, $ATP_{\alpha}S$, and $ATP_{\beta}S$ by the 43kDa protein.

The fluorescent phosphate coupled assay offered a way of measuring the kinetics of hydrolysis of ATP and the phosphorothioate analogues with different metal ions since the coupling reaction, namely the nucleoside phosphorylase-catalysed phosphorolysis of m^7Guo (see Fig. 4.20), was thought not to require a divalent metal ion. This was confirmed by control experiments which showed an identical decrease in fluorescence on addition of a given amount of phosphate in the presence and absence of Mg^{2+} ions. Thus it was intended to use the assay to probe for any changes in stereospecificity of the 43kDa protein towards the phosphorothioate ATP analogues on switching from Mg^{2+} to Cd^{2+} as the activating metal ion.

Further controls therefore investigated the effect of Cd^{2+} ion concentration on the activity of nucleoside phosphorylase in the coupled assay. It was found that up to 0.5mM Cd^{2+}, there was no measurable effect on the activity of the phosphorylase enzyme. However, at higher concentrations, Cd^{2+} was found to be inhibitory, reducing the rate of formation of m^7Gua such that this step was partially rate limiting. The effect of Cd^{2+} ions on the 43kDa protein was also examined. At high Cd^{2+} concentrations (2mM and above) the protein (at 15μM concentration) was clearly seen to precipitate. A more sensitive assay for protein precipitation was found to be an absorbance scan across the wavelength range of the protein absorbance peak centred on 280nm where precipitation produced deviations from a smooth peak, presumably due to light scattering. This method detected some protein precipitation at a concentration of 0.5mM Cd^{2+} while below this level the protein appeared to be fully soluble. In order to avoid the problem with excess Cd^{2+} ions, it was

decided to limit the concentration of free Cd^{2+} in experiments with the 43kDa protein to below 0.2mM.

For a rigorous analysis of reversal of stereospecificity with hard and soft metal ions, it is desirable to do a full kinetic analysis. This involves measuring initial rates of reaction at various concentrations of metal-nucleotide complex. However, such an experiment is difficult to do within the constraint that the free divalent metal ion concentration must be less than 0.2mM. One approach was to vary the concentration of metal-nucleotide complex by employing an excess of nucleotide over metal ions calculated so that a fixed proportion of the total metal ion concentration was in the complexed form. Thus the total metal ion concentration was varied systematically and the appropriate nucleotide concentration in each assay was calculated from the published stability constants of the metal-nucleotide complex (Pecoraro *et al.*, 1984). An example of the calculation of the nucleotide concentration required to give 90% of the total metal ion concentration in the complexed form is outlined below:

In the reaction,

$$M^{2+} + ATP \rightleftharpoons M.ATP \qquad \text{(eqn. 5.1)}$$

the stability constant (K_s) is given by the following expression:

$$K_s = \frac{[M.ATP]}{[M^{2+}][ATP]} \qquad \text{(eqn. 5.2)}$$

For a 90% metal-nucleotide complex, at equilibrium the concentrations of components are:

$$M^{2+} + ATP \rightleftharpoons M.ATP \qquad \text{(eqn.5.3)}$$

$$(0.1y) \quad (x\text{-}0.9y) \qquad (0.9y)$$

where y = total metal concentration, and x = total nucleotide concentration required.

The stability constant (K_S) for the metal-nucleotide complex is therefore given by:

$$K_S = \frac{0.9y}{(0.1y)(x-0.9y)} \qquad \text{(eqn. 5.4)}$$

$$\therefore \quad \frac{0.9y}{K_S(0.1y)} = x-0.9y \qquad \text{(eqn. 5.5)}$$

$$\therefore \quad x = \frac{0.9y}{K_S(0.1y)} + 0.9y \qquad \text{(eqn. 5.6)}$$

Substituting in values for the total metal ion concentration (y), and knowing the stability constant, the total nucleotide concentration required (x) can be calculated. The same procedure can be used to determine the concentration of nucleotide required to give any proportion of complexed metal ions over total metal ion concentration by reappraising the equilibrium concentrations of components (as in Eqn. 5.3) in terms of y as appropriate.

The results of experiments measuring the rates of hydrolysis of MgATP and CdATP at various calculated concentrations of the complexes are shown graphically in Figs. 5.13 and 5.14 respectively. The stability constants used were based on those for the metal-ATP^{4-} species and nucleotide concentrations were calculated so that 97% of the metal ion concentration was in the complex. If the only species interacting with the enzyme was the metal-nucleotide complex, it was anticipated that the plots would be hyperbolic characteristic of saturation kinetics. However, the observed plots deviated markedly from this behaviour. There are three possible explanations for this result. The first possibility is that the values for the stability constants may be wrong. The values used were measured at an ionic strength (μ) of 0.1M while the ionic strength of the 43kDa ATPase reactions was probably around 70mM but this was not believed to give a large difference in stability constant values. Additionally there is some variability in the values of stability

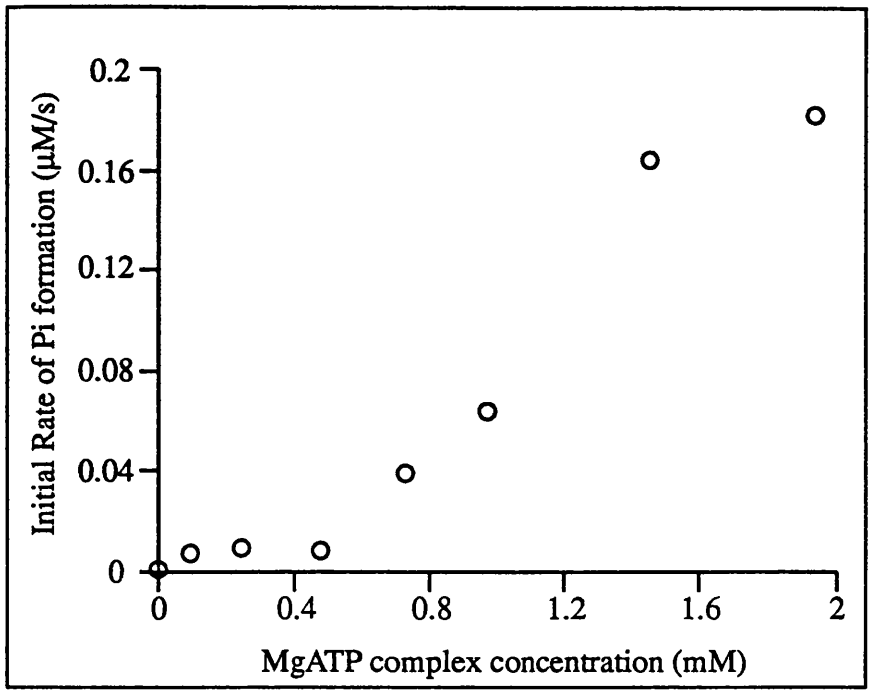

Figure 5.13. Steady-state analysis of MgATP hydrolysis in the presence of excess nucleotide over metal ion. The free ATP concentration was between 0.56 and 0.70mM. Note that each point on the graph represents only one measurement.

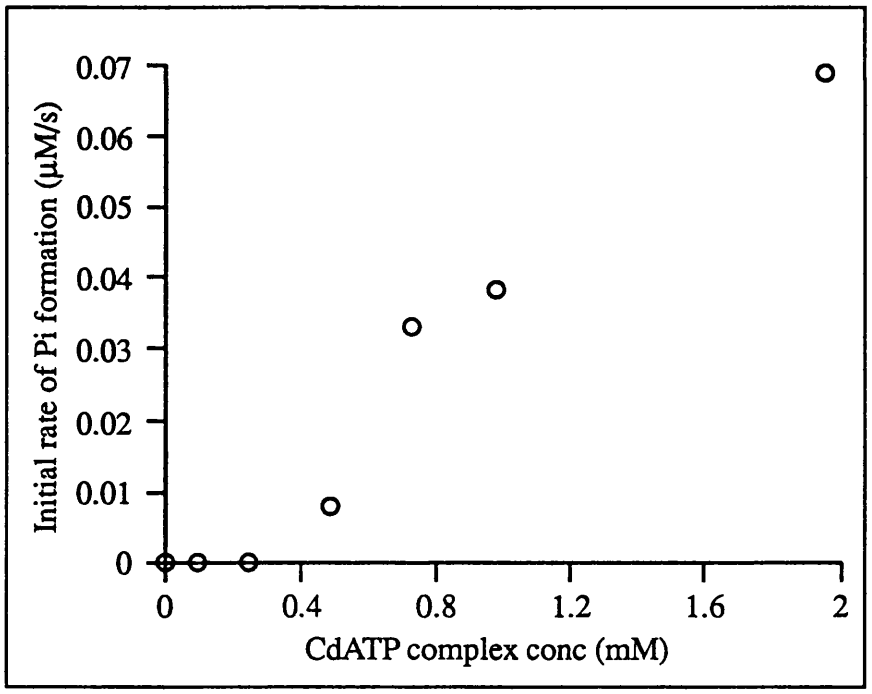

Figure 5.14. Steady-state analysis of CdATP hydrolysis in the presence of excess nucleotide over metal ion. The free ATP concentration was between 2.24 and 2.36mM. Note that each point on the graph only represents one measurement. Note also that the rates obtained in this experiment cannot be directly compared to Fig. 5.13 since the free ATP concentration is greater. This is a consequence of the lower stability constant for CdATP than MgATP.

constants for MgATP and MgADP in the literature. However, taking the lowest reported values for the stability constants for MgATP (Smith and Alberty, 1956), would still give between 68 and 75% of the total Mg^{2+} in the complexed form. Thus even if the stability constants were different under the conditions used the plots of Figs. 5.13 and 5.14 would still be expected to be hyperbolic. The second possibility is that another species in the reaction mixture was sequestering metal ions in competition with ATP. A low level of EDTA (less than 0.1mM final concentration in the assay) was present which may partly explain the deviation from hyperbolic plots. Another potential metal ion chelator in the reaction mixture was the polyamine, spermidine (4-azaoctane-1,8-diamine). Polyamines have been shown to form strong complexes with some metal ions such as Cu^{2+}. However, in solution at neutral pH, they are protonated and do not appear to complex Mg^{2+} ions (Wojciechowska *et al.*, 1991). The third, and most likely, possibility is that free ATP inhibits the hydrolysis of MgATP and CdATP by the 43kDa protein presumably *via* non-productive binding to the active site. In the experiments of Figs. 5.13 and 5.14, the free ATP concentration is almost constant at 0.56-0.70mM and 2.24-2.36mM respectively. Therefore these experiments can be considered as plots of rates against substrate concentration in the presence of a constant concentration of inhibitor (free ATP). Thus the sigmoidal curves obtained suggest that the inhibition does not follow Michaelis-Menten kinetics and point towards cooperativity in the hydrolysis of MgATP in the same way as has been shown for intact gyrase from ATPase experiments in the presence of ADP (Maxwell *et al.*, 1986). Recently the kinetics of ATP hydrolysis in the presence of ADP have been analysed for the 43kDa protein (Ali *et al.*, 1992) and similar sigmoidal plots have been obtained as for the free ATP inhibition in Figs. 5.13 and 5.14.

In view of the apparent inhibition of free ATP discussed above, it was not possible to perform a full kinetic study of the hydrolysis of ATP, $ATP_{\alpha}S$ and $ATP_{\beta}S$ in the presence of hard and soft metal ions to probe for reversal of stereospecificity. However, a simpler experiment was performed where rates were compared with a single concentration of nucleotide. The results of this experiment are summarised in Table 5.2 on page 166. The

concentration of each nucleotide was chosen to be near to a saturating level and an excess metal ion concentration was calculated to ensure that 90% of the nucleotide was complexed to the metal.

Table 5.2. Rates of hydrolysis of ATP, $ATP_{\alpha}S$, and $ATP_{\beta}S$ with Mg^{2+} and Cd^{2+}.

Nucleotide	Nucleotide conc. (mM)	Mg^{2+} ion conc. (mM)	Rate of hydrolysis (μM/s)	Cd^{2+} ion conc. (mM)	Rate of hydrolysis (μM/s)	Rate Mg / Rate Cd
ATP	2.0	1.98	0.162	2.19	0.067	**2.4**
$ATP_{\alpha}S$ (Rp)	0.3	0.57	0.49	0.38	0.014	**35**
$ATP_{\alpha}S$ (Sp)	0.3	0.57	-	0.38	-	-
$ATP_{\beta}S$ (Rp)	1.0	1.72	0.10	0.93	0.023	**4.4**
$ATP_{\beta}S$ (Sp)	1.0	1.72	-	0.93	-	-

It can be seen from the table that CdATP gave a rate of hydrolysis only 2.4-fold slower than MgATP. With the phosphorothioate ATP analogues, the Rp isomers were preferred for both $ATP_{\alpha}S$ and $ATP_{\beta}S$ in the presence of either Mg^{2+} or Cd^{2+}. For $ATP_{\alpha}S$(Rp) there was a 35-fold preference for the Mg complex while for $ATP_{\beta}S$(Rp) the preference for the Mg complex was only 4.4-fold. Since this data was obtained at just one nucleotide concentration the effects on the rate could result from changes in either the apparent K_M of V_{max} or both.

5.2.5. Crystallography of the 43kDa protein in the presence of the inactive phosphorothioate ATP analogues.

The crystallisation of proteins can be achieved by a variety of methods (reviewed in Eisenberg and Hill, 1989). All of these procedures are based on the same strategy which is to slowly bring the protein solution to a state of minimum solubility and achieve a limited degree of supersaturation from which crystals may form. Conditions are chosen that allow a protein molecule to explore the maximum number of favourable interactions

with neighbouring molecules in the approach to supersaturation. These intermolecular interactions provide the thermodynamic impetus for the protein to crystallise or precipitate from solution. Crystallisation is favoured by homogeneity of the macromolecule (impurities may interfere with important specific interactions) and an approach to inadequate solvation which is slow enough to allow the molecules to orientate themselves in a highly ordered matrix.

Since the Sp epimers of $ATP_{\alpha}S$ and $ATP_{\beta}S$ were poor substrates for both gyrase and the 43kDa protein, it was decided to attempt to crystallise the 43kDa protein in the presence of these nucleotides. In this way it was hoped that it might be possible to obtain a direct view of the metal-nucleotide complex in these inactive isomers and to complement the crystallography data obtained with ADPNP (Wigley *et al.*, 1991). $ATP_{\gamma}S$ was shown to be very slowly hydrolysed by gyrase in Chapter 4 and this was also used in crystallography experiments.

Protein samples were purified to near homogeneity (as described in Section 5.2.4), and concentrated to 5-10 mg/ml in low salt buffer (20mM Tris.HCl at the appropriate pH, 5mM $MgCl_2$, and 1mM DTT). Crystallisation trials were performed by the hanging drop method (Eisenberg and Hill, 1989; McPherson, 1982) which enables rapid screening of a variety of crystallisation conditions on a fairly small scale (each well required between 20 and 100µg of protein). Various molecular weight preparations of polyethylene glycol (PEG) were used as the protein precipitants. Results of all the trials with different nucleotides are shown in Fig. 5.15.

As can be seen from the results, various conditions for crystal growth were screened. Thus the effect of pH, protein concentration, and nucleoside phosphorothioate concentration was investigated. The results at the three different pHs (7.5, 8.3, and 8.8) showed no clear differences, although there appeared to be a slight trend towards lower

Figure 5.15. (shown on the next 6 facing pages). Summary of all of the crystallisation trials with the 43 kDa protein and various nucleotides and inhibitors. Protein in crystallography buffer was mixed with precipitant and nucleotide at the concentration stated, and a 12µl drop was applied to a plastic coverslip (see Section 2.31). The coverslip was then inverted over a well containing 2ml of the mother liquor and a seal was made using high-vacuum grease. The plates, each having 24 wells, were checked at regular intervals and the state of the droplet noted. In the figure, ppt indicates that a thick amorphous precipitate formed in the drop; grainy has been used to indicate the formation of a more finely divided precipitate which appeared to be semi-crystalline; oil indicates the formation of clumped oily globules; and crystal indicates the appearance of protein crystals. Generally the results were scored after a week, except for the trials in the presence of high salt (50mM NaCl) which were scored after 2 weeks, and the trials with $ATP_{\gamma}S$ which were scored after 3 days. The samples were kept for at least 4 months during which time regular inspections were made.

pH 7.5	5%	8%	11%	14%	17%	20%
PEG 1000	clear	clear	clear	clear	clear	clear
PEG 4000	clear	clear	clear	clear	clear	clear
PEG 6000	clear	clear	*Crystals*	*Crystals*	*Crystals*	*Crystals*
PEG 8000	*Crystals*	*Crystals*	*Crystals*	*Crystals*	ppt	ppt

pH 8.3	5%	8%	11%	14%	17%	20%
PEG 1000	clear	clear	clear	clear	clear	clear
PEG 4000	clear	clear	clear	clear	clear	clear
PEG 6000	*Crystals*	*Crystals*	*Crystals*	*Crystals*	*Crystals*	*Crystals*
PEG 8000	*Crystals*	*Crystals*	*Crystals*	*Crystals*	*Crystals*	*Crystals*

pH 8.8	5%	8%	11%	14%	17%	20%
PEG 1000	clear	clear	clear	clear	clear	clear
PEG 4000	clear	clear	clear	clear	clear	clear
PEG 6000	*Crystals*	*Crystals*	*Crystals*	*Crystals*	*Crystals*	grainy
PEG 8000	grainy	ppt	ppt	ppt	ppt	ppt

Crystallisation trials with 43 kDa protein (at 7mg/ml) and ADPNP (at 0.5mM).

Figure 5.15. (continued)

pH 7.5	5%	8%	11%	14%	17%	20%
PEG 1000	ppt	ppt	ppt	ppt	ppt	ppt
PEG 4000	ppt	ppt	ppt	ppt	grainy	grainy
PEG 6000	ppt	ppt	ppt	grainy	grainy	ppt
PEG 8000	grainy	ppt	oily	oily	oily	oily

pH 8.3	5%	8%	11%	14%	17%	20%
PEG 1000	ppt	ppt	ppt	ppt	ppt	ppt
PEG 4000	ppt	ppt	ppt	ppt	ppt	ppt
PEG 6000	ppt	ppt	grainy*	grainy	grainy	grainy
PEG 8000	ppt	oily	oily	oily	oily	oily

pH 8.8	5%	8%	11%	14%	17%	20%
PEG 1000	ppt	ppt	ppt	ppt	ppt	ppt
PEG 4000	ppt	ppt	ppt	ppt	ppt	ppt
PEG 6000	ppt	ppt	ppt	ppt	ppt	ppt
PEG 8000	grainy	grainy	ppt	ppt	ppt	ppt

*Crystals formed after treatment with dilute ammonium hydroxide (see text).

Crystallisation trials with 43 kDa protein (at 7mg/ml) and $ATP_{\alpha}S(Sp)$ (at 1mM).

Figure 5.15. (continued)

pH 7.5	5%	8%	11%	14%	17%	20%
PEG 1000	ppt	ppt	ppt	ppt	ppt	ppt
PEG 4000	ppt	ppt	grainy	grainy	ppt	ppt
PEG 6000	grainy	grainy	grainy	grainy	grainy	ppt
PEG 8000	grainy	ppt	ppt	ppt	ppt	ppt

pH 8.3	5%	8%	11%	14%	17%	20%
PEG 1000	ppt	ppt	ppt	ppt	ppt	ppt
PEG 4000	ppt	ppt	ppt	ppt	ppt	ppt
PEG 6000	ppt	grainy	grainy	grainy	grainy	ppt
PEG 8000	ppt	ppt	grainy	grainy	ppt	ppt

pH 8.8	5%	8%	11%	14%	17%	20%
PEG 1000	ppt	ppt	ppt	ppt	ppt	ppt
PEG 4000	ppt	ppt	grainy	grainy	ppt	ppt
PEG 6000	grainy	grainy	ppt	ppt	ppt	ppt
PEG 8000	ppt	ppt	ppt	ppt	ppt	ppt

Crystallisation trials with 43 kDa protein (at 7mg/ml) and $ATP_{\beta}S(Sp)$ (at 1mM).

Figure 5.15. (continued)

pH 8.3	5%	8%	11%	14%	17%	20%
PEG 1000	ppt	ppt	ppt	oily	oily	oily
PEG 4000	ppt	ppt	oily	oily	oily	oily
PEG 6000	oily	oily	oily	oily	oily	oily
PEG 8000	oily	oily	oily	oily	clear	clear

Nucleotide = $ATP_{\gamma}S$ (at 1mM). Protein conc. = 7mg/ml. (Scored after 3 days).

pH 8.3	1%	2%	4%	6%	8%	10%
PEG 4000	ppt	ppt	ppt	ppt	ppt	ppt
PEG 6000	ppt	ppt	ppt	ppt	ppt	ppt
PEG 8000	ppt	ppt	ppt	ppt	ppt	ppt
PEG 20000	ppt	ppt	ppt	ppt	ppt	ppt

Nucleotide = ADPNP (at 0.5mM). Protein conc. = 7mg/ml.

pH 8.3	1%	2%	4%	6%	8%	10%
PEG 4000	ppt	ppt	ppt	ppt	ppt	grainy
PEG 6000	ppt	ppt	ppt	ppt	ppt	ppt
PEG 8000	ppt	ppt	ppt	ppt	ppt	ppt
PEG 20000	ppt	ppt	ppt	ppt	ppt	ppt

Nucleotide = $ATP_{\alpha}S(Sp)$ (at 1mM). Protein conc. = 7mg/ml.

pH 8.3	1%	2%	4%	6%	8%	10%
PEG 4000	ppt	ppt	ppt	ppt	ppt	ppt
PEG 6000	ppt	ppt	ppt	ppt	ppt	ppt
PEG 8000	ppt	ppt	ppt	ppt	ppt	ppt
PEG 20000	ppt	ppt	ppt	ppt	ppt	ppt

Nucleotide = $ATP_{\beta}S(Sp)$ (at 1mM). Protein conc. = 7mg/ml.

Figure 5.15. (continued)

pH 8.3	1%	2%	4%	6%	8%	10%
PEG 4000	ppt	ppt	ppt	ppt	ppt	ppt
PEG 6000	ppt	ppt	ppt	ppt	ppt	ppt
PEG 8000	ppt	ppt	ppt	ppt	ppt	ppt
PEG 20000	ppt	ppt	ppt	ppt	ppt	ppt

Nucleotide = $ATP_{\gamma}S$ (at 1mM). Protein conc. = 7mg/ml. Scored after 3 days

pH 8.3	5%	8%	11%	14%	17%	20%
PEG 4000 (ADPNP)	*Crystals*	*Crystals*	*Crystals*	*Crystals*	*Crystals*	*Crystals*
PEG 6000 (ADPNP)	*Crystals*	clear	*Crystals*	*Crystals*	*Crystals*	*Crystals*
PEG 6000 ($ATP_{\alpha}S$(Sp)	clear	clear	clear	ppt	clear	ppt
PEG 6000 ($ATP_{\beta}S$(Sp)	clear	clear	clear	clear	ppt	ppt

Low protein concentration (2mg/ml). $ATP_{\alpha}S$ and $ATP_{\beta}S$ concs. = 5mM.

pH 8.3	5%	8%	11%	14%	17%	20%
PEG 6000 (ADPNP)	*Crystals*	*Crystals*	*Crystals*	*Crystals*	*Crystals*	*Crystals*
PEG 6000 ($ATP_{\alpha}S$(Sp)	ppt	grainy	grainy	grainy	oily	ppt
PEG 6000 ($ATP_{\beta}S$(Sp)	ppt	ppt	ppt	grainy	ppt	ppt

$ATP_{\alpha}S$ and $ATP_{\beta}S$ concs. = 5mM. Protein conc. = 7mg/ml

Figure 5.15. (continued)

pH 8.3	5%	8%	11%	14%	17%	20%
PEG 6000 (ADPNP)	*Crystals*	*Crystals*	*Crystals*	*Crystals*	*Crystals*	*Crystals*
PEG 6000 ($ATP_{\alpha}S(Sp)$)	ppt	grainy	grainy	grainy	ppt	ppt
PEG 6000 ($ATP_{\beta}S(Sp)$)	ppt	ppt	grainy	grainy	ppt	ppt

$ATP_{\alpha}S$ and $ATP_{\beta}S$ concs. = 5mM. Protein conc. = 7mg/ml. 50mM NaCl present.

pH 8.3	5%	8%	11%	14%	17%	20%
PEG 1000 (novobiocin)	ppt	clear	ppt	ppt	ppt	ppt
PEG 4000 (novobiocin)	ppt	ppt	ppt	ppt	ppt	ppt
PEG 6000 (novobiocin)	grainy	grainy	ppt	ppt	ppt	ppt
PEG 8000 (novobiocin)	ppt	ppt	ppt	clear	ppt	ppt

Novobiocin conc. = 0.1mM. Protein conc. = 3mg/ml.

pH 8.3	5%	8%	11%	14%	17%	20%
PEG 4000 (ADPNP)	*Crystals*	*Crystals*	*Crystals*	*Crystals*	*Crystals*	*Crystals*
PEG 6000 (ADPNP)	clear	*Crystals*	*Crystals*	*Crystals*	*Crystals*	*Crystals*
PEG 4000 (ADPNP and Novobiocin)	clear	clear	clear	clear	clear	clear
PEG 6000 (ADPNP and Novobiocin)	clear	clear	clear	oily	oily	oily

ADPNP conc. = 0.5mM. Novobiocin conc. = 0.1mM. Protein conc. = 3mg/ml

Figure 5.15. (continued)

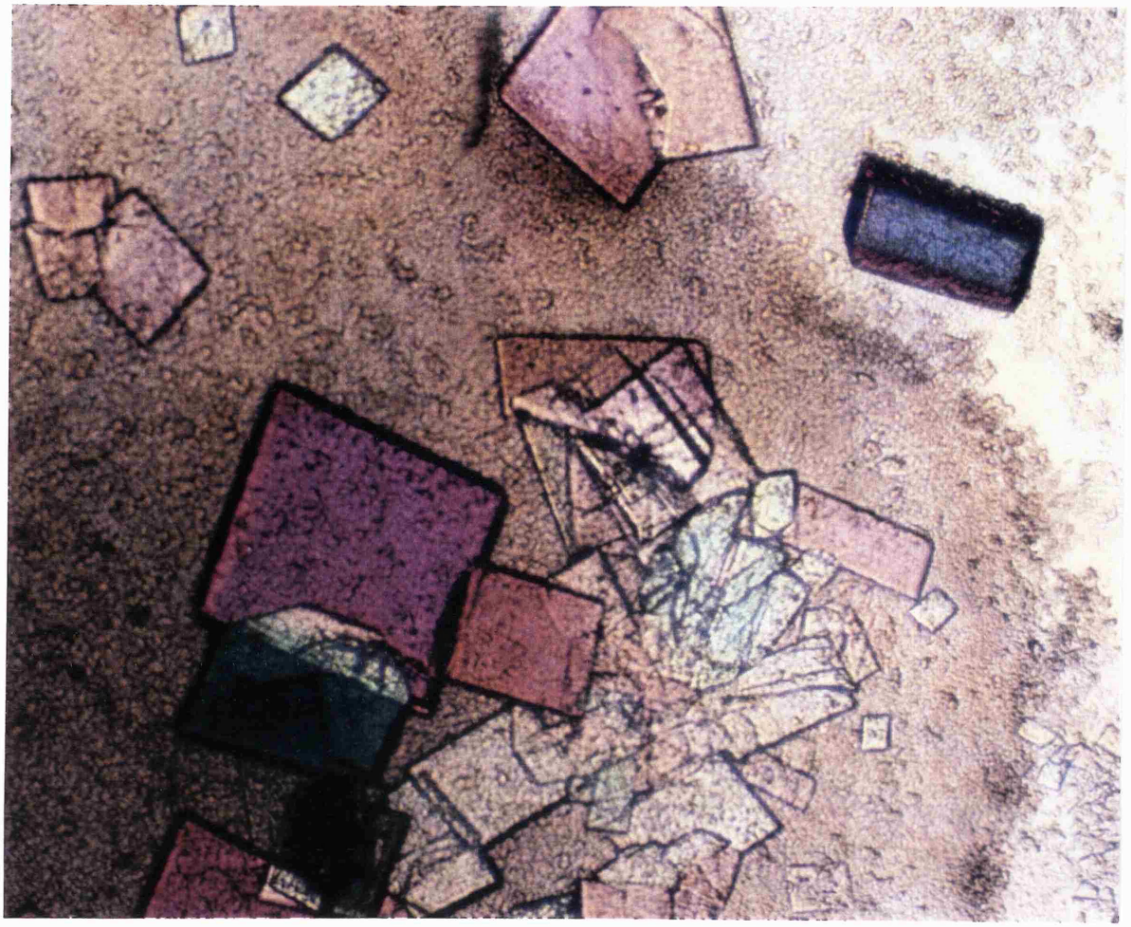

Figure 5.16. Crystals of the 43kDa protein in the presence of ADPNP. The crystals were formed at pH 8.3, at a protein concentration of 7mg/ml and nucleotide concentration of 0.5mM. The photograph was taken at a magnification of X40 using an Olympus OM1 camera mounted on an Olympus microscope. Plane-polarised light was provided from 2 polarising filters, 1 in front of the light source and the other in front of the microscope lens.

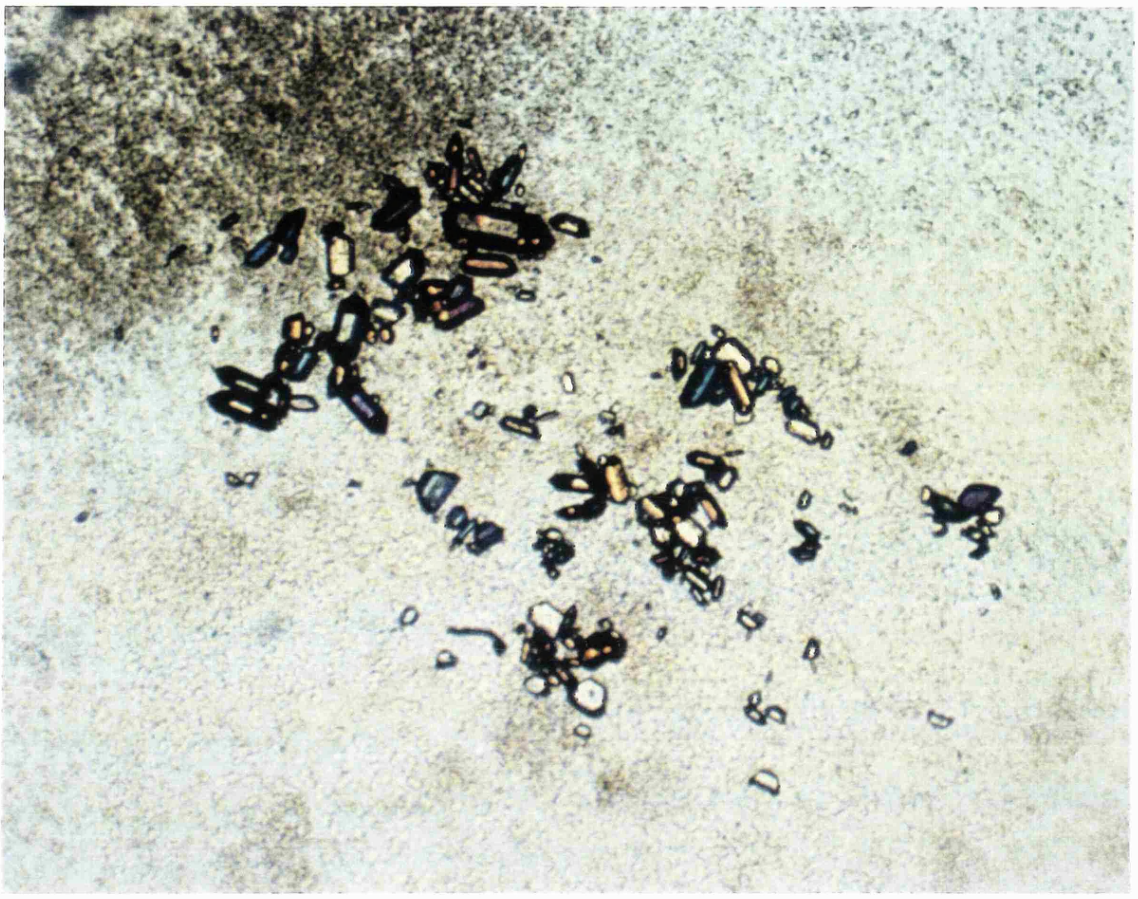

Figure 5.17. Putative protein crystals of the 43 kDa protein in the presence of $ATP_{\alpha}S(Sp)$ (1mM), 11 % PEG 6000, pH 8.3, 22°C. The crystallisation tray was laid down on 24/5/91. After a few days a grainy precipitate formed (see tabulated results in Fig. 5.15) which did not change markedly after about 7 months. 5 µl of 0.1M ammonium hydroxide was added to the hanging drop on 23/1/92 and the tray was laid down again for crystallisation at 22°C. The tray was examined one week after addition of ammonium hydroxide and no crystals were detected. It was not looked at again until 10/7/92 when the crystals were seen and photographed.

protein solubility at higher pHs. The best crystals with ADPNP were obtained at pH 8.3. Crystals grown at a protein concentration of 7mg/ml often existed together with precipitate (Fig. 5.16) whereas at lower protein concentrations (such as 2mg/ml) crystals would tend to grow in the absence of any precipitate. Also larger crystals were obtained at the lower protein concentration. Unfortunately no crystals were obtained with the phosphorothioate ATP analogues. In some cases, grainy precipitates were obtained which appeared to have a semi-crystalline nature. In other cases clumped oil-like droplets were formed. Presumably, both of these states represent some interaction of protein molecules but not in a sufficiently ordered fashion to form crystals.

The grainy precipitate formed with $ATP_{\alpha}S(Sp)$ (1mM) and 43kDa protein (7mg/ml) at pH 8.3 and 14% PEG 6000 was used to attempt to seed crystal growth in samples containing 43kDa protein (2mg/ml) and the usual range of PEG 6000 between 5 and 20%. However, in all six droplets, precipitates were formed.

The inhibition of the gyrase ATPase experiments in Chapter 4 suggest that $ATP_{\alpha}S(Sp)$ and $ATP_{\beta}S(Sp)$ are bound rather weakly by the enzyme. Therefore, crystallography trials were also carried out with $ATP_{\alpha}S(Sp)$ and $ATP_{\beta}S(Sp)$ at high concentrations (5mM). However, as shown in Fig 5.15, no crystals were formed in these experiments.

Crystals of the 43kDa protein formed at a protein concentration of 7mg/ml, pH 8.3, and PEG 6000 were harvested in crystallography buffer containing 5% PEG 6000. Individual crystals were then transferred in a minimum of solution (approximately 15µl) *via* a mini-pipette to coverslips. Two concentrations of Mg-$ATP_{\alpha}S(Sp)$ (1:1 complex; 5µl) were added to different droplets to give a total concentration of 1mM and 20mM respectively. Control experiments where 5µl of water was added to the harvested crystals were also performed. The droplets containing crystals with added water or $ATP_{\alpha}S(Sp)$ (1mM) were stable for at least 3 months. On adding the high concentration of

$ATP_{\alpha}S(Sp)$ to the harvested crystals, the nucleotide immediately came out of solution as a micro-crystalline precipitate. It is therefore possible that experiments at different PEG concentrations with this nucleotide may provide a method for its crystallisation which to my knowledge has not been achieved before.

Fig. 5.15 also shows the results of crystallography trials with the gyrase inhibitor, novobiocin. This coumarin drug has been shown to be a potent inhibitor of the gyrase ATPase (Staudenbauer and Orr, 1981; Sugino and Cozzarelli, 1980; Sugino *et al.*, 1978) and of the 43kDa protein (Ali *et al.*, 1992). In the presence of novobiocin no crystals were obtained with only precipitates being formed. An experiment was also performed with ADPNP and novobiocin together. This showed that in the absence of novobiocin, crystals formed as expected. However, in the presence of the drug, no crystals were formed. Thus the drug appeared to inhibit the formation of crystals, which is consistent with the hypothesis that nucleotide binding and novobiocin binding are mutually exclusive.

After several months, selected crystallisation drops, in which considerable protein precipitation had occurred (or in which grainy precipitates were present), were subjected to a final attempt at obtaining crystals known as "McPherson's last gasp" (McPherson, 1982). In this procedure, 5µl of a 0.1M solution of ammonium hydroxide was added to the "hanging drops" which were then replaced above their respective wells and left to form crystals. The strategy behind this treatment is that addition of ammonium hydroxide will raise the pH of the samples to ~10 which may redissolve the precipitated protein. Evaporation of ammonia from the samples into the vapour phase will then gradually decrease the pH back to the original pH which will slowly bring the protein solution back towards supersaturation and crystallisation may occur.

In several samples, some of the precipitate appeared to dissolve on the addition of ammonium hydroxide. Samples were checked for the appearance of crystals after two weeks with no crystals being found. The trays were then left for about 5 months at 22°C without further observation. One week before submission of this thesis the trays were looked at again. In one sample, containing 1mM $ATP_{\alpha}S$ (Sp), 11% PEG 6000, and 7mg/ml 43 kDa protein at a starting pH of 8.3, crystals had formed (see Fig. 5.17).

5.3. DISCUSSION.

In Chapter 4 of this thesis the specificity of gyrase towards the diastereoisomers of $ATP_{\alpha}S$ and $ATP_{\beta}S$ in the presence of Mg^{2+} ions was characterised and from this data the probable configuration of the active metal-ATP complex was deduced. Confirmation of this prediction has been sought from experiments investigating the stereospecificity of the enzyme with these ATP analogues in the presence of other metal ions in an approach which exploits the differing propensities of the metal ions to coordinate the sulphur.

As a first step it was necessary to investigate the activity of gyrase with different metal ions. In 5.2.1, it was shown that in both the supercoiling and relaxation reactions, a divalent metal ion was required which could be Mg^{2+}, Ca^{2+}, or Mn^{2+} but not Co^{2+}, Ni^{2+}, Zn^{2+}, and Cd^{2+}. Furthermore, it was found that the Mg^{2+} ion concentration required for optimum relaxation of DNA was 4mM. This relatively high level may reflect the metal ion binding constants of important ligands involved in the relaxation reaction such as the phosphates of DNA or acidic amino-acid residues on the surface of the protein. However, at present, the precise role of divalent metal ions in the reactions of gyrase is unclear. For example, the translocation of DNA through the enzyme in the proposed mechanisms for DNA supercoiling and relaxation may require further specific metal ion interactions with, for example, internal amino-acids.

In 5.2.3, the metal ion specificity of quinolone-directed DNA cleavage by gyrase was investigated. This reaction showed a greater tolerance for metal ions than the supercoiling or relaxation reactions. One explanation for this would be that DNA cleavage does not require the formation of such a specific DNA-protein complex as the relaxation or supercoiling reactions. This hypothesis is supported from cleavage experiments using short linear DNA fragments bearing a preferred cleavage site, which have shown that cleavage occurs preferentially at this site regardless of its position in the DNA fragment (Dobbs *et al.*, in press). It is clear that further studies are required but the results

presented here suggest that a more detailed examination of the metal ion requirements of the different gyrase reactions may provide useful mechanistic information.

Monitoring DNA supercoiling provides a convenient assay for gyrase activity since it is fairly simple and quick and is unique to gyrase. Section 5.2.2 has described experiments where a gyrase-DNA complex was formed in the presence of excess Mg^{2+} ions and then isolated *via* gel filtration into a buffer without Mg^{2+} ions. The ability of such complexes to catalyse DNA supercoiling with different metal-nucleotide complexes was then analysed. In the experiment of Fig. 5.5, the observation that, in addition to Mg-ATP, Ca-ATP, and Mn-ATP, Co-ATP was a substrate for supercoiling, was interpreted as evidence that the ATPase reaction of gyrase had a greater tolerance for metal ions than the supercoiling reaction. (This was confirmed for Cd^{2+} by experiments on the ATPase of the 43kDa fragment in Section 5.2.4.2 and discussed later). The interpretation of the experiments with $ATP_{\alpha}S$ and different metal ions was complicated by the fact that significant levels of metal ions were found to leak through the column in this experiment. Because the K_M^{app} for $ATP_{\alpha}S(Rp)$ is approximately 10-fold lower than for ATP, the Mg^{2+} leakage or exchange was more critical in this instance. Thus the results for $ATP_{\alpha}S(Rp)$ were not significant. However, the finding that $ATP_{\alpha}S(Sp)$ was more active with Mn^{2+} and Co^{2+} than with Mg^{2+} cannot be readily dismissed in terms of the the presence of contaminating Mg^{2+} ions since it has already been shown that Mg-$ATP_{\alpha}S(Sp)$ only poorly supports supercoiling. This result is difficult to fully interpret but is consistent with the metal ion binding to the sulphur atom on the α-phosphate.

Further application of spin-columns in isolating gyrase-DNA complexes in the absence of Mg^{2+} ions may be facilitated by the use of a radioisotope of Mg^{2+}. This would allow quantitation of the leakage of Mg^{2+} ions through the column.

In view of the problems with the spin-column approach to investigating reversal of stereospecificity with the ATP analogues and different metals, a more direct approach was taken by focussing on the ATPase of the 43kDa fragment. The characterisation of the hydrolysis of ATP, $ATP_{\alpha}S$ and $ATP_{\beta}S$ in the presence of Mg^{2+} is described in Section 5.2.4.1. As expected, the 43kDa protein exhibited the same stereospecificity towards the phosphorothioate ATP analogues as the intact gyrase tetramer. This provides further evidence that the 43kDa protein is a good model for the ATP binding site of intact gyrase. However, there were significant differences in the kinetics of hydrolysis of the ATP analogues with 43kDa and gyrase. Most dramatic was the differences between $ATP_{\alpha}S$(Rp) compared to ATP in the two proteins. With gyrase the difference was manifested in a lower K_M for $ATP_{\alpha}S$ and with the 43kDa protein the difference was expressed in both a lower K_M and a higher V_{max}. A simple model for the hydrolysis of ATP by the 43kDa protein has recently been suggested based on steady-state kinetics of ATP hydrolysis (as shown in Fig. 5.18) and a rate equation has been derived (Ali *et al.*, 1992). This mechanism shows many similarities to the proposed scheme for intact gyrase (Tamura *et al.*, 1992). For example both are thought to involve the association of ATP-binding domains prior to hydrolysis. However, in the 43kDa protein this association is intermolecular while in the full gyrase structure it is intramolecular since the A_2B_2 tetramer is believed not to dissociate during the reaction. The difference in the kinetics of the phosphorothioate ATP analogues compared to ATP in the two proteins (particularly the higher V_{max} value for $ATP_{\alpha}S$(Rp) compared to ATP with the 43kDa protein) may reflect this difference in the proposed mechanisms.

Since the simplest kinetic scheme for the 43 kDa protein ATPase (Fig. 5.18) involves dimerisation of two enzyme-substrate complexes it is not surprising that the kinetics deviate from the Michaelis-Menten model. Thus K_M values derived from plots of rate *versus* substrate concentration will not represent a dissociation constant of the enzyme

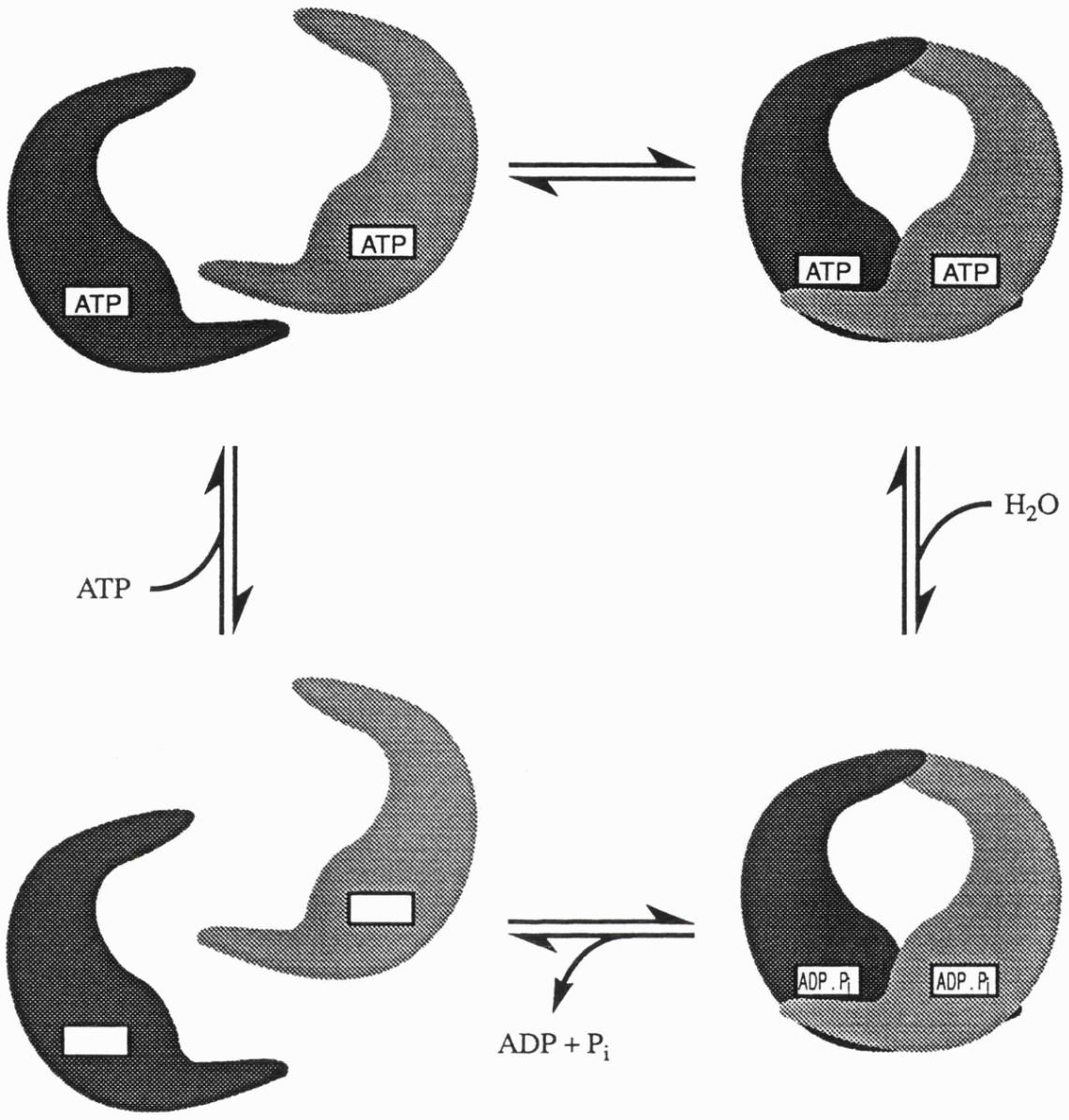

$$2E + 2S \underset{k_{-1}}{\overset{k_1}{\rightleftharpoons}} ES + ES \xrightarrow{k_2} E_2S_2 \xrightarrow{k_3} 2E + 2P$$

(E = enzyme; S = ATP; P = ADP)

Figure 5.18. A model for the ATPase reaction of the 43kDa protein. The model is based on that proposed by Ali *et al.* (1992). The protein binds ATP as a monomer and, once bound, ATP facilitates protein dimerisation. Hydrolysis of ATP can then occur followed by product release. Either the hydrolysis step or the product release step may facilitate dissociation of the protein dimer back into monomers. Also shown is simplest kinetic scheme for the 43kDa ATPase for which a rate equation has been derived algebraically and is currently being tested by computer fitting to experimental data (Ali *et al.*,1992).

substrate complex and it may be more useful to consider K_M values simply as the substrate concentration required to give half V_{max} ($S_{0.5}$).

In Section 5.2.4.2, the specificity of the 43kDa protein towards hard and soft metal ion complexes of ATP and the phosphorothioate ATP analogues was addressed. This analysis was complicated by the inhibitory effects of Cd^{2+} on the protein which made it necessary to perform experiments with only a low level of this metal ion in excess. This made it impossible to carry out a full kinetic analysis in the presence of excess Cd^{2+}. One approach to circumvent this problem was to use an excess of nucleotide calculated to complex a given proportion of metal ions and thus limit the proportion of free metal ions in solution. The results of such studies for ATP were presented in Fig. 5.13 and 5.14. These were interpreted in terms of free nucleotide, not complexed to a divalent metal, inhibiting the hydrolysis of the metal-ATP species. It is possible that the inhibiting species was a complex between ATP and the monovalent cation, K^+, since KCl was present in the reaction mixture and K-ATP has been found to be a substrate for myosin (Connolly and Eckstein, 1981; Seidel, 1969). Interestingly, the sigmoidal curves produced in the presence of free ATP are similar to the results of studies of ADP inhibition on the ATPase of gyrase and the 43kDa protein.

In view of the potential complication of free nucleotide inhibition, the hydrolysis of ATP and the thio-nucleotides with different Mg^{2+} and Cd^{2+} was measured at a single concentration of metal and nucleotide (see Table 5.2). For ATP, the rate in the presence of Cd^{2+} was only 2.4-fold slower than the rate in the presence of Mg^{2+}. For $ATP_{\alpha}S$(Rp) the discrimination was greater with a ratio of the Mg^{2+} rate over the Cd^{2+} rate of 35, and for $ATP_{\beta}S$(Rp) a ratio of 4.4 was obtained. No activity was observed for the Sp epimers of $ATP_{\alpha}S$ and $ATP_{\beta}S$ with either metal. Thus no reversal of stereospecificity was observed. If a more sensitive assay was used to monitor the hydrolysis reaction it may be possible to detect hydrolysis of the inactive epimers of

$ATP_{\alpha}S$ and $ATP_{\beta}S$ and thus observe any small increases in activity of the Sp epimers with Cd^{2+} compared to Mg^{2+}. For example it could be possible to detect a slow rate of hydrolysis if the reaction was allowed to progress for some time before measuring the amount of product formation by either HPLC or the fluorescent phosphate assay (used as a single point determination of the phosphate concentration). The current data indicate that no dramatic reversal of stereospecificity occurred. Given the mode of binding of ATP predicted from the crystallographic data, (see Fig. 4. 30), it may be the case that constraints imposed by the enzyme favour coordination of all metals to oxygen in the Rp epimers of $ATP_{\alpha}S$ and $ATP_{\beta}S$ with the sulphur atom occupying the exposed site unliganded to the metal. As discussed in Chapter 4, sulphur may be favoured in the non-coordinated positions of $ATP_{\alpha}S$ and $ATP_{\beta}S$ in view of the low apparent solvation of these sites in the enzyme. This would allow the Rp epimers of $ATP_{\alpha}S$ and $ATP_{\beta}S$ to assume the correct screw sense geometry with either Mg^{2+} or Cd^{2+}. Indeed, forced coordination of Cd^{2+} to oxygen (as in Cd-ATP) appears well tolerated, with the results in this chapter showing a drop in rate of hydrolysis of only 2.4-fold compared to Mg-ATP. In the case of the Sp epimers, it would be consistent with the crystal structure if the Cd-chelate was more active than the Mg-chelate.

The fact that the Sp epimers are very poor substrates for hydrolysis by gyrase and by the 43kDa protein suggested that they might prove to be good substrate analogues for crystallography of the 43kDa protein. It was anticipated that the information obtained from such crystals would be useful to confirm the protein structure obtained with ADPNP bound and also to give further insights into the metal-nucleotide configuration in these inactive ATP analogues. The results of the crystal trials were presented in 5.2.5 and Fig. 5.15. While crystals were obtained with ADPNP under a variety of conditions, no crystals were formed with the phosphorothioate ATP analogues. Many pieces of evidence point to why ADPNP supports the formation of crystals with the 43kDa protein. Firstly, it has been shown not to be hydrolysed by gyrase (Tamura *et al.*, 1992).

Secondly, it has a relatively low K_i of the order of 10^{-6}M, and thus, at the concentrations used in crystallography, the enzyme would be saturated. Thirdly, it has been found to have a very slow off-rate with gyrase (3.5×10^{-4} min^{-1}; Tamura *et al.*, 1992) and also with the 43kDa protein (J. Ali, personal communication). Thus it appears that ADPNP stabilises the 43kDa protein in a dimerised form of restricted conformational mobility amenable to crystallisation. The failure of the phosphorothioate analogues to support crystals suggests that this conformation is not stabilised sufficiently. This may be because they are hydrolysed (albeit slowly) or because they do not bind sufficiently tightly to the enzyme and a mixture of free enzyme and enzyme bound to nucleotide is present. If the ATP analogues stabilise a different conformation, screening of further crystallography conditions may prove fruitful.

The recent observation of crystals with the 43 kDa protein in the presence of $ATP_{\alpha}S$ (Sp) obtained by the ammonium hydroxide treatment is subject to several qualifications. Firstly, the wells were originally set up on 25/5/91, over a year before the crystals were noticed. Thus desulphurisation of the ATP analogue may well have occurred and the nature of any nucleotide bound to the protein must be uncertain. Nevertheless, since the only crystals of the 43 kDa protein obtained to date are with ADPNP bound, the crystals with $ATP_{\alpha}S$ (Sp) are interesting regardless of whether they represent a protein-nucleotide complex or just the apoprotein. It will be interesting to see whether the crystals diffract to a reasonable resolution to allow structure determination.

5.4. SUMMARY

The divalent metal ion specificity of the DNA supercoiling, DNA relaxation, and DNA cleavage reactions of gyrase have been characterised. It was found that the cleavage reaction exhibited a greater tolerance towards different metal ions than the relaxation and supercoiling reactions. This probably represents the greater complexity of the latter processes.

In an attempt to confirm the predictions from Chapter 4 on the active metal-ATP complex handled by gyrase, reversal of stereoselectivity with the diastereoisomers of $ATP_{\alpha}S$ and $ATP_{\beta}S$ in the presence of hard and soft Lewis acid metals was investigated. Experiments were focussed on the ATPase of the 43kDa protein as a simple model. This protein showed the same stereospecificity towards $ATP_{\alpha}S$ and $ATP_{\beta}S$, in the presence of Mg^{2+}, as intact gyrase (Chapter 4) with the Rp epimers being the preferred substrates. However, there were significant differences in their kinetics of hydrolysis compared to ATP with the 43kDa fragment and intact gyrase which may reflect differences in the kinetic mechanisms of the two proteins.

Cd^{2+} ions at levels of 0.5mM and above (at a protein concentration of 15μM) were found to be inhibitory. In experiments with excess nucleotide over metal, free ATP was found to inhibit the hydrolysis of metal-bound nucleotides in a non-Michaelian fashion similar to the inhibition seen with ADP. This limited the possibility of investigating reversal of stereoselectivity to single concentrations of metals and nucleotides. Such experiments showed that the Rp epimers of $ATP_{\alpha}S$ and $ATP_{\beta}S$ were the preferred substrates with either Mg^{2+} or Cd^{2+}. No activity was detected with the Sp epimers with either metal. Thus, any reversal of stereoselectivity may have gone undetected. It would therefore be interesting to probe the hydrolysis of the Sp-epimers with a more sensitive assay.

The ability of the inactive Sp epimers of $ATP_{\alpha}S$ and $ATP_{\beta}S$ to substitute for ADPNP in supporting the formation of crystals of the 43kDa protein was investigated. Under most of the conditions screened no crystals were formed although very recently crystals in the presence of $ATP_{\alpha}S$ (Sp) were obtained.

Chapter 6

Energy Transduction in DNA Gyrase: A Thermodynamic Limit to the Extent of DNA Supercoiling

6.1. INTRODUCTION

It has been suggested that the extent of DNA supercoiling achievable by gyrase in pBR322 is limited by the free energy of hydrolysis of ATP (Bates and Maxwell, 1989; Maxwell and Gellert, 1986; Reece and Maxwell, 1991b). This stems from the fact that there is an approximate equivalence between the estimated free energy required for the final two superhelical turns and the energy available from the hydrolysis of two ATP's. Specifically for pBR322 it has been found that the maximum specific linking difference (SLD) achievable by gyrase is -0.11 (Bates and Maxwell, 1989; Westerhoff *et al.*, 1988) which corresponds to a free energy for the final round of supercoiling of approximately 116 kJ/mol. This is similar to the free energy of hydrolysis of two ATP's which has been estimated to be approximately -120 kJ/mol (Simmons and Hill, 1976).

Experiments on gyrase-catalysed supercoiling of small DNA circles have determined that the lower limit to the size of circle that can be supercoiled is 174 bp (Bates and Maxwell, 1989). Moreover, a similar limit for the SLD as pBR322 of -0.11 was observed. Two explanations for the limit to the size of DNA circle that could be supercoiled were suggested: either, the introduction of two negative supercoils into circles below this limit would produce a SLD that required more free energy than that available from ATP hydrolysis (a thermodynamic limit), or, the size of smaller circles was insufficient to allow the necessary complexation and conformational changes associated with the catalytic cycle (a steric limit). It was shown that although gyrase could not supercoil circles smaller than 174 bp, it could relax circles as small as 116 bp when they were positively supercoiled in a nucleotide-dependent reaction mechanistically analogous to negative supercoiling. This clearly suggested that the steric limit was unlikely and pointed towards the thermodynamic explanation although the calculated free energy required for the supercoiling of the small circles is considerably greater than that available from the hydrolysis of two ATP's. It was suggested that this apparent energetic paradox could be due to uncertainties in the energetic calculations for small circles.

It has been shown from displacements of several kinase equilibria that the free energy available from the hydrolysis of $ATP_{\beta}S$ is approximately 10.5 kJ/mol greater than ATP (Jaffe and Cohn, 1980; Lee and O'Sullivan, 1985; Lerman and Cohn, 1980). Accordingly, $ATP_{\beta}S$ has been used to probe the energy coupling in sarcoplasmic reticulum vesicles (Pintado *et al.*, 1982). This system couples the hydrolysis of ATP to the transport of Ca^{2+} across its membrane producing a gradient similar to that expected from the free energy of hydrolysis of ATP (see also Section 1.3). It was found that the Ca^{2+} gradients obtained with either ATP or $ATP_{\beta}S$ were the same and it was thus concluded that there was not a 1:1 correspondence between the free energy of the hydrolytic reaction and the free energy associated with the Ca^{2+} gradient.

In this work, it was proposed to investigate the energy coupling in gyrase with ATP and $ATP_{\beta}S$ by comparing the extent of supercoiling achievable with each nucleotide. In addition, the extent of supercoiling with $ATP_{\alpha}S$ was also investigated for further comparison.

6.2. RESULTS

6.2.1. Extent of supercoiling with ATP, $ATP_{\beta}S$ and $ATP_{\alpha}S$.

In Chapter 4 it was shown that the active epimer of $ATP_{\beta}S$ was a very poor substrate for DNA supercoiling despite being reasonably efficiently hydrolysed. Fig 4.15. showed that, at a gyrase concentration of 25nM, only 8 negative supercoils were introduced into pBR322 after 8 hours. This lack of activity made it impossible to measure the extent of supercoiling achievable with this analogue. As part of the same study, however, the extent of supercoiling with ATP and $ATP_{\alpha}S$ was compared. Fig. 6.1. shows that, with a gyrase concentration of 2nM, the supercoiling reaction appeared to reach a maximum by 8 hours after which no further change in the DNA topology was seen. Interestingly, $ATP_{\alpha}S$ appeared to be able to support one additional superhelical turn as compared to ATP. Comparisons with DNA standards, whose ΔLk's were known to ± 1, revealed that the ΔLk with ATP was -(n) and the ΔLk with $ATP_{\alpha}S$ was -(n+1) where $n = 46 \pm 1$; i.e. the ΔLk with ATP was -46 and the ΔLk with $ATP_{\alpha}S$ was -47. The values with ATP are similar to those previously reported (Bates and Maxwell, 1989; Westerhoff *et al.*, 1988) and correspond to a specific linking difference (SLD) of -0.11. Note that in all the extent of supercoiling experiments, the gyrase to DNA ratio was approximately one so that, on average, only one molecule of gyrase was bound to each DNA molecule. At higher ratios where many gyrase molecules are bound to each plasmid, the level of supercoiling may be limited by the lack of conformational freedom imposed by the protein-DNA interactions. For example, the positive wrapping of the DNA around the protein may prevent the full potential extent of supercoiling from being realised when many copies of gyrase are bound to each plasmid.

Fig. 6.2. shows another comparison of the extent of supercoiling obtained with ATP and $ATP_{\alpha}S$ using a high activity preparation of gyrase (gift of J. Tamura, NIH, Bethesda, Maryland, USA). Again $ATP_{\alpha}S$ supported a greater extent of supercoiling than ATP giving the same values for the ΔLk's as those above. This figure also shows that

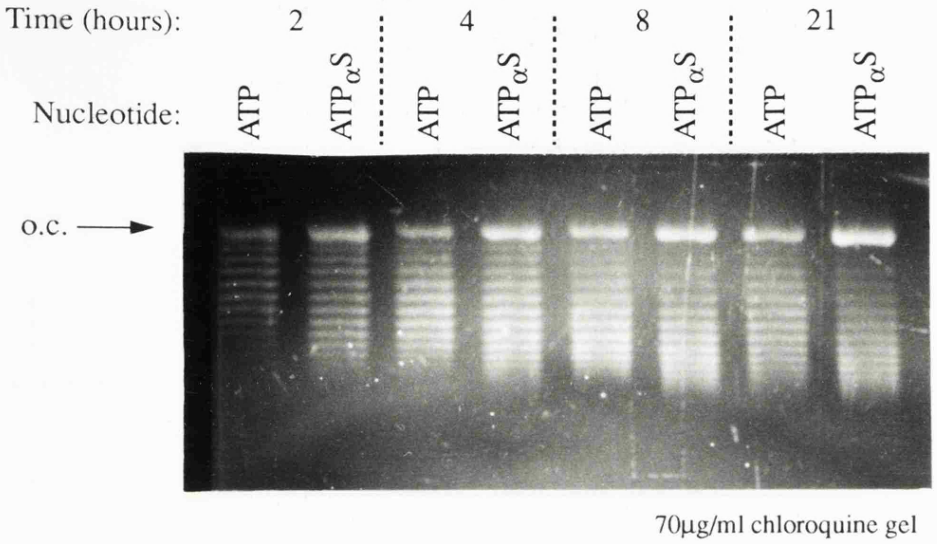

Figure 6.1. Extent of supercoiling with ATP and $ATP_{\alpha}S$(Rp). Gyrase concentration was 2nM; DNA concentration was 3.4nM; nucleotide concentration was 1mM. The figure shows the later time-points of the supercoiling reactions where the specific linking difference of the DNA is approaching a maximum. At apparent equilibrium, the most supercoiled topoisomer corresponded to a ΔLk of -46 in the ATP reaction, and -47 in the $ATP_{\alpha}S$ reaction.

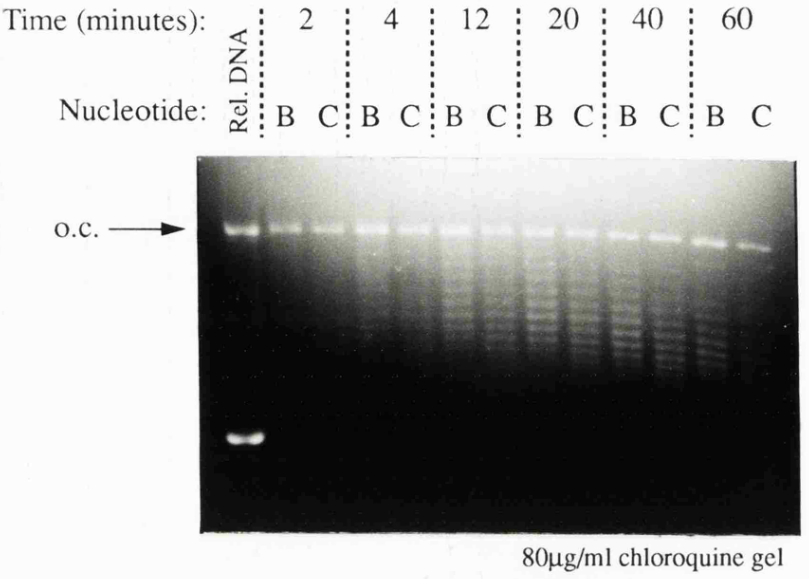

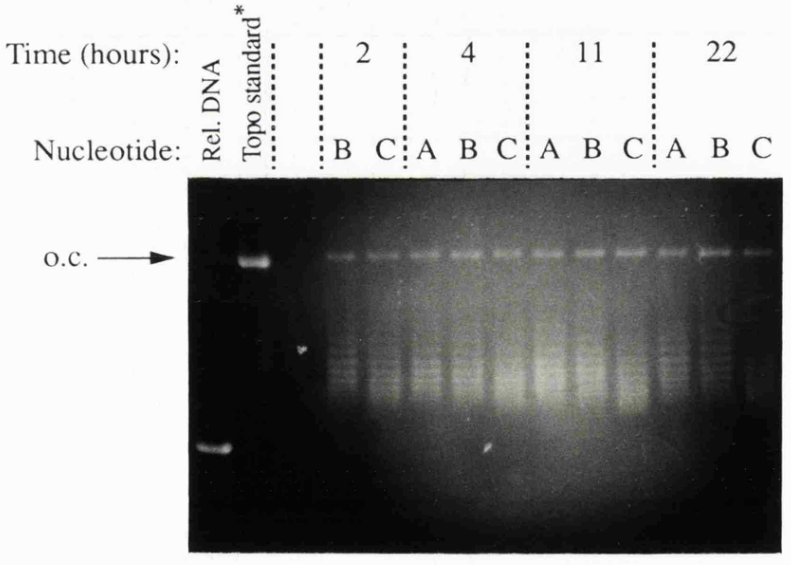

Figure 6.2. Extent of supercoiling with ATP and $ATP_{\alpha}S(Rp)$ with high activity gyrase. Enzyme concentration was 5nM; nucleotide concentration was 1mM. A: ATP(Na salt); B: ATP(triethylammonium salt); C: $ATP_{\alpha}S$(triethylammonium salt)

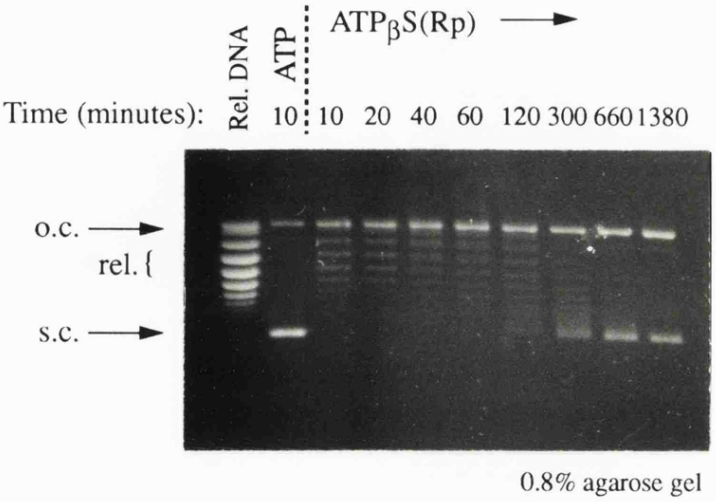

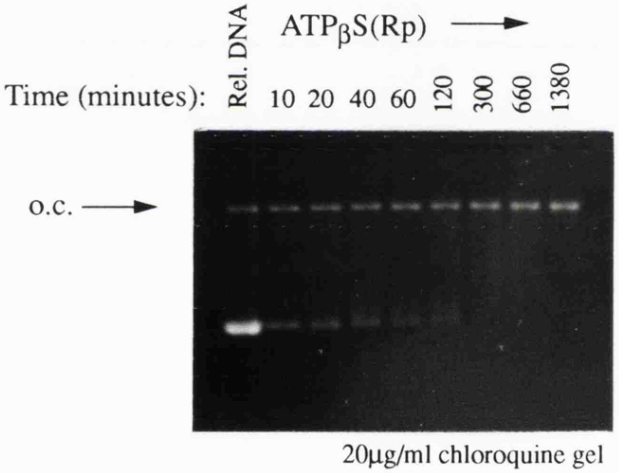

Figure 6.3. Time course of supercoiling with $ATP\beta S(Rp)$ with high activity gyrase. Nucleotide concentration was 1mM; gyrase concentration was 5nM.

different salts of ATP behaved identically with gyrase. It can be seen that the rate of DNA supercoiling became much slower near to the supercoiling limit; after 12 mins. a ΔLk of approximately -42 was achieved while the last 4 supercoils introduced required at least 120 mins.

If the limit to the extent of supercoiling is thermodynamic, the observations on the extent of supercoiling with $ATP_{\alpha}S$ suggest that this nucleotide, like $ATP_{\beta}S$, may have a greater free energy of hydrolysis than ATP. With the availability of the high activity gyrase preparation, a further experiment was performed with $ATP_{\beta}S$ in an attempt to confirm the dependence of the extent of supercoiling on the free energy of nucleotide hydrolysis. The results are presented in Fig. 6.3. which shows that, even with the active enzyme preparation, the level of supercoiling did not reach a limit after 23 hours and the ΔLk was only about -20. Longer incubations were also attempted (up to 72 hours) but the level of nicking of the DNA in these experiments was unacceptably high.

6.2.2. Theoretical estimation of the free energy differences of hydrolysis of ATP, $ATP_{\alpha}S$ and $ATP_{\beta}S$.

If the assumption is made that the ionisation of the different nucleotides is a measure of the relative stabilities of these species, an estimate of the free energies for hydrolysis of the various nucleotides on the basis of differences in their pK_a's can be made. Implicit in this approach is the assumption that the difference in the pK_a's arises principally from the difference in thermodynamic stabilities of the fully ionised nucleoside polyphosphates. Although this may seem to be an oversimplification, the strong electrostatic interaction between the adjacent negative charges in the *gem*-dianion which is generated in the last ionisation together with the likely strong interaction of the fully ionised species with solvent may be dominant factors that justify this assumption.

This approach can be applied to the case of $ATP_{\beta}S$ for which the free energy of hydrolysis in relation to that of ATP is known. Consider the thermodynamic cycle shown below:

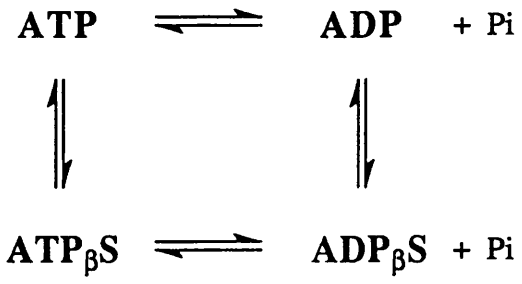

(eqn. 6.1)

The hypothetical equilibria between ATP and $ATP_{\beta}S$, and between ADP and $ADP_{\beta}S$, represent the relative stabilities of these species to be estimated from the differences in pK_a's. These pK_a's are given in Table 6.1 below.

Table 6.1. pK_a values for adenine nucleotides and their Mg complexes.

Nucleotide	**pK_a's**	
	(Values from ref.[a])	(Values from ref.[b])
ATP	6.63	6.7
ADP	6.66	6.8
MgATP	4.72	5.3
MgADP	5.46	-
$ATP_{\alpha}S$	6.65	-
$ADP_{\alpha}S$	6.77	-
$MgATP_{\alpha}S$	5.12	-
$MgADP_{\alpha}S$	5.27	-
$ATP_{\beta}S$	6.64	6.5
$ADP_{\beta}S$	-	5.2
$MgATP_{\beta}S$	5.05	-
$MgADP_{\beta}S$	-	-

[a]Determined by Pecoraro *et al* (1984) from ^{31}P-NMR. Values refer to the Sp epimer of $ATP_{\alpha}S$ and the Rp epimer of $ATP_{\beta}S$.

[b]Determined by Jaffe and Cohn (1978a) from ^{31}P-NMR. Values refer to the Sp epimer of $ATP_{\beta}S$.

Within experimental error, the ΔpK_a for ATP and $ATP_\beta S$ is zero whereas for ADP and $ADP_\beta S$ the ΔpK_a is 1.6. This can be converted to an energy term using Eqn 6.2 below:

$$\Delta G = -RT \ln \frac{K_{thio}}{K_{oxy}} \qquad \text{(eqn. 6.2)}$$

where (K_{thio}/K_{oxy}) is the antilog_{10} of the ΔpK_a. Because of the nature of a thermodynamic cycle, the ratio of the equilibrium constants for these two hypothetical equilibria must be the same as the ratio of equilibrium constants for the two hydrolysis reactions. The free energy difference calculated in this way is 9.3 kJ/mol which compares favourably with the published measured value of 10.5 kJ/mol (Lerman and Cohn, 1980). If valid, this approach would imply that the more favourable free energy of hydrolysis of $ATP_\beta S$ arises almost completely from the greater thermodynamic stability of $ADP_\beta S$ as compared to ADP, which seems intuitively correct.

Applying this approach to $ATP_\alpha S$, the following hypothetical thermodynamic cycle can be set up:

$$\begin{array}{ccc} \mathbf{MgATP} & \rightleftharpoons & \mathbf{MgADP} + \mathrm{Pi} \\ \Vert\downarrow\uparrow\Vert & & \Vert\downarrow\uparrow\Vert \\ \mathbf{MgATP_\alpha S} & \rightleftharpoons & \mathbf{MgADP_\alpha S} + \mathrm{Pi} \end{array}$$

(eqn. 6.3).

From the pK_a values shown in Table 1, it can be seen that ATP and $ATP_\alpha S$ have pK_a's that are the same within experimental error and that ADP has a slightly lower pK_a than $ADP_\alpha S$. This would lead to the conclusion that, if anything, ATP should have a marginally greater free energy of hydrolysis than $ATP_\alpha S$. However, in reactions with gyrase there is always an excess of Mg^{2+} ions present at a concentration such that >95% of the nucleotides are complexed. The correct pK_a's to use are therefore those for the

nucleotide/Mg complexes. From Table 6.1, the ΔpK_a for $MgADP_{\alpha}S$ and MgADP is 0.19, with the thiophosphate being more stable. For MgATP and $MgATP_{\alpha}S$, the ΔpK_a is 0.40 but this time the thiophosphate is the least stable. Combining these ΔpK_a's and converting to a free energy term using eqn. 2 gives a value of 3.4 kJ/mol as an upper estimate for the difference in free energy of hydrolysis of ATP and $ATP_{\alpha}S$. Since the higher pK_a of $MgATP_{\alpha}S$ is the major source of the overall ΔpK_a, it would appear that the more favourable free energy of hydrolysis of $MgATP_{\alpha}S$ is likely to arise from the relative destabilisation of the $MgATP_{\alpha}S$ with respect to MgATP.

Unfortunately, an analysis of the free energy of $MgATP_{\beta}S$ by this approach could not be done since the pK_a for $MgADP_{\beta}S$ has not been published. However in this case the ΔpK_a is much larger and the effects of Mg will presumably be less significant.

6.2.3. Measurement of the free energy differences of hydrolysis between ATP, $ATP_{\alpha}S$(Rp) and $ATP_{\beta}S$(Rp) by displacement of the equilibrium in the arginine kinase reaction.

It has been reported that $ATP_{\alpha}S$(Sp) displaces the equilibrium of the reaction catalysed by phosphomevalonate kinase by a factor of approximately 2, compared to ATP, in favour of the formation of $ADP_{\alpha}S$ and mevalonate 5-diphosphate (Lee and O'Sullivan, 1985). This would imply that, under the conditions of this experiment (9.9mM ATP, 12mM Mg^{2+}, 9.8mM phosphomevalonate (PM) for the ATP experiment; 6mM $ATP_{\alpha}S$(Sp) and 6mM PM for the $ATP_{\alpha}S$ experiment), $ATP_{\alpha}S$(Sp) has a greater free energy of hydrolysis than ATP of approximately 1.7 kJ/mol. These conditions differ considerably from those used in the gyrase supercoiling assays (where nucleotide concentration was 1mM, Mg^{2+} ion concentration was 5mM, and the Rp epimer of $ATP_{\alpha}S$ was used). In view of these differences and the relatively small energy difference between ATP and $ATP_{\alpha}S$ suggested from the supercoiling results (see Section 6.3 and Table 6.3) together with the uncertainties concerning the assumptions inherent in the theoretical free energy

calculations above, it was decided to measure the energy difference directly. The method chosen was to assess the displacement of the equilibrium between the various nucleotides and arginine/phosphoarginine and thus gauge the difference in free energy of hydrolysis between ATP and $ATP_{\alpha}S$. The arginine kinase reaction was particularly suitable because the equilibrium constant is poised near unity thus facilitating the measurement of equilibrium concentrations of components (Lerman and Cohn, 1980). In addition, arginine kinase exhibits the same stereoselectivity as gyrase towards $ATP_{\alpha}S$ and $ATP_{\beta}S$, preferring the Rp epimers (Cohn *et al.*, 1982).

In the original measurements of the free energy differences between ATP and $ATP_{\beta}S$, ^{31}P-NMR was used to determine equilibrium concentrations of nucleotides. In the work described here an HPLC method was used which had the advantage of greater sensitivity which was important in view of the small energy differences anticipated. This greater sensitivity also allowed the equilibria to be measured under conditions analogous to those used for the supercoiling reaction (1mM nucleotide; 5mM Mg^{2+}). The method involved allowing the equilibrium between nucleoside di- and triphosphates and phosphoarginine and arginine to be attained and then quenching the reaction before analysing the relative concentrations of the nucleotides by reverse phase HPLC. Thus it was imperative to completely stop the reaction before the HPLC analysis and various ways of achieving this were investigated. The obvious method was to treat with EDTA and extract the protein with chloroform. However, ADP has been found to be significantly soluble in chloroform (Lerman and Cohn, 1980) and so this method was inappropriate. In addition, control experiments indicated that the reaction was not stopped by the addition of 200mM EDTA to a reaction containing 30mM nucleotide. Further control experiments investigated the possibility of stopping reactions by heat denaturation of the enzyme. However, these showed that the conditions used (heating at 100°C for 2min) caused significant nucleotide hydrolysis and could therefore not be used. The best method was found to be denaturation of the enzyme with the detergent, SDS, followed by treatment

with proteinase K. The proteinase treatment was found to give a much flatter base line in chromatograms and also ensured that no active arginine kinase remained. The noisier chromatograms obtained without proteinase K were presumably due to protein binding to the column. A control experiment, with just ATP and proteinase K, ensured that the proteinase sample was free of any contaminating ATPase.

As a final check that the conditions described above did not displace the equilibrium, identical reactions were analysed by both the HPLC method and a ^{31}P-NMR method. Reactions consisted of 30mM ATP and 30mM arginine as described in Section 2.30. A typical NMR trace is shown in Fig. 6.4 together with the results for the equilibrium concentrations of ADP and ATP obtained from the HPLC analysis. It can be seen that the two approaches gave closely similar results which confirmed the validity of the HPLC method. In addition, experiments with ATP as the Na salt or the triethylammonium salt gave identical equilibria within experimental error (data not shown).

In all equilibrium experiments, 0.1mM Ap_5A was included to inhibit adenylate kinase that was present in the arginine kinase preparation as identified by the formation of significant levels of AMP in reactions without Ap_5A. This also had the advantage of acting as an internal standard on the total nucleotide concentrations in the reactions.

The results for equilibria with ATP, $ATP_\alpha S$ and $ATP_\beta S$ are shown in Table 6.2 below along with the calculated differences in free energy of hydrolysis.

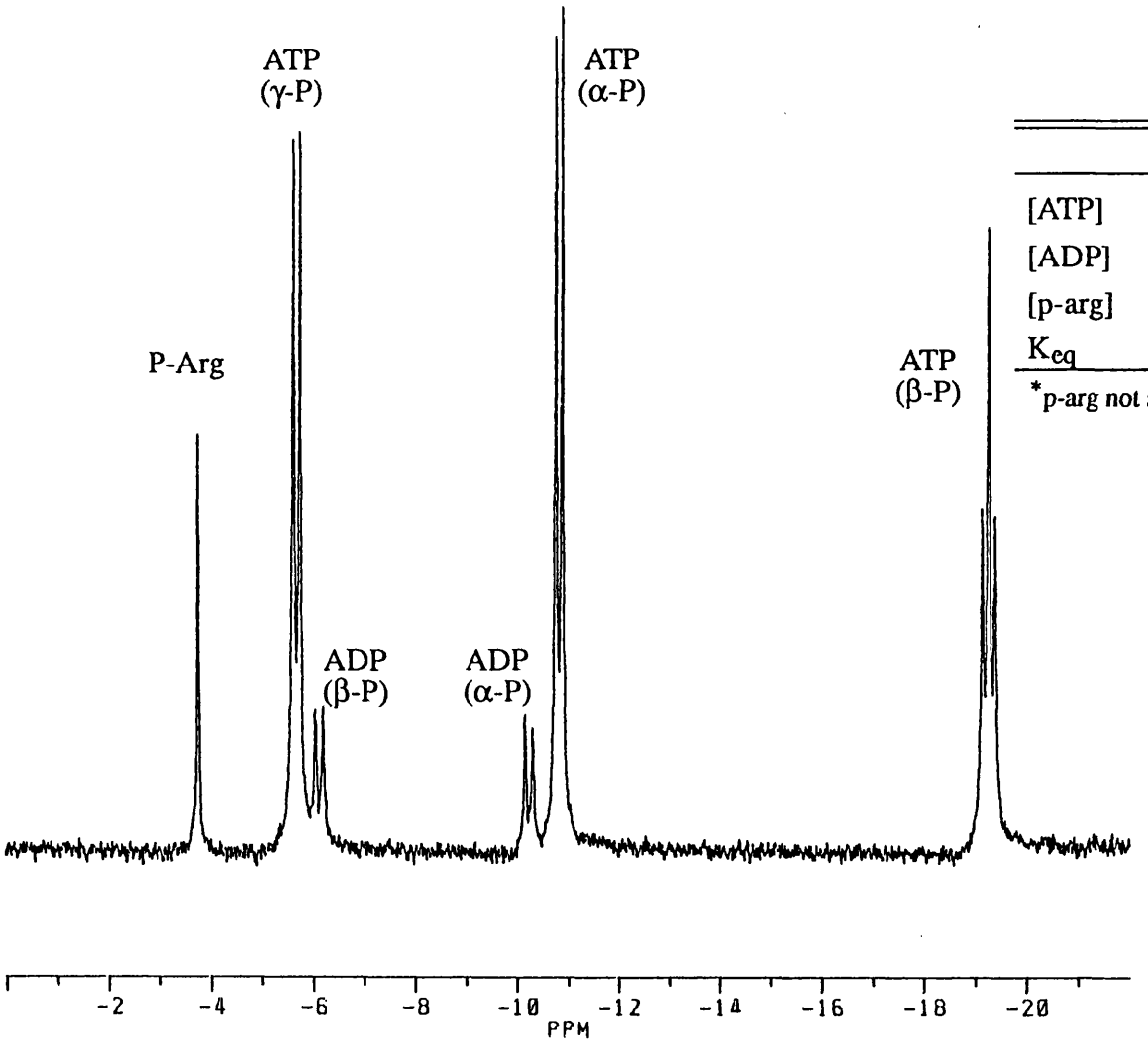

	^{31}P-NMR	HPLC
[ATP]	24.25mM	24.50mM
[ADP]	5.75mM	5.50mM
[p-arg]	5.75mM	N/A*
K_{eq}	0.050	0.056

*p-arg not seen in HPLC.

Figure 6.4. ^{31}P-NMR spectrum of the ATP-ADP equilibrium with arginine kinase. Also shown is a table of the equilibrium concentrations as determined by the NMR and HPLC methods. Note that the pH was 7.35.

Table 6.2. Differences in the free energy of hydrolysis of the ATP analogues measured at pH 8.0.

Nucleotide	Equilibrium concs. (mM)		Apparent	K_{thio}/K_{oxy}	$\Delta\Delta G_{thio-oxy}$
	After 30min.	After 120min.	K_{eq}*		(kJ/mol)
ATP	0.668	0.665	0.252	-	-
ADP	0.332	0.335			
$ATP_{\alpha}S$	0.623	0.625	0.363	1.44	0.92
$ADP_{\alpha}S$	0.377	0.375			
$ATP_{\beta}S$	0.151	0.168	27.76	110	11.8
$ADP_{\beta}S$	0.849	0.832			

*The equilibrium constants K_{oxy} and K_{thio} reported here are apparent values and are not equal to the thermodynamic equilibrium constants because the hydrogen ion released in the reaction has been neglected. (Since the pH's were the same for all the reactions, however, this does not affect ratios of K_{oxy} and K_{thio}).

It should be noted that the results in the above table were obtained at pH 8.0 while the control experiments in Fig. 6.4 were performed at pH 7.35. The apparent equilibrium constant is highly pH dependent as shown in the equation below:

$$K_{eq} = \frac{[MgADP][p\text{-}arg][H^+]}{[MgATP][arg]} = K_{eq}^{app}[H^+] \qquad \text{(eqn. 6.4)}$$

Extrapolating the value of K_{oxy}, obtained at pH 7.35, to pH 8.0 gives a value of 0.237. This compares fairly closely with the value of 0.252 for K_{oxy} measured at pH 8.0 shown in the above table. It has been shown that equilibrium constants for creatine kinase vary considerably with differing concentrations of free Mg^{2+} ions (Lawson and Veech, 1979). The close parity in the values of K_{oxy} described above, which were measured at quite different concentrations of free Mg^{2+} ions, suggests that within this range of free Mg^{2+} ions, K_{oxy} is largely unaffected. Previous studies have determined values of K_{oxy} for

arginine kinase at pH 8.0 and 30°C of 0.17, 0.31, and 0.46 (Lerman and Cohn, 1980; Smith and Morrison, 1969; Uhr *et al.*, 1966) respectively. While it is hard to compare these constants directly, in view of differences in ionic strength, Mg^{2+} and substrate concentrations, and solvent (D_2O as opposed to H_2O in the data of Lerman and Cohn, 1980), the value of K_{oxy} determined here is compatible with the previously published values.

It is clear from Table 6.2 that the equilibrium was displaced markedly in favour of the nucleoside diphosphate and phosphoarginine in the $ATP_{\beta}S$ reaction as compared to ATP. The difference in the free energy of hydrolysis for $ATP_{\beta}S$ over ATP calculated from this displacement was found to be -11.8 kJ/mol. This value is in reasonable agreement with the value of -10.5 kJ/mol obtained by Lerman and Cohn (1980). It is also evident from Table 6.2 that $ATP_{\alpha}S$ was found to have a greater free energy of hydrolysis than ATP of 0.92 kJ/mol. This value is rather less than the 3.4 kJ/mol predicted from the argument based on pK_a's in Section 6.2.2, although it was pointed out that this approach represented an upper estimate since not all of the ΔpK_a may be attributable to the difference in thermodynamic stabilities of the fully ionised species.

6.3. DISCUSSION

The thermodynamics of supercoiling have been investigated extensively either by determinations of the binding affinity of ethidium bromide to various topoisomers (Bauer and Vinograd, 1970; Hsieh and Wang, 1975) or by analysis of the Gaussian distribution of topoisomers as visualised on an agarose gel (Depew and Wang, 1975; Dugaiczyk *et al.*, 1975; Keller, 1975; Keller and Wendel, 1974; Pulleyblank *et al.*, 1975). It has been found that the supercoiling of DNA is an elastic process with the free energy of supercoiling being proportional to the square of the linking difference as shown in equation 6.5 below:

$$\Delta G_{sc} = K.\Delta Lk^2 \qquad \text{(eqn. 6.5)}$$

K is the elastic constant of the DNA. This equation can be normalised to give the free energy of supercoiling per bp by dividing through by N (the number of bp in the DNA circle) to give Eqn 6.6:

$$\frac{\Delta G_{sc}}{N} = NK\left(\frac{\Delta Lk}{N}\right)^2 \qquad \text{(eqn.6.6)}$$

In Eqn. 6.6, NK has been shown to be a constant largely independent of the size of the DNA circle in molecules above approximately 2kb (Horowitz and Wang, 1984; Shore and Baldwin, 1983b). The value for pBR322 was determined by Horowitz and Wang (1984) to be 1130RT and this value has been used in the following calculations. Table 6.3 shows the calculated free energy of supercoiling of various topoisomers of pBR322 compared to relaxed DNA (see also Fig. 6.5). Also included in the table are the free energies required to perform various reductions in linking number in steps of two at high levels of supercoiling. It should be pointed out that the free energy of supercoiling calculations are based on experiments with DNA of relatively low extents of supercoiling (SLD's up to approximately -0.06). While these results are often extrapolated to higher

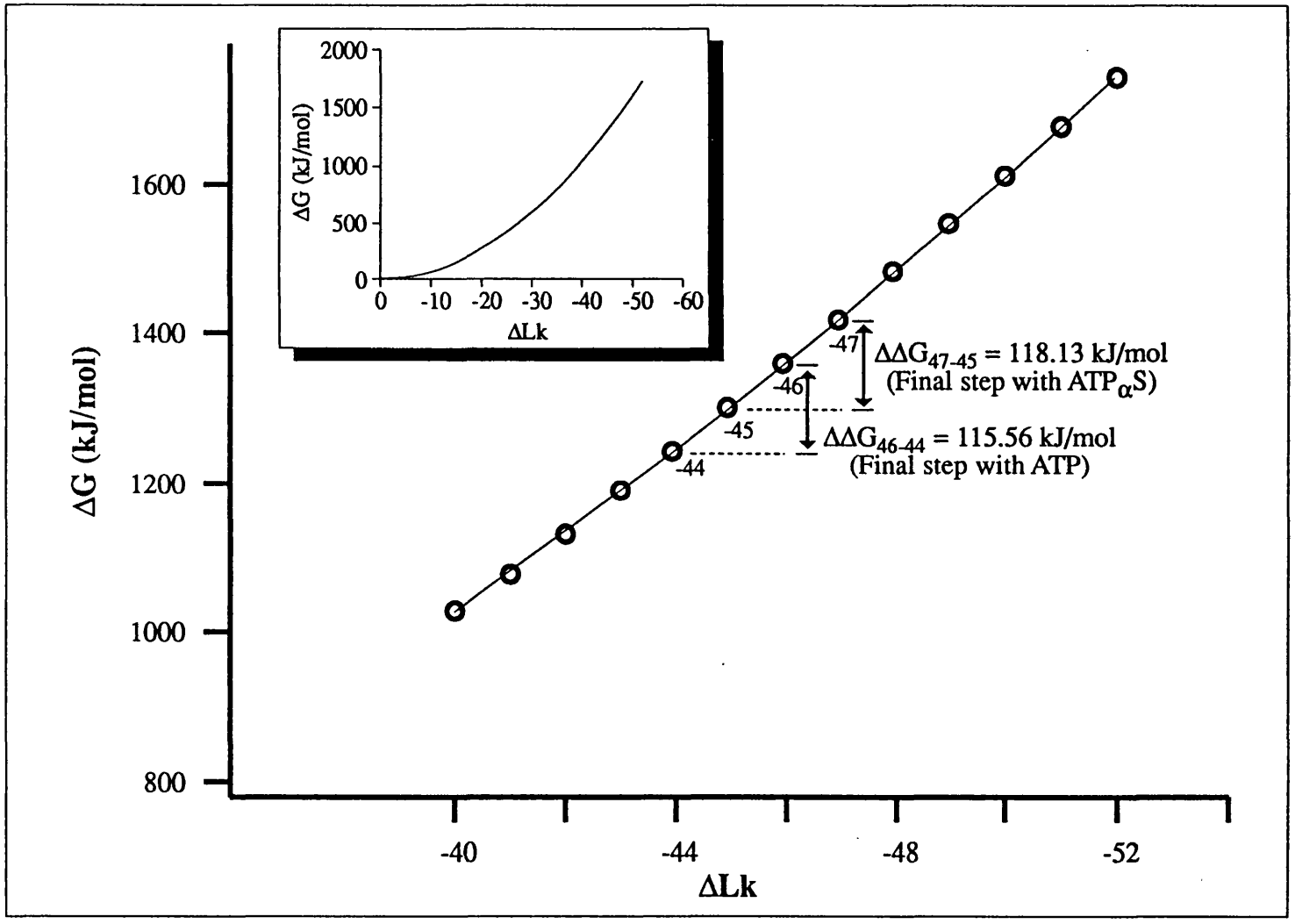

Figure 6.5. Theoretical variation of the free energy of supercoiling (ΔG) with the change in linking number (ΔLk) in pBR322 based on the data of Horowitz and Wang (1984). The main graph shows the free energy at high ΔLk's, while inset, the energy profile over a more extensive range of Lk's is shown. The free energy required to go from ΔLk = -44 to ΔLk = -46, and ΔLk = -45 to ΔLk = -47 is highlighted.

extents of supercoiling, this assumes that the quadratic relationship between the free energy of supercoiling and the linking difference is still valid which may not be the case.

Table 6.3. Free energies associated with various linking differences in pBR322[a]

SLD	ΔLk[b]	ΔG (kJ/mol)	Step in ΔLK	ΔΔG(kJ/mol)
-0.097	-40	1027.21		
-0.100	-41	1079.21		
-0.102	-42	1132.50	-40 to -42	105.29
-0.104	-43	1187.07	-41 to -43	107.56
-0.107	-44	1242.93	-42 to -44	110.43
-0.109	-45	1300.07	-43 to -45	112.99
-0.112	-46	1358.49	-44 to -46	115.56
-0.114	-47	1418.19	-45 to -47	118.13
-0.116	-48	1479.19	-46 to -48	120.70
-0.119	-49	1541.46	-47 to -49	123.31
-0.121	-50	1605.02	-48 to -50	125.83
-0.124	-51	1669.86	-49 to -51	128.40
-0.126	-52	1735.99	-50 to -52	130.97

[a]Values in the above table calculated from the data of Horowitz and Wang (1984).

[b]ΔLk values approximated to the nearest whole number.

It has been shown in Section 6.2.1 that $ATP_{\alpha}S$(Rp) consistently supported a greater extent of supercoiling than ATP. Specifically, it appears that one extra supercoil was introduced with $ATP_{\alpha}S$ giving a ΔLk of -47 compared to -46 with ATP. At first, it may seem paradoxical that the topoisomer with the greatest linking difference for the ATP and $ATP_{\alpha}S$ reactions differed in Lk by one when gyrase catalyses topoisomerisation in steps of two. However, this is readily explained when it is considered that the relaxed DNA starting material (prepared by relaxation of native supercoiled DNA with topoisomerase I) consisted of a Gaussian distribution of topoisomers differing in Lk by one. The ΔLk's produced with ATP and $ATP_{\alpha}S$ correspond to a final step in DNA supercoiling of -44 to -46, and -45 to -47 respectively. From Table 6.3 and Fig. 6.5, it can be seen that the free energy required for the final step of supercoiling is 115.56 kJ/mol in the ATP reaction

and 118.13 kJ/mol in the $ATP_{\alpha}S$ reaction. Thus the extra free energy required for the $ATP_{\alpha}S$ reaction was 2.57 kJ/mol. This value appears to be generally correct for the energy difference between any two consecutive rounds of supercoiling as shown in Table 6.3 and proven as follows. Consider the reactions involved in achieving one additional topoisomer in consecutive rounds of supercoiling (i.e. ΔLk of n to n - 2, or n -1 to n - 3). The free energy for these gyrase reactions are:

$$\Delta G_{n \text{ to } (n-2)} = K\,[(n-2)^2 - n^2] \qquad \text{(eqn. 6.7)}$$

$$\Delta G_{(n-1) \text{ to } (n-3)} = K\,[(n-3)^2 - (n-1)^2] \qquad \text{(eqn. 6.8)}$$

The excess free energy of Eqn 6.8 over Eqn. 6.7 is therefore given by:

$$\Delta\Delta G = K\,\{[(n-3)^2 - (n-1)^2] - [(n-2)^2 - n^2]\}$$

$$= 4K$$

As previously mentioned, NK for pBR322 has been found to be 1130 RT (Horowitz and Wang, 1984), which gives:

$$\Delta\Delta G = \frac{4 \text{ X } 1130 \text{ RT}}{4361} = 2.57 \text{ kJ/mol (at 25°C).}$$

Thus this value remains unaltered when the uncertainty in the quantitation of the absolute ΔLk's with ATP and $ATP_{\alpha}S$ (Section 6.2.1) is taken into account. In Section 6.2.3 it was found that an extra 0.92 kJ/mol was available from the hydrolysis of $ATP_{\alpha}S$ compared with ATP. This compares with a value of 1.7 kJ/mol derived from the work of Lee and O'Sullivan (1985). Since two ATP's are thought to be hydrolysed per round of supercoiling (see Section 4.3 and references cited therein), the extra free energy from the hydrolysis of $ATP_{\alpha}S$ by gyrase should be between 1.8 kJ/mol (this study) and 3.4 kJ/mol (Lee and O'Sullivan, 1985); the difference between these values may be due to the

different conditions used and the fact that opposite diastereoisomers were used (Rp *versus* Sp respectively). Significantly, these values are close to the predicted free energy required of 2.6 kJ/mol for the extra round of supercoiling that is observed. Thus the close parity between the extra free energy available from the hydrolysis of $ATP_{\alpha}S$ and the additional supercoiling that it supports suggests that the maximum extent of supercoiling achievable by gyrase is limited thermodynamically. This would be the first demonstration of a direct thermodynamic relationship between the input and output reactions in an energy transduction process. Furthermore, these results support the conclusions of Bates and Maxwell (1989) who suggested that gyrase is limited by thermodynamic factors in its failure to supercoil DNA circles smaller than 174 bp.

It was shown in Chapter 4 that $ATP_{\alpha}S$(Rp) had a K_M^{app} approximately 11-fold lower than ATP and a similar V_{max}^{app}. Thus it is possible that the greater extent of supercoiling with $ATP_{\alpha}S$ may be due to its apparent tighter binding; at the concentration of nucleotide used in the experiments (1mM) the calculated initial rate of hydrolysis would be 0.75 V_{max} for ATP and 0.96 V_{max} for $ATP_{\alpha}S$. However, the extent of supercoiling experiments were allowed to progress until no further change in Lk could be seen and an apparent equilibrium was obtained. Nevertheless, it is possible that this equilibrium is not a thermodynamic equilibrium but a dynamic one where the rate of the supercoiling reaction is balanced by the rate of the nucleotide-independent relaxation reaction.

It has been shown that the ATP/ADP ratio affects the extent of supercoiling with gyrase (Westerhoff *et al.*, 1988) and it is therefore possible that this was important here. However, it can be calculated from the kinetic data in Chapter 4, that only a relatively small amount of ADP and $ADP_{\alpha}S$ (less than 10%) would be produced in the supercoiling experiments when equilibrium was reached. A control experiment to check the effect of this low level of ADP was attempted by including PK/LDH and PEP in the reaction to regenerate ATP from the ADP formed. However, there appeared to be a nuclease present

in the enzyme mix which gave rise to considerable DNA nicking and making it impossible to follow the supercoiling reaction; further purification of the commercial material may overcome this. In order to rule out any effect of ADP or $ADP_{\alpha}S$ and also further investigate the thermodynamic hypothesis above it should be possible to approach the supercoiling equilibrium from the direction of higher SLD's; pBR322 with SLD's of up to 0.2 have been prepared by the same method used for the preparation of the topoisomer standards in Section 2.20 (N.Noble and A. Maxwell, unpublished results). If the same equilibrium was reached with ATP and $ATP_{\alpha}S$ then this would confirm that ADP and $ADP_{\alpha}S$ were not significant. This experiment would not rule out the possibility of the pseudo-equilibrium between supercoiling and relaxation mentioned above however.

Considering the various arguments above, the hypothesis involving a thermodynamic limit to the extent of supercoiling is favoured at present. It was unfortunate that $ATP_{\beta}S$ was such a poor substrate in the supercoiling reaction since it would be anticipated that, if all the extra free energy of hydrolysis of $ATP_{\beta}S$ compared with ATP was manifested in supercoiling, an extra 8 superhelical turns should be supported and a final ΔLk step of -52 to -54 catalysed. While it may be possible to explore the thermodynamic limit further with this ATP analogue if gyrase preparations of greater specific activity become available in the future, it remains unlikely in view of the slowness of the supercoiling reaction near to its limit (as shown in Fig. 6.2).

It would be interesting to investigate the supercoiling of small DNA circles (Bates and Maxwell, 1989) with $ATP_{\alpha}S$ and $ATP_{\beta}S$. As with pBR322, the reaction with $ATP_{\beta}S$ would probably be too slow. With $ATP_{\alpha}S$, however, it would be interesting to see if any of the circles not supercoiled with ATP could be supercoiled. While the extra free energy available from $ATP_{\alpha}S$ is small, it is possible that circles of 142 bp and 152 bp, which would give supercoiled products with a SLD of -0.11 and -0.10 respectively and are not substrates for supercoiling with ATP, may become substrates with $ATP_{\alpha}S$. In

addition, new small DNA circles could be specifically designed to be just beyond the limit of supercoiling with ATP and prepared using the same recombination method as used by Bates and Maxwell (1989).

6.4. SUMMARY

The extent of supercoiling of pBR322 by gyrase was investigated with ATP, $ATP_{\alpha}S(Rp)$ and $ATP_{\beta}S(Rp)$. With $ATP_{\beta}S$, it was found that the supercoiling reaction was very slow and did not approach a limit even after 23 hours which was consistent with the results in Chapter 4. In the presence of ATP or $ATP_{\alpha}S$ the supercoiling reaction appeared to reach a limit: ATP gave a ΔLk of -46 and $ATP_{\alpha}S$ gave a ΔLk of -47. A theoretical approach using pK_a's of the nucleotides to model the relative stability of their ionised forms predicted that $MgATP_{\alpha}S$ should have a greater free energy of hydrolysis than MgATP. This was confirmed experimentally by measurements of the displacement of the equilibrium of a reaction catalysed by arginine kinase. It was found that an extra 0.92 kJ/mol was available from the hydrolysis of $MgATP_{\alpha}S$ compared to MgATP. Calculations on the free energy of supercoiling gave a value of 2.6 kJ/mol for the extra energy required for the additional round of supercoiling supported by $ATP_{\alpha}S$ over ATP. Taking into account the fact that two ATP's are thought to be hydrolysed per round of supercoiling, the extra free energy available from $MgATP_{\alpha}S$ is approximately 1.8 kJ/mol which is similar to the calculated free energy required for the additional round of supercoiling. The implications of these results are discussed with respect to energy coupling in gyrase and it is proposed that the limit to the extent of supercoiling of pBR322 is determined by the free energy available from the hydrolysis of the nucleotide.

Chapter 7

General Discussion and Future Directions

7.1. GENERAL DISCUSSION

The intention of the work in this thesis has been to further the understanding of the mechanistic events involved in the supercoiling of DNA by gyrase. Most of the work described has focussed on the hydrolysis of ATP and the way in which this is coupled to the supercoiling reaction; thiophosphate analogues of ATP have provided useful tools to probe these processes.

In Chapter 3, positional isotope exchange experiments showed that the off-rate for ATP was slow relative to the overall turnover of the nucleotide. This suggests that the binding of ATP is a two step process with an initial fast and reversible binding step being followed by a largely irreversible conformational change of the enzyme. As discussed in Chapter 3, this work is in agreement with other isotope exchange studies on gyrase by Hackney *et al.* (unpublished manuscript). The proposed two-step binding of ATP with an associated enzyme conformational change is consistent with transient electric dichroism studies by Rau *et al.* (1987) where a nucleotide-induced conformational change was detected, and with ADPNP binding experiments by Tamura *et al.* (1992). On the basis of this evidence, and the fact that two ATP's have been implicated in one ATPase cycle (Section 4.3 and references therein), a simple kinetic scheme for ATP hydrolysis by gyrase is proposed in Eqn. 3.3 (Section 3.3). This scheme is compatible with the model for the interaction of nucleotides with gyrase proposed by Tamura *et al.* (1992).

Also in Chapter 3, experiments on the utilisation of $ATP_{\gamma}S$ by gyrase were described. This work was performed with a view to determining whether it is feasible to analyse the stereochemical course of the gyrase ATPase by using isotopically chiral $ATP_{\gamma}S$. The finding that $ATP_{\gamma}S$ supports catalytic supercoiling has given a minimum value on the presumed rate of hydrolysis of this nucleotide by gyrase and has suggested that it should be possible to perform a stereochemical analysis of the ATPase reaction, although large quantities of enzyme will be required. It is anticipated that such a study will provide

direct evidence as to whether a phosphoenzyme intermediate is involved in gyrase-catalysed ATP hydrolysis.

Chapter 4 presented evidence that, with gyrase, the active Mg^{2+} ion complex of ATP is tridentate with the metal ion coordinated to the *pro*-S oxygens of the α- and β-phosphates and to the γ-phosphate. This was based on the pronounced stereospecificity of the enzyme for the Rp epimers of $MgATP_{\alpha}S$ and $MgATP_{\beta}S$, and the strong preference of Mg^{2+} to coordinate to O as opposed to S (Jaffe and Cohn, 1978a; Pecoraro *et al.*, 1984). Subsequent independent data from X-ray crystallography of the binary complex of the N-terminal fragment of GyrB (43kDa protein) with MgADPNP is consistent with this configuration of the active MgATP complex (Wigley *et al.*, 1991).

It would have been desirable to have confirmed the above prediction on the active MgATP complex by demonstrating that the stereospecificity of gyrase towards $ATP_{\alpha}S$ and $ATP_{\beta}S$ could be reversed when going from a hard Lewis acid metal ion such as Mg^{2+} to a soft metal ion such as Cd^{2+}. However, as described in Chapter 5 this proved to be technically impossible with gyrase or with the 43kDa protein. It was shown, however, that the stereospecificity of the 43kDa protein towards $MgATP_{\alpha}S$ and $MgATP_{\beta}S$ was the same as the full gyrase tetramer which provides valuable evidence in support of the 43kDa protein as a useful model for gyrase-ATP interactions. In addition, significant differences were seen in the kinetics of hydrolysis of the active isomers of $ATP_{\alpha}S$ and $ATP_{\beta}S$ between gyrase and the 43kDa fragment which probably reflect differences in their kinetic mechanisms of nucleotide hydrolysis, resulting from important interdomain and intersubunit interactions in gyrase.

As part of the studies discussed above, the dependence of various gyrase reactions on different metal ions was characterised. This showed that while DNA supercoiling and relaxation were specific towards Mg^{2+}, Ca^{2+}, or Mn^{2+}, double-stranded DNA cleavage

exhibited a much greater tolerance towards other metal ions (such as Cd^{2+}). One explanation for this is that DNA cleavage may not require such a specific gyrase-DNA interaction as DNA supercoiling or relaxation. For example, DNA cleavage may not require the DNA to be wrapped around the protein in the same way as the other two reactions. Interestingly, it has been shown that DNA cleavage can occur close to the end of an oligonucleotide which tends to support this hypothesis (Dobbs *et al.*, in press).

Aspects of the coupling of nucleotide hydrolysis to DNA supercoiling were investigated in Chapter 4. It was shown that for ATP and $ATP_{\alpha}S(Rp)$, there was a good correlation between the relative rates of hydrolysis of these nucleotides and their ability to support the supercoiling reaction. Conversely $ATP_{\beta}S(Rp)$ was relatively efficiently hydrolysed by gyrase but was very inefficient at supporting DNA supercoiling. Two hypotheses regarding the uncoupling of the hydrolysis and supercoiling reactions with this nucleotide were presented in Section 4.3 and it is hoped that this nucleotide may be useful in future experiments on the mechanism of energy transduction in gyrase. Interestingly, preliminary experiments with the ATP analogue AMPNPP [adenosine 5'-(α,β-imidotriphosphate)] have shown that a similar uncoupling of its hydrolysis to DNA supercoiling may occur (M. Congreve, D.P. Weiner, P.M. Cullis, and A. Maxwell, unpublished observations).

In addition to gyrase, there are many examples in nature of energy transduction systems such as muscle contraction, active transport, and oxidative phosphorylation (see Section 1.3). Of these, however, gyrase represents one of the simplest systems since both the energy input and output reactions (namely ATP hydrolysis and the introduction of torsional stress into DNA) are fairly amenable to investigations. In Chapter 6, thermodynamic aspects of energy coupling in gyrase are addressed. It is shown that $MgATP_{\alpha}S(Rp)$ supports a greater extent of supercoiling than ATP. Using the data of Horowitz and Wang (1984) on the free energy of supercoiling, the observed extra DNA

supercoiling with $MgATP_{\alpha}S$ compared to MgATP can be estimated to require approximately 2.6kJ/mol. Measurements of the equilibrium of a reaction catalysed by arginine kinase in the presence of ATP and $ATP_{\alpha}S$(Rp) showed that the hydrolysis of the thionucleotide is more exergonic by approximately 1 kJ/mol. Given that two ATP's are thought to be required per round of supercoiling, the extra energy available from $MgATP_{\alpha}S$(Rp) compared to MgATP should be approximately 2 kJ/mol. This compares favourably with the value of 2.6 kJ/mol for the extra supercoiling achieved with $MgATP_{\alpha}S$(Rp) and it is proposed therefore that the extent of supercoiling by gyrase is determined by the free energy available from the hydrolysis of the nucleotide.

It has been demonstrated previously that the Ca^{2+} gradient produced by the sarcoplasmic reticulum ATPase is the same regardless of whether ATP or $ATP_{\beta}S$ is used as an energy source (Pintado *et al.*, 1982). These authors therefore concluded that the extent of the Ca^{2+} gradient produced was not determined by the free energy of hydrolysis of the nucleotide. In Chapter 1, it was advanced that an explanation for this result may be that the factor determining the magnitude of the Ca^{2+} gradient may be the free energy of hydrolysis of the phosphoenzyme involved in the mechanism (Fig. 1.13); this would be the same with either ATP or $ATP_{\beta}S$. Building on this argument, in energy transduction systems where there is no formation of a nucleotide-derived phosphoenzyme, a limit to the extent of the endergonic reaction could come directly from the free energy difference between ATP and ADP and P_i. In view of the extent of supercoiling results for gyrase, it will be interesting to see whether gyrase is phosphorylated by ATP during the DNA supercoiling reaction; future stereochemical experiments should address this (see above). Current evidence from kinetics and the observation of limited supercoiling with ADPNP (Sugino *et al.*, 1978; Tamura *et al.*, 1992) exclude a mechanism for gyrase which places all the emphasis on a phosphoenzyme intermediate such as in the sarcoplasmic reticulum ATPase and is most easily reconciled with the absence of a phosphoenzyme.

7.2. FUTURE WORK

The experiments described in this thesis open up several interesting possibilities for further study. Some ideas are listed below:

(1) There are a number of possible approaches to confirm the nature of the Mg-ATP complex predicted in Chapter 4.

In Mg^{2+} ATP complexes the metal ion is in rapid dynamic equilibrium in aqueous solution and therefore the active configuration in enzymatic reactions cannot be isolated. Co^{III} and Cr^{III} complexes of ATP have been prepared and found to be kinetically stable with half-times for ligand exchange of several days such that different diastereoisomers of the complexes can be isolated (Cornelius and Cleland, 1978; Dunaway-Mariano and Cleland, 1980a; Dunaway-Mariano and Cleland, 1980b). These exchange-inert complexes have been used to probe the geometry of the active metal-nucleotide complexes in many of the kinases. In the case of CrATP, β,γ-bidentate complexes with Λ and Δ configurations (nomenclature according to Cornelius and Cleland, 1978) were prepared and found to be substrates (albeit poor ones) for several kinases (Dunaway-Mariano and Cleland, 1980a; Dunaway-Mariano and Cleland, 1980b). Based on the prediction of the active metal-ATP complex with gyrase as having Λ-exo tridentate geometry from the work with $ATP_{\alpha}S$ and $ATP_{\beta}S$ in this thesis, it would be anticipated that, if gyrase can accept bidentate CrATP as a substrate, it will be specific for the Λ isomer. This type of analysis would need to be performed at a fairly low pH (between 6 and 6.5) because, at higher pH's, the rate of epimerisation of the CrATP isomers is significant, but this should be feasible since gyrase has been shown to have a fairly broad pH supercoiling activity profile (D.P. Weiner and A. Maxwell, unpublished observations). Tridentate CrATP has also been prepared and was found not to be a substrate for any of the kinases tested (including creatine kinase which is thought to be specific for the tridentate MgATP complex; Leyh *et al.*, 1985) but Dunaway-Mariano and Cleland (1980a) have suggested

that the K_i of tridentate CrATP compared with that of bidentate CrATP may signify whether the nucleotide is bound at an enzyme's active site in an extended form or a compact form (as would be required for coordination of all three phosphates to the metal ion). Similar inhibition studies with tridentate CrATP may give further evidence for a tridentate MgATP complex with gyrase.

Another approach that has been used to characterise the metal ATP complex involved in an enzyme reaction is based on electron paramagnetic resonance (EPR). Specifically, this method exploits the fact that Mn^{2+} is paramagnetic and its unpaired electron spins can couple with the nuclear spin of ^{17}O. Thus, when ^{17}O is a direct ligand for the Mn^{2+} ion, the coupling can often be detected in the EPR spectrum. The coordination of Mn to the nucleotide in the creatine kinase reaction has been extensively studied by EPR using ATP and ADP both regiospecifically and stereospecifically labelled with ^{17}O (Leyh *et al.*, 1985; Leyh *et al.*, 1982; Reed and Leyh, 1980). These studies have confirmed that the active Mn-ATP complex is tridentate and has the Λ-exo configuration (the same as that proposed in this thesis for gyrase). It may be possible to use a similar approach with gyrase since the metal ion studies in Chapter 5 show that this enzyme is active in the presence of Mn^{2+}. However, it would be necessary to use the 43kDa protein which does not require DNA for full ATPase activity since the presence of DNA would introduce additional binding sites for the Mn^{2+} ion that would greatly complicate the EPR spectrum. A complication in the EPR studies is that very high enzyme concentrations are required since the concentration of enzyme active sites has to be higher than the binding constant of the nucleotide (usually mM) and there is no certainty that an interpretable spectrum will be obtained with a given enzyme. Nevertheless, Leyh *et al.* (1985) point out:
"The spectrum for the enzyme-Mn(II)ATP complex (with creatine kinase) is characteristic of the α,β,γ-tridentate species of Mn(II)ATP, and knowledge of this diagnostic pattern should be useful in EPR studies of other enzymes that select this isomer for activity".

In order to specifically probe whether the α-phosphate of ATP is involved in metal ion coordination in the active metal-nucleotide complex with various kinases, the diastereoisomers of $ATP_{\alpha}S$ have been methylated at sulphur (Connolly and Eckstein, 1982). The resulting compounds triesterified at the α-phosphate can be readily purified by reverse-phase HPLC. The lack of a full charge at P_{α} in the diastereoisomers of $ATP_{\alpha}SCH_3$ will presumably reduce dramatically the strength of coordination to Mg^{2+} at this position. However, the failure of these compounds to act as substrates which would signal an important metal ion coordination to the a-phosphate is likely to be ambiguous since failure to function as a substrate could also arise from steric problems introduced by the $-SCH_3$ group. It was found by Connolly and Eckstein that, for enzymes where there was compelling evidence for the involvement of the α-phosphate (creatine kinase and 3-phosphoglycerate kinase) in the active ATP complex, the isomers of $ATP_{\alpha}SCH_3$ were not active, whereas with other enzymes which had been postulated to select a β,γ-bidentate Mg-ATP complex (hexokinase, acetate kinase, and phosphofructokinase), either one or both of the isomers of $ATP_{\alpha}SCH_3$ were found to be substrates. Thus it would be interesting to determine whether these methylated derivatives of $ATP_{\alpha}S$ were substrates with gyrase. If they were, this would argue against the involvement of the α-phosphate in Mg^{2+} coordination. Lack of activity with $ATP_{\alpha}SCH_3$ would be compatible with the predicted tridentate Mg-ATP coordination in Chapter 4 but, as discussed above, it would not *prove* this hypothesis on its own.

Recently, the synthesis and isolation of all four diastereoisomers of guanosine 5'-O-(1,2-dithiotriphosphate) has been reported (Ludwig and Eckstein, 1991). The synthesis of the analogous adenosine compounds should be possible by the same method. It would be interesting to determine whether any of these compounds are substrates with gyrase. Based on the fact that $ATP_{\alpha}S$(Rp) and $ATP_{\beta}S$(Rp) are the preferred isomers in the monothio-ATP analogues, it would be anticipated that $ATP_{\alpha}S_{\beta}S$(Rp,Rp) would be the best substrate in the 1,2-dithio-ATP analogues.

(2) It has been well documented that ADPNP is not hydrolysed by gyrase and that this analogue supports stoichiometric supercoiling. This has been rationalised in terms of nucleotide binding giving one round of supercoiling with enzyme turnover requiring ATP hydrolysis (Sugino *et al.*, 1978). It would appear from the work in this thesis that, while some of the thiophosphate analogues of ATP are either not hydrolysed or only very slowly hydrolysed by gyrase, they do not behave like ADPNP in supporting stoichiometric supercoiling. This probably explains why they did not give rise to crystals with the 43kDa protein (Section 5.2.5). It would be interesting to further explore the ability of the inactive thiophosphate analogues of ATP [namely $ATP_{\alpha}S(Sp)$ and $ATP_{\beta}S(Sp)$] to support relaxation of positive supercoiling which is a nucleotide-dependent reaction mechanistically analogous to negative supercoiling except that it is energetically down-hill (see Section 6.1).

Vanadate has been reported to be a good analogue of phosphate (eg. Goodno, 1982) and is thought to be able to bind at the enzyme active site together with ADP to form a transition-state analogue for ATP hydrolysis. It would be interesting to discover whether such a transition-state mimic would be capable of promoting stoichiometric supercoiling by gyrase in the same way as ADPNP which acts as a ground-state analogue of ATP. Aluminofluoride and beryllofluoride complexes with ADP have been reported to be analogues of ATP (Chabre, 1990). In the case of the beryllium complex the structure is thought to mimic the ground state of ATP since beryllium cannot adopt the trigonal bipyramidal structure of the transition state and this complex is therefore complementary to the vanadate complex described above. In addition to experiments on stoichiometric supercoiling and relaxation of positively supercoiled DNA with these complexes, it may be possible to crystallise the 43kDa protein in their presence. This could provide further information on the way Mg^{2+} is bound to the nucleotide on the enzyme.

(3) It was suggested in Section 5.3 that the cleavage reaction of gyrase requires a less extensive DNA-protein interaction than the reactions involving DNA strand passage (DNA supercoiling and relaxation). This could be further explored by determining the minimum length of double-stranded DNA that can be cleaved by the enzyme.

(4) The thermodynamic analysis in Chapter 6 has provided evidence that the extent of supercoiling by gyrase is limited by the free energy available from ATP. As discussed in Section 6.3, it may be possible to confirm this conclusion by supercoiling experiments with ATP and $ATP_{\alpha}S$(Rp) using small DNA circles. The demonstration that $ATP_{\alpha}S$ has a greater free energy of hydrolysis than ATP may be useful in probing the energetics of other energy coupling systems.

(5) DNA gyrase is the only topoisomerase known to introduce negative supercoils into DNA at the expense of ATP hydrolysis. However, other topoisomerases also possess an ATPase activity such as reverse gyrase (Section 1.2.1), eukaryotic type II topoisomerase (Section 1.2.4), and phage T4 topoisomerase (Section 1.2.5). The latter two enzymes catalyse the thermodynamically favourable relaxation of supercoiled DNA and the reason for the requirement of ATP hydrolysis in this process remains obscure. Phosphorothioate ATP analogues could be used to study the ATPase activity and its coupling to the DNA relaxation (eukaryotic and T4 topoisomerases) or positive supercoiling (reverse gyrase) reactions of the above topoisomerases in approaches analogous to those taken in this thesis on DNA gyrase.

The initial aims of this project were to investigate the interaction of gyrase with ATP and the way in which the energy of hydrolysis of this nucleotide is coupled to DNA supercoiling. Some of these aims have been achieved and it is hoped that future work will give further insights into the process of energy transduction by gyrase. In order to

obtain a complete picture of how gyrase works a combination of kinetic, biochemical and biophysical approaches will be required.

References

Adachi, T., Mizuuchi, M., Robinson, E.A., Appella, E., O'Dea, M.H., Gellert, M., and Mizuuchi, K. (1987). DNA sequence of the *E. coli gyrB* gene: Application of a new sequencing strategy. *Nucleic Acids Res.* **15**, 771-784.

Adrian, M., ten Heggeler-Bordier, B., Wahli, W., Stasiak, A. Z., Stasiak, A., and Dubochet, J. (1990). Direct visualisation of supercoiled DNA molecules in solution. *EMBO J.* **9**, 4551-4554.

Akerfeldt, S. (1960). Cysteamine S-phosphoric acid. *Acta. Chem. Scand.* **14**, 1980-1984.

Ali, J.A., Jackson, A.P., Howells, A.J., and Maxwell, A. (1992). Manuscript in preparation.

Aoyama, H., Sato, K., Fujii, T., Fujimaki, K., Inoue, M., and Mitsuhashi, S. (1988). Purification of *Citrobacter freundii* DNA gyrase and inhibition by quinolones. *Antimicrob. Agents Chemother.* **32**, 104-109.

Armstrong, V.W, Yee, D., and Eckstein, F. (1979). Mechanistic studies on deoxyribonucleic acid dependent ribonucleic acid polymerase from *Escherichia coli* using phosphorothioate analogues. 2. The elongation reaction. *Biochemistry* **18**, 4120-4123.

Arnold, J. (1986). *The stereochemical course of some enzyme reactions.* PhD Thesis, Oxford.

Arnold, J.R.P., Cheng, M.S., Cullis, P.M., and Lowe, G. (1986). The stereochemical course of phosphoryl transfer catalysed by herpes simplex virus type I-induced thymidine kinase. *J. Biol. Chem.* **261**, 1985-1987.

Arnold, J.R.P. and Lowe, G. (1986). Synthesis and stereochemical analysis of chiral inorganic [^{16}O,^{17}O,^{18}O] thiophosphate. *J. Chem. Soc., Chem. Commun.* 865-867.

Baase, W.A. and Wang, J.C. (1974). An ω protein from *Drosophila melanogaster. Biochemistry.* **13**, 4299-4303.

Bagshaw, C.R. (1982). *Muscle contraction.* 1st ed. Outline studies in biology. Chapman and Hall, London.

Banik, U. and Roy, S. (1990). A continuous fluorimetric assay for ATPase activity. *Biochem. J.* **266**, 611-614.

Bates, A. D. and Maxwell, A. (1989). DNA gyrase can supercoil DNA circles as small as 174 base pairs. *EMBO J.* **8**, 1861-1866.

Bates, A.D. and Maxwell, A. (In press). *DNA topology.* IRL press, Oxford, U.K.

Bauer, W. and Vinograd, J. (1970). Interaction of closed circular DNA with intercalative dyes II. The free energy of superhelix formation in SV40 DNA. *J. Mol. Biol.* **47**, 419-435.

Bauer, W.R., Ressner, E.C., Kates, J., and Patzke, J.V. (1977). A DNA nicking-closing enzyme encapsidated in *vaccinia* virus: Partial purification and properties. *Proc. Natl. Acad. Sci. USA.* **74**, 1841-1845.

Been, M.D. and Champoux, J.J. (1980). Breakage of single-stranded DNA by rat liver nicking-closing enzyme with the formation of a DNA-enzyme complex. *Nucleic Acids Res.* **8**, 6129-6142.

Been, M.D. and Champoux, J.J. (1981). DNA breakage and closure by rat liver type I topoisomerase: separation of the half-reactions by using a single-stranded DNA substrate. *Proc. Natl. Acad. Sci. USA* **78**, 2883-2887.

Been, M.D. and Champoux, J.J. (1984). Breakage of single-stranded DNA by eukaryotic type I topoisomerase occurs only at regions with the potential for base-pairing. *J. Mol. Biol.* **180**, 515-531.

Bejar, S. and Bouche, J.P. (1984). The spacing of *Escherichia coli* DNA gyrase sites cleaved *in vivo* by treatment with oxolinic acid and sodium dodecyl sulphate. *Biochimie.* **66**, 693-700.

Beran-Steed, R.K. and Tse-Dinh, Y.-C. (1989). The corboxyl terminal domain of *Escherichia coli* DNA topoisomerase I confers higher affinity to DNA. *Proteins: Struct. Funct. Genet.* **6**, 249-258.

Birnboim, H. C. and Doly, J. (1979). A rapid alkaline extraction procedure for screening recombinant plasmid DNA. *Nucleic Acids Res.* **7**, 1513-1523.

Bjornsti, M.-A. and Wang, J.C. (1987). Expression of yeast DNA topoisomerase I can complement a conditional-lethal DNA topoisomerase I mutation in *Escherichia coli. Proc. Natl. Acad. Sci. USA.* **84**, 8971-8975.

Blättler, W.A. and Knowles, J.R. (1979). Stereochemical course of glycerol kinase, pyruvate kinase, and hexokinase: phosphoryl transfer from chiral [γ(S)-^{16}O, ^{17}O, ^{18}O]ATP. *J. Am. Chem. Soc.* **101**, 510-511.

Boles, T.C., White, J.H., and Cozzarelli, N.R. (1990). Structure of plectonemically supercoiled DNA. *J. Mol. Biol.* **213**, 931-951.

Bolivar, F., Rodriguez, R.L., Greene, P.J., Betlach, M.C., Heyneker, H.L., Boyer, H.W., Crosa, J.H., and Falkow, S. (1977). Construction and characterisation of new cloning vehicles. II. A multipurpose cloning system. *Gene* **2**, 95-113.

Boyer, P.D. (1989). A perspective of the binding change mechanism for ATP synthesis. *FASEB J.* **3**, 2164-2178.

Bradford, M. M. (1976). A rapid and sensitive method for the quantitation of microgram quantities of protein utilizing the principle of protein-dye binding. *Anal. Biochem.* **72**, 248-254.

Breslow, R. and Katz, I. (1968). Relative reactivities of *p*-nitrophenyl phosphate and phosphorothioate toward alkaline phosphatase and in aqueous hydrolysis. *J. Am. Chem. Soc.* **90**, 7376-7377.

Brown, P.O. and Cozzarelli, N.R. (1979). A sign inversion mechanism for enzymatic supercoiling of DNA. *Science.* **206**, 1081-1083.

Brown, P.O. and Cozzarelli, N.R. (1981). Catenation and knotting of duplex DNA by type I topoisomerases: A mechanistic parallel with type II topoisomerases. *Proc. Natl. Acad. Sci. USA.* **78**, 843-847.

Brown, P.O., Peebles, C.L., and Cozzarelli, N.R. (1979). A topoisomerase from *Escherichia coli* related to DNA gyrase. *Proc. Natl. Acad. Sci. USA.* **76**, 6110-6114.

Bryant, F.R., Benkovic, S.J., Sammons, D., and Frey, P.A. (1981). The stereochemical course of thiophosphoryl group transfer catalysed by T4 polynucleotide kinase. *J. Biol. Chem.* **256**, 5965-5966.

Buchwald, S.C., Hansen, D.E., Hassett, A., and Knowles, J.R. (1982). Chiral (^{16}O, ^{17}O, ^{18}O)phosphoric monoesters as stereochemical probes of phosphotransferases. *Methods Enzymol.* **87**, 279-301.

Burgers, P.M.J. and Eckstein, F. (1980). Structure of the metal-nucleotide complex in the creatine kinase reaction. *J. Biol. Chem.* **255**, 8229-8233.

Caserta, M., Amadei, A., Di Mauro, E., and Camilloni, G. (1989). *In vitro* preferential topoisomerisation of bent DNA. *Nucleic Acids Res.* **17**, 8463-8474.

Chabre, M. (1990). Aluminofluoride and beryllofluoride complexes: new phosphate analogues in enzymology. *Trends Biochem. Sci* **15**, 6-10.

Champoux, J.C. (1990). *Mechanistic aspects of type I topoisomerases.* In *DNA topology and its biological effects.* Edited by Wang, J.C. and Cozzarelli, N.R. 217-242. Cold Spring Harbor Laboratory Press, New York.

Champoux, J.J. (1977a). Renaturation of complementary single-stranded DNA circles: complete rewinding facilitated by the DNA untwisting enzyme. *Proc. Natl. Acad. Sci. USA* **74**, 5328-5332.

Champoux, J.J. (1977b). Strand breakage by the DNA untwisting enzyme results in covalent attachment of the enzyme to DNA. *Proc. Natl. Acad. Sci. USA* **74**, 3800-3804.

Champoux, J.J. (1978). Mechanism of the reaction catalysed by the DNA untwisting enzyme: attachment of the enzyme to the 3'-terminus of the nicked DNA. *J. Mol. Biol.* **118**, 441-446.

Champoux, J.J. and Dulbecco, R. (1972). An activity from mammalian cells that untwists superhelical DNA - A possible swivel for DNA replication. *Proc. Natl. Acad. Sci. USA* **69**, 143-146.

Chan, K., Delfert, D., and Junger, K.D. (1986). A direct colorimetric assay for Ca^{2+}-stimulated ATPase activity. *Anal. Biochem.* **157**, 375-380.

Cohn, M. (1982). Some properties of the phosphorothioate analogues of adenosine triphosphate as substrates of enzymic reactions. *Acc. Chem. Res.* **15**, 326-332.

Cohn, M. (1991). Structural and chemical properties of ATP and its metal complexes in solution. *Annals New York Academy of Sciences* **603**, 151-164.

Cohn, M. and Hu, A. (1978). Isotopic (^{18}O) shift in ^{31}P nuclear magnetic resonance applied to a study of enzyme-catalysed phosphate exchange and phosphate (oxygen)-water exchange reactions. *Proc. Natl. Acad. Sci. USA* **75**, 200-203.

Cohn, M., Shih, H., and Nick, J. (1982). Reactivity and metal-dependent stereospecificity of the phosphorothioate analogues of ATP in the arginine kinase reaction. *J. Biol. Chem.* **257**, 7646-7649.

Colman, S. D., Hu, P. C., and Bott, K. F. (1990). *Mycoplasma pneumoniae* DNA gyrase genes. *Molec. Microbiol.* **4**, 1129-1134.

Connolly, B.A. and Eckstein, F. (1981). Structures of the mono-and divalent metal nucleotide complexes in the myosin ATPase. *J. Biol. Chem.* **256**, 9450-9456.

Connolly, B.A. and Eckstein, F. (1982). S-methylated nucleoside phosphorothioates as probes of enzyme metal•nucleotide binding sites. *Biochemistry* **21**, 6158-6167.

Connolly, B. A., Eckstein, F., and Grotjahn, L. (1984). Direct mass spectroscopic method for determination of oxygen isotope position in adenosine 5'-O-(1-thiotriphosphate). Determination of the stereochemical course of the yeast phenylalanyl-tRNA synthetase reaction. *Biochemistry* **23**, 2026-2031.

Contreras, A. and Maxwell, A. (1992). Effects of *gyrB* mutations conferring coumarin resistance on DNA supercoiling and ATP hydrolysis by *Escherichia coli* DNA gyrase. *Mol. microbiol.* **6**, 1617-1624.

Cook, A.F. (1970). Nucleoside S-alkyl phosphorothioates. IV. Synthesis of nucleoside phosphorothioate monoesters. *J. Am. Chem. Soc.* **92**, 190-195.

Corbett, A.H., Zechiedrich, E.L., and Osheroff, N. (1992). A role for the passage helix in the DNA cleavage reaction of eukaryotic topoisomerase II. A two-site model for enzyme-mediated DNA cleavage. *J. Biol. Chem.* **267**, 683-686.

Cornelius, R.D. and Cleland, W.W. (1978). Substrate activity of (adenosine triphosphato) tetraamminecobalt (III) with yeast hexokinase and separation of diastereoisomers using the enzyme. *Biochemistry* **17**, 3279-3286.

Cotton, F.A. and Wilkinson, G. (1972). *Advanced inorganic chemistry. A comprehensive text.* 3rd ed. John Wiley and Sons, New York.

Cozzarelli, N. R. (1980a). DNA gyrase and the supercoiling of DNA. *Science.* **207**, 953-960.

Cozzarelli, N. R. (1980b). DNA topoisomerases. *Cell.* **22**, 327-328.

Crick, F.C.H., Wang, J.C., and Bauer, W.R. (1979). Is DNA really a double helix? *J. Mol. Biol.* **129**, 449-461.

Crick, F. H. C. (1976). Linking numbers and nucleosomes. *Proc. Natl. Acad. Sci. USA* **73**, 2639-2643.

Crothers, D. M., Haran, T. E., and Nadeau, J. G. (1990). Intrinsically bent DNA. *J. Biol. Chem.* **265**, 7093-7096.

Cullis, P.M. (1988). *Acyl group transfer - phosphoryl transfer.* In *Enzyme mechanisms.* pp178-220. Royal Society of Chemistry, London.

D'Arpa, P., Machlin, P.S., Ratrie, H., Rothfield, N.F., Cleveland, D.W., and Earnshaw, W.C. (1988). cDNA cloning of human DNA topoisomerase I: Catalytic activity of a 67.7kDa carboxyl-terminal fragment. *Proc. Natl. Acad. Sci. USA.* **85**, 2543-2547.

Dale, M.P. and Hackney, D.D. (1987). Analysis of positional isotope exchange in ATP by cleavage of the βP-Oγ P bond. Demonstration of negligible positional isotope exchange by myosin. *Biochemistry* **26**, 8365-8372.

Darby, M.K. and Vosberg, H.-P. (1985). Relaxation of supercoiled phosphothioate DNA by mammalian topoisomerases is inhibited in a base-specific manner. *J. Biol. Chem.* **260**, 4501-4507.

Dean, F.B. and Cozzarelli, N.R. (1985). Mechanism of strand passage by *Escherichia coli* topoisomerase I. *J. Biol. Chem.* **260**, 4984-4994.

de Meis, L. and Vianna, A.L. (1979). Energy interconversion by the Ca2+ dependent ATPase of the sarcoplasmic reticulum. *Ann. Rev. Biochem.* **48**, 275-292.

del Castillo, I., Vizán, J.L., Rodríguez-Sáinz, M.C., and Moreno, F. (1991). An unusual mechanism for resistance to the antibiotic coumermycin A_1. *Proc. Natl. Acad. Sci. USA* **88**, 8860-8864.

Depew, R.E., Liu, L.F., and Wang, J.C. (1978). Interaction between DNA and *Escherichia coli* protein ω. Formation of a complex between single-stranded DNA and ω protein. *J. Biol. Chem.* **253**, 511-518.

Depew, R. E. and Wang, J. C. (1975). Conformational fluctuations of DNA helix. *Proc. Natl. Acad. Sci. USA* **72**, 4275-4279.

DiGate, R.J. and Marians, K.J. (1988). Identification of a potent decatenating enzyme from *Escherichia coli. J. Biol. Chem.* **263**, 13366-13373.

Digate, R.J. and Marians, K.J. (1989). Molecular cloning and DNA sequence analysis of *Escherichia coli top*B, the gene encoding topoisomerase III. *J. Biol. Chem.* **264**, 17924-17930.

Dimri, G.P. and Das, H.K. (1990). Cloning and sequence analysis of *gyrA* gene of *Klebsiella pneumoniae. Nucleic Acids Res.* **18**, 151-156.

DiNardo, S., Voelkel, K., and Sternglanz, R. (1984). DNA topoisomerase II mutant of *Saccharomyces cerevisiae:* topoisomerase II is required for segregation of daughter molecules at the termination of DNA replication. *Proc. Natl. Acad. Sci. USA* **81**, 2616-2620.

DiNardo, S., Voelkel, K.A., Sternglanz, R., Reynolds, A.E., and Wright, A. (1982). *Escherichia coli* DNA topoisomerase I mutants have compensatory mutations in DNA gyrase genes. *Cell* **31**, 43-51.

Dobbs, S.T., Cullis, P.M., and Maxwell, A. (In Press). The cleavage of DNA at phosphorothioate internucleotidic linkages by DNA gyrase. *Nucleic Acids Res.*

Domanico, P.L. and Tse-Dinh, Y.C. (1988). Cleavage of dT_8 and dT_8 phosphorothioyl analogues by *Escherichia coli* DNA topoisomerase I: product and rate analysis. *Biochemistry* **27**, 6365-6371.

Drlica, K. (1990). Bacterial topoisomerases and the control of DNA supercoiling. *Trends in Genet.* **6**, 433-437.

Drlica, K. and Coughlin, S. (1989). Inhibitors of DNA gyrase. *Pharmac. Ther.* **44**, 107-121.

Dugaiczyk, A., Boyer, H. W., and Goodman, H. M. (1975). Ligation of *Eco*RI endonuclease-generated DNA fragments into linear and circular structures. *J. Mol. Biol.* **96**, 171-184.

Dunaway-Mariano, D. and Cleland, W.W. (1980a). Investigation of substrate specificity and reaction mechanism of several kinases using chromium(III) adenosine 5'-triphosphate and chromium(III) adenosine 5'-diphosphate. *Biochemistry* **19**, 1506-1515.

Dunaway-Mariano, D. and Cleland, W.W. (1980b). Preparation and properties of chromium(III) adenosine 5'-triphosphate, chromium(III) adenosine 5'-diphosphate, and related chromium(III) complexes. *Biochemistry* **19**, 1496-1505.

Dustin, I., Furrer, P., Stasiak, A., Dubochet, J., Langowski, J., and Egelman, E. (1991). Spatial visualisation of DNA in solution. *J. Struct. Biol.* **107**, 15-21.

Earnshaw, W.C., Halligan, B., Cooke, C.A., Heck, M.M.S., and Liu, L.F. (1985). Topoisomerase II is a structural component of mitotic chromosome scaffolds. *J. Cell Biol.* **100**, 1706-1715.

Earnshaw, W.C. and Heck, M.M.S. (1985). Localization of topoisomerase II in mitotic chromosomes. *J. Cell Biol.* **100**, 1716-1725.

Eccleston, J.F. and Webb, M.R. (1982). Characterisation of the GTPase reaction of elongation factor Tu. Determination of the stereochemical course in the presence of antibiotic X5108. *J. Biol. Chem.* **257**, 5046-5049.

Eckstein, F. (1980). Nucleotide analogues for the study of enzyme mechanisms. *Trends Biochem. Sci.* **5**, 157-159.

Eckstein, F. (1985). Nucleoside phosphorothioates. *Ann. Rev. Biochem.* **54**, 367-402.

Eckstein, F. and Goody, R.S. (1976). Synthesis and properties of diastereoisomers of adenosine 5'-(O-1-thiotriphosphate) and adenosine 5'-(O-2-thiotriphosphate). *Biochemistry* **15**, 1685-1691.

Eisenberg, D. and Hill, C.P. (1989). Protein crystallography: More surprises ahead. *Trends Biochem. Sci.* **14**, 260-264.

Eisenberg, E. and Greene, L.E. (1980). The relation of muscle biochemistry to muscle physiology. *Ann. Rev. Physiol.* **42**, 293-309.

Eisenberg, E. and Hill, T, L. (1985). Muscle contraction and free energy transduction in biological systems. *Science* **227**, 999-1006.

Fairfield, F.R., Bauer, W.R., and Simpson, M.V. (1979). Mitochondria contain a distinct DNA topoisomerase. *J. Biol. Chem.* **254**, 9352-9354.

Fairfield, F.R., Bauer, W.R., and Simpson, M.V. (1985). Studies on mitochondrial type I topoisomerase and on its function. *Biochim. et Biophys. Acta.* **824**, 45-57.

Ferro, A.M. and Olivera, B.M. (1984). Poly(ADP-ribosylation) of DNA topoisomerase I from calf thymus. *J. Biol. Chem.* **259**, 547-559.

Fersht, A. (1985). *Enzyme structure and mechanism.* 2nd ed. W.H. Freeman and Company, New York.

Feuerstein, J., Goody, R.S., and Webb, M.R. (1989). The mechanism of guanosine nucleotide hydrolysis by p21 c-Ha-*ras*. The stereochemical course of the GTPase reaction. *J. Biol. Chem.* **264**, 6188-6190.

Fisher, L. M., Barot, H. A., and Cullen, M. E. (1986). DNA gyrase complex with DNA: Determinants for site specific DNA breakage. *EMBO J.* **5**, 1411-1418.

Fisher, L. M., Mizuuchi, K., O'Dea, M. H., Ohmori, H., and Gellert, M. (1981). Site-specific interaction of DNA gyrase with DNA. *Proc. Natl. Acad. Sci. USA* **78**, 4165-4169.

Foglesong, P.D. and Bauer, W.R. (1984). Effects of ATP and inhibitory factors on the activity of vaccinia virus type I topoisomerase. *J. Virol.* **49**, 1-8.

Franco, R.J. and Drlica, K. (1988). DNA gyrase on the bacterial chromosome: Oxolinic acid-induced DNA cleavage in the *dnaA-gyrB* region. *J. Mol. Biol.* **201**, 229-233.

Frey, P.A. (1982). Stereochemistry of enzymatic reactions of phosphates. *Tetrahedron* **38**, 1541-1567.

Frey, P.A. (1989). Chiral phosphorothioates: stereochemical analysis of enzymatic substitution at phosphorus. *Adv. Enzymol. Relat. Areas Mol. Biol.* **62**, 119-201.

Frey, P.A., Reimschüssel, W., and Paneth, P. (1986). Phosphorus-sulphur bond order in phosphorothioate anions. *J. Am. Chem. Soc.* **108**, 1720-1722.

Frey, P.A. and Sammons, D.R. (1985). Bond order and charge localization in nucleoside phosphorothioates. *Science* **228**, 541-545.

Fuller, F.B. (1971). The writhing number of a space curve. *Proc. Natl. Acad. Sci. USA.* **68**, 815-819.

Garner, M.M. and Revzin, A. (1986). The use of gel electrophoresis to detect and study nucleic acid-protein interactions. *Trends Biochem. Sci* **11**, 395-396.

Gellert, M. (1981). DNA topoisomerases. *Ann. Rev. Biochem.* **50**, 879-910.

Gellert, M., Fisher, L. M., and O'Dea, M. H. (1979). DNA gyrase: purification and catalytic properties of a fragment of gyrase B protein. *Proc. Natl. Acad. Sci. USA* **76**, 6289-6293.

Gellert, M., Fisher, L. M., Ohmori, H., O'Dea, M. H., and Mizuuchi, K. (1980). DNA gyrase: site-specific interactions and transient double-strand breakage of DNA. *Cold Spring Harbor Symp. Quant. Biol.* **45**, 391-398.

Gellert, M., Mizuuchi, K., O'Dea, M. H., Itoh, T., and Tomizawa, J. (1977). Nalidixic acid resistance: A second genetic character in DNA gyrase activity. *Proc. Natl. Acad. Sci. USA* **74**, 4772-4776.

Gellert, M., Mizuuchi, K., O'Dea, M. H., and Nash, H. N. (1976a). DNA gyrase: An enzyme that introduces superhelical turns into DNA. *Proc. Natl. Acad. Sci. USA* **73**, 3872-3876.

Gellert, M., O'Dea, M.H., Itoh, T., and Tomizawa, J. (1976b). Novobiocin and coumermycin inhibit DNA supercoiling catalysed by DNA gyrase. *Proc. Natl. Acad. Sci. USA.* **73**, 4474-4478.

Giaever, G. N. and Wang, J. C. (1988). Supercoiling of intracellular DNA can occur in eukaryotic cells. *Cell* **55**, 849-856.

Gonzalez, M.A., Webb, M.R., Welsh, K.M., and Cooperman, B.S. (1984). Evidence that catalysis by yeast inorganic pyrophosphatase proceeds by direct phosphoryl transfer to water and not via a phosphoryl enzyme intermediate. *Biochemistry* **23**, 797-801.

Goodno, C.C. (1982). Myosin active-site trapping with vanadate ion. *Methods Enzymol.* **85**, 116-123.

Goody, R.S. and Eckstein, F. (1971). Thiophosphate analogs of nucleoside di- and triphosphates. *J. Am. Chem. Soc.* **93**, 6252-6257.

Goody, R.S. and Hofmann, W. (1980). Stereochemical aspects of the interaction of myosin and actomyosin with nucleotides. *J. Muscle Research and Cell Motility* **1**, 101-115.

Goto, T., Laipis, P., and Wang, J.C. (1984). The purification and characterization of DNA topoisomerases I and II of the yeast *Saccharomyces cerevisiae*. *J. Biol. Chem.* **259**, 10422-10429.

Greenfield, L., Simpson, L., and Kaplan, D. (1975). Conversion of closed circular DNA molecules to single-nicked molecules by digestion with DNAse I in the presence of ethidium bromide. *Biochim. et Biophys. Acta.* **407**, 365-375.

Hackney, D.D. (1980). Theoretical analysis of distribution of [^{18}O]Pi species during exchange with water. *J. Biol. Chem.* **255**, 5320-5328.

Hallett, P., Grimshaw, A. J., Wigley, D. B., and Maxwell, A. (1990). Cloning of the DNA gyrase genes under *tac* promoter control: over-expression of the gyrase A and B proteins. *Gene.* **93**, 139-142.

Hames, B.D. (1981). *An introduction to polyacrylamide gel electrophoresis.* In *Gel electrophoresis of proteins. A practical approach.* Edited by Hames, B.D. and Rickwood, D. 1-91. IRL Press., Oxford and Washington DC.

Hansen, D.E. and Knowles, J.R. (1981). The stereochemical course of the reaction catalysed by creatine kinase. *J. Biol. Chem.* **256**, 5967-5969.

Herschlag, D. and Jencks, W.P. (1987). The effect of divalent metal ions on the rate and transition-state structure of phosphoryl-transfer reactions. *J. Am. Chem. Soc.* **109**, 4665-4674.

Higgins, N.P. and Cozzarelli, N.R. (1982). The binding of gyrase to DNA: Analysis by retention by nitrocellulose filters. *Nucleic Acids Res.* **10**, 6833-6847.

Higgins, N.P., Ferro, A.M., and Olivera, B.M. (1990). *DNA topoisomerase modification.* In *DNA topology and its biological effects.* Edited by Wang, J.C. and Cozzarelli, N.R. 361-370. Cold Spring Harbor Laboratory Press, New York.

Higgins, N.P., Peebles, C.L., Sugino, A., and Cozzarelli, N.R. (1978). Purification of subunits of *Escherichia coli* DNA gyrase and reconstitution of enzymatic activity. *Proc. Natl. Acad. Sci. USA.* **75**, 1773-1777.

Hilscher, L.W., Hanson, C.D., Russell, D.H., and Raushel, F.M. (1985). Measurement of positional isotope exchange rates in enzyme-catalysed reactions by fast atom bombardment mass spectrometry: Application to argininosuccinate synthetase. *Biochemistry* **24**, 5888-5893.

Hine, J. (1975). *Structural effects on equilibria in organic chemistry (Chapter 5).* 1st ed. John Wiley & Sons, New York.

Hine, J. and Mookerjee, P.K. (1975). The intrinsic hydrophilic character of organic compounds. Correlations in terms of structural contributions. *J. Org. Chem.* **40**, 292-298.

Hiratsuka, T. (1983). New ribose-modified fluorescent analogs of adenine and guanine nucleotides available as substrates for various enzymes. *Biochim. Biophys. Acta* **742**, 496-508.

Holmes, M.L. and Dyall-Smith, M.L. (1991). Mutations in DNA gyrase result in novobiocin resistance in halophilic archaebacteria. *J. Bacteriol.* **173**, 642-648.

Hopewell, R., Oram, M., Briesewitz, R., and Fisher, L. M. (1990). DNA cloning and organization of the *Staphylococcus aureus gyrA* and *gyrB* genes: Close homology among gyrase proteins and implications for 4-quinolone action and resistance. *J. Bacteriol.* **172**, 3481-3484.

Horowitz, D.S. and Wang, J.C. (1984). Torsional rigidity of DNA and length dependence of the free energy of DNA supercoiling. *J. Mol. Biol.* **173**, 75-91.

Horowitz, D. S. and Wang, J. C. (1987). Mapping the active site tyrosine of *Escherichia coli* DNA gyrase. *J. Biol. Chem.* **262**, 5339-5344.

Hsiang, Y.-H., Lihou, M.G., and Liu, L.F. (1989). Arrest of replication forks by drug-stabilized topoisomerase I - DNA cleavable complexes as a mechanism of cell killing by camptothecin. *Cancer Res.* **49**, 5077-5082.

Hsiang, Y.R., Hertzberg, R., Hecht, S., and Liu, L.F. (1985). Camptothecin induces protein-linked DNA breaks via mammalian DNA topoisomerase I. *J. Biol. Chem.* **260**, 14875-14878.

Hsieh, T. (1990a). DNA topoisomerases. *Current Opinion in Cell Biology* **2**, 461-463.

Hsieh, T-S. (1990b). *Mechanistic aspects of type II DNA topoisomerases.* In *DNA topology and its biological effects.* Edited by Wang, J.C. and Cozzarelli, N.R. 243-263. Cold Spring Harbor Laboratory Press, New York.

Hsieh, T.-S. and Brutlag, D. (1980). ATP-dependent DNA topoisomerase from *D. melanogaster* reversibly catenated duplex DNA rings. *Cell.* **21**, 115-125.

Hsieh, T.-S. and Wang, J. C. (1975). Thermodynamic properties of superhelical DNAs. *Biochemistry* **14**, 527-535.

Huang, S.L. and Tsai, M-D. (1982). Does the magnesium(II) ion interact with the α-phosphate of adenosine triphosphate? An investigation by oxygen-17 nuclear magnetic resonance. *Biochemistry* **21**, 951-959.

Huang, W.M. (1986a). The 52-protein of T4 DNA topoisomerase is homologous to the *gyrA*-protein of gyrase. *Nucleic Acids Res.* **14**, 7379-7390.

Huang, W.M. (1986b). Nucleotide sequence of a type II DNA topoisomerase gene. Bacteriophage T4 gene 39. *Nucleic Acids Res.* **14**, 7751-7765.

Huang, W.M. (1990). *Virus-encoded DNA topoisomerases.* In *DNA topology and its biological effects.* Edited by Wang, J.C. and Cozzarelli, N.R. 265-284. Cold Spring Harbor Laboratory Press, New York.

Huang, W.M., Ao, S., Casjens, S., Orlandi, R., Zeikus, R., Weiss, R., Winge, D., and Fang, M. (1988). A persistent untranslated sequence within bacteriophage T4 DNA topoisomerase gene 60. *Science* **239**, 1005-1012.

Jackson, A.P., Maxwell, A., and Wigley, D.B. (1991). Preliminary crystallographic analysis of the ATP-hydrolysing domain of the *Escherichia coli* DNA gyrase B protein. *J. Mol. Biol.* **217**, 15-18.

Jaffe, E.K. and Cohn, M. (1978a). ^{31}P nuclear magnetic resonance spectra of the thiophosphate analogues of adenine nucleotides; effects of pH and Mg^{2+} binding. *Biochemistry* **17**, 652-657.

Jaffe, E.K. and Cohn, M. (1978b). Divalent cation-dependent stereospecificity of adenosine 5'-O-(2-thiotriphosphate) in the hexokinase and pyruvate kinase reactions. *J. Biol. Chem.* **253**, 4823-4825.

Jaffe, E.K. and Cohn, M. (1979). Diastereomers of the nucleoside phosphorothioates as probes of the structure or the metal nucleotide substrates and of the nucleotide binding site of yeast hexokinase. *J. Biol. Chem.* **21**, 10839-10845.

Jaffe, E.K. and Cohn, M. (1980). Shift of the equilibrium constant of the 3-P-glycerate kinase reaction towards 1,3-Bis-P-glycerate with adenosine 5'-O-(2-thiotriphosphate) (ATPβS) as substrate. *J. Biol. Chem.* **255**, 3240-3241.

Jarvest, R.L. and Lowe, G. (1981). The stereochemical course of phosphoryl transfer catalysed by polynucleotide kinase (bacteriophage-T_4-infected *Escherichia coli* B. *Biochem. J.* **199**, 273-276.

Jarvest, R.L., Lowe, G., and Potter, B.V.L. (1981). The stereochemical course of phosphoryl transfer catalysed by Bacillus stearothermophilus and rabbit

skeletal-muscle phosphofructokinase with a chiral [^{16}O, ^{17}O, ^{18}O]phosphate ester. *Biochem. J.* **199**, 427-432.

Johnson, R. C., Glasgow, A. C., and Simon, M. I. (1987). Spatial relationship of the Fis binding sites for Hin recombinational enhancer activity. *Nature* **329**, 462-465.

Jones, J.P., Weiss, P.M., and Cleland, W.W. (1991). Secondary ^{18}O isotope effects for hexokinase-catalysed phosphoryl transfer from ATP. *Biochemistry* **30**, 3634-3639.

Jones, S.R., Kindman, L.A., and Knowles, J.R. (1978). Stereochemistry of phosphoryl group transfer using a chiral [^{16}O, ^{17}O, ^{18}O] stereochemical course of alkaline phosphatase. *Nature* **275**, 564-565.

Kaiserman, H.B., Ingebritsen, T.S., and Benbow, R.M. (1988). Regulation of *Xenopus laevis* DNA topoisomerase I activity by phosphorylation *in vitro*. *Biochemistry* **27**, 3216-3222.

Kanaar, R., van de Putte, P., and Cozzarelli, N. R. (1989). Gin-mediated recombination of catenated and knotted DNA substrates: implications for the mechanism of interaction between *cis*-acting sites. *Cell* **58**, 147-159.

Kato, J., Nishimura, Y., Imamura, R., Niki, H., Hiraga, S., and Suzuki, H. (1990). New topoisomerase essential for the chromosome segregation in *E. coli*. *Cell* **63**, 393-404.

Keller, W. (1975). Determination of the number of superhelical turns in simian virus 40 DNA by gel electrophoresis. *Proc. Natl. Acad. Sci. USA* **72**, 4876-4880.

Keller, W. and Wendel, I. (1974). Stepwise relaxation of supercoiled SV40 DNA. *Cold Spring Harbor Symp. Quant. Biol.* **39**, 199-208.

Kikuchi, A. and Asai, K. (1984). Reverse gyrase - a topoisomerase which introduces positive superhelical turns into DNA. *Nature* **309**, 677-681.

Kim, R. A. and Wang, J. C. (1989). Function of DNA topoisomerases as replication swivels in *Saccharomyces cerevisiae*. *J. Mol. Biol.* **208**, 257-267.

Kirchhausen, T., Wang, J.C., and Harrison, S.C. (1985). DNA gyrase and its complexes with DNA: Direct observation by electron microscopy. *Cell.* **41**, 933-943.

Kirkegaard, K. and Wang, J.C. (1978). *Escherichia coli* DNA topoisomerase I catalysed linking of single-stranded rings of complementary base sequence. *Nucleic Acids Res.* **5**, 3811-3820.

Kirkegaard, K. and Wang, J. C. (1981). Mapping the topography of DNA wrapped around gyrase by nucleolytic and chemical probing of complexes of unique DNA sequence. *Cell* **23**, 721-729.

Kirkegaard, K. and Wang, J.C. (1985). Bacterial DNA topoisomerase I can relax positively supercoiled DNA containing a single-stranded loop. *J. Mol. Biol.* **185**, 625-637.

Klevan, L. and Wang, J.C. (1980). DNA gyrase-DNA complex containing 140bp of DNA and an $\alpha_2\beta_2$ protein core. *Biochemistry.* **19**, 5229-5234.

Klippel, A., Mertens, G., Patschinsky, T., and Kahmann, R. (1988). The DNA invertase Gin of phage Mu: Formation of a covalent complex with DNA via a phosphoserine at amino acid position 9. *EMBO J.* **7**, 1229-1237.

Knowles, J.R. (1980). Enzyme-catalysed phosphoryl transfer reactions. *Ann. Rev. Biochem.* **49**, 877-919.

Kreuzer, K.N. and Cozzarelli, N.R. (1980). Formation and resolution of DNA catenanes by DNA gyrase. *Cell.* **20**, 245-254.

Krueger, S., Zaccai, G., Wlodawer, A., Langowski, J., O'Dea, M., Maxwell, A., and Gellert, M. (1990). Neutron and light-scattering studies of DNA gyrase and its complex with DNA. *J. Mol. Biol.* **211**, 211-220.

Kung, V.T. and Wang, J.C. (1977). Purification and characterization of an ω protein from *Micrococcus luteus*. *J. Biol. Chem.* **252**, 5398-5402.

Laemmli, U. (1970). Cleavage of structural proteins during the assembly of the head of bacteriophage T4. *Nature* **227**, 680-682.

Lanzetta, P.A., Alvarez, L.J., Reinach, P.S., and Candia, O.A. (1979). An improved assay for nanomole amounts of inorganic phosphate. *Anal. Biochem.* **100**, 95-97.

Lawson, R.J.W. and Veech, R.L. (1979). Effects of pH and free Mg^{++} on the K_{eq} of the creatine kinase reaction and other phosphate hydrolyses and phosphate transfer reactions. *J. Biol. Chem.* **254**, 6528-6537.

Lazewska, D. and Granowski, A. (1990). P_α-chiral phosphorothioate analogues of bis(5'-adenosyl)tetraphosphate (Ap_4A); their enzymatic synthesis and degredation. *Nuc. Acid. Res.* **18**, 6083-6088.

Lebeau, L., Regnier, E., Schultz, P., Wang, J.C., Mioskowski, C., and Oudet, P. (1990). Two-dimensional crystallization of DNA gyrase B subunit on specifically designed lipid monolayers. *FEBS Lett.* **267**, 38-42.

Lebon, J.M., Kado, C.I., Rosenthal, L.J., and Chirikjan, J.G. (1978). DNA modifying enzymes of *Agrobacterium tumefaciens*: Effect of DNA topoisomerases, restriction endonucleases, and unique DNA endonuclease on plasmid and plant DNA. *Proc. Natl. Acad. Sci. USA.* **75**, 4097-4101.

Lee, C.S. and O'Sullivan, W.J. (1985). The interaction of phosphorothioate analogues of ATP with phosphomevalonate kinase. *J. Biol. Chem.* **260**, 13909-13915.

Lee, M. P., Sander, M., and Hsieh, T. (1989). Nuclease protection by *Drosophila* DNA topoisomerase II. Enzyme-DNA contacts at the strong topoisomerase II cleavage sites. *J. Biol. Chem.* **264**, 21779-21787.

Lerman, C.L. and Cohn, M. (1980). ^{31}P NMR quantitation of the displacement of equilibria of arginine, creatine, pyruvate, and 3-P-glycerate kinase reactions by

substitution of sulphur for oxygen in the β phosphate of ATP. *J. Biol. Chem.* **255**, 8756-8760.

Leyh, T.S., Goodhart, P.J., Nguyen, A.C., Kenyon, G.L., and Reed, G.H. (1985). Structures of manganese(II) complexes with ATP, ADP, and phosphocreatine in the reactive central complexes with creatine kinase: electron paramagnetic resonance studies with oxygen-17-labelled ligands. *Biochemistry* **24**, 308-316.

Leyh, T.S., Sammons, D.R., Frey, P.A., and Reed, G.H. (1982). The stereochemical configuration of Mn(II)-ADP at the active site of creatine kinase elucidated by electron paramagnetic resonance with Rp[α-^{17}O]ADP and Sp [α-^{17}O]ADP. *J. Biol. Chem.* **257**, 15047-15053.

Liang, C. and Allen, L.C. (1987). Sulfur does not form double bonds in phosphorothioate anions. *J. Am. Chem. Soc.* **109**, 6449-6453.

Lienhard, G.E. and Secemski, I.I. (1973). P^1,P^5-Di(adenosine-5')pentaphosphate, a potent multisubstrate inhibitor of adenylate kinase. *J. Biol. Chem.* **248**, 1121-1123.

Lindsley, J.E. and Wang, J.C. (1991). Proteolysis patterns of epitopically labelled yeast DNA topoisomerase II suggest an allosteric transition in the enzyme induced by ATP binding. *Proc. Natl. Acad. Sci. USA* **88**, 10485-10489.

Liu, L.F. (1983). DNA topoisomerases - Enzymes that catalyse the breaking and rejoining of DNA. *CRC Crit. Rev. Biochem.* **15**, 1-24.

Liu, L.F. (1990). *Anticancer drugs that convert DNA topoisomerases into DNA damaging agents.* In *DNA topology and its biological effects.* Edited by Wang, J.C. and Cozzarelli, N.R. 371-389. Cold Spring Harbor Laboratory Press, New York.

Liu, L.F., Depew, R.E., and Wang, J.C. (1976). Knotted single-stranded DNA rings: A novel topological isomer of circular single-stranded DNA formed by treatment with *Escherichia coli* ω protein. *J. Mol. Biol.* **106**, 439-452.

Liu, L.F., Liu, C.-C., and Alberts, B.M. (1979). T4 DNA topoisomerase: A new ATP-dependent enzyme essential for initiation of T4 bacteriophage DNA replication. *Nature.* **281**, 456-461.

Liu, L. F., Liu, C.-C., and Alberts, B. M. (1980). Type II DNA topoisomerases: enzymes that can unknot a topologically knotted DNA molecule *via* a reversible double-strand break. *Cell* **19**, 697-707.

Liu, L.F. and Miller, K.G. (1981). Eukaryotic DNA topoisomerases: Two forms of the type I DNA topoisomerases from HeLa cell nuclei. *Proc. Natl. Acad. Sci. USA.* **78**, 3487-3491.

Liu, L. F. and Wang, J. C. (1978a). DNA-DNA gyrase complex: the wrapping of the DNA duplex outside the enzyme. *Cell* **15**, 979-984.

Liu, L. F. and Wang, J. C. (1978b). *Micrococcus luteus* DNA gyrase: active components and a model for its supercoiling of DNA. *Proc. Natl. Acad. Sci. USA* **75**, 2098-2102.

Liu, L.F. and Wang, J.C. (1979). Interaction between DNA and *Escherichia coli* DNA topoisomerase I. *J. Biol. Chem.* **254**, 11083-11088.

Liu, L. F. and Wang, J. C. (1987). Supercoiling of the DNA template during transcription. *Proc. Natl. Acad. Sci. USA* **84**, 7024-7027.

Lockshon, D. and Morris, D. R. (1983). Positively supercoiled plasmid DNA is produced by treatment of *Escherichia coli* with DNA gyrase inhibitors. *Nucleic Acids Res.* **11**, 2999-3017.

Lockshon, D. and Morris, D. R. (1985). Sites of reaction of *Escherichia coli* DNA gyrase on pBR322 *in vivo* as revealed by oxolinic acid-induced plasmid linearisation. *J. Mol. Biol.* **181**, 63-74.

Lother, H., Lurz, R., and Orr, E. (1984). DNA binding and antigenic specifications of DNA gyrase. *Nucleic Acids Res.* **12**, 901-914.

Lowe, G. (1983). Chiral[^{16}O,^{17}O,^{18}O]phosphate esters. *Acc. Chem. Res.* **16**, 244-251.

Lowe, G., Cullis, P.M., Jarvest, R.L., Potter, B.V.L., and Sproat, B.S. (1981). Stereochemistry of phosphoryl transfer. *Philos. Trans. R. Soc. London, Ser. B* **293**, 75-92.

Lowe, G. and Potter, B.V.L. (1981). The stereochemical course of yeast hexokinase-catalysed phosphoryl transfer by using adenosine 5'-[γ(S)-^{16}O, ^{17}O, ^{18}O]triphosphate as substrate. *Biochem. J.* **199**, 227-233.

Lowe, G. and Potter, B.V.L. (1982). The stereochemical course of phosphoryl transfer catalysed by glucose 6-phosphatase. *Biochem. J.* **201**, 665-668.

Ludwig, J. and Eckstein, F. (1989). Rapid and efficient synthesis of nucleoside 5'-O-(1-thiotriphosphates), 5'-triphosphates and 2',3',-cyclophosphorothioates using 2-chloro-4H-1,3,2-benzodioxaphosphorin-4-one. *J. Org. Chem.* **54**, 631-635.

Ludwig, J. and Eckstein, F. (1991). Stereospecific synthesis of guanosine 5'-O-(1,2-dithiotriphosphates). *J. Org. Chem.* **56**, 5860-5865.

Lynn, R., Giaever, G., Swanberg, S.L., and Wang, J.C. (1986). Tandem regions of yeast DNA topoisomerase II share homology with different subunits of bacterial gyrase. *Science.* **233**, 647-649.

Lynn, R.M., Bjornsti, M.-A., Caron, P.R., and Wang, J.C. (1989). Peptide sequencing and site-directed mutagenesis identify tyrosine-727 as the active site tyrosine of *Saccharomyces cerevisiae* DNA topoisomerase I. *Proc. Natl. Acad. Sci. USA.* **86**, 3559-3563.

Lynn, R.M. and Wang, J.C. (1989). Peptide sequencing and site-directed mutagenesis identify tyrosine-319 as the active site tyrosine of *Escherichia coli* DNA topoisomerase I. *Proteins* **6**, 231-239.

Marquetant, R. and Goody, R.S. (1983). An improved separation of diastereomers of nucleoside phosphorothioates using reversed-phase high-performance liquid chromatography. *J. Chromat.* **280**, 386-389.

Maxwell, A. and Gellert, M. (1984). The DNA dependence of the ATPase activity of DNA gyrase. *J. Biol. Chem.* **259**, 14472-14480.

Maxwell, A. and Gellert, M. (1986). Mechanistic aspects of DNA topoisomerases. *Adv. in Prot. Chem.* **38**, 69-107.

Maxwell, A., Gellert, M., and McTurk, P. (1989). *Electron microscopy of 'phased' gyrase-DNA complexes.* In *Highlights of Modern Biochemistry.* Edited by Kotyk, A. 97-114. VSP International Science Publishers., Zeitz.

Maxwell, A., Rau, D.C., and Gellert, M. (1986). *Mechanistic studies of DNA gyrase.* In *Proc. Fourth Conversation in Biomol. stereodynamics III.* Edited by Sarma, R.H. and Sarma, M.H. 137-146. Adenine Press, NY.

McCoubrey, W.K. and Champoux, J.J. (1986). The role of single strand breaks in the catenation reaction catalysed by the rat type I topoisomerase. *J. Biol. Chem.* **261**, 5130-5137.

McPherson, A. (1982). *Preparation and analysis of protein crystals.* John Wiley & Sons, New York.

Meek, T. D., Karsten, W. E., and DeBrosse, C. W. (1987). Carbamoyl-phosphate synthetase II of the mammalian CAD protein: kinetic mechanism and elucidation of reaction intermediates by positional isotope exchange. *Biochemistry* **26**, 2584-2593.

Mejillano, M. R., Jahansouz, H., Matsunaga, T.O., Kenyon, G.L., and Himes, R.H. (1989). Formation and utilization of formyl phosphate by N10-formyltetrahydrofolate synthetase: Evidence for formyl phosphate as an intermediate in the reaction. *Biochemistry* **28**, 5136-5145.

Mensa-Wilmot, K., Seaby, R., Alfano, C., Wold, M.S., Gomes, B., and McMackan, R. (1989). Reconstitution of a nine-protein system that initiates bacteriophage λ DNA replication. *J. Biol. Chem.* **264**, 2853-2861.

Menzel, R. and Gellert, M. (1983). Regulation of the genes for *E. coli* DNA gyrase: homeostatic control of supercoiling. *Cell* **34**, 105-113.

Merz, K.M. and Kollman, P.A. (1989). Free energy perturbation simulations of the inhibition of thermolysin: prediction of the free energy of binding of a new inhibitor. *J, Am. Chem. Soc.* **111**, 5649-5658.

Michelson, A.M. (1964). Synthesis of nucleotide anhydrides by anion exchange. *Biochim. Biophys. Acta* **91**, 1-13.

Midelfort, C. F. and Rose, I. A. (1976). A stereochemical method for detection of ATP terminal phosphate transfer in enzymatic reactions. *J. Biol. Chem.* **251**, 5881-587.

Miller, K.G., Liu, L.F., and Englund, P.T. (1981). A homogenous type II DNA topoisomerase from HeLa cell nuclei. *J. Biol. Chem.* **256**, 9334-9339.

Miller, R.V. and Scurlock, T.R. (1983). DNA gyrase (topoisomerase II) from *Pseudomonas aeruginosa. Biochem. Biophys. Res. Comm.* **110**, 694-700.

Minden, J.S. and Marians, K.J. (1986). *Escherichia coli* topoisomerase I can segregate replicating pBR322 daughter DNA molecules *in vitro*. *J. Biol. Chem.* **261**, 11906-11917.

Mirambeau, G., Duguet, M., and Forterre, P. (1984). ATP-dependent topoisomerase from the archaebacterium *Sulfolobus acidocaldarius*. *J. Mol. Biol.* **179**, 559-563.

Miziorki, H. and Eckstein, F. (1984). The stereochemical course of the ribulose-5-phosphate kinase-catalysed reaction. *J. Biol. Chem.* **259**, 13037-13040.

Mizuuchi, K., Fisher, L. M., O'Dea, M. H., and Gellert, M. (1980). DNA gyrase action involves the introduction of transient double-stranded breaks in DNA. *Proc. Natl. Acad. Sci. USA* **77**, 1847-1851.

Mizuuchi, K., Mizuuchi, M., O'Dea, M. H., and Gellert, M. (1984). Cloning and simplified purification of *Escherichia coli* DNA gyrase A and B proteins. *J. Biol. Chem.* **259**, 9199-9201.

Mizuuchi, K., O'Dea, M. H., and Gellert, M. (1978). DNA gyrase: Subunit structure and ATPase activity of the purified enzyme. *Proc. Natl. Acad. Sci. USA* **75**, 5960-5963.

Moffat, J.G. (1964). General synthesis of nucleoside 5'-triphosphates. *Can. J. Chem.* **42**, 599-604.

Moore, C.L., Klevan, L., Wang, J.C., and Griffith, J.D. (1983). Gyrase:DNA complexes visualised as looped structures by electron microscopy. *J. Biol. Chem.* **258**, 4612-4617.

Morgan, B.P., Scholtz, J.M., Ballinger, M.D., Zipkin, I.D., and Bartlett, P.A. (1991). Differential binding energy: a detailed evaluation of the influence of hydrogen-bonding and hydrophobic groups on the inhibition of thermolysin by phosphorus-containing inhibitors. *J. Am. Chem. Soc.* **113**, 297-307.

Moriya, S., Ogasawara, N., and Yoshikawa, H. (1985). Structure and function of the region of the replication origin of the *Bacillus subtilis* chromosome. III. Nucleotide sequence of some 10,000 base pairs in the origin region. *Nucleic Acids Res.* **13**, 2251-2265.

Morrison, A. and Cozzarelli, N.R. (1979). Site-specific cleavage of DNA by *E. coli* DNA gyrase. *Cell.* **17**, 175-184.

Morrison, A. and Cozzarelli, N.R. (1981). Contacts between DNA gyrase and its binding site on DNA: Features of symmetry and asymmetry revealed by protection from nucleases. *Proc. Natl. Acad. Sci. USA.* **78**, 1416-1420.

Morrison, A., Higgins, N.P., and Cozzarelli, N.R. (1980). Interaction between DNA gyrase and its cleavage site on DNA. *J. Biol. Chem.* **255**, 2211-2219.

Nadal, M., Jaxal, C., Portemer, C., Forterre, P., Mirambeau, G., and Duguet, M. (1988). Reverse gyrase of *Sulfolobus*: Purification to homogeneity and characterization. *Biochemistry* **27**, 9102-9108.

Nadal, M., Mirambeau, G., Forterre, P., Reiter, W-D., and Duguet, M. (1986). Positively supercoiled DNA in a virus-like particle of an archaebacterium. *Nature* **321**, 256-258.

Nakasu, S. and Kikuchi, A. (1985). Reverse gyrase; ATP-dependent type I topoisomerase from *Sulfolobus*. *EMBO J.* **4**, 2705-2710.

Neal, S.E., Eccleston, J.F., and Webb, M.R. (1990). Hydrolysis of GTP by $p21^{NRAS}$, the *NRAS* protooncogene product, is accompanied by a conformational change in the wild-type protein: Use of a single fluorescent probe at the catalytic site. *Proc. Natl. Acad. Sci. USA* **87**, 3562-3565.

Ogita, T. and Knowles, J.R. (1988). On the intermediacy of carboxyphosphate in biotin-dependent carboxylations. *Biochemistry* **27**, 8028-8033.

Orr, G.A., Simon, J., Jones, S.R., Chin, G.J., and Knowles, J.R. (1978). Adenosine 5'-O-([γ-18O]γ-thio)triphosphate chiral at the γ-phosphorus: stereochemical consequences of reactions catalysed by pyruvate kinase, glycerol kinase, and hexokinase. *Proc. Natl. Acad. Sci. USA* **75**, 2230-2233.

Osheroff, N., Shelton, E.R., and Brutlag, D.L. (1983). DNA topoisomerase II from *Drosophila melanogaster*: Relaxation of supercoiled DNA. *J. Biol. Chem.* **258**, 9536-9543.

Pai, E.F., Krengel, U., Petsko, G.A., Goody, R.S., Kabsch, W., and Wittinghofer, A. (1990). Refined crystal structure of the triphosphate conformation of H-ras p21 at 1.35 Å resolution: implications for the mechanism of GTP hydrolysis. *EMBO J.* **9**, 2351-2359.

Pastorcic, M. (1982). *Purification and characterization of a new type I topoisomerase in E. coli.* PhD Thesis, Chicago, Illenois.

Pearson, R.G. (1966). Acids and bases. Hard acids prefer to associate with hard bases, and soft acids prefer to associate with soft bases. *Science* **151**, 172-177.

Pecoraro, V.L., Hermes, J.D., and Cleland, W.W. (1984). Stability constants of Mg^{2+} and Cd^{2+} complexes of adenine nucleotides and thionucleotides and rate constants for formation and dissociation of MgATP and MgADP. *Biochemistry* **23**, 5262-5271.

Perrin, D.D. and Armarego, W.L.F. (1988). *Purification of laboratory chemicals.* Pergamon Press, Oxford.

Pintado, E., Scarpa, A., and Cohn, M. (1982). Calcium transport and ATPase activities of sarcoplasmic reticulum with adenosine 5,-O-(2-thiotriphosphate) diastereomers as substrates. *J. Biol. Chem.* **257**, 11346-11352.

Pluira, D.H., Schomberg, D., Richard, J.P., Frey, P.A., and Knowles, J.R. (1980). Stereochemical course of a phosphokinase using a chiral (^{18}O)phosphorothioate. Comparison with the transfer of a chiral (^{16}O, ^{17}O, ^{18}O)phosphoryl group. *Biochemistry* **19**, 325-329.

Pollard-Knight, D., Potter, B.V.L., Cullis, P.M., Lowe, G., and Cornish-Bowden, A. (1982). The stereochemical course of phosphoryl transfer catalysed by glucokinase. *Biochem. J.* **201**, 421-423.

Prell, B. and Vosberg, H.-P. (1980). Analysis of covalent complexes formed between calf thymus DNA topoisomerase and single-stranded DNA. *Eur. J. Biochem.* **108**, 389-398.

Pruss, G.J. (1985). DNA topoisomerase I mutants. Increased heterogenity in linking number and other replicon-dependent changes in DNA supercoiling. *J. Mol. Biol.* **185**, 51-63.

Pruss, G.J., Franco, R.J., Chevalier, S.G., Manes, S.H., and Drlica, K. (1986). Effects of DNA gyrase inhibitors in *Escherichia coli* topoisomerase I mutants. *J. Bacteriol.* **168**, 276-282.

Pruss, G.J., Manes, S.H., and Drlica, K. (1982). *Escherichia coli* DNA topoisomerase I mutants: Increased supercoiling is corrected by mutations near gyrase genes. *Cell.* **31**, 35-42.

Pulleyblank, D. E., Shure, M., Tang, D., Vinograd, J., and Vosberg, H.-P. (1975). Action of nicking-closing enzyme on supercoiled and nonsupercoiled closed circular DNA: formation of a Boltzmann distribution of topological isomers. *Proc. Natl. Acad. Sci. USA* **72**, 4280-4284.

Radloff, R., Bauer, W., and Vinograd, J. (1967). A dye-buoyant-density method for the detection and isolation of closed circular duplex DNA: the closed circular DNA in HeLa cells. *Proc. Natl. Acad. Sci. (USA)* **57**, 1514-1521.

Ran, D.C., Gellert, M., Thoma, F., and Maxwell, A.M. (1987). Structure of the DNA gyrase-DNA complex as revealed by transient electric dichroism. *J. Mol. Biol.* **193**, 555-569.

Raushel, F. M and Villafranca, J. J. (1980). Phosphorus-31 nuclear magnetic resonance application to positional isotope exchange reactions catalysed by *Escherichia coli* carbamoyl-phosphate synthetase: analysis of forward and reverse enzymatic reactions. *Biochemistry* **19**, 3170-3174.

Reece, R.J. (1990). *Investigation of the domain structure of the Escherichia coli DNA gyrase A protein.* PhD Thesis, Leicester University.

Reece, R.J., Dauter, Z., Wilson, K.S., Maxwell, A., and Wigley, D.B. (1990). Preliminary crystallographic analysis of the breakage-reunion domain of the *Escherichia coli* DNA gyrase A protein. *J. Mol. Biol.* **215**, 493-495.

Reece, R.J. and Maxwell, A. (1989). Tryptic fragments of the *Escherichia coli* DNA gyrase A protein. *J. Biol. Chem.* **264**, 19648-19653.

Reece, R.J. and Maxwell, A. (1991a). The C-terminal domain of the *Escherichia coli* DNA gyrase A subunit is a DNA-binding protein. *Nucleic Acids Res.* **19**, 1399-1405.

Reece, R.J. and Maxwell, A. (1991b). DNA gyrase: structure and function. *Crit. Rev. Biochem. Mol. Biol.* **26**, 335-375.

Reece, R.J. and Maxwell, A. (1991c). Probing the limits of the DNA breakage-reunion domain of the *Escherichia coli* DNA gyrase A protein. *J. Biol. Chem.* **266**, 3540-3546.

Reed, G.H. and Leyh, T.S. (1980). Identification of the six ligands to manganese(II) in transition-state-analogue complexes of creatine kinase: oxygen-17

superhyperfine coupling from selectively labelled ligands. *Biochemistry* **19**, 5472-5480.

Reed, R.R. and Moser, C.D. (1984). Resolvase-mediated recombination intermediates contain a serine residue covalently linked to DNA. *Cold Spring Harbor Symp. Quant. Biol.* **49**, 245-249.

Rhodes, D. and Klug, A. (1980). Helical periodicity of DNA determined by enzyme digestion. *Nature* **286**, 573-578.

Richard, J.P., Carr, M.C., Ives, D.H., and Frey, P.A. (1980). The stereochemical course of thiophosphoryl group transfer catalysed by adenosine kinase. *Biochem. Biophys. Res. Commun.* **94**, 1052-1056.

Richard, J.P. and Frey, P.A. (1978). Stereochemical course of thiophosphoryl group transfer catalysed by adenylate kinase. *J. Am. Chem. Soc.* **100**, 7757-7758.

Richard, J.P., Prasher, D.C., Ives, D.H., and Frey, P.A. (1979). Chiral (^{18}O)phosphorothioates. The stereochemical course of thiophosphoryl group transfer catalysed by nucleoside phosphotransferase. *J. Biol. Chem.* **254**, 4339-4341.

Rosenfeld, S.S. and Taylor, E.W. (1984). The ATPase mechanism of skeletal and smooth muscle acto-subfragment 1. *J. Biol. Chem.* **259**, 11908-11919.

Rowe, T.C., Tewey, K.M., and Liu, L.F. (1984). Identification of the breakage-reunion subunit of T4 DNA topoisomerase. *J. Biol. Chem.* **259**, 9177-9181.

Rubio, V, Britton, H.G., Grisolia, S., Sproat, B.S., and Lowe, G. (1981). Mechanism of activation of bicarbonate ion by mitichondrial carbamoyl-phosphate synthetase: formation of enzyme-bound adenosine diphosphate from the adenosine triphosphate that yields inorganic phosphate. *Biochemistry* **20**, 1969-1974.

Saenger, W. (1984). *Principles of nucleic acid structure.* Edited by Cantor, C.R. Advanced texts in chemistry. Springer-Verlag, New York.

Saenger, W. and Eckstein, F. (1970). Crystal and molecular structure of the triethylammonium salt of uridine 2',3'-O,O-cyclophosphorothioate. *J. Am. Chem. Soc.* **92**, 4712-4718.

Saini, M.S., Buchwald, S., VanEtten, R.L., and Knowles, J.R. (1981). Stereochemistry of phospho transfer catalysed by bovine liver acid phosphatase. *J. Biol. Chem.* **256**, 10453-10455.

Sander, M. and Hsieh, T.-S. (1983). Double strand DNA cleavage by the type II DNA topoisomerases from *Drosophila melanogaster*. *J. Biol. Chem.* **258**, 8421-8428.

Schlichting, I., Almo, S.C., Rapp, G., Wilson, K., Petratos, K., Lentfer, A., Wittinghofer, A., Kabsch, W., Pai, E.F., Petsko, G.A., and Goody, R.S. (1990). Time-resolved X-ray crystallographic study of the conformational change in Ha-Ras p21 protein on GTP hydrolysis. *Nature* **345**, 309-315.

Seidel, J.C. (1969). Effects of salts of monovalent ions on the adenosine triphosphatase activities of myosin. *J. Biol. Chem.* **244**, 1142-1148.

Senter, P.D., Eckstein, F., and Kagawa, Y. (1983). Substrate metal-adenosine 5'-triphosphate chelate structure and stereochemical course of reaction catalysed by the adenosinetriphosphatase from the thermophilic bacterium PS3. *Biochemistry* **22**, 5514-5518.

Shaffer, R. and Traktman, P. (1987). Vaccinia virus encapsidates a novel topoisomerase with the properties of a eukaryotic type I enzyme. *J. Biol. Chem.* **262**, 9309-9315.

Shen, L.L., Baranowski, J., and Pernet, A.G. (1989a). Mechanism of inhibition of DNA gyrase by quinolone antibacterials: Specificity and cooperativity of drug binding to DNA. *Biochemistry.* **28**, 3879-3885.

Shen, L. L., Kohlbrenner, W. E., Weigl, D., and Baranowski, J. (1989b). Mechanism of quinolone inhibition of DNA gyrase: Appearance of unique norfloxacin binding sites in enzyme-DNA complexes. *J. Biol. Chem.* **264**, 2973-2978.

Shen, L.L., Mitscher, L.A., Sharma, P.N., O'Donnell, T.J., Chu, D.W.T., Cooper, C.S., Rosen, T., and Pernet, A.G. (1989c). Mechanism of inhibition of DNA gyrase by quinolone antibacterials: A cooperative drug-DNA binding model. *Biochemistry* **28**, 3886-3894.

Shen, L.L. and Pernet, A.G. (1985). Mechanism of inhibition of DNA gyrase by analogs of nalidixic acid: The target of the drugs is DNA. *Proc. Natl. Acad. Sci. USA.* **82**, 307-311.

Sheu, K-F.R., Richard, J.P., and Frey, P.A. (1979). Stereochemical courses of nucleotidyltransferase and phosphotransferase action. Uridine diphosphate glucose pyrophosphorylase, galactose-1-phosphate uridylyltransferase, adenylate kinase, and nucleoside diphosphate kinase. *Biochemistry* **18**, 5548-5556.

Shibata, T., Nakasu, S., Yasui, K., and Kikuchi, A. (1987). Intrinsic DNA-dependent ATPase activity of reverse gyrase. *J. Biol. Chem.* **262**, 10419-10421.

Shishido, K., Noguchi, N., and Ando, T. (1983). Correlation of enzyme-induced cleavage sites on negatively superhelical DNA between prokaryotic topoisomerase I and S1 nuclease. *Biochim. Biophys. Acta* **740**, 108-117.

Shore, D. and Baldwin, R. L. (1983a). Energetics of DNA twisting. 1. Relation between twist and cyclization probability. *J. Mol. Biol.* **170**, 957-981.

Shore, D. and Baldwin, R. L. (1983b). Energetics of DNA twisting. II. Topoisomer analysis. *J. Mol. Biol.* **170**, 983-1007.

Shore, D., Langowski, J., and Baldwin, R. L. (1981). DNA flexibility studied by covalent closure of short fragments into circles. *Proc. Natl. Acad. Sci. USA* **78**, 4833-4837.

Shuman, S. and Moss, B. (1987). Identificaiton of a vaccinia virus gene encoding a type I topoisomerase. *Proc. Natl. Acad. Sci. USA.* **84**, 7478-7482.

Siedlecki, J., Zimmerman, W., and Weissbach, A. (1983). Characterisation of a prokaryotic topoisomerase I activity in chloroplast extracts from spinach. *Nucleic Acids Res.* **11**, 1523-1536.

Simmons, R.M. and Hill, T.L. (1976). Definitions of free energy levels in biochemical reactions. *Nature.* **263**, 615-618.

Simpson, R.T., Thoma, F., and Brubaker, J.M. (1985). Chromatin reconstituted from tandemly repeated cloned DNA fragments and core histones: A model system for the study of higher order structure. *Cell* **42**, 799-808.

Sines, J.J. and Hackney, D.D. (1986). Anomalous oxygen-18 exchange during ATP synthesis in oxidative phosphorylation. *Biochemistry* **25**, 6144-6149.

Skerra, A., Pfitzinger, I., and Plückthun, A. (1991). The functional expression of antibody Fv fragments in *Escherichia coli*: improved vectors and a generally applicable purification technique. *Bio/Technology* **9**, 273-278.

Sleep, J.A. and Hackney, D.D. (1980). The equivalence of phosphate oxygens for exchange and the hydrolysis characteristics revealed by the distribution of $[^{18}O]P_i$ species formed by myosin and actomyosin ATPase. *J. Biol. Chem.* **255**, 4094-4099.

Smith, E. and Morrison, J.F. (1969). Kinetic studies on the arginine kinase reaction. *J. Biol. Chem.* **244**, 4224-4234.

Smith, R.M. and Alberty, R.A. (1956). The apparent stability constants of ionic complexes of various adenosine phosphates with divalent cations. *J. Am. Chem. Soc.* **78**, 2376-2380.

Snyder, M. and Drlica, K. (1979). DNA gyrase on the bacterial chromosome: DNA cleavage induced by oxolinic acid. *J. Mol. Biol.* **131**, 287-302.

Srivenugopal, K.S., Lockshon, D., and Morris, D.R. (1984). *Escherichia coli* DNA topoisomerase III: Purification and characterization of a new type I enzyme. *Biochemistry*. **23**, 1899-1906.

Staudenbauer, W.L. and Orr, E. (1981). DNA gyrase: affinity chromatography on novobiocin-sepharose and catalytic properties. *Nucleic Acids Res.* **9**, 3589-3602.

Steck, T.R. and Drlica, K. (1984). Bacterial chromosome segregation: Evidence for DNA gyrase involvement in decatenation. *Cell*. **36**, 1081-1088.

Stein, L.A., Schwarz, R., Chock, P.B., and Eisenberg, E. (1979). Mechanism of actomyosin adenosine triphosphatase. Evidence that adenosine 5'-triphosphate hydrolysis can occur without dissociation of the actomyosin complex. *Biochemistry* **18**, 3895-3909.

Sternglanz, R., Dinardo, S., Voelken, K.A., Nishimura, Y., Hirota, Y., Becherer, K., Zumstein, L., and Wang, J.C. (1981). Mutations in the gene encoding for *Escherichia coli* DNA topoisomerase I affect transcription and transposition. *Proc. Natl. Acad. Sci. USA*. **78**, 2747-2751.

Stryer, L. (1988). *Biochemistry*. Third ed. W. H. Freeman and Company, New York.

Sugino, A. and Cozzarelli, N.R. (1980). The intrinsic ATPase of DNA gyrase. *J. Biol. Chem.* **255**, 6299-6306.

Sugino, A., Higgins, N.P., Brown, P.O., Peebles, C.L., and Cozzarelli, N.R. (1978). Energy coupling in DNA gyrase and the mechanism of action of novobiocin. *Proc. Natl. Acad. Sci. USA*. **75**, 4838-4842.

Sugino, A., Higgins, N.P., and Cozzarelli, N.R. (1980). DNA gyrase subunit stoichiometry and the covalent attachment of subunit A to DNA during DNA cleavage. *Nucleic Acids Res.* **8**, 3865-3875.

Sugino, A., Peebles, C.L., Kreuzer, K.N., and Cozzarelli, N.R. (1977). Mechanism of action of Nalidixic acid: Purification of *Escherichia coli nalA* gene product and its relationship to DNA gyrase and a novel nicking-closing enzyme. *Proc. Natl. Acad. Sci. USA.* **74**, 4767-4771.

Swanberg, S. L. and Wang, J. C. (1987). Cloning and sequencing of the *Escherichia coli gyrA* gene coding for the A subunit of DNA gyrase. *J. Mol. Biol.* **197**, 729-736.

Tamura, J.K., Bates, A.D., and Gellert, M. (1992). Slow interaction of 5'-adenylyl-β,γ-imidodiphosphate with *Escherichia coli* DNA gyrase. Evidence for cooperativity in nucleotide binding. *J. Biol. Chem.* **267**, 9214-9222.

Tamura, J. K. and Gellert, M. (1990). Characterisation of the ATP binding site on *Escherichia coli* DNA gyrase. Affinity labelling of lys-103 and lys-110 of the B subunit by pyridoxal 5'-diphospho-5'-adenosine. *J. Biol. Chem.* **265**, 21342-21349.

Thiara, A.S. and Cundliffe, E. (1988). Cloning and characterization of a DNA gyrase B gene from *Streptomyces sphaeroides* that confers resistance to novobiocin. *EMBO J.* **7**, 2255-2259.

Tipton, P.A. and Cleland, W.W. (1988). Carbon-13 and deuterium isotope effects on the catalytic reactions of biotin carboxylase. *Biochemistry* **27**, 4325-4331.

Trask, D.K. and Muller, M.T. (1983). Biochemical characterization of topoisomerase I purified from avian erythrocytes. *Nucleic Acids Res.* **11**, 2779-2800.

Travers, A. A. (1990). Why bend DNA? *Cell* **60**, 177-180.

Trentham, D.R., Eccleston, J.F., and Bagshaw, C.R. (1976). Kinetic analysis of ATPase mechanisms. *Quart. Rev. Biophys.* **9**, 217-281.

Tsai, M-D. and Chang, T.T. (1980). Chirality at a pro-pro-prochiral phosphorus center. Stereochemical course of the 5'-nucleotidase-catalysed reaction. *J. Am. Chem. Soc.* **102**, 5416-5418.

Tse, Y.-C., Kirkegaard, K., and Wang, J.C. (1980). Covalent bonds between protein and DNA: Formation of phosphotyrosine linkage between certain DNA topoisomerases and DNA. *J. Biol. Chem.* **255**, 5560-5565.

Tse, Y.-C. and Wang, J.C. (1980). *E. coli* and *M. luteus* DNA topoisomerase I can catalyse catenation or decatenation of double-stranded DNA rings. *Cell.* **22**, 269-276.

Tse-Dinh. (1986). Uncoupling of the DNA breaking and rejoining steps of *Escherichia coli* type I DNA topoisomerase. *J. Biol. Chem.* **261**, 10931-10935.

Tse-Dinh, Y.-C. (1985). Regulation of the *Escherichia coli* DNA topoisomerase I gene by DNA supercoiling. *Nucleic Acids Res.* **13**, 4751-4763.

Tse-Dinh, Y-C. (1991). Zinc(II) coordination in *Escherichia coli* DNA topoisomerase I is required for cleavable complex formation with DNA. *J. Biol. Chem.* **266**, 14317-14320.

Tse-Dinh, Y.-C. and Beran-Steed, R.K. (1988). *Escherichia coli* DNA topoisomerase I is a zinc metalloprotein with three repetitive zinc-binding domains. *J. Biol. Chem.* **263**, 15857-15859.

Tse-Dinh, Y.-C., McMarron, B.G.H., Arentzen, R., and Chowdhry, V. (1983). Mechanistic study of *E. coli* DNA topoisomerase I: Cleavage of oligonucleotides. *Nucleic Acids Res.* **11**, 8691-8701.

Tse-Dinh, Y.-C. and Wang, J.C. (1986). Complete nucleotide sequence of the *topA* gene encoding *Escherichia coli* DNA topoisomerase I. *J. Mol. Biol.* **191**, 321-331.

Uemura, T., Morikawa, K., and Yanagida, M. (1986). The nucleotide sequence of the fission yeast DNA topoisomerase II gene: structural and functional relationships to other DNA topoisomerases. *EMBO J.* **5**, 2355-2361.

Uhr, M.L., Marcus, F., and Morrison, J.F. (1966). Studies on adenosine triphosphate: arginine phosphotransferase. Purification and reaction mechanism. *J. Biol. Chem.* **241**, 5428-5435.

Usher, D.A., Richardson, D.I., and Eckstein, F. (1970). Absolute stereochemistry of the second step of ribonuclease action. *Nature* **228**, 663-665.

Vinograd, J., Lebowitz, J., Radloff, R., Watson, R., and Laipis, P. (1965). The twisted circular form of polyoma viral DNA. *Proc. Natl. Acad. Sci. USA.* **53**, 1104-1111.

von de Saal, W., Anderson, P. M., and Villfranca, J. J. (1985). Mechanistic Investigations of *Escherichia coli* Cytidine-5'-triphosphate Synthetase. *J. Biol. Chem.* **260**, 14993-14997.

Vosberg, H.-P. (1985). DNA topoisomerases: Enzymes that control DNA conformation. *Current Topics Microbiol. Immunol.* **114**, 19-102.

Vosberg, H.-P., Grossman, L.I., and Vinograd, J. (1975). Isolation and partial characterization of the relaxation protein from nuclei of cultured mouse and human cells. *Eur. J. Biochem.* **55**, 79-93.

Wallis, J.W., Chrebet, G., Brodsky, G., Rolfe, M., and Rothstein, R. (1989). A hyper-recombination mutation of *S. cerevisiae* identifies a novel eukaryotic topoisomerase. *Cell.* **58**, 409-419.

Wang, J.C. (1969). Degree of superhelicity of covalently closed cyclic DNA's from *Escherichia coli*. *J. Mol. Biol.* **43**, 263-272.

Wang, J.C. (1971). Interaction between DNA and an *Escherichia coli* protein ω. *J. Mol. Biol.* **55**, 523-533.

Wang, J. C. (1982). DNA topoisomerases. *Sci. Am.* **247**, 84-109.

Wang, J. C. (1985). DNA topoisomerases. *Annu. Rev. Biochem.* **54**, 665-697.

Wang, J. C. (1987a). DNA topoisomerases: nature's solution to the topological ramifications of the double-helix structure of DNA. *The Harvey Lectures* **81**, 93-110.

Wang, J.C. (1987b). Recent studies of DNA topoisomerases. *Biochim. et Biophys. Acta.* **909**, 1-9.

Wang, J. C. (1991). DNA topoisomerases: why so many? *J. Biol. Chem.* **266**, 6659-6662.

Wang, J.C. and Becherer, K. (1983). Cloning of the gene topA encoding for DNA topoisomerase I and the physical mapping of the *cysB-topA-trp* region of *Escherichia coli. Nucleic Acids Res.* **11**, 1773-1790.

Wang, J.C. and Liu, L.F. (1990). *DNA replication: topological aspects and the roles of DNA topoisomerases.* In *DNA topology and its biological effects.* Edited by Wang, J.C. and Cozzarelli, N.R. 321-340. Cold Spring Harbor Laboratory Press, New York.

Wasserman, S.A. and Cozzarelli, N.R. (1986). Biochemical topology: Applications to DNA recombination and replication. *Science* **232**, 951-960.

Watson, J.D. and Crick, F.C.H. (1953). Molecular structure of nucleic acid. A structure for deoxyribo nucleic acid. *Nature.* **171**, 373-378.

Watson, N. (1988). A new revision of the sequence of plasmid pBR322. *Gene* **70**, 399-403.

Webb, M.R. (1982). The stereochemical course of nucleoside triphosphatase reactions. *Methods Enzymol.* **87**, 301-316.

Webb, M.R. and Eccleston, J.F. (1981). The stereochemical course of the ribosome-dependent GTPase reaction of elongation factor G from *Escherichia coli. J. Biol. Chem.* **256**, 7734-7737.

Webb, M.R., Grubmeyer, C., Penefsky, H.S., and Trentham, D.R. (1980). The stereochemical course of phosphoric residue transfer catalysed by beef heart mitochondrial ATPase. *J. Biol. Chem.* **255**, 11637-11639.

Webb, M.R. and Trentham, D.R. (1980a). Analysis of chiral inorganic (^{16}O, ^{17}O,^{18}O)thiophosphate and the stereochemistry of the 3-phosphoglycerate kinase reaction. *J. Biol. Chem.* **255**, 1775-1779.

Webb, M.R. and Trentham, D.R. (1980b). The stereochemical course of phosphoric residue transfer during the myosin ATPase reaction. *J. Biol. Chem.* **255**, 8629-8632.

Webb, M.R. and Trentham, D.R. (1981). The stereochemical course of phosphoric residue transfer catalysed by sarcoplasmic reticulum ATPase. *J. Biol. Chem.* **256**, 4884-4887.

Westerhoff, H. V., O'Dea, M. H., Maxwell, A., and Gellert, M. (1988). DNA supercoiling by DNA gyrase. A static head analysis. *Cell Biophysics.* **12**, 157-181.

Westheimer, F.H. (1987). Why nature chose phosphates. *Science* **235**, 1173-1178.

White, J.H. (1969). Self-linking and the Gauss integral in higher dimensions. *Am. J. Math.* **91**, 693-728.

White, J.H., Cozzarelli, N.R., and Bauer, W.R. (1988). Helical repeat and linking number of surface-wrapped DNA. *Science* **241**, 323-327.

Wigley, D.B., Davies, G.J., Dodson, E.J., Maxwell, A., and Dodson, G. (1991). Crystal structure of an N-terminal fragment of the DNA gyrase B protein. *Nature* **351**, 624-629.

Wimmer, M. J., Rose, I.A., Powers, S.G., and Meister, A. (1979). Evidence that carboxyphosphate is a kinetically competent intermediate in the carbamyl phosphate synthetase reaction. *J. Biol. Chem.* **254**, 1854-1859.

Wojciechowska, A., Bolewski, L., and Lomozik, L. (1991). A study of polyamine complex formation with H^+, Cu(II), Zn(II), Pb(II), and Mg(II) in aqueous solution. *Monatsh. Chem.* **122**, 131-138.

Wolfenden, R.V., Cullis, P.M., and Southgate, C.C.F. (1979). Water, protein folding, and the genetic code. *Science* **206**, 575-577.

Worland, S. T. and Wang, J. C. (1989). Inducible overexpression, purification and active site mapping of DNA topoisomerase II from the yeast *Saccharomyces cerevisiae*. *J. Biol. Chem.* **264**, 4412-4416.

Wu, H.-Y., Shyy, S., Wang, J. C., and Liu, L. F. (1988). Transcription generates positively and negatively supercoiled domains in the template. *Cell.* **53**, 433-440.

Wyckoff, E., Natalie, D., Nolan, J. M., Lee, M., and Hsieh, T. (1989). Structure of the *Drosophila* DNA topoisomerase II gene. Nucleotide sequence and homology among topoisomerases II. *J. Mol. Biol.* **205**, 1-13.

Yamagishi, J.-I., Yoshida, H., Yamayoshi, M., and Nakamura, S. (1986). Nalidixic acid-resistant mutations of the *gyrB* gene of *Escherichia coil. Mol. Gen. Genet.* **204**, 367-373.

Yanagida, M. and Sternglanz, R. (1990). *Genetics of DNA topoisomerases.* In *DNA topology and its biological effects.* Edited by Wang, J.C. and Cozzarelli, N.R. 299-320. Cold Spring Harbor Laboratory Press, New York.

Zumstein, L. and Wang, J.C. (1986). Probing the structural domains and function *in vivo* of *Escherichia coli* DNA topoisomerase I by mutagenesis. *J. Mol. Biol.* **191**, 333-340.

Appendix I

On the Specific Activities of DNA Gyrase Preparations

Since the isolation and purification of the DNA gyrase A and B proteins in the early 1980's, the specific activities of GyrB have always been lower than that of GyrA with the most active GyrB preparations being approximately 3-fold less active than GyrA (Mizuuchi *et al.*, 1984).

During the preparation of the gyrase subunits in this work, it was noticed that the specific supercoiling activity of the B subunit was again less than that of the A subunit and that the activities were considerably less than those reported by Mizuuchi *et al.*, (1984). Fig. A1 shows the supercoiling assays to determine the specific activities of the purified A and B subunits and the A_2B_2 tetramer reconstituted from these subunits. The specific activities of the A and B subunits were 7 X 10^5 units/mg and 6 X 10^4 units/mg respectively. These values were determined from the concentration of one subunit required to give 50% supercoiling in the presence of an excess of the other subunit. If the preparations of the A and B subunits contained only active protein, similar values for the specific activities of the two subunits would be expected since their molecular weights are similar (97kDa and 90kDa respectively). The observation that the specific activity of the B preparation was approximately 10-fold lower than the A preparation suggested that the B preparation contained either a non-homogeneous mixture of active and inactive protein or a homogeneous sample of protein with greatly reduced activity. In Fig. A1, the specific activity of the full enzyme reconstituted from an equimolar mixture of the two subunits was found to be 6 X 10^4 units/mg based on total protein concentration. The activity of a gyrase sample reconstituted from a molar ratio of A subunit to B subunit of 1:10 was found to increase approximately 10-fold based of the concentration of the A protein (data not shown). This would favour the hypothesis that the B protein preparation was a mixture of active and inactive (or much less active) enzyme. Similar low specific activities for the B protein (produced from the same overexpressing clone as in this study) have been obtained by other colleagues in this laboratory. Furthermore, an extensive investigation of the supercoiling activity of gyrase with a constant level of the A protein in

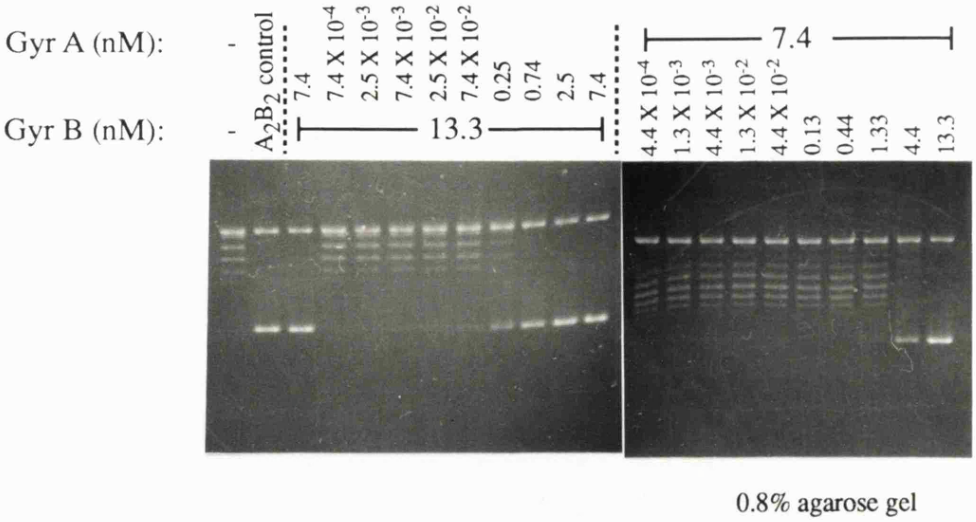

Figure A1(a). Supercoiling assays to determine the specific activities of the gyr A and gyr B preparations. The reactions (30µl) were performed as described in Section 2.27. To determine the specific activity of the A and B proteins, the protein concentration was varied in the presence of the other subunit as shown in the figure. (Protein concentrations are expressed in terms of protein dimers). 1 unit of activity is defined as the amount of protein required to give 50% supercoiling under the conditions of the assay. For the A protein it can be seen that 50% supercoiling occurred with 0.74nM protein which gave a specific activity of 7 X 10^5 units/mg. For the B protein 50% supercoiling occurred between 13.3 and 4.4nM protein which gave a specific activity of 6 X 10^4 units/mg.

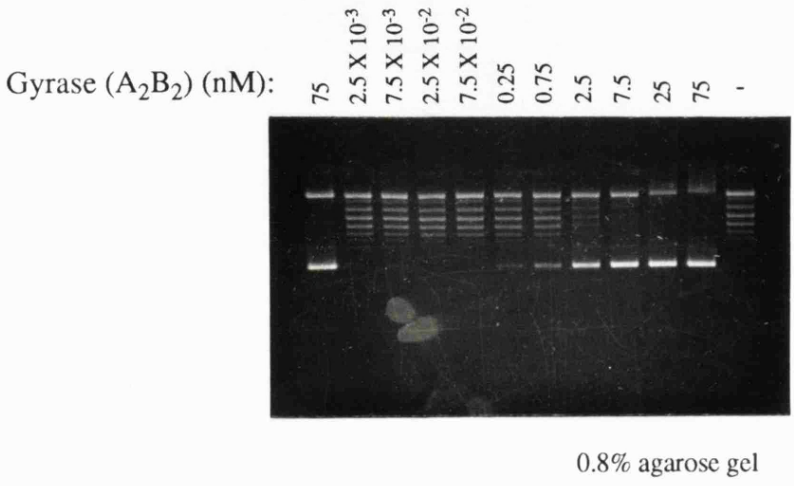

Figure A1(b). Supercoiling assay to determine the specific activity of gyrase reconstituted from an equimolar amount of gyr A and gyr B. The reactions (30µl) comprised the usual supercoiling reaction mixture (Section 2.27). 50% supercoiling is seen between tracks 7 and 8 (ie. at approximately 1.5nM gyrase). This corresponds to a specific activity of 6 X 10^4 units/mg)

the presence of varying molar excesses of the B subunit suggested that approximately 10% of the B protein was in the active form and 90% was inactive (J. Ali, personal communication) which is consistent with the conclusion above that the B preparation contained active and inactive protein.

It is well established that the gyrase ATPase is activated by DNA (Maxwell and Gellert, 1984; Mizuuchi *et al.*, 1978; Staudenbauer and Orr, 1981; Sugino and Cozzarelli, 1980; Sugino *et al.*, 1978) although there has been some discrepancy in the reported magnitude of this activation. This discrepancy may reflect different preparations and different conditions of the ATPase assays by different investigators.

Using the PK/LDH assay and an ATP concentration of 1mM, a considerable ATPase activity was observed in the absence of DNA which increased by only 1.3 to 1.5-fold in the presence of linear pBR322 (data not shown). This small activation in the presence of DNA is much less than that reported by Maxwell and Gellert (1984) although their experiments employed a lower ATP concentration.

The binding of the gyrase preparation to DNA was investigated with various proportions of A and B subunits as shown in Fig. A2. It was found that, with an excess of the A subunit, a ratio of the B subunit to DNA of approximately 11 was required to fully bind the DNA.

The above observations that the B protein preparation has a lower than expected specific supercoiling activity and that the ATPase of this gyrase preparation is only moderately stimulated by DNA support the hypothesis that the B protein is present in two conformations, only one of which is active towards DNA supercoiling. The DNA binding data suggests that the inactive form of the B protein is less able to form a complex with the A protein that can bind to DNA. Assuming that only the active proportion of the

A protein present:	-	+	-	+	+	+	+	+
B dimer conc. (nM):	-		296	74	148	296	592	1184

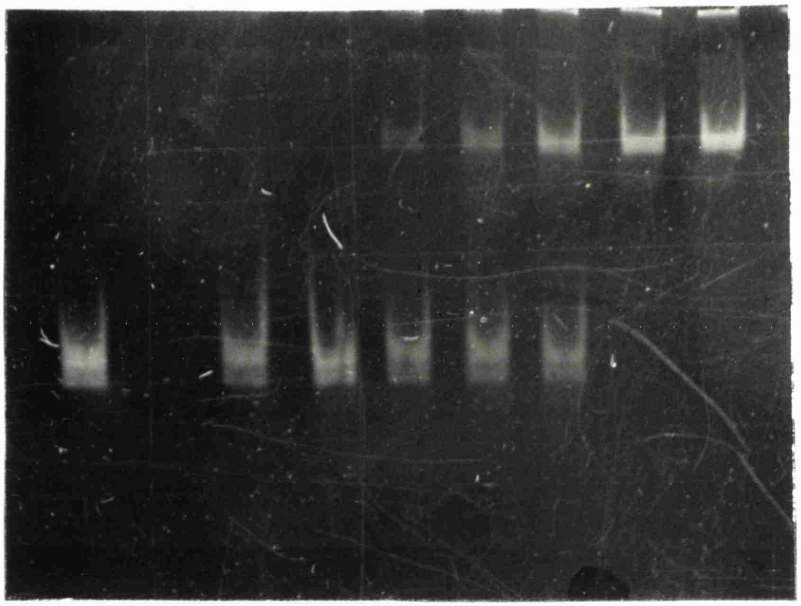

Figure A2. A gel retardation assay to determine the proportion of GyrB to DNA required, in the presence of an excess of GyrA, to fully bind to the DNA. Linear 172bp DNA was used at a concentration of 54nM. GyrA was at a concentration of 69nM. Free DNA can be seen as the high mobility band and protein-bound DNA can be seen as the lower mobility band.

B protein can form complexes capable of DNA binding, the gel retardation assay would be consistent with a maximum of 9% of the total protein concentration being in the active form. It has been shown previously that the B protein exhibits a DNA-independent ATPase which is increased by treatment with urea or heat (Maxwell and Gellert, 1984). These workers also speculated that the increase in the DNA-independent ATPase activity may be due to a protein conformational change induced by the treatment with heat or urea which may be identical to that adopted in the presence of the A protein and DNA. It is possible that the B preparation described in this chapter contained more of this altered conformation than the preparation described by Maxwell and Gellert (1984). Alternative hypotheses are also possible to explain the low supercoiling and DNA binding characteristics of the B preparation where an altered conformation of the protein not involved in the supercoiling mechanism of gyrase was present.

It would appear that the low supercoiling activity of the B protein is a consequence of the *gyrB* clone and is probably due to the high level of overexpression of the protein (up to 40% of cell extract). It was reasoned that it may be possible to improve the activity of the B protein if it could be produced at the same time as the A protein in the cell since the A protein might stabilise the active conformation. Moreover, for many applications, only the gyrase tetramer and not the separate A and B proteins are required. In addition, it was thought that it may be possible to purify the whole gyrase complex produced in this way *via* ion exchange chromatography (if the components stayed together at the salt concentration required to elute the protein) or *via* gel filtration. Two procedures could be used in attempting to clone both gyrase proteins together; either the two genes could be expressed on the same plasmid, or they could be expressed on separate plasmids and cells could be transformed with both of the vectors. The second of these approaches was deemed to be the most straight-forward. The existing plasmids harbouring the *gyrA* and *gyrB* genes (pPH3 and pAG111 respectively) both contained the ampicillin resistance gene. In order to select for cells containing both *gyrA* and *gyrB* plasmids one of these

vectors needed to be changed so that it contained a difference resistance determinant. Accordingly, the *gyrB* gene was cloned into a vector containing the gene for tetracycline resistance and *E. coli* was transformed with both this vector and the pPH3 vector. This work was performed by R. Reece of this laboratory. I then went on to analyse the *E. coli* cells harbouring these vectors.

Fig. A3 shows that the cells did express both gyrase proteins. The proportion of GyrA to GyrB was approximately 1:1 taking into account the fact that GyrA gives a two-fold lower staining intensity with coomassie stain than GyrB (see Section 2.23). Growth under varying concentrations of ampicillin and tetracycline did not appear to have any significant effect on the relative expression of the two proteins. A supercoiling assay of the cell extract revealed a specific activity of 7 X 10^3 units/mg. This was of the same order as the cell extract for the B protein produced in the normal way and therefore suggested that the B protein produced from the A/B clone consisted of a considerable proportion of inactive protein in the same way as the B clone. In view of this, attempts to further purify the gyrase protein from the cell extracts were not attempted. Fig. A4 shows a series of supercoiling assays with the double clone cell extracts in which various amounts of additional A or B proteins were added. It can be seen that the activity was unaffected by the addition of extra A protein but was increased slightly in the presence of additional B protein. This is consistent with some of the B protein in the A/B cell extract being in the inactive form for DNA supercoiling. One possibility for the low activity of the protein was that the cells were dying after induction by IPTG. To investigate this the specific activities of cell extracts harvested at various times after induction were measured. Samples harvested 2, 3, and 4 hours after induction showed no significant differences in activity.

In order to study the detailed kinetic mechanism of the gyrase ATPase a pre-steady-state approach will be required. This will probably require fully active protein and therefore

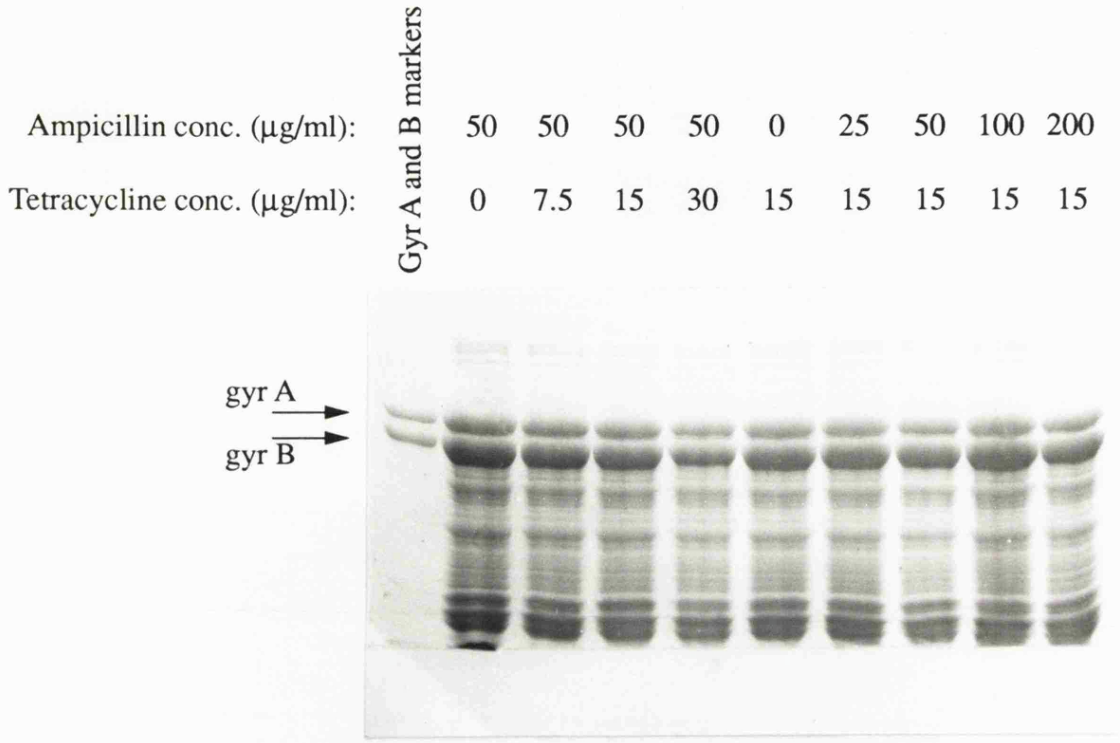

Figure A3. SDS-PAGE gel showing cell extracts of the A/B double clone grown under varying antibiotic concentrations. The cell extracts were prepared as follows. A single colony of *E.coli* containing the *gyrA* and *gyrB* vectors was picked from an AMP(100μg/ml)/TET(15μg/ml) plate and grown overnight in LB containing AMP and TET at the concentrations above. The following day, 200μl aliquots of the cell culture were pipetted into nine 10 ml sterilin tubes containing LB and the various antibiotic concentrations shown in the figure. The cells were grown up to an optical density (A_{595}) of 0.5 and IPTG was added to a final concentration of 50μM. Cell growth was continued for a further 4.5 hours. After harvesting, the cell pellets were resuspended in Enzyme Buffer (300μl) and the cells were disrupted by sonication. The protein concentration in all the samples was found to be approximately 4.7 mg/ml.

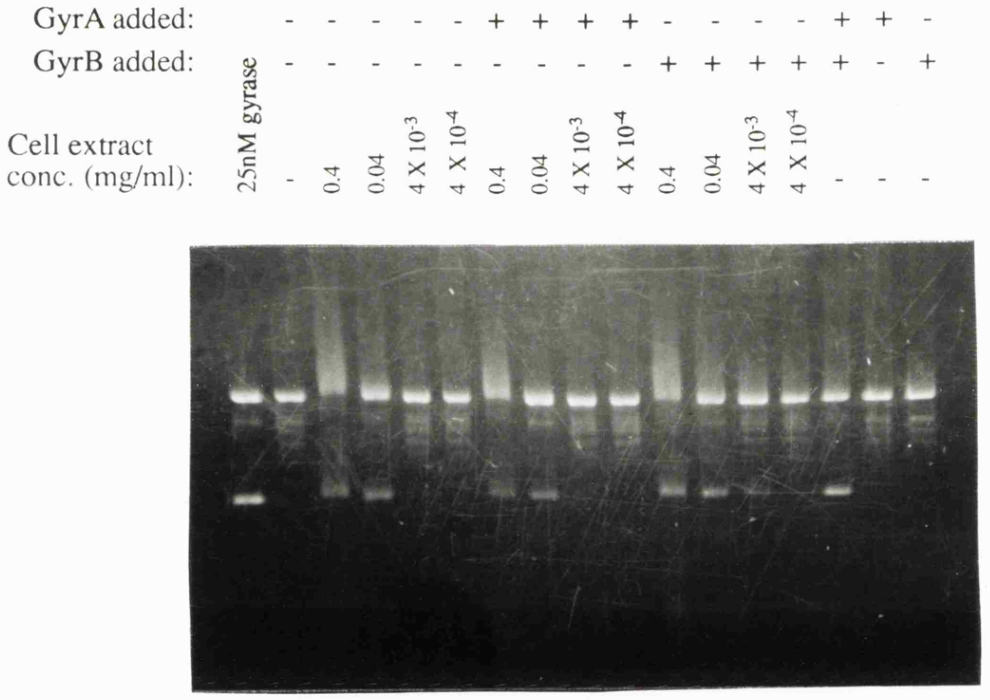

Figure A4. Supercoiling assays of the double clone cell extracts in which various amounts of additional GyrA or GyrB proteins were added. The final concentration of the additional GyrA added was 4.4 X 10^{-3} mg/ml and the final concentration of the GyrB added was 0.022 mg/ml.

methods to improve the activity of the B subunit would be very important. It has been shown that the specific activity of the B protein is increased by approximately 6-fold if the protein is unfolded in 6M guanidine hydrochloride and then allowed to refold (A. Maxwell, personal communication). This suggests that up to 18% of the B preparation (before unfolding and refolding) is in the active form and offers a way of increasing the proportion of active protein. However, it would seem excessive to produce mainly inactive enzyme which required this unfolding and refolding step and a more desirable method would be to produce active enzyme directly. One possibility may be to grow the cells and induce at a lower temperature (Skerra *et al.*, 1991).

In conclusion the supercoiling data is consistent with the B protein preparation containing approximately 10 to 20% active protein. The proportion of inactive protein possesses a DNA-independent ATPase similar to that of the DNA stimulated ATPase of the active B protein. DNA binding studies suggest that either the inactive proportion of the B protein does not bind DNA at all (in the presence of the A protein) or that the binding is considerably reduced.

Appendix II

Publications resulting from this and related work are:

Modha, J., Weiner, D.P., Cullis, P.M., and Rivett, A.J. (1990). Effects of ATP analogues on the activity of the Lon protease in *Escherichia coli*. *Biochem. Soc. Trans.* **18**, 589.

Weiner, D.P. (1991). Catalytic antibodies. *Chemistry & Industry* **No. 10**, 20 May, 347-349.

Weiner, D.P. (1992). Expanding the chemistry of nature: catalytic antibodies. *Gen. Engineer & Biotechnologist* **12**, No. 2, 9-13.

Cullis, P.M., Maxwell, A., and Weiner, D.P. (1992). Energy coupling in DNA gyrase: a thermodynamic limit to the extent of DNA supercoiling. *Biochemistry* (In press).